



Universitat Autònoma de Barcelona

ADVERTIMENT. L'accés als continguts d'aquesta tesi queda condicionat a l'acceptació de les condicions d'ús establertes per la següent llicència Creative Commons:  http://cat.creativecommons.org/?page_id=184

ADVERTENCIA. El acceso a los contenidos de esta tesis queda condicionado a la aceptación de las condiciones de uso establecidas por la siguiente licencia Creative Commons:  <http://es.creativecommons.org/blog/licencias/>

WARNING. The access to the contents of this doctoral thesis it is limited to the acceptance of the use conditions set by the following Creative Commons license:  <https://creativecommons.org/licenses/?lang=en>



Study of the crosstalk between microglia and oligodendrocyte-related cells in central nervous system myelination through interactomics

Jennifer Enrich Bengoa

Ph.D supervisors: Dr. Alejandro Perálvarez Marín and Dr. Irene Román Degano

Biophysics Unit, Department of Biochemistry and Molecular Biology, School of
Medicine, Universitat Autònoma de Barcelona,

I. ACKNOWLEDGEMENTS

Ante todo, quisiera decir que esta tesis doctoral no habría sido posible sin el soporte de innumerables personas que van desde profesionales del ámbito científico hasta aquellos más allegados. Así que empecemos.

Ante todo, quisiera agradecer a Enrique Querol por haberme presentado a mi supervisor de tesis. Sin ti, Enrique, posiblemente esta aventura en la UAB en la Unidad de Biofísica jamás habría empezado. Así que siempre te estaré enormemente agradecida por haberme brindado la oportunidad de conocer a Alex y poder empezar mi aventura como doctoranda. Por otra parte Enrique, quiero decirte que eres un profesor al que admiro muchísimo, todavía recuerdo lo mucho que me fascinó una clase que diste en la cual hablabas sobre la enfermedad de Huntington. Por otro caso familiar, aunque distinto al de dicha patología, decidí pedirte consejo profesional. Por suerte a mi edad y teniendo en cuenta la cantidad de deporte que hago, me he librado de la mala fortuna. Así que gracias por tu increíble sinceridad, consejo y soporte cuando estaba muy perdida. Creo que nunca tendré palabras suficientes para agradecerte tantas cosas Enrique. Gracias de todo corazón Enrique.

Alex, gracias por haberme dado la oportunidad de formar parte de tu grupo. Ha sido una experiencia muy gratificante y cabe decir, que estoy contenta de que hayas sido mi supervisor. Me has enseñado muchas cosas tanto a nivel profesional como personal, quizás ahora mismo no lo tengas en mente pero me has dado consejos que me van a venir muy bien para crecer como persona. Gracias por todo Alex y ¡sigue haciendo que la investigación avance!

Irene, moltes gràcies per haver-me ajudat a descobrir una part de la ciència tan bonica i fascinant com la bioinformàtica i les omiques. Vaig descobrir lo que més m'apassionava de la ciència gràcies a tu. Llàstima haver-ho descobert el darrer any de la tesi però així també vaig tenir l'oportunitat de treballar a poyata. Gràcies per aquesta gran oportunitat, va ser tot un plaer treballar amb eines bioinformàtiques i omiques, i sobre tot poder comptar amb una professional tan experimentada en aquest camp com tu. Mil gràcies Irene!

Gracias al resto de miembros de la Unidad de Biofísica, tanto aquellos que aún seguís por ahí como aquellos que pasasteis un tiempo y dejasteis vuestra huella. Muchas gracias Ramón, Pep, Núria, Mireia, David, Elodia, Tzevetana, Sonia, Gisela, Elena, Marta S., Mateo y Xavi. Posiblemente me haya dejado gente pero ya sabemos que algo de memoria de pez tengo para los nombres. Así que disculpad aquellos de los cuales me haya podido dejar de nombrar.

Gracias a aquellas personas de los distintos servicios técnicos que me han permitido aprender técnicas de biología molecular y de cultivos celulares. Muchísimas gracias Javier por tu

increíble paciencia y por ser capaz de transmitir tus conocimientos de biología molecular, gracias a ti he aprendido muchísimo. Gracias a las técnicas de cultivos celulares Cris y Neus por ser tan profesionales y transmitir esa pasión que tienen por los cultivos.

Quisiera también agradecer a Francesc Jiménez por los días que me tuvo en su laboratorio y lo muchísimo que aprendí. Moltíssimes gràcies Francesc per aquesta oportunitat i per transmetre aquesta passió per la ciència i per el teus projectes. T'he de dir que em va fascinar el que esteu fent en el vostre grup de recerca. Gràcies per transmetre d'aquesta manera tan especial aquesta passió que tens per la ciència i gràcies per haver-me deixa't passar uns dies al teu laboratori. T'he de dir que ho vaig gaudir moltíssim.

Moltes gràcies també al grup d'Histologia Mèdica, ha estat un plaer poder treballar amb vosaltres i treure aquests magnífics resultats. Sense el vostre enorme esforç i els vostres coneixements, mai hauria estat possible.

Gràcies també als membres del meu comitè de seguiment: Carles Saura, Rubén Lopez i Carles Gil. Cal a dir que sóc tot un nervi i anava força nerviosa a totes les comissions de seguiment però un cop allà els nervis marxaven de seguida. He après moltíssim de les vostres observacions, suggeriments, dubtes, preguntes... Ara sí que em sento capaç de defensar aquesta tesi doctoral i ja s'ha acabat aquesta tonteria del nervi de parlar en públic. Gràcies de tot cor.

Ahora sí, toca hablar sobre aquellas personas externas del ámbito académico y que habéis estado ahí en todo momento. Así que me lo voy a tomar con calma y voy a ir uno por uno.

Albert, aquell germà que mai vaig tenir. Gràcies per tots aquests anys, dintre de poc dècada i mitja d'amistat. Gràcies per haver estat en els bons i en els mals moments, per rebrem sempre amb un somriure i amb una abraçada. Tu i la teva família sempre m'heu acceptat com a una més i és algo que sempre us agrairé. Me n'alegro tant que segueixis present a la meua vida i espero que sempre sigui així. Això sí, les festes de la Llagosta seguiran forever and ever i el mandanga style en las noches de borrachera y no borrachera también! T'estimo nino!

Eugenia, mi argentina favorita. Quien iba a decir que después de tantos años aún nos seguiríamos riendo como el primer día, eres de las personas más nobles y sinceras que conozco. Hemos pasado por muchas cosas y cuando más lo necesitaba me has recibido con los brazos abiertos. Que suerte de que todavía sigas en mi vida. Te quiero amiga.

A mi italiana favorita, Giada. Buah, contigo todo siempre ha sido genial. Que bien nos lo pasábamos aquellas noches de fiesta, eran lo más de lo más. También aquellos momentos en los que se necesitaba una amiga y tú estabas ahí, jamás me has fallado Giada. Hablo en pasado, no por qué no tengamos una excelente amistad, sino porqué lamentablemente para nosotros te has

vuelto a Italia. Nos encanta que vengas a visitarnos pero se nos queda muy corto Giada. Estamos deseando que vuelvas a vivir aquí y te invito a un mojito, coca-cola, beer, water o vater (creo que ambos son válidos), tú ya me entiendes jajaja. Gracias amiga, ¡qué fácil es quererte tanto!

Eloy, el meu gran amic des de l'adolescència. Que genial que estiguis present a la meva vida, hem passat per molt però som molt forts i no hi ha res que no puguem superar. Recordo aquells anys on tancàvem discoteques, no hi havia cap de setmana sense festa, un amic per els bons i els mals moments... Encara recordo entre riures quan tothom creia que acabaríem sortint junts i en lloc d'això, vam acabar sortint junts però de l'armari i no pas de la mà jajaja! vam ser els primers en sortir de l'armari l'un amb l'altre, best moment ever! Gràcies Eloy per seguir a la meva vida, gràcies per saber que puc comptar amb tu tant per els bons com per els mals moments. Ara, ja no comptis amb mi per lo de de tancar discoteques, ja veig que a tu l'edat et perdona però a mi no. T'estimo Eloiè!

Claudia, una de las personas que más aprecio. No podemos ser más distintas, somos como la noche y el día pero ¿quién dice que los polos opuestos no puedan llevarse bien? Lo cierto es que nadie entiende como somos tan amigas con lo distintas que somos pero hay algo que me encanta de ti, eres una persona de lo más noble que te puedas encontrar por ahí. Que genial todos estos años compartiéndolos con una amiga como tú y que sean muchos más. ¡No me faltes nunca Claudia!

Alex Rodal, para los amigos el Rodi, mi gran amigo de la carrera. No sé qué habría sido de la carrera sin ti, conocí mucha gente y con algunos aún sigo manteniendo el contacto pero tú eres el más especial de todos. Eres un friki, un otaku, te encanta el monstruo del espagueti... buahh cuantas cosas he descubierto en la vida gracias a ti, aunque creo que todavía no has logrado convencerme del todo. Me quedo con ser una gamer y una friki del final fantasy pero no me saques de ahí jajaja. Está genial conservar tu amistad, poder salir los fines por ahí, hacer un pulso cada finde para ver como llevamos el tema pesas (aixx....a medida que me crece la espalda ya casi ni puedes conmigo. Recuerda, hay vídeos jajja) y sobre todo ¡que la buena birra nunca falte! Eso sí que sepas que como te pases de alcohol voy a intentar robarte a los clientes, recuerda “somos amigos en la vida personal y enemigos en la laboral” jajaj que bueno acabar trabajando en la competencia. Gracias por todo amigo, ¡se te quiere mucho!

A mi Hospi, otra biotec fugada. Buahhh tengo demasiadas cosas que decirte Hospi, como me alegro de tenerte como amiga y haber descubierto ese lado que intentas no mostrar y que solo poquitas personas conocen. Nos ha tocado vivir situaciones muy difíciles, pero ¿sabes qué? Lo que no te mata, te hace más fuerte. Así que **¡tú y yo somos invencibles!** Ya te lo he dicho y te

lo vuelvo a repetir, en Terrassa tienes una casa cuando lo necesites. Te quiero amiga, eres más fuerte y valiente de lo que te imaginas.

A la meva mallorquina exiliada a Barcelona, la Mar. Tindria tantes coses a escriure sobre tu que podria escriure una tesi doctoral només amb les nostres histories. Ja saps que farà cosa d'una dècada vas ser una de les persones més importants per mi. Gràcies a tu vaig aprendre moltes coses, que absurd és lligar el gènere amb els sentiments i que absurd és no normalitzar que cadascú utilitzi els pronoms que vulgui, veritat? Vas ser una persona molt important en la meva vida i ara encara ho continues siguent, amiga. Hem viscut coses molt similars i dures però sempre et dic, confio en que tot anirà bé. Bé, no confio, ho sé. Et conec i sé la fortalesa que tens, a més a més, tens gent que et recolza i els importes, a mi m'importes. Gràcies amiga, no em faltis mai si us plau.

A li Martta, la persona més real i amb menys mascares que mai he conegut. Persona queer, no binarie, pansexual, feminista, sense complexes i que es mostra tal i com és. Ho tens tot amore! No sé si t'ho he dit mai però des de el moment 1 que et vaig conèixer, vaig saber que possiblement fossis una de les persones més autèntiques que mai arribaria a conèixer. De moment, ho continuo mantenint. Martta no sé que faria sense els teus consells, xerrades llargues, un bon martini al migdia y que no falte el candy! Ets tan autèntiqui i natural que de vegades em fas enveja, que genial poder viure siguent uni mateixi i passant de tot i de totis. Gràcies per haver aparegut a la meva vida, t'estimo amigui!

A Lucía, mi médica favorita. Bueno Lucía, creo que ya sabes el gran aprecio que te tengo y me alegra muchísimo que sigas formando parte de mi vida. Es todo un regalo poder seguir disfrutando de tu amistad y que sigamos celebrando cumpleaños juntas como buenas amigas. Sé que has pasado una mala época este año pero me alegro de que las cosas hayan salido bien y ya sabes que estoy aquí para lo que necesites. También, aunque lo conozca poco, quiero darle las gracias a tu pareja Sergi. ¡A todos nos encantó! es un encanto de chico y me alegro mucho que hayas encontrado a una persona que te quiera y te cuide tanto. Sergi, ¡cuida bien de Lucía o te las verás conmigo! Felicidades pareja, sois geniales.

A Mateo, mi ex compi de lab, intento fallido de minion... Como hemos hecho el tonto en el lab y como nos hemos reído. Jamás olvidaré esa papelera con la cara de Chucky. ¿Crees que alguien se la habrá llevado a su casa? Hay gente con gustos siniestros, así que ¡para gustos los colores! Me alegro de haber podido sacar un buen amigo del lab. Me da penita que estés en Valencia pero sé que es lo mejor para ti, así que ¡dale duro a la tesis campeón! Ya estoy deseando que vuelvas y ya sabes, cada vez que vuelvas a Barna hay plan, yo siempre tengo un plan. Es lo que tiene ser un culo inquieto. ¡Un abrazo amigo y nos vemos en tu próxima visita!

A la persona que está detrás de la revista Autiblog (me abstengo de poner nombre y pronombres por respeto a su decisión de anonimato). Me alegro muchísimo de habernos conocido en persona y sobre todo de saber que tengo a otra persona a la cual puedo añadir a mi círculo de amistades. Ya sabes que me encanta la visibilidad que das al autismo y te doy las gracias por permitirme formar parte de dicha visibilidad. Muchísimas gracias por estar presente en mi vida y ya sabes que tienes casa en Terrassa siempre que lo necesites.

A Guti, Vanesa y a su pequeña Celia. Que gran suerte haberos conocido, sois una de esas parejas mejor avenidas que conozco y que están criando a una hija con unos muy buenos valores y rodeada de cariño y amor, como siempre debería ser. Que sepáis que nos encanta ir a vuestra casa, ir con la peque al parque, bailar el remix de la vaca Lola durante mínimo 1 hora... Habéis despertado nuestro instinto maternal, ¿no tenía suficiente ya con dos cobayas que dan más guerra que 3 críos juntos? Bueno, tendrán a sus tíos Guti y Vanesa, y a su prima Celia. Celia, cuando crezcas te haré leer este párrafo en el cual a tus 3 añitos preguntabas si había escuelas para ratitas para que así nuestras cobayas, Rocky y Cloud (según tú las ratitas), pudiesen ir al colegio también. ¡Gracias por formar parte de nuestras vidas!

A los amigos y familia de mi pareja que me han acogido como a una más: Luis, Míriam, Sílvia, Manu, mi cuñado Ricky y a su compañero gatuno Simón que posiblemente quiera zamparse a nuestras cobayas, Camila...y a toda la peña de Euskadi que me tratasteis como a una más del grupo. Que suerte tiene mi mujer de tener estas dos familias tan maravillosas, la de sangre y la que ella ha escogido.

A mi fisio Sergio, el guaperas que las tiene a todas locas por él y que colecciona los colorines de la parte de arriba de las agujas con las que pincha a sus pacientes. Merezco estar en agradecimientos de dicho bote ya que por lo menos me habrás pinchado 30 veces la mandíbula y las que me quedan aún... Gracias por hacerme pasar tan buenos ratos en tu consulta, cotilleos varios, historias varias de tus ex, la nueva churri que en 2 meses ya se ha tatuado la S de Sergio. ¿Sergio, que les haces a las mujeres para que se vuelvan locas por ti? ¿Me cuentas el secreto? Entre paciente y fisio, esto me interesa. Estoy comprometida pero si algún día la cosa no fuese bien, agradecería saber el truco jaja. Bueno Sergio, nos hemos conocido porque tengo una mandíbula que está para que me la cambien por otra pero al menos he sacado algo bueno de todo esto. Te vas a librar de mí unos meses cuando me pinchen toxina botulínica pero tranquilo, en unos meses vuelvo a estar por ahí. ¡Que siga la misma churri por favor, me voy a volver loca con tanto nombre!

A Antonio, mi profesor de Hapkido. Ciertamente Antonio, como tú bien decías, tenía mucho miedo. Miedo a las caídas de Hapkido, miedo a tirarme al suelo, miedo a hacerme daño.... Hasta que un día estuvimos hablando y ahí reaccioné. Una tía que hoy en día está musculada, se

pasa horas en la sala de máquinas, hace artes marciales... ¿Miedo a qué? ¿A un pasado marcado por alguien que no merece la pena? Ahora he pasado a ser lo que tú decías “las tías que hacen artes marciales tiene muy mala hostia cuando pelean”. ¡Que le peten a las caídas! En Hapkido te tiras al suelo, te tiran...pero sobre todo te lo pasas bien. Gracias a ti, ahora ya no tengo miedo ni del pasado ni de todo lo que me pueda pasar en Hapkido (suerte que sabes recolocar hombros, espero no ser la siguiente a la que le suceda algo así). ¡Gracias de todo corazón Antonio!

Y ya por último queda dar las gracias a mi familia.

A Miren, mi preciosa mujer. Sí, mi prometida es mi familia, de hecho es la persona más importante de mi familia. Recuerdo el primer día que te vi y me dije “¿dónde estaba metida esta chica de los ojazos verdes durante todo este tiempo?”. No sé si fue amor a primera vista, solo sé que me impacté de ti y que desde que empezamos a hablar ya no nos separamos. Vamos que poco más y pierdes el último tren, ¡vaya si nos gustamos! Y desde aquel día aquí estamos 3 años después, pensando en ser madres y en la boda que hemos tenido que posponer por causas externas. A partir de aquí, sé que quien lea esto posiblemente no entenderá nada pero lo que realmente importa es que todas y cada una de las personas nombradas más arriba y mi mujer, sí conocen la historia. Miren, no solo me enamoré de ti, sino que también me salvaste la vida. Que duro es tener que fugarte de tu propia casa, hay días en los que no sabía si iba a volver a ver la luz del nuevo amanecer. En situaciones tan extremas, el miedo se apodera de ti y ya no sabes cuál es la respuesta correcta que te permitirá seguir un día más. Por suerte, tú estabas ahí y no tuviste miedo, lograste sacarme de esa casa. Así que aquí estamos, juntas, felices y con ganas de formar nuestra propia familia. ¡Te quiero 3,1 Miren!

A mis cobayas, Cloud y Rocky. Sí, mis animales son parte de mi familia y esta es mi tesis. Ha habido momentos muy duros durante esta tesis, sobre todo cuando cambias radicalmente tu vida de un día para otro. Ellos han hecho que los momentos más duros se conviertan en los más tiernos. Así que merecen salir en los agradecimientos de esta tesis.

A mi tía Susana, mis primas Hellen y Jessabell, mis sobrinas Xiomara, Domenica, Juliet y mi sobrino Esteban. Gracias por estar presentes en mi vida aunque ahora mismo sea en la distancia. Sé que perdisteis a una hermana, una tía, una tía abuela...pero como ya sabéis cada cual debe ser responsable de sus propios actos y los hijos no siempre se parecen a sus progenitores. Así que bueno, ahora tenéis a una sobrina, una prima y una tía. Sois uno de los pilares más importantes de mi vida y os quiero muchísimo, no os podéis ni imaginar las ganas que tengo de abrazaros. Sois posiblemente lo único bueno, pero que muy bueno, que me ha dejado esa mujer y jamás podría dejar de quererlos tanto. ¡Os quiero familia!

A mi padre, el hombre más importante de toda mi vida a fecha de hoy. Te debo mis estudios, mi educación, momentos de felicidad, y sobre todo el saber lo que significa querer...Te debo tantísimas cosas pero se nos acabó el tiempo hace ya unos años. Se nos acabó el tiempo aunque esa no era tu hora. ¿Qué triste verdad, papi? No supimos pedir ayuda pero que sepas que tu hija se fue lejos de esa casa y aquí sigue, dando guerra. Papi, te faltaron muchas cosas por vivir pero haré que tus futuros nietos sepan quien fuiste y vamos a dejarlo en que yo solo he tenido padre. Te quiero y estés donde estés, espero que te sientas orgulloso de mí. Nos vemos en unos años, tenemos muchas cosas que contarnos. Te quiero.

A mis abuelos paternos y a mi abuela materna. Gràcies padrí i iaia per haver-me cuida't de petita quan el meu pare estava sobrepassat amb la feina i necessitava ajuda. Gràcies per haver vingut a Àvila amb nosaltres i per estimar-me tant. Padrí sento molt que ja no hi siguis però vas ser com un segon pare per mi. Iaia lamento el temps que ens van robar i el que et van fer passar. Tan de bo pogués tornar enrere, suposo de que vegades la vida és molt injusta, ho sento iaia. Espero que quan ens tornem a veure ho puguem parlar i recuperar el temps perdut. A mi abuela materna, abuelita, sé que nos permitieron tener el tiempo justo de conocernos y que no recibiste el cariño que merecías por parte de tu hija, fue muy injusto pero nadie tiene la culpa de los hijos que le tocan. Abuelita, fuiste una buena madre así que nada de lo que haya podido suceder a posterior ha sido culpa tuya. ¿Sabes qué abuelita? Todavía recuerdo aquel cumpleaños en Los Angeles y los regalos que me hiciste, eras increíble y solo con recordar aquel día todavía sonrío. ¡Ojalá poder abrazarte de nuevo!

A la meva cosina Mariona. Gràcies per haver-me escoltat, per haver-me cregut i per ser la meva cosina. Al cap i a la fi hi ha moltes víctimes i un sola culpable. Que bé poder recuperar tot el temps perdut.

Y finalmente, **a mí misma**. He tenido apoyo de amigos, familia, pareja, soporte profesional (María y Elisabet, gracias) pero el **trabajo para salir adelante y superar cualquier bache es tuyo y solamente tuyo**. Nadie entiende como pude redactar parte de la tesis en la casa de los horrores (redactar la tesis era lo más relajante de esa casa), los ovarios tan grandes que hay que tener para hacer una tesis doctoral cuando no sabes si te van a intentar clavar algo hoy o no, el valor para fugarte con todo lo que puedas de la que fue tu casa y seguir escribiendo la tesis, artículos... no lo voy a negar, al principio cuesta levantarse pero yo soy de aquellas que siempre que se cae, encuentra la forma de levantarse. Así que me merezco dedicarme esta tesis doctoral a mí misma y está claro que ni alguien que vive en plena locura ni una tesis doctoral son suficientes para frenarme. **I am invincible!**

¡GRACIAS A TODES POR HABER HECHO POSIBLE MI TESIS!

Las cicatrices del pasado marcan de dónde vienes pero no hacia dónde vas.

I am invincible!

A mi mujer Miren

A mi padre, que en paz descansa

Y a mí misma

II. ABSTRACT

Demyelinating disorders such as multiple sclerosis (MS) are characterized by myelin destruction and impaired remyelination due to a failure in oligodendrocyte progenitor cells (OPCs) differentiation to mature oligodendrocytes. This thesis aims to expand the knowledge about the microglia-OPCs crosstalk in (re)myelination and demyelination. Several studies support that microglia is necessary for OPCs differentiation, besides, previous interactomic studies from our lab studies found that Transient Receptor Potential Vanilloid 2 (TRPV2), which is expressed in the central nervous system (CNS), OPCs and glial cells, interact with key myelin proteins, suggesting a possible function of TRPV2 in myelination.

First, in a single-protein-focused study, we have compiled information about TRPV2 trafficking to the membrane as a tool to understand the function and regulation of the channel towards the plasma membrane, followed by the validation of TRPV2 interaction with the important key myelin proteins. Then, we analyzed the effect on TRPV2 expression of pro- and anti-inflammatory environments, but also in experimental mice models such as jimpy mutant mice, cuprizone, experimental autoimmune encephalomyelitis (EAE), and in human MS samples. These results observed that TRPV2 expression is altered in these animal models and MS human samples, and also that trafficking and subsequent activation is found in microglia and OPCs in pro-inflammatory environments.

Second, we performed a transcriptomic data analysis of microarray studies performed in cuprizone-treated mice to infer the ligand-receptor and the ligand-target pairs regarding microglia-OPCs crosstalk. This last part of the work led us to the discovery of new microglia/OPCs biomarkers with relevant in the pathophysiology of de-/re-myelination, also providing an omics tool which could be used to analyze the cross-talk of any pair of cell types with transcriptomic data available.

II. RESUMEN

Los trastornos desmielinizantes como la esclerosis múltiple (EM) se caracterizan por la destrucción de la mielina y el deterioro de la remielinización debido a fallos en la diferenciación de las células progenitoras de oligodendrocitos (OPCs) a oligodendrocitos maduros. Esta tesis tiene como objetivo ampliar el conocimiento sobre la comunicación microglia-OPCs en (re)mielinización y desmielinización. Varios estudios respaldan que la microglía es necesaria para la diferenciación de las OPC, además, estudios interactómicos previos de nuestro laboratorio encontraron que el Receptor de Potencial Transitorio Vanilloide 2 (TRPV2), que se expresa en el sistema nervioso central (SNC), las OPC y las células gliales, interactúa con proteínas clave de la mielina, lo que sugiere una posible función de TRPV2 en la mielinización.

En primer lugar, en un estudio centrado en una sola proteína, recopilamos información sobre el tráfico de TRPV2 a la membrana como una herramienta para comprender la función y la regulación del canal hacia la membrana plasmática, seguido de la validación de la interacción de TRPV2 con proteínas clave de la mielina. Luego, analizamos el efecto sobre la expresión de TRPV2 de entornos proinflamatorios y antiinflamatorios, pero también en modelos de ratones experimentales como ratones mutantes jimpy, cuprizona, encefalomiелitis autoinmune experimental (EAE) y en muestras de EM humana. Estos resultados observaron que la expresión de TRPV2 está alterada en estos modelos animales y muestras humanas de EM, y también que el tráfico y la activación posterior se encuentran en microglía y OPCs en entornos proinflamatorios.

En segundo lugar, realizamos un análisis de datos transcriptómicos de estudios de microarrays realizados en ratones tratados con cuprizona para inferir los pares ligando-receptor y ligando-diana con respecto a la comunicación microglía-OPCs. Esta última parte del trabajo nos lleva al descubrimiento de nuevos biomarcadores de microglía/OPC con relevancia en la fisiopatología de la desmielinización/remielinización, y también proporciona una herramienta ómica que podría usarse para analizar la comunicación de cualquier par de células, con datos transcriptómicos disponibles.

II. RESUM

Els trastorns desmielinitzants com l'esclerosi múltiple (EM) es caracteritzen per la destrucció de la mielina i el deteriorament de la remielinització a causa de fallades en la diferenciació de les cèl·lules progenitores d'oligodendròcits (OPCs) a oligodendrocits madurs. Aquesta tesi té com a objectiu ampliar el coneixement sobre la comunicació microglia-OPCs en (re)mielinització i desmielinització. Diversos estudis donen suport a que la microglia és necessària per a la diferenciació de les OPCs, a més, estudis interactòmics previs del nostre laboratori van trobar que el Receptor de Potencial Transitori Vanilloide 2 (TRPV2), que s'expressa al sistema nerviós central (SNC), les OPCs i les cèl·lules glials, interactua amb proteïnes clau de la mielina, cosa que suggereix una possible funció de TRPV2 en la mielinització.

En primer lloc, en un estudi centrat en una sola proteïna, recopilem informació sobre el trànsit de TRPV2 a la membrana com una eina per comprendre la funció i la regulació del canal cap a la membrana plasmàtica, seguit de la validació de la interacció de TRPV2 amb proteïnes clau de la mielina. Després, analitzem l'efecte sobre l'expressió de TRPV2 d'entorns proinflamatoris i antiinflamatoris, però també en models de ratolins experimentals com ara ratolins mutants jimpy, cuprizona, encefalomiелitis autoimmune experimental (EAE) i en mostres d'EM humana. Aquests resultats van observar que l'expressió de TRPV2 està alterada en aquests models

animals i mostres humanes d'EM, i també que el trànsit i l'activació posterior es troben en microglia i OPCs en entorns proinflamatoris.

En segon lloc, realitzem una anàlisi de dades transcriptòmiques d'estudis de microarrays realitzats en ratolins tractats amb cuprizona per inferir els parells lligant-receptor i lligant-diana respecte a la comunicació microglia-OPCs. Aquesta darrera part del treball ens porta al descobriment de nous biomarcadors de microglia/OPC amb rellevància en la fisiopatologia de la desmielinització/remielinització, i també proporciona una eina òmica que es podria fer servir per analitzar la comunicació de qualsevol parell de cèl·lules, amb dades transcriptòmiques disponibles.

III. ABBREVIATIONS

CNS	Central nervous system
PNS	Peripheral nervous system
OPCs	Oligodendrocyte progenitor cells
IL	Interleukin
IFN	Interferon
EAE	Experimental autoimmune encephalomyelitis
MBP	Myelin basic protein
PLP	Proteolipid protein
PDGF	Platelet-derived growth factor
MS	Multiple sclerosis
BDNF	Brain-derived neurotrophic factor
LPS	Lipopolysaccharide
NO	Nitric oxide
MD	Myelinating disorders
PMD	Palizaues-Merzbacher Disease
WM	Whitematter
SPG2	Spastic paraplegia type 2
RRMS	Relapsing-remitting multiple sclerosis
PPMS	Primary-progressive multiple sclerosis
SPMS	Secondary-progressive multiple sclerosis
PRMS	Progressive-relapsing multiple sclerosis
BBB	Blood-brain barrier
GM	Grey matter
MOG	Myelin oligodendrocyte glycoprotein
MAG	Myelin associated glycoprotein
Th	T-helper
CC	Corpus callosum
TRP	Transient Receptor Potential
TRPA	Transient Receptor Potential Ankyrin
TRPC	Transient Receptor Potential Canonical
TRPM	Transient Receptor Potential Melastin
TRPV	Transient Receptor Potential Vanilloid
TRPML	Transient Receptor Potential Mucolipin
TRPP	Transient Receptor Potential Polycystic

TRPV2	Transient Receptor Potential Vanilloid 2
GBM	Glioblastoma multiforme
AD	Alzheimer's disease
PD	Parkinson's disease
VRL-1	Vanilloid-receptor-like protein 1
NTM	Neurotrimin
CSF	Cerebrospinal fluid
PBMCs	peripheral blood mononuclear cells
DEGs	Differentially expressed genes
ARD	Ankyrin repeat domain
MET	Methionine
ROS	Reactive oxygen species
Met-SO	Methionine-S-sulfoxide
Met-RO	Methionine-R-sulfoxide
PPIs	Protein-protein interactions
DRG	Dorsal root ganglion

TABLE OF CONTENTS

I. Acknowledgments	3
II. Abstract	13
III. Abbreviations	16
IV. List of figures	20
V. List of tables	21
Introduction	22
1. Transient Receptor Potential (TRP) Channels in the nervous system	22
2. TRPV2 involvement in CNS and related disorders	24
3. Understanding myelin	27
3.1 Microglia, astrocytes and oligodendrocytes crosstalk for CNS (re)myelination	28
4. Recapitulation hypothesis of the CNS	30
5. Myelinating disorders of the CNS	31
5.1 Pelizaeus-Merzbacher Disease and the jimpy mice model	32
5.2 Multiple sclerosis and experimental mice models	35
5.2.1 The Experimental autoimmune encephalomyelitis mice model	39
5.2.2 The Cuprizone de-/remyelinating mice model	40
6. Interactomics, biomarkers and OMICS data analysis	41
7. Biomarkers in demyelinating disorders	42
Hypothesis and objectives	45
Results	46
Chapter I. Trafficking of Stretch-Regulated TRPV2 and TRPV4 Channels Inferred Through Interactomics	47
1. Introduction	48
2. Sequence and Structure Determinants in Channel Trafficking	51
3. Interactomics	52
4. Understanding Channel Trafficking through Protein–Protein Interactions	52
5. Concluding remarks	55
6. References	56
7. Supplementary information	61
Chapter II. TRPV2: A Key Player in Myelination Disorders of the Central Nervous System	66
1. Introduction	67
2. Results	68
3. Discussion	77
4. Material and Methods	80
5. Conclusions	86
6. References	88
7. Supplementary information	91
Chapter III. Deciphering the genetic crosstalk between microglia and	

oligodendrocyte precursor cells during demyelination and remyelination using transcriptomic data	93
1. Introduction	95
2. Material and methods	96
3. Results	99
4. Discussion	103
5. Conclusion	106
6. References	106
7. Supplementary information	109
General discussion	169
1. Protein-protein interactions of TRPV2 and TRPV4 are related to CNS biological processes and protein trafficking	170
2. NO is responsible of TRPV2 activation in glial cells by TRPV2 translocation to the membrane	171
3. TRPV2 interaction with important key myelin proteins	172
4. TRPV2 involvement in CNS myelin related disorders	173
4.1 TRPV2 expression in jimpy mutant mice	173
4.2 TRPV2 in cuprizone mouse model of MS	174
4.3 TRPV2 in EAE mouse model of MS	175
4.4 How MSRA affects on TRPV2 expression in MS mouse models?	176
4.5 TRPV2 and MSRA expression in MS human brains	177
4.6 TRPV2 points out oligodendrocytes-microglia cross-talk to achieve (re)myelination	178
5. The importance of microglia and OPCs crosstalk during (re)myelination and demyelination	179
Conclusions	190
Bibliography	193

IV. LIST OF FIGURES

Figure 1. TRP superfamily	23
Figure 2. A myelinated neuron along its axon	27
Figure 3. Different stages of oligodendrocytes maturation; from OPCs to mature myelin forming oligodendrocytes	28
Figure 3. PMD classification	34
Figure 4. Main clinical symptoms in MS	36
Figure 5. Time course of de- and remyelination in acute cuprizone model	41

V. LIST OF TABLES

Table 1. Main characteristics of existing <i>in vivo</i> models to study multiple sclerosis	38
Table 2. Types of biomarkers and their relevance in MS	43
Table 3. Comparison of the 10 most DEGs found in CC during early and late demyelination, and remyelination in cuprizone model	180
Table 4. Associated functions of the differentially expressed OPC receptors	188

INTRODUCTION

1. Transient Receptor Potential (TRP) Channels in the nervous system

TRP ion channels superfamily was discovered in a mutant strain of *Drosophila melanogaster* by Cosens and Manning in 1969 (Cosens and Manning, 1969). This TRP superfamily comprises a group of non-selective cation channels that act as polymodal cellular sensors, acting in response to a wide spectrum of chemical and physical stimuli (Zheng, 2013). In humans, TRP superfamily comprises 27 TRP channels that are classified in function of their sequence homology (**Figure 6A**). Also, this superfamily is divided into six subfamilies based on founding members; TRPA (ankyrin), TRPC (canonical), TRPM (melastatin), TRPV (vanilloid), TRPML (mucolipin) and TRPP (polycystic) (**Figure 1A**) (Clapham et al., 2003; Perálvarez-Marín et al., 2013). The current existing TRPs repertoire came from gene duplications from Choanoflagellates, the common ancestor of teleost fishes and terrestrial vertebrates (Saito et al., 2011). TRPs structure consist of six-segment (S1-S6) transmembrane domains, with a pore forming between S5 and S6, and have two cytosolic domains N- and C-terminal (**Figure 1B**) (Wang et al., 2020).

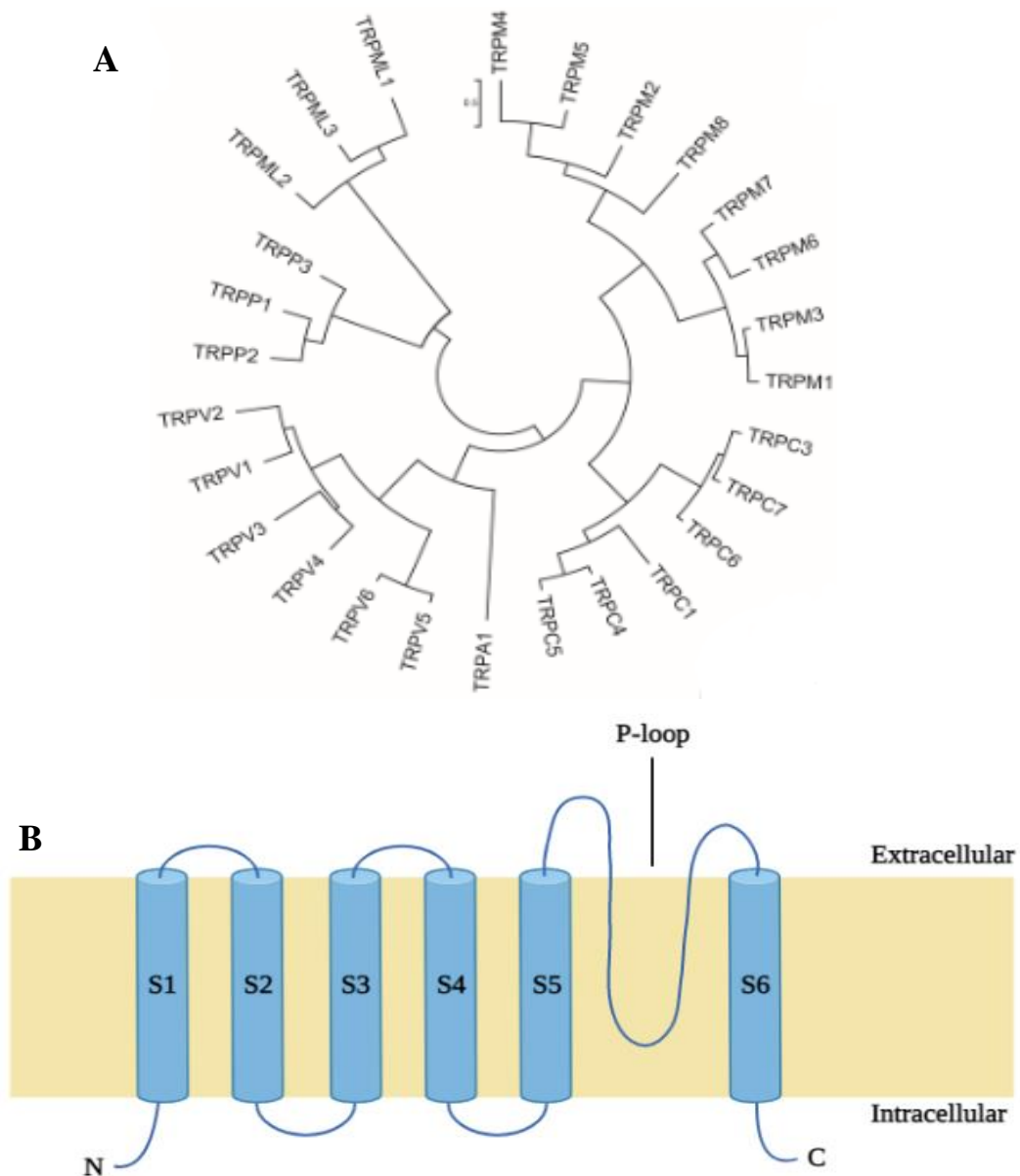


Figure 1. TRP superfamily. (A) Phylogenetic relationships of the human TRP superfamily, showing 27 TRPs classified by their sequence homology. (B) Illustration of TRPs protein structure. The illustration shows six-transmembrane segments, the six transmembrane domains (S1-S6) forming a pore loop (P-loop) between S5-S6 and the intracellular N- and C-termini.

TRPs have been related to a variety of physiological processes in the brain and also with pathologies of the nervous system (Wang et al., 2020). TRPs are widely expressed in the central nervous system (CNS) at different brain regions, neurons and also in glial cells (astrocytes, microglia and ependymal cells) (Vennekens et al., 2012; Verkhratsky et al., 2014; Wang et al., 2020). Some of these TRPs, such as TRPM3 (Hoffmann et al., 2010), TRPV1 (Gonzalez-Reyes et al., 2013) and TRPCs (Paez et al., 2011) have also been reported in oligodendrocytes. Regarding the physiological roles of TRPs in the nervous system, several of them have been related with important functions of the nervous system. TRPC4 and TRPC5 have been reported involved in the neuronal growth cone morphology that is necessary for correct brain

development (Greka et al., 2003; Jeon et al., 2013). TRPC6 is involved in synaptic and behavioral plasticity (Zhou et al., 2008). In general, TRPCs play an important role in modulating neurite outgrowth, axon guidance and nerve regeneration (Kumar et al., 2012). TRPV1 detects noxious stimuli in the peripheral nervous system (PNS) (Caterina and Julius, 2001). TRPV2 is widely expressed through the nervous system and it is involved into the nervous system physiology, however, its role is widely discussed on the next sections. TRPM2 has been described as associated to hippocampal synaptic plasticity oxidative stress induced by glutathione leading to neuronal cell death, neuronal development and synaptic plasticity (Vennekens et al., 2012; Wang et al., 2020). TRPM7 is linked to physiological conditions, plays a role on synaptic transmission and cognitive functions (Abumaria et al., 2019) and is also necessary for CNS development (Abumaria et al., 2019). TRPMLs has been reported associated with different functions, being the maintenance of neuronal development one of them (Morelli et al., 2019). As observed, TRPs play an important role in normal physiological conditions of the nervous system but also in pathological conditions. TRPM2 has been described as related to ischemic stroke, providing TRPM2 agonists protection to ischemic strokes (Alim et al., 2013; Shimizu et al., 2016). Other studies also found an association between TRPM2 and the risk of suffering bipolar disorder (Xu et al., 2009, 2006). TRPC1 has been associated with the progression of different types of cancer, including glioblastoma multiforme (GBM) (Bomben and Sontheimer, 2010; Cuddapah et al., 2013; Elzamzamy et al., 2020). And other TRPCs such as TRCP3, TRPC5 and TRPC6 has been found involved in cellular abnormalities in GBM (Bomben and Sontheimer, 2008). TRPC3 is also linked to hypertension and hypoxic conditions in human cerebral vascular tissue (Thilo et al., 2011). TRPM2 is involved in neuronal toxicity and memory impairment in Alzheimer's disease (AD) (Lee et al., 2021; Wang et al., 2020). TRPA1 lack hinders AD progression (Bosson et al., 2017). TRPC6 inhibition results in protection of brain damage against cerebral ischemia (Du et al., 2010).

2. TRPVs involvement in CNS and related disorders

TRPV subfamily in mammals comprises six members that are divided in two groups, TRPV1-4 and TRPV5-6, in accordance to their sequence homology and cation selectivity. TRPV1-4 channels share a global sequence identity of 20% and are non-selective low calcium permeable channels. TRPV5-6 channels share a global sequence identity of 75% and display a high selectivity for calcium (Montell, 2005; Perálvarez-Marín et al., 2013). TRPVs have also been associated to important functions of the CNS but also with CNS diseases. TRPV1 expression in the CNS has been described in hippocampus, cortex, cerebellum, olfactory bulb, mesencephalon, hindbrain and spinal cord (Ho et al., 2012; Tóth et al., 2005). At cellular level, TRPV1 expression has been found in astrocytes (Doly et al., 2004), microglia (Sappington and

Calkins, 2008) and different types of neurons (El Andaloussi-Lilja et al., 2009; Goswami et al., 2010; Puntambekar et al., 2005; Tóth et al., 2005). To date, it is known that TRPV1 expression changes influences on addictive behavior, anxiety and depression. Also, TRPV1 mediates glial and neuronal functions, and has been related to Parkinson's disease (PD) (Ho et al., 2012). TRPV3 expression in the CNS has been detected in brain and spinal cord (Xu et al., 2002). Studies in rat cerebellum demonstrated that TRPV3 plays an important role on motor coordination (Singh et al., 2020). TRPV5 has been reported in neurons, astrocytes and in important brain regions such as olfactory bulb, cortex, hypothalamus, hippocampus, midbrain, brainstem and cerebellum (S. Kumar et al., 2017). TRPV5 function has been related to neuroendocrine modulation (S. Kumar et al., 2017). TRPV6 in the CNS expression has been widely observed in brain, suggesting a plausible involvement in CNS physiology (Santosh Kumar et al., 2017).

TRPV2 is the most unknown member of the TRPV subfamily and was firstly named as vanilloid-receptor-like protein 1 (VRL-1) due to the 50% of sequence homology with TRPV1 that is the most characterized member of this subfamily (Perálvarez-Marín et al., 2013). TRPV2 is a temperature dependent ion channel as TRPV1 and TRPV3, being activated by noxious heat (>52 °C) (Caterina et al., 1999; Perálvarez-Marín et al., 2013). TRPV2 can be also activated by mechanical stimuli, chemical compounds (Perálvarez-Marín et al., 2013) and oxidative stress (Fricke et al., 2019). Interestingly, TRPV2 activation and subsequent function has been related to TRPV2 trafficking to the membrane (Perálvarez-Marín et al., 2013), Regarding TRPV2 pharmacology, although there is some information, it is still limited. Some of these drugs and compounds are not specific for TRPV2 and are also specie-dependent (Perálvarez-Marín et al., 2013). The compounds with higher affinity to TRPV2 are probenecid and tranilast, acting as agonist and antagonist, respectively (Perálvarez-Marín et al., 2013). Some recent studies of Hainz *et al.* (Hainz et al., 2017b, 2017a, 2016) demonstrated that the very specific activator of TRPV2, probenecid, in two multiple sclerosis (MS) models is capable to prevent and arrest the clinical progression in experimental autoimmune encephalomyelitis (EAE) mice and diminish demyelination in cuprizone model. TRPV2 is ubiquitously distributed through the human body but is also widely expressed through the PNS and CNS body (Kojima and Nagasawa, 2014; Perálvarez-Marín et al., 2013). In the CNS, TRPV2 has been described in medium-to-large neurons bearing myelinated fibers (Caterina et al., 1999), microglia (Maksoud et al., 2019), astrocytes (Shibasaki et al., 2013) and oligodendrocyte progenitor cells (OPCs) (Cahoy et al., 2008) but not in oligodendrocytes. Therefore, to our knowledge this is the first time that TRPV2 expression is found in oligodendrocytes (further discussed). In mammals CNS tissues, TRPV2 expression has also been detected in important brain regions as for example the forebrain and hindbrain regions (Nedungadi et al., 2012) and the cerebral cortex (Liapi and Wood, 2005) in

rats, the mature forebrain in mice (Cahoy et al., 2008) and the hypothalamo-neurohypophysial system in macaques (Wainwright et al., 2004). Among all these regions, TRPV2 has been highly expressed in neurons of mouse forebrain regions (Cahoy et al., 2008). The function of TRPV2 is unknown but in the CNS it is necessary for the axon and neurite outgrowth of motor and sensory neurons (Cohen et al., 2015; Shibasaki et al., 2010) and also, in microglia and macrophages has been linked to phagocytosis of cellular debris (Link et al., 2010). Previous results in our laboratory (Pau Doñate-Macián et al., 2018) showed that TRPV2 interacts with important key myelin proteins such as proteolipid protein 1 (PLP1), Opalin, Neurotrimin (NTM) and also with other important proteins (i.e. ABR, FGF1, KCNJ10, PEBP1, PLP1 and SCD3) that are related to neoplasms and neurological conditions of the CNS (Santoni and Amantini, 2019). TRPV2 involvement has been described in GBM, acting as a negative regulator of glioma cell survival and proliferation (Nabissi et al., 2010). TRPV2 activation by cannabidiol agonist results in increased chemosensitivity and subsequent death of human glioma cell lines (Nabissi et al., 2013). All these evidences confirm a TRPV2 involvement in CNS physiology and neurological conditions, and also suggest a TRPV2 role in CNS myelin and related disorders.

TRPV4 is also widely expressed through human body as TRPV2, including in the CNS. TRPV4 ion channel has been detected in microglia, astrocytes, neurons and oligodendrocytes (Feng et al., 2020) and has been linked to neuronal toxicity observed in AD (Bai and Lipski, 2014), astrogliosis (Butenko et al., 2012) and neuronal excitability (Shibasaki et al., 2015, 2007). Previous studies have demonstrated the involvement of TRPV4 in cerebral ischemia (Butenko et al., 2012) and epilepsy (Chen et al., 2016). Studies in cuprizone model demonstrated that TRPV4 activation in microglia is related to oligodendrocytes apoptosis leading to CNS demyelination, however, TRPV4 inhibition results in improved myelination and diminished inflammation and glial reactivity (Liu et al., 2018). In addition, mutations in TRPV4 have been linked to some nervous system pathologies such as Charcot–Marie–Tooth disease type 2C, spinal muscular atrophy and hereditary motor and sensory neuropathy type 2 (Velilla et al., 2019; Verma et al., 2010). As happens with TRPV2, TRPV4 is also trafficked to the membrane and requires its translocation to the plasma membrane to be functional (Cao et al., 2018), mutations on TRPV4 also affects on its trafficking and then to its activity (Doñate-Macián et al., 2019). For that reason in our laboratory was performed a wet lab omics approach to identify functions and signaling pathways in which TRPV4 is involved (P. Doñate-Macián et al., 2018).

The lack of information about the function of TRPV2 and TRPV4, the knowledge that both of them are related to nervous system and that its activation is linked to membrane trafficking lead

to the importance to further investigate the TRPV2 and TRPV4 trafficking to plasma membrane.

3. Understanding myelin

Myelin is a modified plasma membrane that wraps nerve axons to allow the correct transmission of electrical impulses and protect nerves. This plasma membrane is composed by a high proportion of lipids (70-85%) and a low proportion of proteins (15-30%) (Morell and Quarles, 1999). A myelinated axon is composed by: cell body or soma, myelin sheaths, nodes of Ranvier, paranodes, juxtaparanodes and axon terminal (Suminaite et al., 2019) (**Figure 2**).

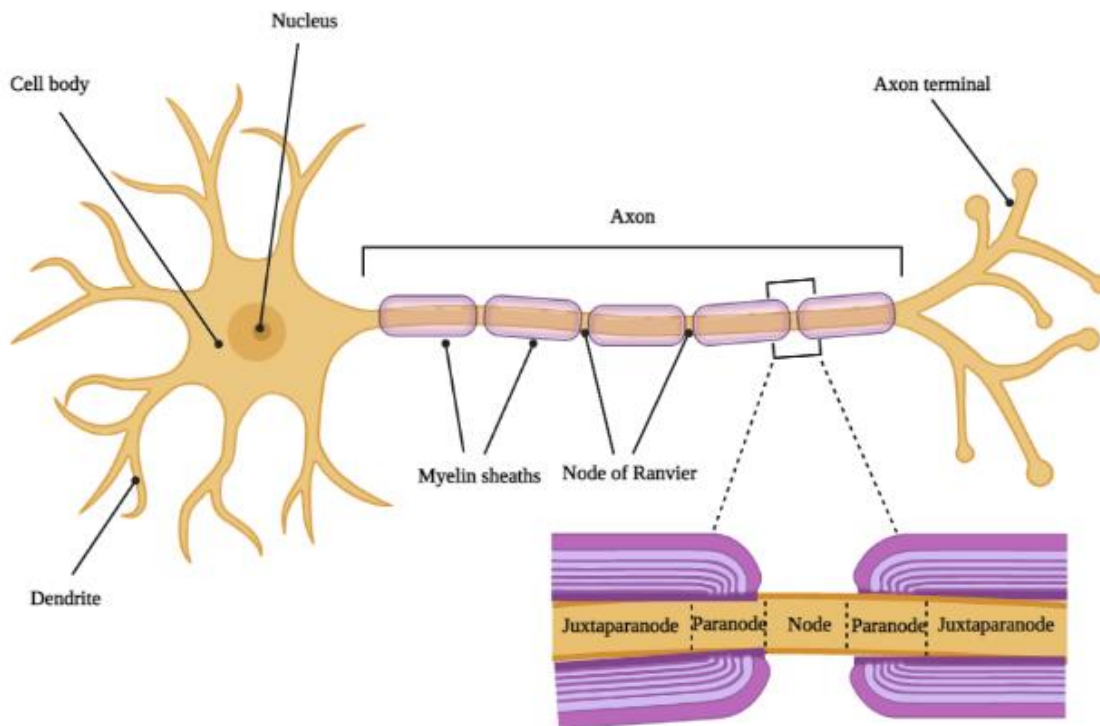


Figure 2. A myelinated neuron along its axon. The different parts of a myelinated axon are shown and in a magnified view it is shown the structure around the node of Ranvier.

Cell body contains the nucleus and other organelles, also the soma is branched into a dendritic tree that is in charge to receive inputs from other cells (Ludwig et al., 2021). Myelin sheaths surround nerve axons in a spiral fashion, acting as an electrical insulator and allow a fast signal conduction in the nervous system (Purves et al., 2001; Suminaite et al., 2019). In myelinated axons, electrical impulses are spread through the myelinated nerve by saltatory conduction, skipping from node to node down until axon terminal that make synaptic contacts with other cells. These connections between neurons and synapses result in the nervous system network. The nervous system is divided into the PNS and CNS, being the CNS composed by brain and spinal cord, and the PNS by the nerves that lie outside of brain and spinal cord. The myelination

of the nervous system is necessary for the correct nervous system functioning. In the CNS, myelin is generated by oligodendrocytes and in the PNS by Schwann cells. Each Schwann cell generates a single myelin sheath around an axon, however, a single oligodendrocyte sheaths multiple axons (Salzer and Zalc, 2016).

3.1 Microglia, astrocytes and oligodendrocytes crosstalk for CNS (re)myelination

In the CNS, the oligodendrocytes capable to generate myelin are mature myelinating oligodendrocytes that came from OPCs. Oligodendrocytes are originated from OPCs that migrate, proliferate, differentiate and mature into these oligodendrocytes capable to form myelin (Domingues et al., 2016) (**Figure 3**).

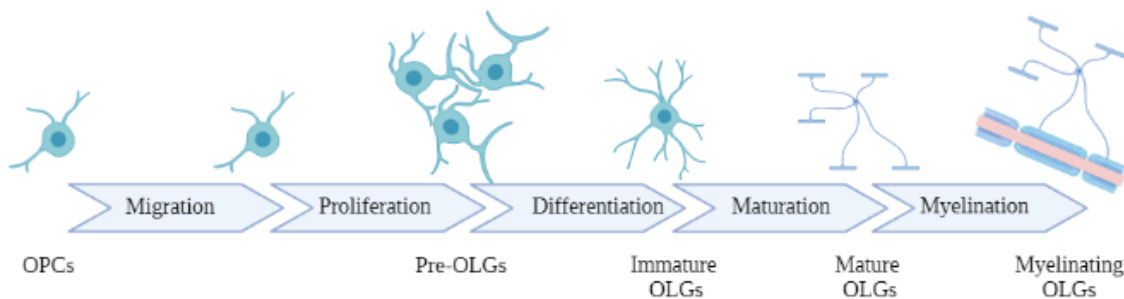


Figure 3. Different stages of oligodendrocytes maturation; from OPCs to mature myelin forming oligodendrocytes. The different stages are characterized by oligodendroglial cells at different stages (OPCs, preoligodendrocytes, immature oligodendrocytes, mature oligodendrocytes and myelin forming oligodendrocytes. Abbreviations: OLGs, oligodendrocytes.

A large number of OPCs are widespread through the CNS and remain undifferentiated, also continue to proliferate during the whole life-span of the individual but declining their capacity of proliferation with age (Bergles and Richardson, 2016). During embryogenesis OPCs arise from neural stem cells in the ventricular neuroepithelium in the neural tube (Hardy and Reynolds, 1993; Levine et al., 1993; Warf et al., 1991), however, in the adulthood arise from the subventricular zone of the forebrain (Menn et al., 2006; Richardson et al., 2006). When CNS myelin is damaged, OPCs proliferation and migration takes place, and get differentiated into oligodendrocytes as an attempt to repair damaged myelin (Fernandez-Castaneda and Gaultier, 2016). The different steps that are necessary to obtain mature oligodendrocytes from OPCs, is an orchestrated process that is possible due to the oligodendrocytes, microglia and astrocyte crosstalk (Domingues et al., 2016). In general terms, microglia are the immune cells of the CNS and are in charge to maintain the homeostasis of the CNS (Yin et al., 2017), phagocytic clearance of cell debris (Neumann et al., 2009), synaptic integrity (Wang et al., 2016), surveillance and injury repair (Evilsizor et al., 2015). Astrocytes are a cell type of the CNS that participates in guidance and synaptic support, control of the blood brain barrier (BBB) and

blood flow (Blackburn et al., 2009), and myelination (Molina-Gonzalez and Miron, 2019). However, both microglia and astrocytes have been associated at different degrees with CNS development processes such as neuronal differentiation, migration, programmed cell death, neurite growth, axon guidance, and synaptic formation (Pang et al., 2000). Microglia has been extensively reported to contribute with myelination, supporting OPCs survival, migration, differentiation and maturation (Kalafatakis and Karagogeos, 2021). During development activated microglia secrete TNF α , interleukin (IL)-1 β , IL-6 and interferon (IFN)- γ that promote oligodendrocytes development (Kalafatakis and Karagogeos, 2021). Microglia expresses the chemokine CXCL1 that favors oligodendrocytes survival in a viral model of demyelination (Hosking et al., 2010), shows neuroprotective effects and reduces severity in the EAE model (Omari et al., 2009). Microglia has also been reported to enhance the expression the important key myelin proteins such as myelin basic protein (MBP) and PLP (Hamilton and Rome, 1994). Other studies revealed that IL-4-activated microglia promotes oligodendrogenesis (Butovsky et al., 2006). OPC survival is related to modulation of platelet-derived growth factor (PDGF)- α receptor and NF- κ B activation by microglia, at the same time NF- κ B activation is also related to OPCs maturation (Nicholas et al., 2001). MS patients during early remyelinating lesions, microglia shows a high expression of the chemokine receptor CCR5, suggesting a role of microglia at the beginning of remyelination (Trebst et al., 2008). Galectin-3 is highly expressed in microglia and supports remyelination onset and oligodendrocytes differentiation (Hoyos et al., 2014; Pasquini et al., 2011).

The involvement of astrocytes in oligodendrocytes has also been extensively reviewed (Nutma et al., 2020). Astrocytes have been related to OPCs proliferation, differentiation and migration. The PDGF secreted by astrocytes results in results in OPCs proliferation and migration but at the same time inhibits premature oligodendrocyte differentiation (Traiffort et al., 2020). Astrocytes also secrete the brain-derived neurotrophic factor (BDNF) that promotes myelination and is also involved in OPCs maturation (Traiffort et al., 2020). Astrocytes promotes OPCs proliferation via Cx47 and via ERK/Id4 activation (Liu et al., 2017), and secrete extracellular vesicles that supports OPCs differentiation (Willis et al., 2020). Astrocytes promote cholesterol production and express ciliary neurotrophic factor both of them supporting remyelination (Molina-Gonzalez and Miron, 2019). Modification of extracellular matrix via astrocytes can also favor oligodendrocytes and subsequent remyelination (Nutma et al., 2020).

Although microglia and astrocytes have beneficial effects for oligodendrocytes, also have detrimental effects on oligodendrocytes. Lipopolysaccharide (LPS)-activated microglia promotes OPCs death and a failure in the MBP key myelin protein production (Pang et al., 2000). In vitro studies show that CD137L-activated microglia promotes oligodendrocytes apoptosis (Yeo et al., 2012). Microglia activation via IFN- γ release cytotoxic factors such as

glutamate, nitric oxide (NO), superoxide, and pro-inflammatory cytokines (Takeuchi et al., 2006). TNF α is a pro-inflammatory cytokine expressed in astrocytes and microglia in inflammatory lesions in the CNS (Klinkert et al., 1997) and has been associated to inhibit OPCs differentiation (Nash et al., 2011). Microglia as previously said, expresses CXCL1, this molecule have beneficial effects on some animal models of demyelination but also diminishes OPCs migration during development (Kalafatakis and Karageos, 2021). Some secreted factors by astrocytes can also inhibit myelination and remyeliantion, such as tenascin C, bone morphogenetic proteins and hyaluronan (Domingues et al., 2016). Reactive astrocytes in demyelinated lesions, express Endothelin-1 that inhibits OPCs differentiation and remyelination via Notch activation (Hammond et al., 2014). Activated astrocytes also secrete TNF- α , IL-1 β , IL-6, BDNF, leukemia inhibitory factor and CCL2 that leads to immune system response but also to OPCs and oligodendrocytes damage (Nutma et al., 2020). Reactive astrocytes secrete the chemokine CXCL10 that inhibits myelination and oligodendrocytes maturation (Nash et al., 2011). Microglia and astrocytes can have beneficial and detrimental roles on the microglia, astrocytes and oligodendrocytes crosstalk. These roles by microglia and astrocytes depend on the situation, activated signaling pathways and course of disease, among others. However, the molecular signals that control these beneficial and detrimental roles still remain unknown. A better understanding of this crosstalk could be very beneficial to achieve a normal CNS development and achieve (re)myelination.

4. Recapitulation hypothesis of the CNS

The recapitulation hypothesis of the CNS was proposed as a first time by Franklin and Hinks in 1999 (Franklin and Hinks, 1999). This recapitulation hypothesis argues that myelination during development and remyelination after pathological events may share pretty much the same program and mechanisms (Franklin and Hinks, 1999). It is known that myelination during development and remyelination share a common objective, consisting in forming myelin sheaths along nerve axons to protect axons and increase nerve conduction (Bhatt et al., 2014). Both developmental myelination and remyelination need the microglia-astrocytes-oligodendrocytes crosstalk, and also, the OPCs key stages of migration, proliferation, differentiation and maturation in myelin forming oligodendrocytes. In general terms, the program that occurs during developmental myelination is re-run during remyelination but facing a different environment with several inhibitory signals. Therefore, the main question consist in how much conserved it is the process of developmental myelination during remyelination. Demyelinating diseases of the CNS are characterized by mainly failures OPCs differentiation and subsequent lack of remyelination. Hence, a comprehension of the mechanisms involved in (re)myelination would be very useful to develop novel regenerative therapies. Although both

developmental myelination and remyelination share a common objective and important similarities, there are also important differences. Some of these observed differences are referred to the thickness of myelin sheaths. After remyelination it has been described that there is an important decrease in myelin sheath thickness that results in a significant increase in the ratio of axons (axon diameter/total fiber diameter). Also remyelinated axons show shorten intermodal length (Duncan et al., 2017). Another important difference is the phagocytic activity of macrophages that is necessary to the removal of myelin debris that are generated during this process of demyelination. These myelin debris contain inhibitory compounds for OPCs differentiation (Fancy et al., 2011). Other studies also found that CNS remyelination can be also mediated by Schwann cells (Dusart et al., 1992; Itoyama et al., 1983; Zawadzka et al., 2010). Different studies performed on zebrafish (Udvardia et al., 2001) and mouse dorsal root ganglion (DRG) neurons (Liu and Snider, 2001) show that different signaling pathways are activated between developmental myelination and remyelination. Although developmental myelination and remyelination share a common objective and similarities, important differences are found. However, in spite of important differences, studies on developmental myelination would be key to unravel new mechanisms that could be also necessary for remyelination and drive to CNS regenerative therapies. Therefore, a better understanding of the extracellular factors, signaling pathways, and signals involved in the glial cells and oligodendrocytes crosstalk during (re)myelination are necessary to achieve CNS regeneration

5. Myelinating disorders of the CNS

Myelinating disorders (MD) of the CNS are characterized by myelin damage or abnormal myelination. These MD can be divided into three types: dysmyelination, hypomyelination and demyelination. Dysmyelination is characterized to abnormal, arrested or delayed myelin (Poser, 1978). Demyelination consists in the destruction or damage of myelin. Hypomyelination is referred to an abnormal low quantity of myelin. The etiology of MD can be very different. Dysmyelinating diseases has been described in metabolic hereditary disorders (Kolodny, 1993; Medina, 1993), hypomyelinating disorders has been associated with mutations (Dorboz et al., 2018; Hengel et al., 2017; Hobson and Garbern, 2012; Nahhas et al., 1993) and demyelinating disorders could be caused by inflammatory processes, viral infections, toxic or chemical, acquired metabolic demyelination and focal compression (Love, 2006). In the case of hypomyelinating disorders some of them could be Pelizaeus-Merzbacher Disease (PMD), recessive hypomyelinating leukodystrophy-3, trichothiodystrophy, cockayne syndrome, among others (Ji et al., 2018). As previously said, the etiology of demyelinating disorders is more varied than in the other MD. Some examples of demyelinating disorders are MS, acute-disseminated encephalomyelitis, neuromyelitis optica, acute haemorrhagic leucoencephalitis,

progressive multifocal leucoencephalopathy and central pontine and extrapontine myelinolysis. However, among all demyelinating disorders, MS is the most common and heterogeneous disease (Love, 2006). In this work we are really interested in the hypomyelinating disorder PMD and the demyelinating disease of MS.

5.1 Pelizaeus-Merzbacher Disease and the jimpy mice model

Leukodystrophies comprise genetic disorders that mainly affect CNS myelin in the white matter (WM) (Perlman and Mar, 2012; van der Knaap et al., 2016). In leukodystrophies the most relevant hallmark is the lost (demyelination) or abnormal deficient myelin (hypomyelination), being some leukodystrophies classified as demyelinating or hypomyelinating leukodystrophies (Vanderver et al., 2015). PMD is the most common X-linked recessive hypomyelinating leukodystrophy, having an incidence between 1.45 and 1.9 per 100,000 live male births (Numata et al., 2014). PMD results from a mutation in the PLP1 gene that is located on chromosome Xq22 (Garbern, 2007; Koeppen and Robitaille, 2002). Friedrich Pelizaeus in 1885 was the first person that identified the neurological impairments at early life that presented 5 male individuals of a family (Pelizaeus, 1885). These individuals showed at early childhood the following symptomatology: nystagmus, spastic quadriparesis, ataxia and cognitive delay. In 1910, Ludwig Merzbacher re-investigated the same family that at this point presented 14 affected individuals and two of them were sisters (Merzbacher, 1910), this study served to define a X-linked basis of pathology transmission. Merzbacher also performed a post-mortem analysis of one brain tissue of one affected male and reported a lack of myelin histochemical staining in the WM (Merzbacher, 1910). In 1928, the brain and spinal cord of one of these affected sisters were examined after long storage (Liebers, 1928), showing an identical pattern of myelin expression in the centrum semiovale as Merzbacher previously observed (Merzbacher, 1910). However, cerebellar WM and brainstem showed some little differences and Liebers's (Liebers, 1928) differently from Merzbacher also analyzed a spinal cord and observed only minor myelin loss. Observations by Pelizaeus (Pelizaeus, 1885) and Merzbacher (Merzbacher, 1910) led to conclude that there must be an important heterogeneity in PMD affected members of the same family (Koeppen and Robitaille, 2002). During the following years, subsequent studies were performed and allowed to amplify the diseases identity of PMD. Seitelberger studied the neurological and neuropathological features and proposed a neuropathological classification system for the disease in 1970 that was latter reconciled with molecular-genetic data on 1995 (Seitelberger, 1995; Seitelberger et al., 1970). The first proposed classification included other forms of leukodystrophies than PMD. Zeman et al. (Zeman et al., 1964) speculated that PMD results from a defect in the PLP1 gene as the PNS remains unaffected. The involvement of PLP1 was supported by the mapping of PLP1 gene to the long arm of the human X chromosome (Willard and Riordan, 1985), confirming a X-linked

recessive inheritance of PMD. In 1989, several subsequent studies confirmed PLP1 gene mutations in PMD affected families (Gencic et al., 1989; Hudson et al., 1989; Trofatter et al., 1989). Currently, it is known that PMD shows phenotypic and genotypic heterogeneity, however, all forms leads to CNS hypomyelination and neurological troubles, and are caused by PLP1 mutations (Osorio and Goldman, 2018). PMD has been associated to duplications, point, missense and null mutations in the PLP1 gene (Inoue, 2019; Osorio and Goldman, 2018). Human PLP1 is a 17 kb gene located on the X-chromosome (Xq21-q22) (Inoue, 2019; Osorio and Goldman, 2018). PLP1 encodes the 276-amino acid PLP1 protein and with its alternate splice encodes the 35-amino acid DM20 protein (Inoue, 2019). PLP1 is an extremely hydrophobic membrane protein composed by four transmembrane domains, two extracellular loops containing two cysteine bridges, one cytosolic loop and cytosolic N- and C- termini (Garbern et al., 1999; Inoue, 2019; Osorio and Goldman, 2018). PLP1 is the major component CNS myelin, comprising around 50% of the total protein content (Eng et al., 1968; Knapp, 1996) and is necessary for the compaction of CNS myelin (Nadon and West, 1998). PLP1 is mainly expressed in oligodendrocytes but also in a subset of neurons from caudal medulla and rarely expressed in GABAergic interneurons (Miller et al., 2009). Some studies demonstrated that PLP1 lacking or reduction results in neurological PLP1-related disorders (Garbern et al., 2002; Lüders et al., 2019). PMD can be classified in three different subtypes according to the neuropathological findings, age of onset and age of death: type I or classic PMD, type II or connatal PMD and type III or transitional PMD (Seitelberger et al., 1970). Spastic paraplegia type 2 (SPG2) is considered an expanded spectrum of PLP1 related disorders (Saugier-Weber and Munnich, 1994). *Cailloux et al.* (Cailloux et al., 2000) classify PMD patients into five forms (from 0 to 4) according to the presented clinical severity, being 0 the most severe form and 4 the mildest form. Connatal PMD corresponds to forms 0 and 1, transitional PMD to forms 1 and 2, and classic PMD to forms 2 and 3. SPG2 corresponds to from 4 (Torii et al., 2014). Classic PMD is the most common type of PMD and initiates before first year of life. These patients present hypotonia, nystagmus and delayed development of motor skills involved in walking. The progression of classic PMD is slow during the first 10 years of life, and then slowly deteriorates until mid-adulthood. Connatal PMD is developed during the neonatal period and is the most aggressive PMD. These children present laryngeal stridor, feeding difficulties, optic atrophy, progressive spasticity leading to contractures that restrict movement, dysarthria, ataxia and extremely hypotonia. These patients normally die during infancy or childhood. Transitional PMD combines clinical features of both classic and connatal PMD (Inoue, 2019; Osorio and Goldman, 2018; Torii et al., 2014). The most common mutations in PMD are PLP1 duplications (60–70%) followed by the missense point mutations (15–20%), insertions and deletions (Torii et al., 2014). Point mutations are found in the whole spectrum of PMD and SPG2, being more present in connatal and transitional PMD (Inoue, 2019; Torii et al., 2014).

Point mutations in conserved residues results in the severe phenotypes of PMD, however, point mutations in less conserved regions leads to milder PMD phenotypes (Inoue, 2019). Duplications are mainly found in form 2 of Cailloux classification (Cailloux et al., 2000) but also in forms 1 and 3 (Inoue, 2019; Torii et al., 2014). Null mutations that include deletions and nonsense mutations results on the mild end of the spectrum that corresponds to classic PMD and SPG2 (Inoue, 2019; Torii et al., 2014) (**Figure 4**).

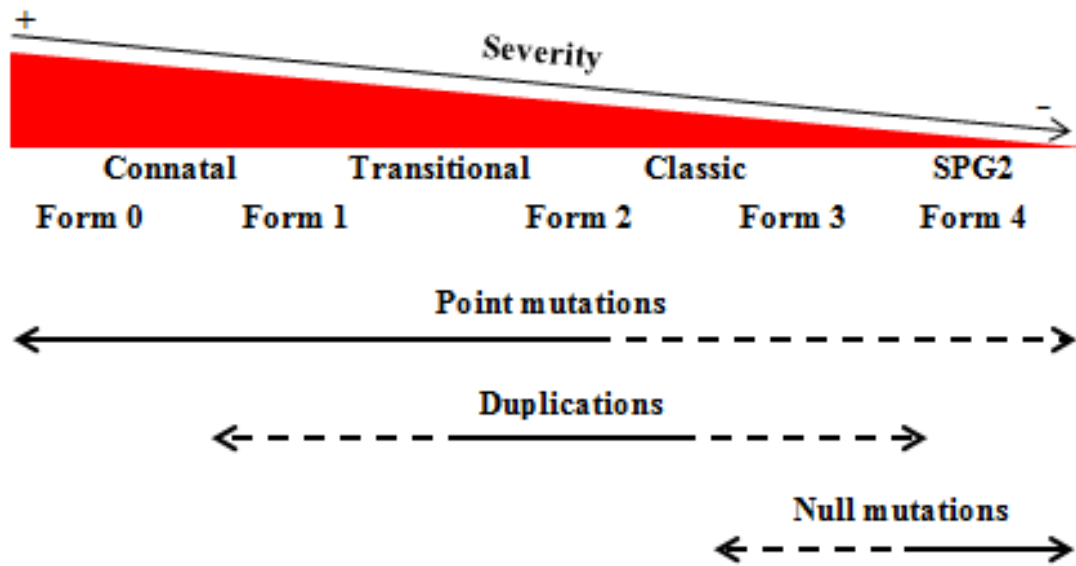


Figure 4. PMD classification. PMD is classified in accordance to the severity of the disease showing both the classification based on neuropathological findings (connatal, transitional, classic and SPG2) and on clinical severity (form0 to 4). The most prominent mutations corresponding to the severity and neuropathological findings are also shown (arrows delimit the mutations and dashed lines indicate that mutations are found but with less frequency).

To date there is no cure for PMD, therefore, several works have been focused on discovering clinical treatments and drugs. Different animal models have been used to study hypomyelinating PLP1-related disorders such as the jimpy mice, myelin deficient rat, shaking pup in dogs, PLP1 deficient-transgenic mice, PLP1 overexpressing mice and PLP1 overexpressing transgenic rat (Duncan et al., 2011). Jimpy model is the best characterized model of PMD and was described in 1964 by *Sidman et al.* (Sidman et al., 1964). Jimpy is a shortened life-span murine (3-4 weeks) that shows a X-linked recessive transmission and results in a radical CNS myelin deficiency in homozygous mice male (Vela et al., 1998). Jimpy results from a single point mutation in the PLP1 gene that results in a A→G base change (Nave et al., 1987). This animal model is characterized by producing fewer ultrasonic vocalizations between 2 to 8 days postpartum and develops motor tremors around 10 days postpartum. These tremors are more accentuated in the hindquarters, disturbing animals. These mice weigh less and spend less time engaged in coordinated activity than their normal littermates. Animals die between 25-30 days due to a

respiratory paralysis, although, during the last week of life these animals also manifest tonic seizures and hind legs are sometimes paralyzed (Bolivar and Brown, 1994; Vela et al., 1998). At biochemical and histological levels, jimpy male mice show a reduction of 90-98% of myelin in the CNS and are characterized by an important oligodendrocytes death (Vela et al., 1998). Jimpy mice is a very accepted model to study PMD because recapitulates many hallmarks of PMD such as the premature oligodendrocytes death, severe neurological deficits and early mortality (Elitt et al., 2020; Knapp et al., 1986).

5.2 Multiple sclerosis and experimental mice models

MS is the most common demyelinating disorder, having around 3.0 million affected people worldwide and affects in a ratio of 2:1 women to men, but in some countries this ratio could achieve a ratio of 4:1, respectively (Walton et al., 2020). MS presents a variable prevalence depending on the geographical area, however, the most affected areas are Canada, Northern United States, most of Northern Europe, New Zealand, Australia (south eastern), and Israel, having a prevalence of 30–80 per 100,000 habitants. Southern Europe, southern United States, and northern Australia have a prevalence of 5–25 per 100,000 habitants. Finally, the low affected regions with a prevalence lower than 5 per 100,000 habitants are Africa, and South America (Wade, 2014). MS typically starts between ages 20 and 40 and is characterized by inflammation, demyelination, gliosis, oligodendrocytes death and neuronal loss (Goldenberg, 2012; Tafti et al., 2021). Although MS is the most common demyelinating disorder and several laboratories make several efforts to discover the main cause of the disease, the etiology still remains unknown. Unfortunately, MS incidence is increasing worldwide and at the moment is considered a multifactorial disease, meaning that is triggered by genetic predisposition and environmental factors (Ghasemi et al., 2017). Some of these environmental factors could be low levels of vitamin D, smoking, childhood obesity and Epstein-Barr virus infection (Dobson and Giovannoni, 2019; Harbo et al., 2013). Regarding genetic factors, it has been reported that biological first-degree relatives of MS patients have high risk to develop the disease (Harirchian et al., 2018). Monozygotic twins have higher susceptibility to develop MS (24-25%) in comparison with dizygotic twins (3–5%) (Hansen et al., 2005; Willer et al., 2003). One of the most identified genetic risk factors from MS is an allele from the major histocompatibility complex class II HLA-DRB1 gene, HLA-DRB1*15:01, that results in a threefold risk to develop MS (Parnell and Booth, 2017). Genome-wide association studies allowed to identify single nucleotide polymorphisms that are related to MS (Beecham et al., 2013; International Multiple Sclerosis Genetics Consortium et al., 2011). Regarding the different sex ratio that presents female and male to develop MS, it has been observed that in EAE mouse model for MS, the presence of two X chromosomes is associated with a higher susceptibility to develop MS (Smith-Bouvier et al., 2008). Clinical features vary from patients and also within one

patient over time, neurological symptoms are the most abundant but symptoms can go beyond neurological involvement (Gelfand, 2014; Ghasemi et al., 2017) (**Figure 5**).

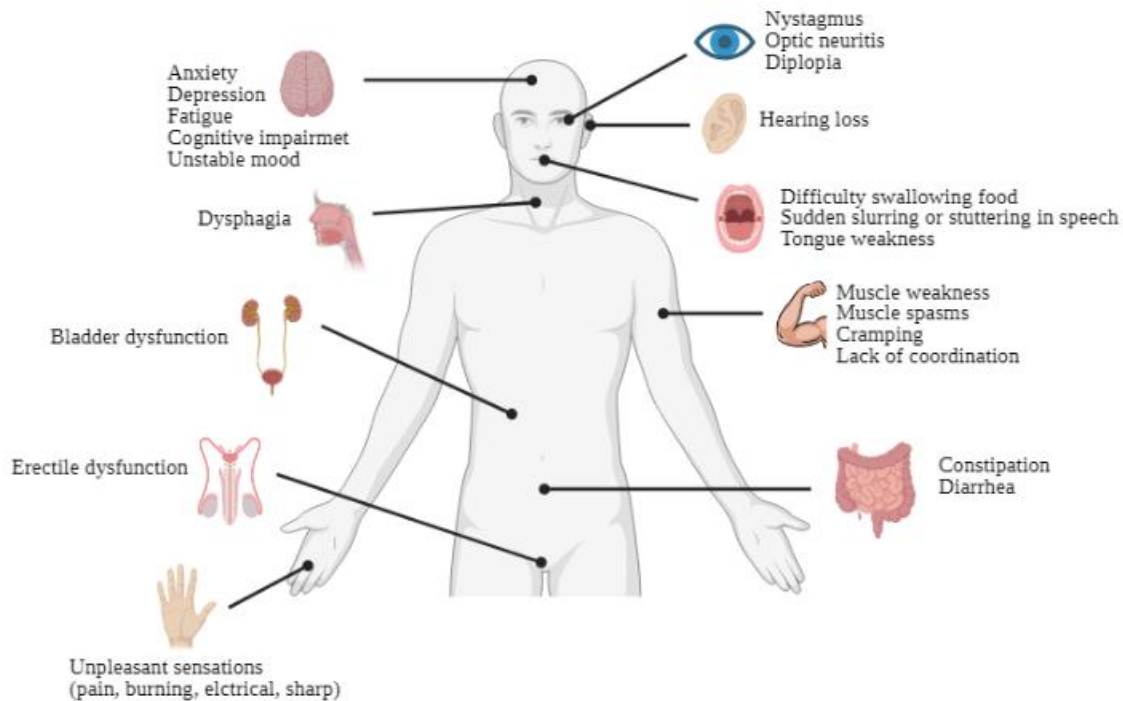


Figure 5. Main clinical symptoms in MS. MS clinician is characterized by a wide varied symptomatology between patients and can affect several organs leading to different conditions.

MS can be classified in the following subtypes according to disease course: relapsing-remitting MS (RRMS), primary-progressive MS (PPMS), secondary-progressive MS (SPMS), and progressive-relapsing MS (PRMS) (Ghasemi et al., 2017; Goldenberg, 2012). RRMS is the most common subtype, affecting around 85% of MS patients and is characterized by acute attacks followed by periods of remission. PPMS is the second subtype most common of MS, affecting from 15 to 20% of MS patients. PPMS is characterized by gradual deterioration from the onset without periods of remission or relapses, however, there may be occasional plateaus. SPMS may be developed in some patients with RRMS. SPMS shows a disease course continuing to worsen with or without periods of remission or plateau. PRMS is the rarest form of MS, affecting less than 5% of MS patients. PRMS presents intermittent flare-ups of worsening symptoms along the way with no periods of remission (Ghasemi et al., 2017; Goldenberg, 2012; Tafti et al., 2021).

Pathologically, MS is characterized by oligodendrocytes death, demyelination, axonal damage, breaching of BBB as well as T and B-cell infiltration (Qureshi et al., 2018). However, as previously said, the mechanisms that trigger MS still remain unknown. At histological level,

MS is characterized by demyelinating lesions or plaques in grey matter (GM) and WM due to a persistent inflammation (Lassmann, 2018; Popescu et al., 2013). The observed plaques are composed by inflammatory cells and their excreted cytokines, demyelinated and transected axons, gliosis and oligodendrocytes death (Ghasemi et al., 2017; Popescu and Lucchinetti, 2012; Popescu et al., 2013). These lesions can be classified into different patterns of lesions: pattern I lesion, pattern II lesion, pattern III lesion and pattern IV lesion (Lucchinetti et al., 2000). Pattern I lesion consist in active demyelinating sites with important presence of lymphocytes and macrophages. This pattern of lesion is mainly found in small veins and venules and show sharply demarcated edges with perivenous extensions. It is also appreciated the loss of some key myelin proteins such as MBP, PLP1, myelin oligodendrocyte glycoprotein (MOG) and myelin associated glycoprotein (MAG). Pattern II lesion differs from pattern I lesion because there is found a prominent deposition of Igs and a complement antigen at regions with active demyelination. Pattern III lesion is characterized by T lymphocytes infiltration, macrophages and activated microglia. There is no deposition of Ig or complement. Pattern III lesion is not found in veins or venules and a preservation of a rim of myelin is most frequently noticed wrapping inflamed vessels in demyelinating areas. In this type of lesion, borders of active lesions are not well defined. In these lesions are found a preferential loss of MAG and oligodendrocytes show nuclear condensation and fragmentation that are apoptotic markers. Also a pronounced loss of oligodendrocytes is observed. Pattern IV lesion differs from pattern III lesion because there is an increase of oligodendrocytes death (Lucchinetti et al., 2000).

To date there is no cure for MS, however, treatments can be divided into disease-modifying therapies and symptomatic therapies (Dobson and Giovannoni, 2019). Disease-modifying therapies consist in suppressing or modulating inflammation in the course of disease (Hauser and Cree, 2020). Currently, immunosuppressant (i.e. fingolimod, natalizumab and ocrelizumab) and immunomodulatory (i.e. interferon beta, glatiramer acetate and teriflunomide) treatments are used to treat MS. Immune reconstitution therapies are also possible and include alemtuzumab and cladribine (Dobson and Giovannoni, 2019). Among different disease-modifying therapies it has been shown that the majority of approved disease-modifying therapies to treat MS are more effective to treat RRMS (Hauser and Cree, 2020). Symptomatic therapies make reference to physical and pharmaceutical therapies that consist on managing the symptoms that result from the course of the disease. It means that are not specific for MS patients. Some of these symptomatic therapies are directed towards bladder dysfunction, neuropathic pain, anxiety, depression etc. MS is a disease involved with a lot of questions with no answers. To date, some risk factors have been proposed to trigger MS, however, at this point no one can confirm what causes MS development in an individual. Although, some therapies are available there is still no cure for MS. A better knowledge of the disease mechanism would

be very helpful to develop novel treatments. To deeper understand MS and discover novel treatments, different *in vivo* models have been developed: autoimmune, viral, chemical, and transgenic models. Each animal model mimics a subset of symptoms and pathological features of MS, therefore, the chosen animal model must be in accordance with your research interests (Torre-Fuentes et al., 2020) (**Table 1**). Among the different existing experimental models, the most used *in vivo* models are the EAE and the cuprizone model. The EAE is induced by autoantigen and Freund's adjuvant administration or transfer of autoreactive T cells (Baker and Amor, 2015; van der Star et al., 2012). The cuprizone model is induced by feeding the cuprizone copper chelator that causes demyelination. However, once cuprizone diet is stopped, remyelination takes place (Torre-Fuentes et al., 2020).

Table 1. Main characteristics of existing *in vivo models* to study multiple sclerosis.

Type of model	Model of MS	Mechanism	Characteristics
Autoimmune	EAE	Immunization with PLP ₁₃₉₋₁₅₁ , MBP ₈₄₋₁₀₄ or MOG ₃₅₋₅₅	Depending on animal species and strain, the obtained phenotype of MS is different (i.e immunization with PLP or MBP in SJL mice mimics RRMS, immunization with MOG in C57BL/6 mice mimics PPMS) Not possible to study remyelination
Viral	TMEV	Infection with Theiler's murine encephalomyelitis virus (TMEV)	Study axonal damage and inflammatory demyelination in PPMS Not possible to know when symptomatology is caused by the virus or the inflammatory response Not possible to study remyelination
	MHV	Infection with Mouse Hepatitis (corona) Virus (MHV)	Accurately replicates MS pathogenesis and allows to study progressive disability Lack of information concerning virus infection and spreading Possible to study remyelination
	SFV	Infection of mice with Semliki Forest Virus (SFV)	Mice do not die Possible to study remyelination
	JME	Infection of japanese macaque encephalomyelitis (JME) with Simian herpesvirus	Animals develop spontaneous neurological disease Limited remyelination Not an experimental model available
Chemical	Cuprizone	Feeding C57BL/6 mice with 0.2% cuprizone for 6 weeks	Study de- and remyelination at precise time Specific to oligodendrocytes Non-inflammatory
	Lysolecithin	Lysolecithin injection in SJL/J mice	Study de- and remyelination Localized region Extremely complex technique
	Ethidium bromide	Injection of ethidium bromide	Study de- and remyelination Localized region

			Complex technique
--	--	--	-------------------

Abbreviations: TMEV, Theiler's murine encephalomyelitis virus; MHV, Mouse Hepatitis Virus; SFV, Semliki Forest Virus; JME, japanese macaque encephalomyelitis.

5.2.1 The Experimental autoimmune encephalomyelitis mice model

The EAE model was initially described in monkeys in 1933 by *Rivers et al.* (Rivers et al., 1933) but referred with the name of acute disseminated encephalomyelitis. Later, this model was described in other species and was firstly described in mice in 1949 (Olitsky and Yager, 1949). EAE mouse model is the most common autoimmune disease model to study MS and many of the existing therapies have been proved in this model (Lassmann, 2011; Robinson et al., 2014). EAE can be induced by active immunization with any of three MBP, MOG and PLP myelin-derived proteins or by y passive transfer of activated myelin-specific CD4⁺ T lymphocytes (Robinson et al., 2014). The mouse strain and myelin antigen will determine the phenotype. For example, EAE induction in C57BL/6 mice with MOG causes a chronic EAE with moderate phenotype useful to study PPMS. EAE induction in SJL results in a model that mimics RRMS, however, immunization with PLP causes a saver phenotype than immunization with MBP (Miller et al., 2007). When EAE mice are immunized with a myelin protein, result in a T-cell and monocyte infiltration in the CNS due to BBB breakdown (Barthelmes et al., 2016; Bennett et al., 2010; Rao and Segal, 2004). EAE is a very used model to study MS because both share common features: immune-inflammatory activation with infiltration to the CNS, microglial activation, demyelination and secretion of inflammatory cytokines (Jahan-Abad et al., 2020; Plastini et al., 2020). EAE is considered a T-helper (Th)1/Th17 mediated inflammatory disease that results in a secretion of inflammatory cytokines, CNS inflammation and demyelination (Jahan-Abad et al., 2020; 't Hart et al., 2011). Although EAE and MS share common hallmarks that make EAE an interesting model to study MS, there are some important differences. For example, T cell-infiltrates differ between MS and EAE. CD4⁺ T-lymphocytes are considered the mediators in EAE pathogenesis, however, CD8⁺ T-cells that are the major T-cell population found in MS are considered as key player in MS pathogenesis (Lassmann and Bradl, 2017; Sinha et al., 2015). Demyelination is mainly found in perivenous regions in EAE mice, however, in MS demyelination is not restricted to this area of WM (Sriram and Steiner, 2005). In EAE mice the localization of lesions is dependent of the myelin-derived proteins used during immunization, being more focused in lumbar regions for MBP and PLP1 EAE mice, and localized in brainstem in MOG mice (Sriram and Steiner, 2005). Immunotherapies can also have different effects between EAE and MS such as the immunosuppressive drug Cyclosporin

A can prevent the BBB breakdown in EAE mice but is not useful for MS patients due to the adverse effects and low efficacy (Mix et al., 2010).

5.2.2 The Cuprizone de-/remyelinating mice model

Cuprizone copper chelator (bis-cyclohexanone oxaldihydrazone) compound was discovered by Gustav Nilsson in 1950 (Nilsson, 1950). Subsequent studies performed in mice revealed that cuprizone administration results in reduced blood copper levels and demyelination (Carlton, 1966). Cuprizone model was developed by William Blakemore in the 70's (Blakemore, 1973a, 1972). Copper is an essential element in mammal's nutrition. However, both copper deficiency and copper excess leads to pathological conditions (Stern et al., 2007). Copper is necessary to preserve cardiovascular integrity, neuroendocrine function, tissue growth, lung elasticity, iron metabolism and neovascularization. However, copper deficiency has been associated with mental retardation, cardiovascular problems, neutropenia, bone fragility, immune failures, impaired brain function, among other's (Vega-Riquer et al., 2019). CNS demyelination has also been associated with copper deficiency (Prodan et al., 2002).

Cuprizone model is the most frequent toxic model to study demyelination and remyelination in a mouse model of MS. In this model, adult mice are fed with 0.2% of cuprizone that leads to demyelination during 4-5 weeks. In cuprizone model, *corpus callosum* (CC) and cerebellar peduncles are the most affected brain regions showing significant demyelination (Blakemore, 1973b). CC is the largest WM bundle in the brain that connects right and left hemispheres of the human brain, allowing interhemispheric communication (Fitsiori et al., 2011; Goldstein et al., 2021). In CC of these mice, different glial cells types have been described: astrocytes (Zhang et al., 2019), microglia (Lee et al., 2019) and oligodendroglial cells (Meyer et al., 2018; Valério-Gomes et al., 2018). During the phase of demyelination, cuprizone model is characterized by a primary mature oligodendrocyte death but not OPCs (Bénardais et al., 2013; Fischbach et al., 2019), contrary, microglia and astrocytes are activated (Gudi et al., 2014). As previously said, animals are fed with cuprizone and exposure to cuprizone during 4-5 weeks which induces an acute demyelination, however, exposures up to 12 weeks results in a chronic demyelination (Hibbits et al., 2009; Zhang et al., 2017). In the case of acute demyelination in cuprizone model, cuprizone withdraw allows to spontaneous remyelination after 4 days (Torkildsen et al., 2008). However, in chronic demyelination the degree of remyelination may be limited or may even fail (Urbanski et al., 2019).

Cuprizone model normally achieves a complete demyelination approximately at 3-4 weeks of cuprizone exposure and then it is stabilized. However, around 4-5 weeks of cuprizone diet there is a OPCs proliferative peak with the attempt to repopulate the loss of mature oligodendrocytes. This observed proliferative peak of OPCs still increases during remyelination (Yamate-Morgan

et al., 2019). In the case of microglia, it arrives to a plateau at 5 weeks of cuprizone treatment and decreases during remyelination, however, astrocytes remain activated during demyelination and remyelination processes (Plastini et al., 2020). A summary with the general characteristics observed during acute demyelination in cuprizone model are shown in **Figure 6**. Although cuprizone model is a very frequent animal model used to study MS, this model as any other, has some advantages and disadvantages. This model allows to study remyelination and molecular mechanisms can be dissect and studied without peripheral cells infiltration, however, this model is not an immune-mediated mouse model as MS pathology is (Gudi et al., 2014; Zhan et al., 2020).

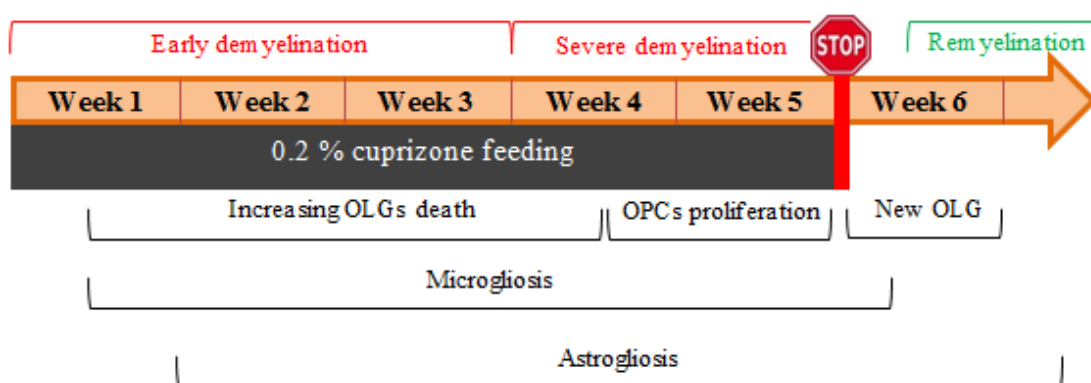


Figure 6. Time course of de- and remyelination in acute cuprizone model. Mice are fed with 0.2% (w/w) of cuprizone during 5 weeks. Early demyelination starts at first week and progress to a severe demyelination that starts at the end of week 3 or beginning of week 4. Severe demyelination culminates at the end of fifth week. Once cuprizone is removed (first day of week 6) from the diet of these animals, remyelination starts spontaneously.

6. Interactomics, biomarkers and OMICS data analysis

Omics technologies make reference to genomics, transcriptomics, interactomics, proteomics and metabolomics. This suffix -omics makes reference to the study of life science on large-scale data/information (Santos et al., 2016). In this thesis, among the different omics technologies, we are interested in interactomics. Interactomics is defined as the discipline between bioinformatics, biochemistry and engineering that is in charge to study the interactions between and among proteins and other components of a cell (Shachuan et al., 2015; Yan et al., 2018, p. 3). Mapping the interaction networks of an organism will be helpful to understand the consequences of these interactions in physiological and pathological conditions, define new biomarkers, possible drug targets and functional associations in cellular networks cell (Shachuan et al., 2015; Yan et al., 2018, p. 3). One of the main interests of interactomics is to discover new biomarkers. Biomarkers are defined as a biological markers that are used to describe a medical sign and can be objectively measured and evaluated (Strimbu and Tavel, 2010; Ziemssen et al., 2019). Biomarkers could be very important for an early diagnosis and

monitoring of different pathologies, as valuable predictive tool, assess the prognostic of a condition and to measure the susceptibility/risk of a condition, treatment selection and measure the pharmacodynamics/response leading to the development of novel therapies and treatments (Califf, 2018; Shachuan et al., 2015). To date, interactomics allowed to discover important biomarkers in different pathophysiological conditions such as genetic variants involved in heart diseases (Gonzalez-Teran et al., 2022), neurodegenerative disorders (AD, PD and amyotrophic lateral sclerosis) (Haenig et al., 2020), chronic respiratory diseases (Maiorino et al., 2020), among other's (Ruiz et al., 2021; Vidal et al., 2011; Yatsenko et al., 2020). Therefore, interatomic studies could be useful to discover the function of some proteins based on guilt-by-association approaches, in means that the function of some proteins can be unraveled by knowing with who they are interacting. Our previous interactomic studies in TRPV2 (Pau Doñate-Macián et al., 2018) and TRPV4 (P. Doñate-Macián et al., 2018) allowed to unravel a wide set of interactors of TRPV2 and TRPV4, being many of the associated to trafficking, myelin components and lipid metabolism.

7. Biomarkers in demyelinating disorders

As previously said, important biomarkers has been found related to neurodegenerative disorders (Haenig et al., 2020) but there are also available data about some biomarkers for demyelinating disorders of the CNS such as MS (Berger and Reindl, 2015; Boziki et al., 2020; Kira, 2017). However, it still lacks plenty of biomarkers to discover so more studies are needed on this field.

In the case of MS, there is no cure and the etiology still remains unknown. Therefore, the discovery of different biomarkers to prevent the MS onset, predict the evolution of the disease or how the disease response to different treatments, would be very useful for the quality of life of these patients. In demyelinating disorders it seems that the main problem to achieve remyelination is the failure of OPCs to get differentiated in mature forming myelin oligodendrocytes. A process that is orchestrated by microglia, astrocytes and OPCs. The discovery of potential biomarkers at big scale would be possible thanks to omics technologies that allow the unraveling of key molecules involved in physiological and pathophysiological processes. MS is an inflammatory and neurodegenerative disease of the CNS that has non-traumatic cause. In MS is important to identify the molecules involved in the immune response and also the other molecules involved in the neurodegenerative process. These biomarkers would be useful to predict the risk to develop MS, provide an early diagnosis, an accurate diagnosis of MS, predict the progression of the diseases and also to predict the response to different treatments (**Table 2**). In MS, biomarkers are normally studied in peripheral blood and cerebrospinal fluid (CSF). However, samples obtained from these different sources have its advantages and disadvantages. Studies performed in peripheral blood are non-invasive for

patients and allow studying the response to different treatments that has been systemically administrated and also arise information about the immune MS onset. However, studies performed in peripheral blood are not limited to CNS. Contrary, studies performed on CSF are CNS specific but are more invasive for patients (Harris and Sadiq, 2009). Therefore, in MS omics analysis are useful to unravel predictive biomarkers, diagnostic biomarkers, prognostic biomarkers, disease associated biomarkers and biomarkers to predict the efficacy to different therapeutic treatments.

Table 2. Types of biomarkers and their relevance in MS.

Types of biomarkers	Interest in MS
Predictive biomarkers	Identify the risk to develop MS
Diagnostic biomarkers	Early diagnosis of MS Confirm the presence of MS and the subtype
Prognostic biomarkers	Predict the course or progression of the diseases of MS
Disease-related biomarkers	Indicator of the diseases activity such as inflammation, demyelination and neurodegeneration in MS
Pharmacodinamic/response biomarkers	Evaluate the response to different therapies

In MS the most notable biomarkers related to pathophysiology are miRNAs, being some of them upregulated or downregulated (Gul et al., 2020). In MS lesions or peripheral blood mononuclear cells (PBMCs) it can be found some upregulated miRNAs such as miR-199a, miR-320, miR-155, miR-142-3p and miR-142. However, miR-219, miR-34a, miR-103, miR-182-5p, miR-124 and miR-15a/b in PBMCs or CSF in MS patients (Gul et al., 2020). Serum levels of tau and BDNF are also MS biomarkers, being tau upregulated and a marker of disease progression, and BDNF downregulated and useful as a biological marker for diagnosis (Islas-Hernandez et al., 2018). The soluble isoform of the IFN- β receptor (sIFNAR2) levels are found decreased in serum of MS patients (Órpez-Zafra et al., 2017). Higher levels of the chemokines CXCL10, CXCL13 and CXCL12 in CSF are also considered MS biomarkers (Jafari et al., 2021; Krumbholz et al., 2006). IL-6 is a pro-inflammatory cytokine that is one of the most studied cytokines involved in MS and it is found severely overexpressed in MS lesions (Harris and Sadiq, 2009). Several studies have found increased levels of NO metabolites in CSF (Miljkovic et al., 2002; Yamashita et al., 1997), serum (Giovannoni et al., 1997) and urine (Giovannoni et al., 1999) in MS subjects. NO is one of the responsables of oligodendrocytes death, axonal degeneration and subsequent impairment of nerve conduction (Smith and Lassmann, 2002). The presence of Oligoclonal Bands is one of the oldest biomarker of MS that can be used as a biomarker of diagnosis (Toscano and Patti, 2021). Neurofilament light chain levels in serum and CSF are increased in MS subjects and can be used as a biomarker of MS progression and

prognosis (Kempen et al., 2020; Malmeström et al., 2003; Salzer et al., 2010). Other biomarkers found in AD have also been suggested as possible biomarkers for MS such as secreted amyloid precursor protein, amyloid- β isoforms, Bri2, tau, phosphorylated tau, and β -amyloid precursor protein-cleaving enzyme-1 (Harris and Sadiq, 2009).

As said before, different biomarkers have been found, however, it still remain many questions about MS mechanisms and other biomarkers. What is known is that in MS there is a failure in OPCs differentiation to mature oligodendrocytes, a process orchestrated by microglia, astrocytes and OPCs. Therefore, identifying the genes involved in this crosstalk and how these cells interact among them would be very useful to unravel new mechanisms and discover new MS biomarkers.

HYPOTHESIS AND OBJECTIVES

The interplay between molecules is key to every physiological process, and myelination and remyelination are not an exception. In this work we put the focus on TRPV channels such as TRPV2 and TRPV4 and their molecular partners to reach specific membrane compartments relevant for their function. Based on TRPV2s molecular partners, we narrow down to the single protein level to characterize the implications of this elusive ion channel in myelin physiology. Finally, we take a wider and unbiased perspective to discover new relevant players in myelin pathophysiology by using available omics public data.

The working hypothesis of this doctoral thesis is that microglia and OPCs crosstalk play a crucial role on developmental myelination and during de-/remyelination. Therefore a better understating of the molecules involved in this crosstalk during physiological myelination, myelinating disorders and remyelination would be of important interest to achieve therapeutic remyelination in myelin related disorders. To study our hypothesis, this thesis is divided into three chapters with their corresponding specific objectives:

Chapter I

- To review and to analyze from scratch the known human brain protein-protein interactions for TRPV2 and TRPV4 to gain insight on how these ion channels are trafficked to the plasma membrane and other membrane compartments.

Chapter II

- To validate and to characterize the interaction of TRPV2 with key myelin proteins proposed through interactomics experiments from our lab.
- To assess the expression of TRPV2 in microglia and OPCs in myelin pro- and anti-inflammatory environments.
- To assess the expression of TRPV2 and to indirectly assess its activity in myelinating disorders by using animal models and MS human clinical samples.

Chapter III

- To identify the molecules involved in the microglia-OPCs crosstalk by using microarray analysis performed in the cuprizone model of MS.
- To determine the differentially expressed genes (DEGs) in microglia, OPCs and CC after cuprizone treatment.
- To identify the microglia ligands and OPCs target genes and receptors involved in the microglia-OPCs crosstalk.




Results

Chapter I

Trafficking of Stretch-Regulated TRPV2 and TRPV4 Channels Inferred Through Interactomics

Review

Trafficking of Stretch-Regulated TRPV2 and TRPV4 Channels Inferred Through Interactomics

Pau Doñate-Macián ^{1,2} , Jennifer Enrich-Bengoa ^{1,3}, Irene R. Dégado ^{4,5,6},
David G. Quintana ¹  and Alex Perálvarez-Marín ^{1,3,*} 

¹ Biophysics Unit, Department of Biochemistry and Molecular Biology, School of Medicine, Universitat Autònoma de Barcelona, 08193 Cerdanyola del Vallés, Catalonia, Spain; pabdoama@gmail.com (P.D.-M.); jennifer.enrich@uab.cat (J.E.-B.); DavidG.Quintana@uab.cat (D.G.Q.)

² Laboratory of Molecular Physiology, Department of Experimental and Health Sciences, Pompeu Fabra University, 08003 Barcelona, Catalonia, Spain

³ Institut de Neurociències, Universitat Autònoma de Barcelona, 08193 Cerdanyola del Vallés, Catalonia, Spain

⁴ CIBER Cardiovascular Diseases (CIBERCVD), Instituto de Salud Carlos III, 28029 Madrid, Spain; iroman@imim.es

⁵ REGICOR Study Group, Cardiovascular Epidemiology and Genetics Group, IMIM (Hospital Del Mar Medical Research Institute), 08003 Barcelona, Catalonia, Spain

⁶ Faculty of Medicine, University of Vic-Central University of Catalonia (UVic-UCC), 08500 Vic, Spain

* Correspondence: alex.peralvarez@uab.cat; Tel.: +34-93-581-4504

Received: 14 October 2019; Accepted: 25 November 2019; Published: 27 November 2019



Abstract: Transient receptor potential cation channels are emerging as important physiological and therapeutic targets. Within the vanilloid subfamily, transient receptor potential vanilloid 2 (TRPV2) and 4 (TRPV4) are osmo- and mechanosensors becoming critical determinants in cell structure and activity. However, knowledge is scarce regarding how TRPV2 and TRPV4 are trafficked to the plasma membrane or specific organelles to undergo quality controls through processes such as biosynthesis, anterograde/retrograde trafficking, and recycling. This revision lists and reviews a subset of protein–protein interactions from the TRPV2 and TRPV4 interactomes, which is related to trafficking processes such as lipid metabolism, phosphoinositide signaling, vesicle-mediated transport, and synaptic-related exocytosis. Identifying the protein and lipid players involved in trafficking will improve the knowledge on how these stretch-related channels reach specific cellular compartments.

Keywords: ion channel trafficking; transient receptor potential channels; TRPV2; TRPV4; phosphatidylinositol signaling; stretch-related channels

1. Introduction

Transient receptor potential (TRP) channels are polymodal cation channels involved in somatosensation at the cellular and tissue levels in vertebrates [1]. Channels in the TRP family are in charge of sensing physical stimuli such as temperature or mechanical changes to trigger cation-mediated cell signal transduction pathways [2]. The vanilloid subfamily (TRPV) has six members (TRPV1–6), where TRPV1–4 have been long related to thermal sensing [3]. More recently, they have also been linked to mechanical stress, especially the TRPV2 and TRPV4 channels [4,5]. Accordingly, the function of TRPV2 and TRPV4 is expected to be essential in tissues with high mechanical shearing, such as skeletal and cardiac muscle.

Expression of TRPV2 is wide (Figure 1a) and TRPV2 is involved in several physiological processes [6], but the particular role of this channel in skeletal and cardiac muscle is gaining much attention [7–12]. The expression of TRPV4 is as ubiquitous as TRPV2 (Figure 1a), but it is prominent in epithelial tissues, evoking calcium currents in response to extracellular stimuli, such as temperature,

osmotic changes, and mechanical stretch [13–15]. Mutations of TRPV4 are related to involved in oligomerization, trafficking, and degradation can result in genetic disorders like Brachyolmia, Charcot–Marie–Tooth disease type 2C, spinal muscular spinal muscular atrophy, arthrogryposis, and hereditary motor and sensory neuropathy type 2 [16,17]. The identification of these mutations is a first step to determine the pathogenesis of the associated diseases and to design specific therapies. In addition, the disruption of the folding-sensitive region of TRPV4 could be a therapeutic option for diseases in which TRPV4 increases its activity such as pain and skeletal dysplasias [18]. Recently, it has also been shown that TRPV4 affects the calcium balance in cardiomyocytes, affecting contractility, leading to cardiac tissue damage in heart pathophysiology [19].

An important question regarding TRPV2 and TRPV4 is how these channels are trafficked to and recycled from the membrane. This is an essential aspect in TRPV2 and TRPV4 function as Ca^{2+} -dependent stretch-modulated channels. It has been shown that trafficking and/or translocation is a highly regulated process, and it may be dependent on channel activity. Translocation of TRPV2 to the membrane is driven by growth factors or chemotactic peptides [6], although it is not clear yet whether TRPV2 is functional when at the plasma membrane and/or internal organelles, mainly because most of the literature regarding TRPV2 trafficking is based on poor detection antibodies against TRPV2 [20]. The function of TRPV4 is exerted mainly at the plasma membrane and TRPV4 trafficking to the membrane is regulated by activators, such as GSK1016790A [18]. Controlled and regulated trafficking of ion channels, especially in excitatory tissues, is fundamental because of the possibility of cation leakage during trafficking, which leads to unbalanced cation homeostasis promoting cell toxicity and/or excitotoxicity. This revision of the published protein–protein interactions for the TRPV2 and TRPV4 channels [21–24] intends to shed light about the proteins involved in the regulated and constitutive trafficking of these two mechanosensory cation channels.

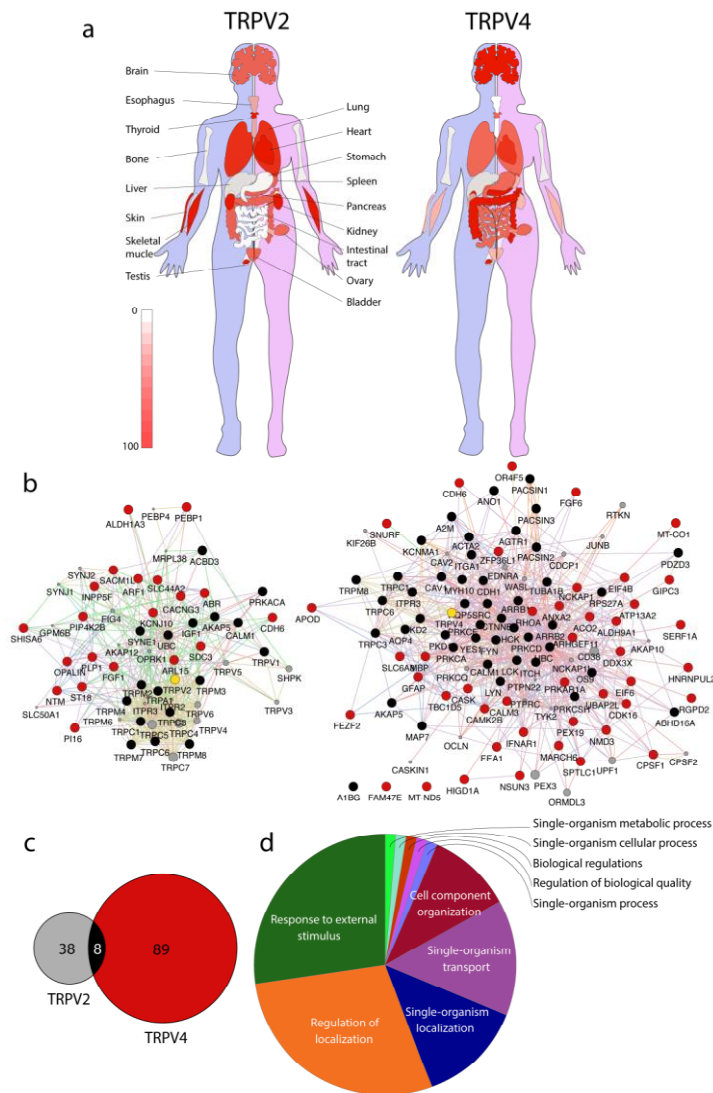


Figure 1. Transient receptor potential vanilloid subfamily TRPV2 and TRPV4 expression and interactomic profiles. (a) TRPV2 and TRPV4 tissue expression in humans; (b) TRPV2 (left) and TRPV4 (right) interactomes crossing published results (see main text for details). (c) Protein interactions overlap among TRPV2 and TRPV4 interactomes. (d) Main biological process terms defined by TRPV2 and TRPV4 gene set enrichment analysis (GSEA).

2. Sequence and Structure Determinants in Channel Trafficking

Beyond TRP biogenesis and oligomerization as tetramers [25], TRP channel trafficking is a complex mechanism, integrating processes such as membrane insertion, glycosylation, Golgi maturation, vesicle trafficking, and protein–protein interaction (PPI) [26]. The balance between these processes results in a correct protein distribution in the plasma membrane or the corresponding membrane compartment, leading to up- and down-regulation of the protein function. The trafficking structural and molecular determinants in TRP sequence are mediators of PPI and/or lipid–protein interactions (LPIs). In TRPV channels, both the N- and C-termini were involved in trafficking. The distal N-terminus of TRPV channels is highly variable and structurally disordered and likely to host several phosphorylation sites and PPI and LPI domains. Deletion of the distal N-terminus of TRPV2 is enough to deplete the channel trafficking to the plasma membrane [23], which has also been observed for TRPV5 [27]. In addition, the N-terminus of TRPV4 interacts with OS-9 in the endoplasmic reticulum (ER), preventing channel trafficking to the plasma membrane [28]. Protein kinase C and casein kinase substrate in neurins proteins (PACSN) also bind to the TRPV4 distal N-terminal domain (interaction exclusive for TRPV4 among TRPV channels), enhancing the relative amount of TRPV4 in the plasma membrane [29]. As for the C-terminus, AKAP79/150 binding has been described [24], as well as the ankyrin repeat domain (ARD), which is involved in PPI, but also in the complex mechanism of trafficking of TRPV channels. The TRPV4 C-terminus is also involved in trafficking, as shown by C-terminus deletion mutants, resulting in TRPV4 accumulation in the ER [30]. The characteristic ankyrin repeat domain (ARD) is involved in PPI, but also in the complex mechanism of trafficking of TRPV channels. Experiments carried out to map in vitro TRPV2 topology [23] were performed with constructs lacking either most of the N-terminal domain of the channel (the first 74 amino acids Δ N74-TRPV2) or the first 336 amino acids at the distal N-terminus (corresponding to the ARD, Δ ARD-TRPV2). Despite the N-terminal truncation, TRPV2 was properly folded within the lipid bilayer. The Δ ARD-TRPV2 mutant was not able to traffic to the plasma membrane, as determined by confocal imaging and biotinylation assay [23]. Such a fact indicates that the N-terminal region may be needed for additional channel processes other than insertion in the ER membranes, such as channel tetramerization, glycosylation, or interaction with chaperone proteins to allow membrane translocation. Although it has not been described for TRPV2 [31], the ARD indeed plays a key role in channel oligomerization for TRPV4, as has been shown for ARD mutants in TRPV4 [32]. TRPV mutants lacking ARD or carrying point mutations in N- or C-terminal domains produce channels that seem unable to tetramerize, which emphasizes the need for the TRPV cytosolic domains to promote the correct oligomerization of the subunits [32,33].

Turnover of TRPV channels in the plasma membrane is also controlled by regulated exocytosis, a process mediated by phosphorylation and interaction with SNAP (soluble N-ethylmaleimide sensitive fusion attachment protein) receptor (SNARE) complex proteins. SNAREs are a protein complex of more than 60 members in mammalian cells that mediate vesicle fusion with their target membrane bound compartment. The complex of SNAREs has a relevant role in cellular processes such as neurotransmitter release in synapses, exocytosis, or autophagy [34,35]. Upon protein kinase C (PKC) activation, TRPV1 is recruited to the plasma membrane by SNARE mediated vesicle transport, leading to a potentiation of TRPV1 currents [36]. Interaction of TRPV1 and TRPV2 with Snapin and SynaptotagminIX (SYT9) [36,37]. For TRPV2, the interaction with SNAREs protein is mapped into the highly conserved region of the membrane proximal domain (MPD), pointing to the conservation of these interactions along the TRPV1–4 subfamily [37].

Regarding LPI, TRPV channels share highly conserved PIP2 binding domains [24]. Binding of PIP2 to TRPV1 [38], TRPV2 [39], and TRPV3 [40] was mapped to the highly conserved proximal C-terminal domain, contiguous to the TRP box. The TRPV4 PIP2 binding domain is pinpointed using bioinformatics [24], although TRPV4 has an additional PIP2 binding site in the distal N-terminal domain [41]. Two recent works suggest that phosphatidic acid (PA) mediates LPIs between the

membrane proximal domain (pre-S1 domain) and the C-terminus of TRPV channels in the trafficking of TRPV channels to the plasma membrane [37,42].

3. Interactomics

Proteomic studies provide useful tools to understand the molecular mechanism of TRPV channels. Guilt-by-association approaches aiming for mid-throughput interactome discovery for TRPV2 and TRPV4 were used, combined with standard techniques such as co-immunoprecipitation in mammalian cell lines and a novel membrane-specific yeast two-hybrid (MYTH) methodology [21,22].

The MYTH is a split-ubiquitin-based system that allows the location of the bait protein (TRPV2, TRPV4) embedded in the membrane. First, a yeast strain is generated that constitutively expresses the ion channel fused to the C-terminus of ubiquitin followed by the transcription factor LexA-VP16 (TF). The bait strain is then transformed with a cDNA library containing more than 10^6 protein preys fused to the N-terminus of ubiquitin. The tag carries a mutation to hinder the spontaneous refolding of ubiquitin, which thus will only occur when a prey protein interacts with the bait. Once the interaction occurs and ubiquitin is refolded, the bait complex is cleaved and the TF is released. The traffic of TF to the nucleus starts the expression of reporter genes integrated in the yeast strain, allowing cells to grow in selective media lacking either Histidine (His) or Adenine (Ade). Moreover, the LacZ reporter gene is activated upon interaction, so that colonies carrying a putative interactor become blue stained in the presence of X-Gal. The blue color intensity may be used to determine whether interactions are strong or constitutive (intense blue color staining) or transient (pale blue color intensity) [43]. Using MYTH, 20 and 44 new interactors were found for TRPV2 and TRPV4, respectively [21,22] (Table S1 and Figure 1b,c).

Available PPIs for TRP channels are listed in the TRIP database [44]. For TRPV2 and TRPV4 PPI, refer to Supporting Table S1 and Figure 1b,c. The TRIP database is an excellent tool to get relevant information of biological processes regarding TRP channels. To the best of our knowledge, the database was last updated in August 2015, not including any new PPIs, such as the TRPV2 and TRPV4 membrane yeast two-hybrid (MYTH) dataset from these studies [21,24]. Figure 1 and Supplementary Table S1 list all the interactions for TRPV2 and TRPV4. However, for the PPI trafficking analysis performed in this study, only the PPIs identified in MYTH studies [21,22] are used. Using the list of TRPV2 and TRPV4 PPIs, a gene set enrichment analysis (GSEA) is performed, and then all ion channels and transporters filtered out to avoid the bias towards transport and cation transport gene ontology terms. Out of the 59 protein list, the GSEA resulted in 10 enriched biological process categories, including the following: neural nucleus development (GO:0048857); phosphatidylinositol biosynthetic process (GO:0006661); myelin sheath (GO:0043209); phospholipid biosynthetic process (GO:0008654); regulation of cellular amide metabolic process (GO:0034248); modulation of chemical synaptic transmission (GO:0050804); regulation of vesicle-mediated transport (GO:0060627); Ras GTPase binding (GO:0017016); regulation of cellular localization (GO:0060341); and cellular lipid metabolic process (GO:0044255).

4. Understanding Channel Trafficking through Protein–Protein Interactions

In this review, the focus lies in terms related to two aspects: (i) lipid and phosphoinositides, and (ii) synaptic and vesicle-regulated trafficking. Because both aspects are tightly entangled, they are difficult to study independently [21–24,37]. Lipids are key effectors in signal transduction and protein function, but also in protein trafficking [45]. Phosphoinositides (PIs) provide cellular organelles with specific lipid signatures, facilitating the binding of specific proteins. Membrane protein traffic is mediated by accessory proteins containing distinct lipid–protein binding domains, which promote binding depending on the lipids physico-chemical nature [45]. Regulated (e.g., synaptic-based exocytosis) and constitutive vesicle-mediated transport for TRP channels have already been reviewed, mostly based on TRPV1 studies [46]. This revision aims to expand the knowledge on vesicle/synaptic-based trafficking by shedding some light on accessory proteins involved in these processes, as listed in Table 1.

Table 1. List of interactors related to trafficking processes derived from a membrane yeast two hybrid approach.

Gene Symbol	Interactor	Gene Name	Gene ID	Process ^a
<i>ABHD16A</i>	TRPV4	abhydrolase domain containing 16A	7920	1
<i>ANXA2</i>	TRPV4	annexin A2	302	1, 2
<i>ARF1</i>	TRPV2	Adenosine diphosphate (ADP) ribosylation factor 1	375	1, 2, 3, 4, 5
<i>ATP13A2</i>	TRPV4	Adenosine triphosphate (ATP)ase cation transporting 13A2	23400	2, 3
<i>CAMK2B</i>	TRPV4	calcium/calmodulin dependent protein kinase II beta	816	4
<i>CASK</i>	TRPV4	calcium/calmodulin dependent serine protein kinase	8573	2, 3, 4
<i>CDK16</i>	TRPV4	cyclin dependent kinase 16	5127	2
<i>INPP5F</i>	TRPV2	inositol polyphosphate-5-phosphatase F	22876	1, 2, 3, 5, 6
<i>PIP4K2B</i>	TRPV2	phosphatidylinositol-5-phosphate 4-kinase type 2 beta	8396	1, 5, 6
<i>SACM1L</i>	TRPV2	SAC1 like phosphatidylinositide phosphatase	22908	1, 5, 6
<i>SDC3</i>	TRPV2	syndecan 3	9672	1, 2, 3, 4, 5
<i>SHISA6</i>	TRPV2	shisa family member 6	388336	2, 4
<i>SNAPIN</i>	TRPV2/TRPV1	SNAP associated protein	23557	2, 3, 4
<i>SPTLC1</i>	TRPV4	serine palmitoyltransferase long chain base subunit 1	10558	1, 6
<i>SYT9</i>	TRPV2/TRPV1	synaptotagmin 9	143425	2, 3, 4
<i>TBC1D5</i>	TRPV4	TBC1 domain family member 5	9779	3

^a Processes: 1, cellular lipid metabolism; 2, regulation of cell localization; 3, regulation of vesicle-mediated transport; 4, modulation of chemical synaptic transmission; 5, phosphatidylinositol biosynthesis; 6, phospholipid biosynthesis. TRPV, transient receptor potential vanilloid subfamily; SNAP, soluble NSF attachment protein.

Among the list of interactors (Table S1), the literature is revised regarding proteins/enzymes related to phosphoinositide signaling as markers of specific lipidic composition among cellular organelles, but also to trafficking and vesicle-mediated accessory proteins (Figure 2). This revision provides an overview of the TRPV2 and TRPV4 trafficking process. Side information on TRPV2 and TRPV4 trafficking is found in the literature, such as the role of PACSIN3 for TRPV4 [29,41], recombinase gene activator (RGA) protein, and ras-related protein 7 (Rab7) for TRPV2 [47,48], and the Snapin/Syt9 pair for TRPV1 and TRPV2 [21,36,37]. However, the role of the lipid-mediated PPI for TRPV channels deserves extra attention, not only because of the complexity of the mechanism, but also because of the diversity of mechanisms depending on the tissue of interest (Figure 1a).

The lipase/acyl-transferase dehydrogenase enzyme (ABHD16A) is a TRPV4 interactor involved in lipid metabolism [49]. Proteins of the ABHD family are involved in lipidic modifications, such as palmitoylation, and in negative regulation of α -amino-3-hydroxy-5-methyl-4-isoxazolepropionic acid (AMPA) receptor trafficking. The depalmitoylase ABHD17A is crucial for synaptic targeting and vesicle sorting of AMPA receptors, through PSD-95 depalmitoylation [49,50]. In line with AMPA, but also to *N*-methyl-D-aspartate (NMDA) receptors trafficking, the calcium/calmodulin dependent protein kinase II beta (CAMK2B) and the calcium/calmodulin dependent serine protein kinase (CASK), both TRPV4 interactors, are trafficking regulatory proteins [51–53]. Another kinase interacting with TRPV4 is the cyclin dependent kinase 16 (CDK16), a key regulator of vesicle trafficking [54–56]. The kinase CDK16 interacts directly with COPII complexes modulating secretory cargo transport.

Annexin 2 (AnxA2) is a lipid raft associated trafficking factor in the plasma membrane and the endosomal system, related to both endo- and exocytosis [57]. Binding of AnxA2 to phospholipids in a Ca^{2+} -dependent manner [58], generating microdomains suitable for the binding of membrane proteins, such as the renal cotransporter NKCC2 [59]. AnxA2 has been shown to interact with fibroblast growth factor 1 (FGF1) (Table S1), forming heterooligomers capable of interacting with acidic membrane lipids, such as PA. Viral infection hijacks AnxA2, which is used for the virus advantage in cell-attachment, replication, and proliferation processes [60]; thus, AnxA2 is a likely candidate protein to play a role in the TRPV4-DDX3X mechanism in viral infectivity [22].

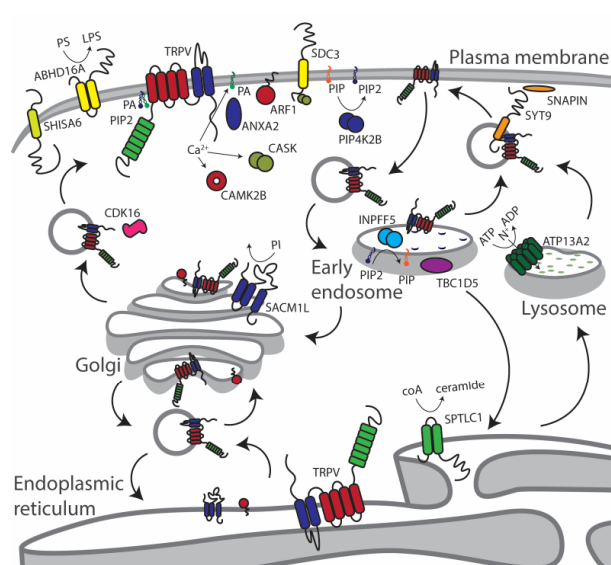


Figure 2. Cellular overview of the main TRPV2 and TRPV4 trafficking-related protein–protein interactions (PPIs) organized by cellular compartment (see main text for details).

The ADP-ribosylation factor (Arf) small G proteins, such as Arf1, are related to lipid droplet metabolism, clathrin independent endocytosis, and other membrane dynamics processes [61–63]. N-terminus miristoylated Arf1 only tethers to the membrane when bound to guanosine triphosphate (GTP) [64]. Guanine exchange factors (GEF) and GTPase activating proteins (GAP) are required by Arfs. Hydrolysis of GTP by Arf and Arf-like proteins regulate the enzymatic activity of proteins, such as PI kinases and phosphatases. Among the TRPV2 interactors, Phosphatidylinositol-5-phosphatase 4-kinase type 2 beta (PIP4K2B), inositol polyphosphate-5-phosphatase F (INPP5F, also known as Sac2), and SAC1 like phosphatidylinositol phosphatase (SACM1L, also known as Sac1) are enzymes involved in phosphoinositide regulation as signals for membrane traffic. The Arf1 pathway is related to phospholipase D (PLD), which is responsible for the production of phosphatidic acid as a signaling molecule, shown to interact with TRPV channels [37,42]. The Arf1–PLD pathways are responsible for vesicle-mediated endocytosis and exocytosis, as well as the formation of multivesicular bodies (MVBs) through phosphoinositides binding/signaling [45]. The putative interaction between TRPV2 and Arf1 is an important hint regarding vesicle-mediated constitutive trafficking of TRPV channels. Other proteins that could be related to the Arf1 pathway, identified as TRPV2 and TRPV4 interactions, are Arl15 (Arf-like protein) and the CALM/CamK2B/Cask subset, respectively (Table S1 and Table 1).

Enzymes involved in phosphoinositide regulation are TRPV2/TRPV4 interactors, such as PIP4K2B and the SACM1L and INPP5F pair, Sac1 and Sac2, respectively. The kinase PIP4K2B regulates the levels of phosphatidylinositol 5-phosphate (PI5P) [65] by converting it to phosphatidylinositol 4,5-bisphosphate (PI(4,5)P2), a lipid involved in TRPV2 and TRPV4 function [6,41]. The non-abundant PI5P phosphoinositide is related to the Akt kinase pathway and relevant for several cellular processes, such as survival and cell growth, with a prominent role in cancer [66]. Hydrolysis of phosphatidylinositol 3-phosphate (PI3P), phosphatidylinositol 4-phosphate (PI4P), and phosphatidylinositol 3,5-bisphosphate (PI(3,5)P2) is carried out by SACM1L/Sac1, which is enriched at the Golgi membrane, but is also present in ER membranes [67]. The preferential substrate for this enzyme is PI4P. The spatial distribution of

PI4P in Golgi is defined by SACM1L/Sac1, creating the optimal conditions to maintain the cisternal identity of the Golgi, which is critical to membrane protein trafficking [68]. Inositol polyphosphate-5-phosphatase F (INPP5F, also known as Sac2) has a specific activity for PI(4,5)P₂ and phosphatidylinositol 3,4,5-trisphosphate (PI(3,4,5)P₃) to generate PI4P and PI(3,4)P₂. INPP5F/Sac2 colocalizes with early endosomal markers and is related to the regulation of endocytic recycling [69].

The ATPase cation transporting 13A2 (ATP13A2 or PARK9) is an endo-/lysosomal associated ATPase related to intracellular trafficking under proteotoxic stress [70]. In a MYTH-based proteomics approach [71], the authors have identified 43 PARK9-interacting proteins related to trafficking. The putative TRPV4-PARK9 and the TRPV2-INPP5F interactions identified in studies [21,22] could be interesting to understand TRPV channels recycling in the endosome/lysosome pathways.

Syndecan-3 (SDC3) is a heparan-sulfate proteoglycan and a TRPV2 interactor, related to leukocyte migration [72]. Modification of cytoskeleton is carried out by SDC3, but no relationship between SDC3 and membrane protein trafficking has been shown so far. However, SDC4 modulates the activity and membrane expression of TRPC6 in glomerular permeabilization [73].

The trafficking of AMPA receptors towards the synapse has been thoroughly studied [74], and among the proteins involved in locating AMPA receptors at the synapse, SHISA6 is found as a TRPV2 interactor. The C-terminal characteristic PDZ domain in SHISA6 binds to post-synaptic density protein 95 (PSD95), which confines AMPA receptors at the postsynaptic density [75]. Proteins, such as SHISA6, ABHD16A, Snapin, and SYT9 (Snapin and SYT9 revised earlier), interact with TRPV channels, mediating synaptic exocytosis, suggesting conservation of some elements in regulated exocytosis of TRPV channels [21,36,37,46].

The TRPV4 interactor serine palmitoyltransferase long chain base subunit 1 (SPTLC1), which resides in the ER, drives the synthesis of sphingomyelin [76], sphingolipid that needs to be trafficked to the plasma membrane. Specific lipid composition in membrane domains may argue for the need of specific lipids bound to TRPV channels during trafficking. SPTLC1, teaming up with ORMDL3, are involved in ceramide synthesis [77,78], in response to ER stress and calcium homeostasis, factors influencing the trafficking of membrane proteins, such as TRPV channels.

The TBC1 domain family member 5 (TBC1D5) plays a significant role in the regulation of the endosomal pathway. TBC1D5 interacts with TRPV4 in a yeast two-hybrid approach [22]. In the endosomal system, TBC1D5 inhibits the retromer and promoting autophagy. It is also a key factor in membrane turnover and membrane protein recycling through Rab7 [79]. The Rab7 and TRPV2 pair has been shown to colocalize in the endosome. As a result of such a trafficking situation, TRPV2 relates to nervous system development by enhancing neurite outgrowth [48]. Among TRPV channels, TRPV2 is the most likely to play a role in the regulation of the endosomal pathway [80].

5. Concluding Remarks

This revision of the literature aims toward a better understanding of the mechanisms driving the trafficking of TRPV2 and TRPV4 to specific membrane compartments, derived from a guilt-by-association approach based on PPI (Table S1). The interaction of TRPV2 and TRPV4 with lipids and/or with lipid modifying enzymes points to the fact that the lipid environment is fundamental for TRPV2 and TRPV4 trafficking, beyond the TRPV2 and TRPV4 lipid requirement for ion channel function. Future perspectives should include the study of the tight inactivation mechanisms of ion channels involved in the trafficking of these proteins, to prevent cation leakage inside the cell. In the case of TRPV2 and TRPV4 (and other TRP channels), the focus so far has resided on which lipid signaling molecules activate/inhibit the channel at the site of function. The identification of LPI and PPI interactions preventing cation leakage during trafficking toward avoiding detrimental cell toxicity effects provides another potentially interesting area of study, which may be especially relevant in tissues under high stretch stress conditions, such as skeletal and cardiac muscle. Knowledge on how TRPV2 and TRPV4 are specifically trafficked in these tissues might provide invaluable benefits in

the therapeutic management of muscle physiopathology, where cation transport and balance play a cardinal role.

Supplementary Materials: The following are available online at <http://www.mdpi.com/2218-273X/9/12/791/s1>, Table S1. TRPV2 and TRPV4 interactomes.

Author Contributions: Conceptualization P.D.-M., J.E.-B., I.R.D., D.G.Q. and A.P.-M.; writing—original draft preparation, P.D.-M. and A.P.-M.; writing—review and editing, P.D.-M., J.E.-B., I.R.D., D.G.Q. and A.P.-M.

Funding: This work was supported by Marie Curie International Outgoing Fellowship within the 7th European Community Framework Programme (PIOF-GA-2009-237120 to A.P.-M.), a Universitat Autònoma de Barcelona-Programa Banco de Santander Fellowship, and the Spanish Government grant MINECO BFU2017-87843-R to A.P.-M. P.D.-M. was a recipient of an FI fellowship from Generalitat de Catalunya (FI-2013FIB00251). I.R.D. was supported by the Carlos III Health Institute, co-financed with European Union *European Regional Development Funds* (CIBERCV CB16/11/00229), and by the Strategic Plan for research and health innovation (PERIS) (SLT006/17/00029).

Conflicts of Interest: The authors declare no conflict of interest. The funders had no role in the design of the study; in the collection, analyses, or interpretation of data; in the writing of the manuscript; or in the decision to publish the results.

References

1. Nilius, B.; Owsianik, G. The transient receptor potential family of ion channels. *Genome Biol.* **2011**, *12*, 218. [[CrossRef](#)]
2. Ramsey, I.S.; Delling, M.; Clapham, D.E. AN INTRODUCTION TO TRP CHANNELS. *Annu. Rev. Physiol.* **2006**, *68*, 619–647. [[CrossRef](#)] [[PubMed](#)]
3. Gunthorpe, M.J.; Benham, C.D.; Randall, A.; Davis, J.B. The diversity in the vanilloid (TRPV) receptor family of ion channels. *Trends Pharmacol. Sci.* **2002**, *23*, 183–191. [[CrossRef](#)]
4. Shibasaki, K. Physiological significance of TRPV2 as a mechanosensor, thermosensor and lipid sensor. *J. Physiol. Sci.* **2016**, *66*, 359–365. [[CrossRef](#)] [[PubMed](#)]
5. Ho, T.C.; Horn, N.A.; Huynh, T.; Kelava, L.; Lansman, J.B. Evidence TRPV4 contributes to mechanosensitive ion channels in mouse skeletal muscle fibers. *Channels* **2012**, *6*, 246–254. [[CrossRef](#)]
6. Perálvarez-Marín, A.; Doñate-Macian, P.; Gaudet, R. What do we know about the transient receptor potential vanilloid 2 (TRPV2) ion channel? *FEBS J.* **2013**, *280*, 5471–5487. [[CrossRef](#)]
7. Robbins, N.; Koch, S.E.; Rubinstein, J. Targeting TRPV1 and TRPV2 for potential therapeutic interventions in cardiovascular disease. *Transl. Res.* **2013**, *161*, 469–476. [[CrossRef](#)]
8. Sabourin, J.; Cognard, C.; Constantin, B. Regulation by scaffolding proteins of canonical transient receptor potential channels in striated muscle. *J. Muscle Res. Cell Motil.* **2009**, *30*, 289–297. [[CrossRef](#)]
9. Watanabe, H.; Murakami, M.; Ohba, T.; Ono, K.; Ito, H. The pathological role of transient receptor potential channels in heart disease. *Circ. J.* **2009**, *73*, 419–427. [[CrossRef](#)]
10. Lorin, C.; Vögeli, I.; Niggli, E. Dystrophic cardiomyopathy: role of TRPV2 channels in stretch-induced cell damage. *Cardiovasc. Res.* **2015**, *106*, 153–162. [[CrossRef](#)]
11. Jones, S.; Mann, A.; Worley, M.C.; Fulford, L.; Hall, D.; Karani, R.; Jiang, M.; Robbins, N.; Rubinstein, J.; Koch, S.E. The role of transient receptor potential vanilloid 2 channel in cardiac aging. *Aging Clin. Exp. Res.* **2017**, *29*, 863–873. [[CrossRef](#)] [[PubMed](#)]
12. Aguetaz, E.; Bois, P.; Cognard, C.; Sebillé, S. Stretch-activated TRPV2 channels: Role in mediating cardiopathies. *Prog. Biophys. Mol. Biol.* **2017**, *130*, 273–280. [[CrossRef](#)] [[PubMed](#)]
13. Güler, A.D.; Lee, H.; Iida, T.; Shimizu, I.; Tominaga, M.; Caterina, M. Heat-evoked activation of the ion channel, TRPV4. *J. Neurosci.* **2002**, *22*, 6408–6414. [[CrossRef](#)] [[PubMed](#)]
14. Liedtke, W.; Choe, Y.; Martí-Renom, M.A.; Bell, A.M.; Denis, C.S.; AndrejŠali; Hudspeth, A.J.; Friedman, J.M.; Heller, S. Vanilloid Receptor–Related Osmotically Activated Channel (VR-OAC), a Candidate Vertebrate Osmoreceptor. *Cell* **2000**, *103*, 525–535. [[CrossRef](#)]
15. Suzuki, M.; Mizuno, A.; Kodaira, K.; Imai, M. Impaired pressure sensation in mice lacking TRPV4. *J. Biol. Chem.* **2003**, *278*, 22664–22668. [[CrossRef](#)] [[PubMed](#)]
16. Velilla, J.; Marchetti, M.M.; Toth-Petroczy, A.; Grosogoeat, C.; Bennett, A.H.; Carmichael, N.; Estrella, E.; Darras, B.T.; Frank, N.Y.; Krier, J.; et al. Homozygous TRPV4 mutation causes congenital distal spinal muscular atrophy and arthrogryposis. *Neurol. Genet.* **2019**, *5*, e312. [[CrossRef](#)]

17. Verma, P.; Kumar, A.; Goswami, C. TRPV4-mediated channelopathies. *Channels* **2010**, *4*, 319–328. [[CrossRef](#)]
18. Lei, L.; Cao, X.; Yang, F.; Shi, D.J.; Tang, Y.Q.; Zheng, J.; Wang, K. A TRPV4 channel C-terminal folding recognition domain critical for trafficking and function. *J. Biol. Chem.* **2013**, *288*, 10427–10439. [[CrossRef](#)]
19. Jones, J.L.; Peana, D.; Veteto, A.B.; Lambert, M.D.; Nourian, Z.; Karasheva, N.G.; Hill, M.A.; Lindman, B.R.; Baines, C.P.; Krenz, M.; et al. TRPV4 increases cardiomyocyte calcium cycling and contractility yet contributes to damage in the aged heart following hypoosmotic stress. *Cardiovasc. Res.* **2019**, *115*, 46–56. [[CrossRef](#)]
20. Cohen, M.R.; Huynh, K.W.; Cawley, D.; Moiseenkova-Bell, V.Y. Understanding the cellular function of TRPV2 channel through generation of specific monoclonal antibodies. *PLoS ONE* **2013**, *8*, e85392. [[CrossRef](#)]
21. Doñate-Macián, P.; Gómez, A.; Dégano, I.R.; Perálvarez-Marín, A. A TRPV2 interactome-based signature for prognosis in glioblastoma patients. *Oncotarget* **2018**, *9*, 18400–18409. [[CrossRef](#)] [[PubMed](#)]
22. Doñate-Macián, P.; Jungfleisch, J.; Pérez-Vilaró, G.; Rubio-Moscardo, F.; Perálvarez-Marín, A.; Diez, J.; Valverde, M.A. The TRPV4 channel links calcium influx to DDX3X activity and viral infectivity. *Nat. Commun.* **2018**, *9*, 1–13. [[CrossRef](#)] [[PubMed](#)]
23. Doñate-Macián, P.; Bañó-Polo, M.; Vázquez-Ibar, J.-L.; Mingarro, I.; Perálvarez-Marín, A. Molecular and topological membrane folding determinants of transient receptor potential vanilloid 2 channel. *Biochem. Biophys. Res. Commun.* **2015**, *462*, 221–226. [[CrossRef](#)] [[PubMed](#)]
24. Doñate-Macián, P.; Perálvarez-Marín, A. Dissecting domain-specific evolutionary pressure profiles of transient receptor potential vanilloid subfamily members 1 to 4. *PLoS ONE* **2014**, *9*, e110715. [[CrossRef](#)] [[PubMed](#)]
25. Huynh, K.W.; Cohen, M.R.; Jiang, J.; Samanta, A.; Lodowski, D.T.; Zhou, Z.H.; Moiseenkova-Bell, V.Y. Structure of the full-length TRPV2 channel by cryo-EM. *Nat Commun* **2016**, *7*, 11130. [[CrossRef](#)] [[PubMed](#)]
26. Cayouette, S.; Boulay, G. Intracellular trafficking of TRP channels. *Cell Calcium* **2007**, *42*, 225–232. [[CrossRef](#)]
27. De Groot, T.; Van Der Hagen, E.A.E.; Verkaar, S.; Te Boekhorst, V.A.M.; Bindels, R.J.M.; Hoenderop, J.G.J. Role of the transient receptor potential vanilloid 5 (TRPV5) protein N terminus in channel activity, tetramerization, and trafficking. *J. Biol. Chem.* **2011**, *286*, 32132–32139. [[CrossRef](#)]
28. Wang, Y.; Fu, X.; Gaiser, S.; Köttgen, M.; Kramer-Zucker, A.; Walz, G.; Wegierski, T. OS-9 regulates the transit and polyubiquitination of TRPV4 in the endoplasmic reticulum. *J. Biol. Chem.* **2007**, *282*, 36561–36570. [[CrossRef](#)]
29. Cuajungco, M.P.; Grimm, C.; Oshima, K.; D’Hoedt, D.; Nilius, B.; Mensenkamp, A.R.; Bindels, R.J.M.; Plomann, M.; Heller, S. PACSINs bind to the TRPV4 cation channel: PACSIN 3 modulates the subcellular localization of TRPV4. *J. Biol. Chem.* **2006**, *281*, 18753–18762. [[CrossRef](#)]
30. Becker, D.; Müller, M.; Leuner, K.; Jendrach, M. The C-terminal domain of TRPV4 is essential for plasma membrane localization. *Mol. Membr. Biol.* **2008**, *25*, 139–151. [[CrossRef](#)]
31. Jin, X.; Touhey, J.; Gaudet, R. Structure of the N-terminal ankyrin repeat domain of the TRPV2 ion channel. *J. Biol. Chem.* **2006**, *281*, 25006–25010. [[CrossRef](#)] [[PubMed](#)]
32. Arniges, M.; Fernández-Fernández, J.M.; Albrecht, N.; Schaefer, M.; Valverde, M.A. Human TRPV4 channel splice variants revealed a key role of ankyrin domains in multimerization and trafficking. *J. Biol. Chem.* **2006**, *281*, 1580–1586. [[CrossRef](#)] [[PubMed](#)]
33. Garcia-Elias, A.; Berna-Erro, A.; Rubio-Moscardo, F.; Pardo-Pastor, C.; Mrkonjić, S.; Sepúlveda, R.V.; Vicente, R.; González-Nilo, F.; Valverde, M.A. Interaction between the Linker, Pre-S1, and TRP Domains Determines Folding, Assembly, and Trafficking of TRPV Channels. *Structure* **2015**, 1–10. [[CrossRef](#)] [[PubMed](#)]
34. Ramakrishnan, N.A.; Drescher, M.J.; Drescher, D.G. The SNARE complex in neuronal and sensory cells. *Mol. Cell. Neurosci.* **2012**, *50*, 58–69. [[CrossRef](#)] [[PubMed](#)]
35. Moreau, K.; Ravikumar, B.; Renna, M.; Puri, C.; Rubinsztein, D.C. Autophagosome precursor maturation requires homotypic fusion. *Cell* **2011**, *146*, 303–317. [[CrossRef](#)] [[PubMed](#)]
36. Morenilla-Palao, C.; Planells-Cases, R.; García-Sanz, N.; Ferrer-Montiel, A. Regulated exocytosis contributes to protein kinase C potentiation of vanilloid receptor activity. *J. Biol. Chem.* **2004**, *279*, 25665–25672. [[CrossRef](#)]
37. Doñate-Macián, P.; Álvarez-Marimón, E.; Sepulcre, F.; Vázquez-Ibar, J.L.; Perálvarez-Marín, A. The Membrane Proximal Domain of TRPV1 and TRPV2 Channels Mediates Protein–Protein Interactions and Lipid Binding In Vitro. *Int. J. Mol. Sci.* **2019**, *20*, 682. [[CrossRef](#)]
38. Prescott, E.D.; Julius, D. A modular PIP2 binding site as a determinant of capsaicin receptor sensitivity. *Science (80-.)*. **2003**, *300*, 1284–1288. [[CrossRef](#)]

39. Mercado, J.; Gordon-Shaag, A.; Zagotta, W.N.; Gordon, S.E. Ca²⁺-dependent desensitization of TRPV2 channels is mediated by hydrolysis of phosphatidylinositol 4,5-bisphosphate. *J. Neurosci.* **2010**, *30*, 13338–13347. [[CrossRef](#)]
40. Doerner, J.F.; Hatt, H.; Ramsey, I.S. Voltage- and temperature-dependent activation of TRPV3 channels is potentiated by receptor-mediated PI(4,5)P₂ hydrolysis. *J. Gen. Physiol.* **2011**, *137*, 271–288. [[CrossRef](#)]
41. Garcia-Elias, A.; Mrkonjić, S.; Pardo-Pastor, C.; Inada, H.; Hellmich, U.A.; Rubio-Moscardó, F.; Plata, C.; Gaudet, R.; Vicente, R.; Valverde, M.A. Phosphatidylinositol-4,5-bisphosphate-dependent rearrangement of TRPV4 cytosolic tails enables channel activation by physiological stimuli. *Proc. Natl. Acad. Sci.* **2013**, *110*, 9553–9558. [[CrossRef](#)] [[PubMed](#)]
42. Nieto-Posadas, A.; Picazo-juárez, G.; Llorente, I.; Jara-oseguera, A.; Morales-Lázaro, S.; Escalante-Alcalde, D.; Islas, L.D.; Rosenbaum, T. Lysophosphatidic acid directly activates TRPV1 through a C-terminal binding site. *Nat. Chem. Biol.* **2012**, *8*, 78–85. [[CrossRef](#)] [[PubMed](#)]
43. Snider, J.; Kittanakom, S.; Damjanovic, D.; Curak, J.; Wong, V.; Stagljar, I. Detecting interactions with membrane proteins using a membrane two-hybrid assay in yeast. *Nat. Protoc.* **2010**, *5*, 1281–1293. [[CrossRef](#)] [[PubMed](#)]
44. Chun, J.N.; Lim, J.M.; Kang, Y.; Kim, E.H.; Shin, Y.-C.; Kim, H.-G.; Jang, D.; Kwon, D.; Shin, S.-Y.; So, I.; et al. A network perspective on unraveling the role of TRP channels in biology and disease. *Pflügers Arch. - Eur. J. Physiol.* **2014**, *466*, 173–182. [[CrossRef](#)]
45. Krauß, M.; Haucke, V. Phosphoinositides: Regulators of membrane traffic and protein function. *FEBS Lett.* **2007**, *581*, 2105–2111. [[CrossRef](#)]
46. Ferrandiz-Huertas, C.; Mathivanan, S.; Wolf, C.J.; Devesa, I.; Ferrer-Montiel, A. Trafficking of ThermoTRP Channels. *Membranes* **2014**, *4*, 525–564. [[CrossRef](#)]
47. Stokes, A.J.; Shimoda, L.M.N.; Koblan-Huberson, M.; Adra, C.N.; Turner, H. A TRPV2-PKA signaling module for transduction of physical stimuli in mast cells. *J. Exp. Med.* **2004**, *200*, 137–147. [[CrossRef](#)]
48. Cohen, M.R.; Johnson, W.M.; Pilat, J.M.; Kiselar, J.; DeFrancesco-Lisowitz, A.; Zigmond, R.E.; Moiseenkova-Bell, V.Y. Nerve Growth Factor Regulates Transient Receptor Potential Vanilloid 2 via Extracellular Signal-Regulated Kinase Signaling To Enhance Neurite Outgrowth in Developing Neurons. *Mol. Cell. Biol.* **2015**, *35*, 4238–4252. [[CrossRef](#)]
49. Xu, J.; Gu, W.; Ji, K.; Xu, Z.; Zhu, H.; Zheng, W. Sequence analysis and structure prediction of ABHD16A and the roles of the ABHD family members in human disease. *Open Biol.* **2018**, *8*, 180017. [[CrossRef](#)]
50. Yokoi, N.; Fukata, Y.; Sekiya, A.; Murakami, T.; Kobayashi, K.; Fukata, M. Identification of PSD-95 Depalmitoylating Enzymes. *J. Neurosci.* **2016**, *36*, 6431–6444. [[CrossRef](#)]
51. Herring, B.E.; Nicoll, R.A. Long-Term Potentiation: From CaMKII to AMPA Receptor Trafficking. *Annu. Rev. Physiol.* **2016**, *78*, 351–365. [[CrossRef](#)] [[PubMed](#)]
52. Kristensen, A.S.; Jenkins, M.A.; Banke, T.G.; Schousboe, A.; Makino, Y.; Johnson, R.C.; Huganir, R.; Traynelis, S.F. Mechanism of Ca²⁺/calmodulin-dependent kinase II regulation of AMPA receptor gating. *Nat. Neurosci.* **2011**, *14*, 727–735. [[CrossRef](#)] [[PubMed](#)]
53. Yan, J.-Z.; Xu, Z.; Ren, S.-Q.; Hu, B.; Yao, W.; Wang, S.-H.; Liu, S.-Y.; Lu, W. Protein kinase C promotes N-methyl-D-aspartate (NMDA) receptor trafficking by indirectly triggering calcium/calmodulin-dependent protein kinase II (CaMKII) autophosphorylation. *J. Biol. Chem.* **2011**, *286*, 25187–25200. [[CrossRef](#)] [[PubMed](#)]
54. Liu, Y.; Cheng, K.; Gong, K.; Fu, A.K.Y.; Ip, N.Y. Pctaire1 phosphorylates N-ethylmaleimide-sensitive fusion protein: implications in the regulation of its hexamerization and exocytosis. *J. Biol. Chem.* **2006**, *281*, 9852–9858. [[CrossRef](#)]
55. Palmer, K.J.; Konkel, J.E.; Stephens, D.J. PCTAIRE protein kinases interact directly with the COPII complex and modulate secretory cargo transport. *J. Cell Sci.* **2005**, *118*, 3839–3847. [[CrossRef](#)]
56. Dixon-Clarke, S.E.; Shehata, S.N.; Krojer, T.; Sharpe, T.D.; von Delft, F.; Sakamoto, K.; Bullock, A.N. Structure and inhibitor specificity of the PCTAIRE-family kinase CDK16. *Biochem. J.* **2017**, *474*, 699–713. [[CrossRef](#)]
57. Rescher, U.; Gerke, V. Annexins - Unique membrane binding proteins with diverse functions. *J. Cell Sci.* **2004**, *117*, 2631–2639. [[CrossRef](#)]
58. Gerke, V.; Creutz, C.E.; Moss, S.E. Annexins: linking Ca²⁺ signalling to membrane dynamics. *Nat. Rev. Mol. Cell Biol.* **2005**, *6*, 449–461. [[CrossRef](#)]

59. Dathe, C.; Daigeler, A.L.; Seifert, W.; Jankowski, V.; Mrowka, R.; Kalis, R.; Wanker, E.; Mutig, K.; Bachmann, S.; Paliege, A. Annexin A2 mediates apical trafficking of renal Na⁺-K⁺ +2Cl⁻ Cotransporter. *J. Biol. Chem.* **2014**, *289*, 9983–9997. [[CrossRef](#)]
60. Taylor, J.R.; Skeate, J.G.; Martin Kast, W. Annexin A2 in virus infection. *Front. Microbiol.* **2018**, *9*, 1–8. [[CrossRef](#)]
61. Kaczmarek, B.; Verbavatz, J.M.; Jackson, C.L. GBF1 and Arf1 function in vesicular trafficking, lipid homeostasis and organelle dynamics. *Biol. Cell* **2017**, *109*, 391–399. [[CrossRef](#)] [[PubMed](#)]
62. Yorimitsu, T.; Sato, K.; Takeuchi, M. Molecular mechanisms of Sar/Arf GTPases in vesicular trafficking in yeast and plants. *Front. Plant Sci.* **2014**, *5*, 1–12. [[CrossRef](#)] [[PubMed](#)]
63. Price, H.P.; Stark, M.; Smith, D.F. *Trypanosoma brucei* ARF1 Plays a Central Role in Endocytosis and Golgi–Lysosome Trafficking. *Mol. Biol. Cell* **2007**, *18*, 864–873. [[CrossRef](#)] [[PubMed](#)]
64. Liu, Y.; Kahn, R.A.; Prestegard, J.H. Dynamic structure of membrane-anchored Arf*GTP. *Nat. Struct. Mol. Biol.* **2010**, *17*, 876–881. [[CrossRef](#)]
65. Bulley, S.J.; Clarke, J.H.; Droubi, A.; Giudici, M.-L.; Irvine, R.F. Exploring phosphatidylinositol 5-phosphate 4-kinase function. *Adv. Biol. Regul.* **2015**, *57*, 193–202. [[CrossRef](#)]
66. Mahajan, K.; Mahajan, N.P. PI3K-independent AKT activation in cancers: a treasure trove for novel therapeutics. *J. Cell. Physiol.* **2012**, *227*, 3178–3184. [[CrossRef](#)]
67. Del Bel, L.M.; Brill, J.A. Sac1, a lipid phosphatase at the interface of vesicular and nonvesicular transport. *Traffic* **2018**, *19*, 301–318. [[CrossRef](#)]
68. Blagoveshchenskaya, A.; Cheong, F.Y.; Rohde, H.M.; Glover, G.; Knödler, A.; Nicolson, T.; Boehmelt, G.; Mayinger, P. Integration of Golgi trafficking and growth factor signaling by the lipid phosphatase SAC1. *J. Cell Biol.* **2008**, *180*, 803–812. [[CrossRef](#)]
69. Hsu, F.; Hu, F.; Mao, Y. Spatiotemporal control of phosphatidylinositol 4-phosphate by Sac2 regulates endocytic recycling. *J. Cell Biol.* **2015**, *209*, 97–110. [[CrossRef](#)]
70. Demirsoy, S.; Martin, S.; Motamedi, S.; van Veen, S.; Holemans, T.; Van den Haute, C.; Jordanova, A.; Baekelandt, V.; Vangheluwe, P.; Agostinis, P. ATP13A2/PARK9 regulates endo-/lysosomal cargo sorting and proteostasis through a novel PI(3,5)P2-mediated scaffolding function. *Hum. Mol. Genet.* **2017**, *26*, 1656–1669. [[CrossRef](#)]
71. Usenovic, M.; Knight, A.L.; Ray, A.; Wong, V.; Brown, K.R.; Caldwell, G.A.; Caldwell, K.A.; Stagljar, I.; Krainc, D. Identification of novel ATP13A2 interactors and their role in α -synuclein misfolding and toxicity. *Hum. Mol. Genet.* **2012**, *21*, 3785–3794. [[CrossRef](#)] [[PubMed](#)]
72. Kehoe, O.; Kalia, N.; King, S.; Eustace, A.; Boyes, C.; Reizes, O.; Williams, A.; Patterson, A.; Middleton, J. Syndecan-3 is selectively pro-inflammatory in the joint and contributes to antigen-induced arthritis in mice. *Arthritis Res. Ther.* **2014**, *16*, 1–14. [[CrossRef](#)] [[PubMed](#)]
73. Liu, Y.; Echtermeyer, F.; Thilo, F.; Theilmeier, G.; Schmidt, A.; Schüle, R.; Jensen, B.L.; Lodenkemper, C.; Jankowski, V.; Marcussen, N.; et al. The proteoglycan syndecan 4 regulates transient receptor potential canonical 6 channels via RhoA/rho-associated protein kinase signaling. *Arterioscler. Thromb. Vasc. Biol.* **2012**, *32*, 378–385. [[CrossRef](#)] [[PubMed](#)]
74. Bissen, D.; Foss, F.; Acker-Palmer, A. AMPA receptors and their minions: auxiliary proteins in AMPA receptor trafficking. *Cell Mol. Life Sci.* **2019**, *76*, 2133–2169. [[CrossRef](#)] [[PubMed](#)]
75. Klaassen, R.V.; Stroeder, J.; Coussen, F.; Hafner, A.-S.; Petersen, J.D.; Renancio, C.; Schmitz, L.J.M.; Normand, E.; Lodder, J.C.; Rotaru, D.C.; et al. Shisa6 traps AMPA receptors at postsynaptic sites and prevents their desensitization during synaptic activity. *Nat. Commun.* **2016**, *7*, 10682. [[CrossRef](#)] [[PubMed](#)]
76. Breslow, D.K. Sphingolipid homeostasis in the endoplasmic reticulum and beyond. *Cold Spring Harb. Perspect. Biol.* **2013**, *5*, a013326. [[CrossRef](#)]
77. Kiefer, K.; Carreras-Sureda, A.; García-López, R.; Rubio-Moscardó, F.; Casas, J.; Fabriàs, G.; Vicente, R. Coordinated regulation of the orosomucoid-like gene family expression controls de novo ceramide synthesis in mammalian cells. *J. Biol. Chem.* **2015**, *290*, 2822–2830. [[CrossRef](#)]
78. Kiefer, K.; Casas, J.; García-López, R.; Vicente, R. Ceramide imbalance and impaired TLR4-mediated autophagy in BMDM of an ORMDL3-Overexpressing mouse model. *Int. J. Mol. Sci.* **2019**, *20*. [[CrossRef](#)]

79. Wang, J.; Fedoseienko, A.; Chen, B.; Burstein, E.; Jia, D.; Billadeau, D.D. Endosomal receptor trafficking: Retromer and beyond. *Traffic* **2018**, *19*, 578–590. [[CrossRef](#)]
80. Abe, K.; Puertollano, R. Role of TRP Channels in the Regulation of the Endosomal Pathway. *Physiology* **2011**, *26*, 14–22. [[CrossRef](#)]



© 2019 by the authors. Licensee MDPI, Basel, Switzerland. This article is an open access article distributed under the terms and conditions of the Creative Commons Attribution (CC BY) license (<http://creativecommons.org/licenses/by/4.0/>).

Supplementary information

TRPV4	transient receptor potential cation channel, subfamily V, member 4 [Source:HGNC Symbol;Acc:18083]	plasma membrane	M	L	L	Yes		
MYTH	FGF6	fibroblast growth factor 6 [Source:HGNC Symbol;Acc:3684]	extracellular/secreted	n	n	n	Yes	
MYTH	ATP13A2	ATPase type 13A2 [Source:HGNC Symbol;Acc:30213]	lysosomal lumen	M	M	M	Yes	
MYTH	PEX19	peroxisomal biogenesis factor 19 [Source:HGNC Symbol;Acc:9713]	cytosol & peroxisome	H	L	L	Yes	
MYTH	MBP	myelin basic protein [Source:HGNC Symbol;Acc:6925]	plasma membrane	n	n	n	No	
MYTH	HNRNPUL2	heterogeneous nuclear ribonucleoprotein U-like 2 [Source:HGNC Symbol;Acc:25451]	nucleus	M	M	L	Yes	
MYTH	TBC1D5	TBC1 domain family, member 5 [Source:HGNC Symbol;Acc:19166]	endosome membrane	L	M	M	Yes	
MYTH	CAMK2B	calcium/calmodulin-dependent protein kinase II beta [Source:HGNC Symbol;Acc:1461]	cytosol & nucleus	M	L	n	Yes	
MYTH	FEZF2	FEZ family zinc finger 2 [Source:HGNC Symbol;Acc:13506]	nucleus	n	n	n	No	
MYTH	ZFP3B1	ZFP36 ring finger protein-like 1 [Source:HGNC Symbol;Acc:1107]	nucleus	n	n	n	Yes	
MYTH	ACO2	acortitase 2, mitochondrial [Source:HGNC Symbol;Acc:118]	cytosol & mitochondrion	H	M	M	Yes	
MYTH	NMD3	NMD3 ribosome export adaptor [Source:HGNC Symbol;Acc:24250]	nucleus	n	n	n	Yes	
MYTH	RHOA	ras homolog family member A [Source:HGNC Symbol;Acc:167]	plasma membrane & cytosol	L	L	L	Yes	
MYTH	GFAP	glial fibrillary acidic protein [Source:HGNC Symbol;Acc:4235]	cytosol & lysosomal membrane	n	n	n	No	
MYTH	ARHGEF11	Rho guanine nucleotide exchange factor (GEF) 11 [Source:HGNC Symbol;Acc:14580]	cytosol	H	M	H	Yes	
MYTH	IFNAR1	interferon (alpha, beta and omega) receptor 1 [Source:HGNC Symbol;Acc:5432]	plasma membrane, lysosome & endosome	n	n	n	Yes	
MYTH	CALM3	calmodulin 3 (phosphorylase kinase, delta) [Source:HGNC Symbol;Acc:1449]	cytosol & nucleus	n	n	L	Yes	
MYTH	SPILC1	serine palmitoyltransferase, long chain base subunit 1 [Source:HGNC Symbol;Acc:11277]	endoplasmic reticulum membrane	L	M	n	Yes	
MYTH	GIPC3	GIPC PDZ domain containing family, member 3 [Source:HGNC Symbol;Acc:18183]	n	L	L	Yes		
MYTH	CDH6	cadherin 6, type 2, K-cadherin (fetal kidney) [Source:HGNC Symbol;Acc:1765]	plasma membrane	M	M	n	Yes	
MYTH	PRKAR1A	protein kinase, cAMP-dependent, regulatory, type I, alpha [Source:HGNC Symbol;Acc:9388]	plasma membrane	M	n	n	Yes	
MYTH	CASK	calcium/calmodulin-dependent serine protein kinase (MAGUK family) [Source:HGNC Symbol;Acc:1497]	plasma membrane & cytosol	L	M	M	Yes	
MYTH	RGPD2	RANBP2-like and GRIP domain containing 2 [Source:HGNC Symbol;Acc:32415]	nucleus	n	n	n	No	
MYTH	EEA1	early endosome antigen 1 [Source:HGNC Symbol;Acc:3185]	endosome membrane	L	L	n	Yes	
MYTH	CDK16	cyclin-dependent kinase 16 [Source:HGNC Symbol;Acc:8749]	plasma membrane & cytosol	M	M	L	Yes	
MYTH	MT-CO1	mitochondrially encoded cytochrome c oxidase I [Source:HGNC Symbol;Acc:7419]	mitochondrion	H	M	H	Yes	
MYTH	SLC6A8	solute carrier family 6 (neurotransmitter transporter), member 8 [Source:HGNC Symbol;Acc:11055]	plasma membrane	n	n	n	Yes	
MYTH	NCKAP1	NCK-associated protein 1 [Source:HGNC Symbol;Acc:7666]	plasma membrane & cytosol	M	L	L	Yes	
MYTH	APOD	apolipoprotein D [Source:HGNC Symbol;Acc:631]	extracellular/secreted	L	n	n	Yes	
MYTH	OR4F5	olfactory receptor, family 4, subfamily F, member 5 [Source:HGNC Symbol;Acc:14825]	plasma membrane	n	n	n	No	
MYTH	EIF6	eukaryotic translation initiation factor 6 [Source:HGNC Symbol;Acc:6159]	cytosol & nucleus	M	n	n	Yes	
MYTH	SNURF	SNRNP upstream reading frame [Source:HGNC Symbol;Acc:11171]	nucleus	n	n	n	Yes	
MYTH	ANXA2	annexin A2 [Source:HGNC Symbol;Acc:537]	extracellular/secreted	n	n	n	Yes	
MYTH	FAM47E	family with sequence similarity 47, member E [Source:HGNC Symbol;Acc:34343]	M	H	H	Yes		
MYTH	ABHD16A	abhydrolase domain containing 16A [Source:HGNC Symbol;Acc:13921]	plasma membrane	M	n	n	Yes	
MYTH	DDX3X	DEAD (Asp-Glu-Ala-Asp) box helicase 3, X-linked [Source:HGNC Symbol;Acc:2745]	cytosol & nucleus	H	H	H	Yes	
MYTH	SERF1A	small EDRK-rich factor 1A (telomeric) [Source:HGNC Symbol;Acc:10755]	nucleus	n	n	n	Yes	
MYTH	NSUN3	NOP2/sun domain family, member 3 [Source:HGNC Symbol;Acc:26208]	mitochondrion	n	n	n	Yes	
MYTH	HGD1A	HG1 hypoxia inducible domain family, member 1A [Source:HGNC Symbol;Acc:29527]	mitochondrion inner membrane	M	n	n	Yes	
MYTH	UBAP2L	ubiquitin associated protein 2-like [Source:HGNC Symbol;Acc:29877]	nucleus	n	n	L	Yes	
MYTH	EIF4B	eukaryotic translation initiation factor 4B [Source:HGNC Symbol;Acc:3295]	cytosol	M	M	n	Yes	
MYTH	CPSF1	cleavage and polyadenylation-specific factor 1, 160kDa [Source:HGNC Symbol;Acc:2324]	nucleus	n	n	n	Yes	
MYTH	ALDH9A1	aldehyde dehydrogenase 9 family, member A1 [Source:HGNC Symbol;Acc:412]	cytosol	L	M	L	Yes	
MYTH	MARCH6	membrane-associated ring finger (C3HC4) 6, E3 ubiquitin protein ligase [Source:HGNC Symbol;Acc:30550]	endoplasmic reticulum membrane	n	n	n	Yes	
MYTH	MTNDS	mitochondrially encoded NADH dehydrogenase 5 [Source:HGNC Symbol;Acc:7461]	mitochondrion inner membrane	n	n	n	Yes	
TRIPDB	AKAP5	A kinase (PRKA) anchor protein 5 [Source:HGNC Symbol;Acc:375]	plasma membrane & cytosol	n	n	n	Yes	
TRIPDB	AQP4	aquaporin 4 [Source:HGNC Symbol;Acc:637]	plasma membrane	n	n	n	Yes	

TRIPDB	AQP5	aquaporin 5 [Source:HGNC Symbol;Acc:638]	plasma membrane	n	n	n	No	
TRIPDB	CALM1	calmodulin 1 (phosphorylase kinase, delta) [Source:HGNC Symbol;Acc:1442]	cytosol & nucleus	n	n	L	Yes	
TRIPDB	FYN	FYN oncogene related to SRC, FGR, YES [Source:HGNC Symbol;Acc:4037]	plasma membrane & cytosol	n	n	n	Yes	
TRIPDB	A1BG	alpha-1-B glycoprotein [Source:HGNC Symbol;Acc:5]	granule lumen	n	n	n	No	
TRIPDB	A2M	alpha-2-macroglobulin [Source:HGNC Symbol;Acc:7]	extracellular/secreted	L	n	n	Yes	
TRIPDB	ITCH (AIP4)	itchy E3 ubiquitin protein ligase [Source:HGNC Symbol;Acc:13890]	cytosol	M	H	M	Yes	
TRIPDB	LOK	lymphocyte-specific protein tyrosine kinase [Source:HGNC Symbol;Acc:6204]	plasma membrane & cytosol	n	n	n	No	
TRIPDB	HOK	hemopoietic cell kinase [Source:HGNC Symbol;Acc:4840]	cytosol	n	n	n	Yes	
TRIPDB	ITPR3	inositol 1,4,5-trisphosphate receptor, type 3 [Source:HGNC Symbol;Acc:6182]	endoplasmic reticulum membrane	n	n	n	Yes	
TRIPDB	LYN	v-src-1 Yamaguchi sarcoma viral related oncogene homolog [Source:HGNC Symbol;Acc:6735]	plasma membrane & cytosol	n	n	n	Yes	
TRIPDB	MAP7	microtubule-associated protein 7 [Source:HGNC Symbol;Acc:6869]	plasma membrane & cytosol	L	n	n	Yes	
TRIPDB	OS9	osteosarcoma amplified 9, endoplasmic reticulum lectin [Source:HGNC Symbol;Acc:16994]	endoplasmic reticulum lumen	M	M	M	Yes	degradation
TRIPDB	PACSIN1	protein kinase C and casein kinase substrate in neurons 1 [Source:HGNC Symbol;Acc:8570]	plasma membrane & cytosol	n	n	n	No	
TRIPDB	PACSIN2	protein kinase C and casein kinase substrate in neurons 2 [Source:HGNC Symbol;Acc:8571]	plasma membrane & cytosol	n	n	M	Yes	
TRIPDB	PACSIN3	protein kinase C and casein kinase substrate in neurons 3 [Source:HGNC Symbol;Acc:8572]	plasma membrane & cytosol	M	M	M	Yes	
TRIPDB	RPS27A	ribosomal protein S27a [Source:HGNC Symbol;Acc:10417]	cytosol & nucleus	L	H	H	Yes	
TRIPDB	SRC	v-src avian sarcoma (Schmidt-Ruppin A-2) viral oncogene homolog [Source:HGNC Symbol;Acc:11261]	plasma membrane & cytosol	L	n	L	Yes	
TRIPDB	ANO1	anoctamin 1, calcium activated chloride channel [Source:HGNC Symbol;Acc:21625]	plasma membrane	L	n	n	Yes	
TRIPDB	TRPC1	transient receptor potential cation channel, subfamily C, member 1 [Source:HGNC Symbol;Acc:12333]	plasma membrane	M	M	M	Yes	
TRIPDB	PKD1 (TRPP1)	polycystic kidney disease 1 (autosomal dominant) [Source:HGNC Symbol;Acc:9008]	cytosol & golgi	n	n	n	Yes	
TRIPDB	UBC	ubiquitin C [Source:HGNC Symbol;Acc:12468]	cytosol, endosome & endoplasmic reticulum membrane	L	H	H	Yes	
TRIPDB	YES1 (Yes)	v-yes-1 Yamaguchi sarcoma viral oncogene homolog 1 [Source:HGNC Symbol;Acc:12841]	plasma membrane & cytosol	M	M	L	Yes	
TRIPDB	PRKCSH	protein kinase C substrate 80K-H [Source:HGNC Symbol;Acc:9411]	endoplasmic reticulum	n	n	L	Yes	
TRIPDB	AGTR1	angiotensin II receptor, type 1 [Source:HGNC Symbol;Acc:236]	plasma membrane & clathrin coated vesicles	n	n	n	Yes	
TRIPDB	KCNMA1	potassium large conductance calcium-activated channel, subfamily M, alpha member 1 [Source:HGNC Symbol;Acc:6284]	plasma membrane	n	n	L	Yes	
TRIPDB	CAV1	caveolin 1, caveolae protein, 22kDa [Source:HGNC Symbol;Acc:1522]	plasma membrane, golgi & endocytic vesicle membrane	M	n	M	Yes	
TRIPDB	CDH1	cadherin 1, type 1, E-cadherin (epithelial) [Source:HGNC Symbol;Acc:1748]	plasma membrane & golgi	n	n	n	No	
TRIPDB	MYH10	myosin, heavy chain 10, non-muscle [Source:HGNC Symbol;Acc:7568]	cytosol	L	n	n	Yes	
TRIPDB	POZD3	POZ domain containing 3 [Source:HGNC Symbol;Acc:19891]	plasma membrane	n	n	n	No	
TRIPDB	TUBA1B	tubulin, alpha 1b [Source:HGNC Symbol;Acc:18809]	cytosol	L	n	M	Yes	
TRIPDB	CTNWB1	catenin (cadherin-associated protein), beta 1, 88kDa [Source:HGNC Symbol;Acc:2514]	plasma membrane, cytosol & nucleus	H	n	n	Yes	
TRIPDB	ACTA2	actin, alpha 2, smooth muscle, aorta [Source:HGNC Symbol;Acc:130]	cytosol	n	n	H	Yes	
TRIPDB	ARRB1	arrestin, beta 1 [Source:HGNC Symbol;Acc:711]	plasma membrane, lysosomal & golgi membrane	n	n	L	Yes	
TRIPDB	ARRB2	arrestin, beta 2 [Source:HGNC Symbol;Acc:712]	cytosol	n	n	n	Yes	
TRIPDB	ITGA1	integrin, alpha 1 [Source:HGNC Symbol;Acc:6334]	plasma membrane	M	L	M	Yes	
TRIPDB	PKD2	polycystic kidney disease 2 (autosomal dominant) [Source:HGNC Symbol;Acc:9009]	golgi & golgi-associated vesicle membrane	M	n	n	Yes	
TRIPDB	TRPC3	transient receptor potential cation channel, subfamily C, member 3 [Source:HGNC Symbol;Acc:12335]	plasma membrane	n	n	n	Yes	
TRIPDB	TRPC6	transient receptor potential cation channel, subfamily C, member 6 [Source:HGNC Symbol;Acc:12338]	plasma membrane	L	n	n	Yes	
TRIPDB	TRPM8	transient receptor potential cation channel, subfamily M, member 8 [Source:HGNC Symbol;Acc:17961]	plasma membrane	n	n	n	No	
TRIPDB	PRKCA	protein kinase C, alpha [Source:HGNC Symbol;Acc:9393]	plasma membrane, cytosol & nucleus	M	M	n	Yes	
TRIPDB	PRKCE	protein kinase C, epsilon [Source:HGNC Symbol;Acc:9401]	plasma membrane, cytosol	n	n	L	Yes	
TRIPDB	PRKCD	protein kinase C, delta [Source:HGNC Symbol;Acc:9399]	plasma membrane, cytosol & nucleus	L	L	L	Yes	

n: not detected
H: high
M: medium
L: low

Interactome	Source	GENE	NAME	LOCATION	Expression in heart	Expression in skeletal muscle	Expression in smooth muscle	RNA Exp	Trafficking Go-Terms	Transported Integral membrane proteins	Secreted Proteins
TRPV2	MYTH	TRPV2	transient receptor potential cation channel, subfamily V, member 2 [Source:HGNC Symbol;Acc:18082]	plasma membrane	H	H	H	Yes			
TRPV2	MYTH	FGF1	fibroblast growth factor 1 (acidic) [Source:HGNC Symbol;Acc:3665]	extracellular/secreted	n	n	n	Yes			
TRPV2	MYTH	ST18	suppression of tumorigenicity 18 (breast carcinoma) (zinc finger protein) [Source:HGNC Symbol;Acc:18695]		M	M	H	Yes			
TRPV2	MYTH	ABR	active BCR-related [Source:HGNC Symbol;Acc:81]	cytosol	M	L	L	Yes			
TRPV2	MYTH	KCNJ10	potassium inwardly-rectifying channel, subfamily J, member 10 [Source:HGNC Symbol;Acc:6256]	plasma membrane	n	n	n	No			
TRPV2	MYTH	PEBP1	phosphatidylethanolamine binding protein 1 [Source:HGNC Symbol;Acc:8639]	cytosol	M	L	n	Yes			
TRPV2	MYTH	SLG4A2	solute carrier family 4A (choline transporter), member 2 [Source:HGNC Symbol;Acc:17292]	plasma membrane & granules	n	n	n	Yes			
TRPV2	MYTH	OPALIN	oligodendrocytic myelin paranodal and inner loop protein [Source:HGNC Symbol;Acc:20707]		n	n	n	No			
TRPV2	MYTH	CDH6	cadherin 6, type 2, K-cadherin (fetal kidney) [Source:HGNC Symbol;Acc:1765]	plasma membrane	M	M	n	Yes			
TRPV2	MYTH	INPP5F	inositol polyphosphate-5-phosphatase F [Source:HGNC Symbol;Acc:17054]	early endosome membrane	n	n	n	Yes			
TRPV2	MYTH	PIP4K2B	phosphatidylinositol-4-phosphate 4-kinase, type II, beta [Source:HGNC Symbol;Acc:8998]	cytosol & nucleoplasm	n	n	n	Yes			
TRPV2	MYTH	ARF1	ADP-ribosylation factor 1 [Source:HGNC Symbol;Acc:652]	Golgi & cytosol	L	L	L	Yes			
TRPV2	MYTH	PLP1	proteolipid protein 1 [Source:HGNC Symbol;Acc:9086]	plasma membrane	n	n	n	No			
TRPV2	MYTH	SDC3	syndecan 3 [Source:HGNC Symbol;Acc:10660]	plasma membrane, golgi and lysosomal lumen	M	M	M	Yes			
TRPV2	MYTH	CAONG3	calcium channel, voltage-dependent, gamma subunit 3 [Source:HGNC Symbol;Acc:1407]	plasma membrane & endocytic vesicle	n	n	n	No			
TRPV2	MYTH	PI16	peptidase inhibitor 16 [Source:HGNC Symbol;Acc:21245]	extracellular/secreted	n	M	n	Yes			
TRPV2	MYTH	SACM1L	SAC1 suppressor of actin mutations 1-like (yeast) [Source:HGNC Symbol;Acc:17659]	Endoplasmic reticulum membrane & golgi	M	M	n	Yes			
TRPV2	MYTH	SHS6A	shisa family member 6 [Source:HGNC Symbol;Acc:34491]	plasma membrane	n	n	n	No			
TRPV2	MYTH	ARL15	ADP-ribosylation factor-like 15 [Source:HGNC Symbol;Acc:25945]	extracellular/secreted	L	M	L	Yes			
TRPV2	MYTH	ALDH1A3	aldehyde dehydrogenase 1 family, member A3 [Source:HGNC Symbol;Acc:409]	cytosol	n	n	n	Yes			
TRPV2	MYTH	NTM	neurotrophin [Source:HGNC Symbol;Acc:17941]	plasma membrane	n	n	n	Yes			
TRPV2	MYTH	ACBD3	acyl-CoA binding domain containing 3 [Source:HGNC Symbol;Acc:15453]	Golgi	M	n	M	Yes			
TRPV2	TRIPDB	AKAP5	A kinase (PKA) anchor protein 5 [Source:HGNC Symbol;Acc:175]	plasma membrane & cytosol	n	n	n	Yes			
TRPV2	TRIPDB	SYNE1	spectrin repeat containing, nuclear envelope 1 [Source:HGNC Symbol;Acc:17089]	Golgi, nucleus & cytoskeleton	H	H	H	Yes			
TRPV2	TRIPDB	TRPV1	transient receptor potential cation channel, subfamily V, member 1 [Source:HGNC Symbol;Acc:12716]	plasma membrane	n	n	n	Yes			
TRPV2	TRIPDB	UBC	ubiquitin C [Source:HGNC Symbol;Acc:12468]	endoplasmic reticulum membrane, endosome membrane, endocytic vesicle membrane & cytosol	H	H	H	Yes			
TRPV2	TRIPDB	CALM1	calmodulin 1 (phosphorylase kinase, delta) [Source:HGNC Symbol;Acc:1442]	cytosol & nucleus	n	n	L	Yes			
TRPV2	TRIPDB	PRKACA	protein kinase, cAMP-dependent, catalytic, alpha [Source:HGNC Symbol;Acc:9380]	cytosol & nucleus	M	M	L	Yes			
TRPV2	TRIPDB	IGF1	insulin-like growth factor 1 (somatomedin C) [Source:HGNC Symbol;Acc:5464]	extracellular/secreted	n	n	n	Yes			
TRPV2	TRIPDB	TRPC1	transient receptor potential cation channel, subfamily C, member 1 [Source:HGNC Symbol;Acc:12333]	plasma membrane	M	M	M	Yes			
TRPV2	TRIPDB	TRPC3	transient receptor potential cation channel, subfamily C, member 3 [Source:HGNC Symbol;Acc:12335]	plasma membrane	n	n	n	Yes			
TRPV2	TRIPDB	TRPC6	transient receptor potential cation channel, subfamily C, member 6 [Source:HGNC Symbol;Acc:12338]	plasma membrane	L	n	n	Yes			
TRPV2	TRIPDB	TRPA1	transient receptor potential cation channel, subfamily A, member 1 [Source:HGNC Symbol;Acc:497]	plasma membrane	n	n	n	No			
TRPV2	TRIPDB	TRPM2	transient receptor potential cation channel, subfamily M, member 2 [Source:HGNC Symbol;Acc:12339]	plasma membrane & granule membrane	n	n	n	Yes			
TRPV2	TRIPDB	TRPM3	transient receptor potential cation channel, subfamily M, member 3 [Source:HGNC Symbol;Acc:17992]	plasma membrane	n	n	n	No			
TRPV2	TRIPDB	TRPM4	transient receptor potential cation channel, subfamily M, member 4 [Source:HGNC Symbol;Acc:17993]	plasma membrane	L	n	M	Yes			
TRPV2	TRIPDB	TRPM7	transient receptor potential cation channel, subfamily M, member 7 [Source:HGNC Symbol;Acc:17994]	plasma membrane	n	n	n	Yes			
TRPV2	TRIPDB	TRPM8	transient receptor potential cation channel, subfamily M, member 8 [Source:HGNC Symbol;Acc:17961]	plasma membrane	n	n	n	No			
TRPV2	TRIPDB	SYT9	synaptotagmin IX [Source:HGNC Symbol;Acc:19265]	plasma membrane	n	n	n	No			
TRPV2	TRIPDB	SNAP25	synaptosomal-associated protein, 25kDa [Source:HGNC Symbol;Acc:11132]	plasma membrane	n	n	n	No			

TRIPDB	AQP5	aquaporin 5 [Source:HGNC Symbol;Acc:638]	plasma membrane	n	n	n	No	
TRIPDB	CALM1	calmodulin 1 (phosphorylase kinase, delta) [Source:HGNC Symbol;Acc:1442]	cytosol & nucleus	n	n	L	Yes	
TRIPDB	FYN	FYN oncogene related to SRC, FGR, YES [Source:HGNC Symbol;Acc:4037]	plasma membrane & cytosol	n	n	n	Yes	
TRIPDB	A1BG	alpha-1-B glycoprotein [Source:HGNC Symbol;Acc:5]	granule lumen	n	n	n	No	
TRIPDB	A2M	alpha-2-macroglobulin [Source:HGNC Symbol;Acc:7]	extracellular/secreted	L	n	n	Yes	
TRIPDB	ITCH (AIP4)	itchy E3 ubiquitin protein ligase [Source:HGNC Symbol;Acc:13890]	cytosol	M	H	M	Yes	
TRIPDB	LCK	lymphocyte-specific protein tyrosine kinase [Source:HGNC Symbol;Acc:6204]	plasma membrane & cytosol	n	n	n	No	
TRIPDB	HCK	hemopoietic cell kinase [Source:HGNC Symbol;Acc:4840]	cytosol	n	n	n	Yes	
TRIPDB	ITPR3	inositol 1,4,5-trisphosphate receptor, type 3 [Source:HGNC Symbol;Acc:6182]	endoplasmic reticulum membrane	n	n	n	Yes	
TRIPDB	LYN	v-src-1 Yamaguchi sarcoma viral related oncogene homolog [Source:HGNC Symbol;Acc:6735]	plasma membrane & cytosol	n	n	n	Yes	
TRIPDB	MAP7	microtubule-associated protein 7 [Source:HGNC Symbol;Acc:6869]	plasma membrane & cytosol	L	n	n	Yes	
TRIPDB	OS9	osteosarcoma amplified 9, endoplasmic reticulum lectin [Source:HGNC Symbol;Acc:16994]	endoplasmic reticulum lumen	M	M	M	Yes	degradation
TRIPDB	PACSIN1	protein kinase C and casein kinase substrate in neurons 1 [Source:HGNC Symbol;Acc:8570]	plasma membrane & cytosol	n	n	n	No	
TRIPDB	PACSIN2	protein kinase C and casein kinase substrate in neurons 2 [Source:HGNC Symbol;Acc:8571]	plasma membrane & cytosol	n	n	M	Yes	
TRIPDB	PACSIN3	protein kinase C and casein kinase substrate in neurons 3 [Source:HGNC Symbol;Acc:8572]	plasma membrane & cytosol	M	M	M	Yes	
TRIPDB	RPS27A	ribosomal protein S27a [Source:HGNC Symbol;Acc:10417]	cytosol & nucleus	L	H	H	Yes	
TRIPDB	SRC	v-src avian sarcoma (Schmidt-Ruppin A-2) viral oncogene homolog [Source:HGNC Symbol;Acc:11261]	plasma membrane & cytosol	L	n	L	Yes	
TRIPDB	ANO1	anoctamin 1, calcium activated chloride channel [Source:HGNC Symbol;Acc:21625]	plasma membrane	L	n	n	Yes	
TRIPDB	TRPC1	transient receptor potential cation channel, subfamily C, member 1 [Source:HGNC Symbol;Acc:12333]	plasma membrane	M	M	M	Yes	
TRIPDB	PKD1 (TRPP1)	polycystic kidney disease 1 (autosomal dominant) [Source:HGNC Symbol;Acc:9008]	cytosol & golgi	n	n	n	Yes	
TRIPDB	UBC	ubiquitin C [Source:HGNC Symbol;Acc:12468]	cytosol, endosome & endoplasmic reticulum membrane	L	H	H	Yes	
TRIPDB	YES1 (Yes)	v-yes-1 Yamaguchi sarcoma viral oncogene homolog 1 [Source:HGNC Symbol;Acc:12841]	plasma membrane & cytosol	M	M	L	Yes	
TRIPDB	PRKCSH	protein kinase C substrate 80K-H [Source:HGNC Symbol;Acc:9411]	endoplasmic reticulum	n	n	L	Yes	
TRIPDB	AGTR1	angiotensin II receptor, type 1 [Source:HGNC Symbol;Acc:236]	plasma membrane & clathrin coated vesicles	n	n	n	Yes	
TRIPDB	KCNMA1	potassium large conductance calcium-activated channel, subfamily M, alpha member 1 [Source:HGNC Symbol;Acc:6284]	plasma membrane	n	n	L	Yes	
TRIPDB	CAV1	caveolin 1, caveolae protein, 22kDa [Source:HGNC Symbol;Acc:1522]	plasma membrane, golgi & endocytic vesicle membrane	M	n	M	Yes	
TRIPDB	CDH1	cadherin 1, type 1, E-cadherin (epithelial) [Source:HGNC Symbol;Acc:1748]	plasma membrane & golgi	n	n	n	No	
TRIPDB	MYH10	myosin, heavy chain 10, non-muscle [Source:HGNC Symbol;Acc:7568]	cytosol	L	n	n	Yes	
TRIPDB	POZD3	POZ domain containing 3 [Source:HGNC Symbol;Acc:19891]	plasma membrane	n	n	n	No	
TRIPDB	TUBA1B	tubulin, alpha 1b [Source:HGNC Symbol;Acc:18809]	cytosol	L	n	M	Yes	
TRIPDB	CTNWB1	catenin (cadherin-associated protein), beta 1, 88kDa [Source:HGNC Symbol;Acc:2514]	plasma membrane, cytosol & nucleus	H	n	n	Yes	
TRIPDB	ACTA2	actin, alpha 2, smooth muscle, aorta [Source:HGNC Symbol;Acc:130]	cytosol	n	n	H	Yes	
TRIPDB	ARRB1	arrestin, beta 1 [Source:HGNC Symbol;Acc:711]	plasma membrane, lysosomal & golgi membrane	n	n	L	Yes	
TRIPDB	ARRB2	arrestin, beta 2 [Source:HGNC Symbol;Acc:712]	cytosol	n	n	n	Yes	
TRIPDB	ITGA1	integrin, alpha 1 [Source:HGNC Symbol;Acc:6334]	plasma membrane	M	L	M	Yes	
TRIPDB	PKD2	polycystic kidney disease 2 (autosomal dominant) [Source:HGNC Symbol;Acc:9009]	golgi & golgi-associated vesicle membrane	M	n	n	Yes	
TRIPDB	TRPC3	transient receptor potential cation channel, subfamily C, member 3 [Source:HGNC Symbol;Acc:12335]	plasma membrane	n	n	n	Yes	
TRIPDB	TRPC6	transient receptor potential cation channel, subfamily C, member 6 [Source:HGNC Symbol;Acc:12338]	plasma membrane	L	n	n	Yes	
TRIPDB	TRPM8	transient receptor potential cation channel, subfamily M, member 8 [Source:HGNC Symbol;Acc:17961]	plasma membrane	n	n	n	No	
TRIPDB	PRKCA	protein kinase C, alpha [Source:HGNC Symbol;Acc:9393]	plasma membrane, cytosol & nucleus	M	M	n	Yes	
TRIPDB	PRKCE	protein kinase C, epsilon [Source:HGNC Symbol;Acc:9401]	plasma membrane, cytosol	n	n	L	Yes	
TRIPDB	PRKCD	protein kinase C, delta [Source:HGNC Symbol;Acc:9399]	plasma membrane, cytosol & nucleus	L	L	L	Yes	

n: not detected
H: high
M: medium
L: low

Chapter II

TRPV2: A Key Player in Myelination Disorders of the Central Nervous System



Article

TRPV2: A Key Player in Myelination Disorders of the Central Nervous System

Jennifer Enrich-Bengoa ^{1,2,†}, Gemma Manich ^{2,3,†}, Tony Valente ^{2,3,4}, Paula Sanchez-Molina ^{2,3} ,
Beatriz Almolda ^{2,3}, Carme Solà ⁵ , Josep Saura ⁶ , Berta González ^{2,3}, Bernardo Castellano ^{2,3},
and Alex Perálvarez-Marín ^{1,2,*}

- ¹ Biophysics Unit, Department of Biochemistry and Molecular Biology, School of Medicine, Universitat Autònoma de Barcelona, 08193 Cerdanyola del Vallès, Catalonia, Spain; jennifer.enrich@uab.cat
 - ² Institut de Neurociències, Universitat Autònoma de Barcelona, 08193 Cerdanyola del Vallès, Catalonia, Spain; gemma.manich@uab.cat (G.M.); tony.valente@uab.cat (T.V.); paula.sanchez@uab.cat (P.S.-M.); beatriz.almolda@uab.cat (B.A.); berta.gonzalez@uab.cat (B.G.); bernardo.castellano@uab.cat (B.C.)
 - ³ Medical Histology Unit, Department of Cell Biology, Physiology and Immunology, School of Medicine, Universitat Autònoma de Barcelona, 08193 Cerdanyola del Vallès, Catalonia, Spain
 - ⁴ Research Group on Methodology, Methods, Models and Outcomes of Health and Social Sciences (M3O), Experimental Sciences and Methodological Department, Faculty of Health Sciences and Welfare, University of Vic-Central University of Catalonia (UVic-UCC), 08500 Vic, Catalonia, Spain
 - ⁵ Department of Cerebral Ischemia and Neurodegeneration, Institut D'Investigacions Biomèdiques de Barcelona-Consejo Superior de Investigaciones Científicas (CSIC), Institut D'Investigacions Biomèdiques August-Pi i Sunyer (IDIBAPS), 08036 Barcelona, Catalonia, Spain; carme.sola@iibb.csic.es
 - ⁶ Biochemistry and Molecular Biology Unit, School of Medicine, Institut D'Investigacions Biomèdiques August-Pi i Sunyer (IDIBAPS), University of Barcelona, 08036 Barcelona, Catalonia, Spain; josepsaura@ub.edu
- * Correspondence: alex.peralvarez@uab.cat; Tel.: +34-93-581-4504
† These authors contribute equally to this work.



Citation: Enrich-Bengoa, J.; Manich, G.; Valente, T.; Sanchez-Molina, P.; Almolda, B.; Solà, C.; Saura, J.; González, B.; Castellano, B.; Perálvarez-Marín, A. TRPV2: A Key Player in Myelination Disorders of the Central Nervous System. *Int. J. Mol. Sci.* **2022**, *23*, 3617. <https://doi.org/10.3390/ijms23073617>

Academic Editors:
Antonio Ferrer-Montiel
and Antonio Felipe

Received: 3 March 2022
Accepted: 22 March 2022
Published: 25 March 2022

Publisher's Note: MDPI stays neutral with regard to jurisdictional claims in published maps and institutional affiliations.



Copyright: © 2022 by the authors. Licensee MDPI, Basel, Switzerland. This article is an open access article distributed under the terms and conditions of the Creative Commons Attribution (CC BY) license (<https://creativecommons.org/licenses/by/4.0/>).

Abstract: Transient potential receptor vanilloid 2 (TRPV2) is widely expressed through the nervous system and specifically found in neuronal subpopulations and some glial cells. TRPV2 is known to be sensitized by methionine oxidation, which results from inflammation. Here we aim to characterize the expression and regulation of TRPV2 in myelination pathologies, such as hypomyelination and demyelination. We validated the interaction between TRPV2 and its putative interactor Opalin, an oligodendrocyte marker, in mixed glial cultures under pro- and anti-inflammatory conditions. Then, we characterized TRPV2 time-course expression in experimental animal models of hypomyelination (jimmy mice) and de-/remyelination (cuprizone intoxication and experimental autoimmune encephalomyelitis (EAE)). TRPV2 showed upregulation associated with remyelination, inflammation in cuprizone and EAE models, and downregulation in hypomyelinated jimmy mice. TRPV2 expression was altered in human samples of multiple sclerosis (MS) patients. Additionally, we analyzed the expression of methionine sulfoxide reductase A (MSRA), an enzyme that reduces oxidated methionines in TRPV2, which we found increased in inflammatory conditions. These results suggest that TRPV2 may be a key player in myelination in accordance with the recapitulation hypothesis, and that it may become an interesting clinical target in the treatment of demyelination disorders.

Keywords: transient potential receptor vanilloid 2; Opalin; oxidative stress; myelination; multiple sclerosis; recapitulation theory

1. Introduction

Transient potential receptor vanilloid 2 (TRPV2) is a thermo-, mechano- and lipid sensor non-selective cation channel, and is a member of the superfamily of TRP channels [1]. Activation of TRPV2 is triggered by noxious heat (>52 °C), but also by mechanical stimuli, different chemical compounds such as probenecid [1], and by oxidative stress through methionine (Met) oxidation [2]. TRPV2 is ubiquitously expressed in many human

tissues, such as skeletal muscle, heart, lung, skin, thyroid, testis, and immune tissues [1,3]. In the central nervous system (CNS), TRPV2 expression has been specifically found in medium-to-large neurons bearing myelinated fibers [4], in microglia [5], astrocytes [6] and, at the mRNA level, in oligodendrocyte precursor cells (OPCs) [7], but so far, not in oligodendrocytes. TRPV2 expression and activity, both at the plasma membrane and/or internal endosomes, has been reported to be necessary for axon and neurite outgrowth of motor and sensory neurons [8,9], and in microglia and macrophages has been consistently related to phagocytosis of cellular debris [10].

Previous work from our lab [11] showed that TRPV2 putatively interacts with important key myelin proteins (i.e., proteolipid protein 1 (PLP1), Opalin, neurotrimin (NTM) and with other proteins involved in neoplasms and CNS diseases (ABR, FGF1, KCNJ10, PEBP1, PLP1 and SCD3) [12]. Intriguingly, Opalin, a protein located in the paranodal loop and soma of oligodendrocytes [13], was one of the proteins that showed the strongest interaction with TRPV2, suggesting that TRPV2 could be related to myelination, although its expression has not been shown in oligodendrocytes [7]. Studies by Hainz et al. [14–16] demonstrated that probenecid, a pannexin-1 antagonist, but also a specific TRPV2 agonist [1], improves the outcome in two experimental mouse models of multiple sclerosis (MS): in the experimental autoimmune encephalomyelitis (EAE) model, it is capable of preventing and arresting the progression of clinical symptoms and promoting oligodendrocyte proliferation [14,15] and in the cuprizone model of demyelination/remyelination, it reduces demyelination [16]. This evidence points to a putative role of TRPV2 as an upstream key player in myelination and remyelination processes in the CNS.

In this study, we characterized the TRPV2–Opalin interaction *in vitro* and in mixed glial cell culture to assess if TRPV2 is expressed in oligodendrocytes. TRPV2 presence in oligodendrocyte-lineage cells, in addition to neurons, astrocytes and microglia, may provide support for the importance of TRPV2 in neuron-glial cells' [7] cross-talk in CNS myelination. In parallel, we characterized TRPV2 expression in the CNS in three different myelination murine models: the hypomyelinating jimpy mice as a pathophysiological model for Pelizaeus–Merzbacher disease (PMD) [17–19] and the cuprizone- and EAE-induced experimental mouse models. To assess the potential role of TRPV2 in human pathophysiology, we determined TRPV2 gene and protein expression in tissue samples of human MS patients.

2. Results

2.1. Opalin Interacts *In Vitro* with the Ankyrin-Repeat Domain (ARD) of TRPV2

Since previous results from our group indicated a possible interaction between TRPV2 and NTM, PLP1 and Opalin [11], we studied these interaction pairs *in vitro*. Purified full-length (FL) rat TRPV2 and rat ARD were immobilized on nitrocellulose membranes, and then rat brain protein extracts were incubated with the membranes. After immunoblotting against the selected interactors, we observed that Opalin interacts with both the whole protein and with the cytosolic ARD of TRPV2 in a stronger fashion than NTM and PLP1 protein (Figure 1A). The mode of interaction between FL and the cytosolic domain of TRPV2 and Opalin indicates intracellular/transmembrane interaction, so both proteins coexist in the same cell, such as an oligodendrocyte-like cell.

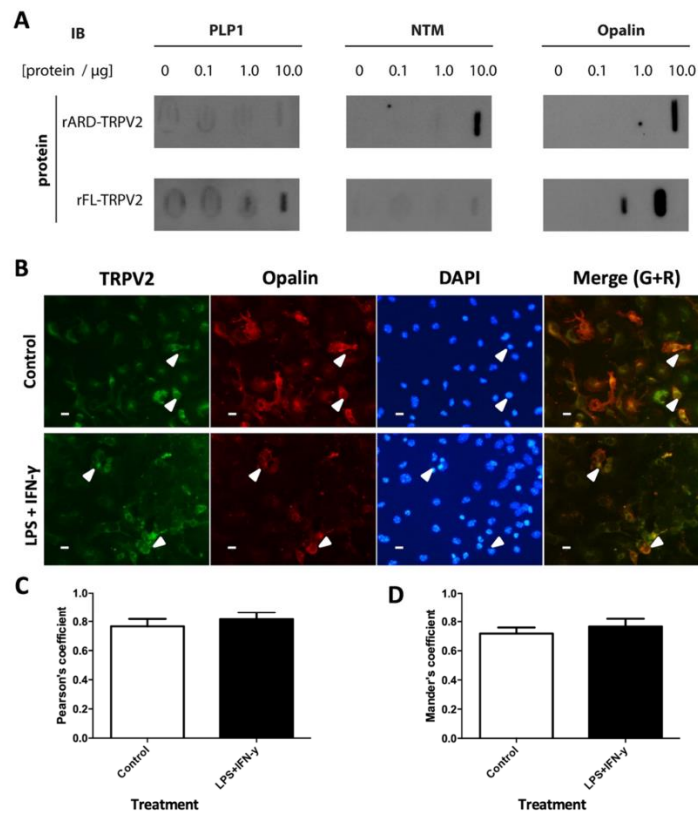


Figure 1. TRPV2 interaction with Opalin, NTM and PLP1 in vitro during basal and inflammatory conditions. (A) Rat TRPV2 FL protein and rat ARD of TRPV2 were immobilized on membranes and incubated with increasing concentrations of rat protein brain lysates (0–10 μg). Opalin, NTM and PLP1 were detected by immunoblot. (B) Immunocytochemistry in mouse mixed glial primary cultures shows TRPV2 (green), Opalin (red) and DAPI (blue). TRPV2-Opalin colocalization is shown as yellow signal (merge) and both proteins are co-expressed in some cells (arrowheads). Expression of these proteins is mainly found in the membrane. (C) TRPV2–Opalin colocalization expressed as Pearson's coefficient in basal and inflammatory conditions. Both proteins show a high degree of colocalization. (D) TRPV2 colocalization with Opalin, expressed as Mander's coefficient M2 (fraction of TRPV2 signal overlapping Opalin) in basal and inflammatory conditions. Both proteins show a high degree of colocalization. Results were expressed as mean \pm SEM. Statistical analysis of the results were performed with an unpaired Student's *t*-test ($p < 0.05$ is statistically significant). Scale bar = 20 μm .

2.2. TRPV2 and Opalin Display a High Degree of Colocalization in Mixed Glial Cultures Enriched in Oligodendrocytes

Next, to assess the possibility that TRPV2 and Opalin co-express in the same cell type, we determined if they were expressed in vitro in mixed glial cell cultures containing microglia, astrocytes and oligodendrocytes (Supplementary Figure S1). Co-expression was determined in basal conditions and after a pro-inflammatory stimulus, since myeli-

nation disorders are associated with inflammatory processes. Results showed that some TRPV2+ cells also expressed Opalin with a high degree of colocalization (Figure 1B), as indicated by ca. 0.8 Mander's and Pearson's coefficients (Figure 1C,D). After exposure to a pro-inflammatory stimulus such as lipopolysaccharide (LPS) + interferon- γ (IFN- γ), levels of colocalization remained unchanged (Figure 1C,D).

2.3. TRPV2 Expression in Microglia and Oligodendrocytes Is Regulated after Pro-Inflammatory, Anti-Inflammatory and Demyelinating Treatments

Cellular expression of TRPV2 was determined with double immunocytochemical staining performed in glial mixed cultures. These cultures were composed of approximately 25% microglia, 30% astrocytes and 35% oligodendrocytes in basal conditions, and their populations varied slightly after pro-inflammatory treatment (Supplementary Figure S1). In basal conditions, TRPV2 was mainly expressed in microglia, detected by lysosomal CD68, and oligodendrocytes, identified by platelet-derived growth factor receptor alpha (PDGFR α) (Figure 2A,G), while no expression was observed in glial fibrillary acidic protein (GFAP)-labelled astrocytes (Figure 2D). In both microglia and oligodendrocytes, TRPV2 was highly expressed and concentrated in the cell body, without labelling in their ramifications. After the pro-inflammatory treatment with LPS, TRPV2 intensity decreased in activated microglia, but its expression was extended to all of the microglial cell body and membrane, with a punctate staining similar to lysosomal CD68 (Figure 2B). In oligodendrocytes, we observed a similar expression pattern, consisting of a decreased intensity of TRPV2 staining spread throughout PDGFR α + cell bodies (Figure 2H). After interleukin (IL)-4 anti-inflammatory treatment, TRPV2 was found in both ramified and activated microglia phenotypes, following the expression patterns explained above (Figure 2C). Similarly, oligodendrocytes showed high TRPV2 expression in their cell bodies, as been observed in the control condition (Figure 2I). In none of the treatments did GFAP+ astrocytes show TRPV2 expression (Figure 2E,F).

Quantification of total TRPV2 expression in mixed glial cultures showed a significant decrease of TRPV2 after LPS pro-inflammatory treatment (Figure 2J, $p < 0.01$) compared to controls. After an anti-inflammatory IL-4 treatment, TRPV2 expression tended to increase (Figure 2J, $p = 0.05$) when compared to controls. Oxidative stress is known to induce oxidation of specific Met residues in TRPV2 (Met528 and Met607 in rat TRPV2) [2,20], endogenously activating the channel. As an indicator of oxidative stress in the cell culture, we measured nitric oxide (NO) concentration in cell media. Indeed, NO is also interesting since it promotes TRPV2 translocation to the plasma membrane [5]. Results showed that IL-4 treated cultures presented lower levels of NO in the cell culture medium compared to the control, while LPS-treated cultures showed a significant increase of NO (Figure 2L).

In an attempt to closely determine the TRPV2 response in demyelination processes, we treated quaternary glial mixed cell cultures containing myelin-binding protein (MBP)-positive mature oligodendrocytes (see cell populations in Supplementary Figure S2) with the demyelinating and apoptotic cell agent L- α -lysophosphatidylcholine (LPC), which is also a direct activator of TRPV2 [21]. TRPV2 levels were significantly decreased in LPC-treated cultures compared to their respective controls, as similarly observed in the LPS pro-inflammatory treatment (Figure 2K, $p < 0.01$). Determination of NO in the cell media of LPC-treated cells, as a measure of oxidative stress, demonstrated similar levels compared to the control condition (Figure 2M).

2.4. TRPV2 and Opalin Expression, but Not Methionine Sulfoxide Reductase A (MSRA) Levels, Are Importantly Reduced in the Hypomyelinating Jimpy Mutant Mice

TRPV2, Opalin and MSRA protein expression was explored in spinal cord sections of control and jimpy mutant mice by immunohistochemistry. First, we determined the degree of hypomyelination in jimpy mice by staining the MBP, one of the most abundant proteins in myelin. As expected, MBP was highly expressed and homogeneously distributed in the white matter (WM) of spinal cord sections of control mice (Figure 3A,a) and slightly

expressed in grey matter (GM) (Figure 3a'). Jimpy mutant mice showed a clear reduction of MBP expression and myelin thickness in both WM and GM (Figure 3B,b',C, $p < 0.0001$).

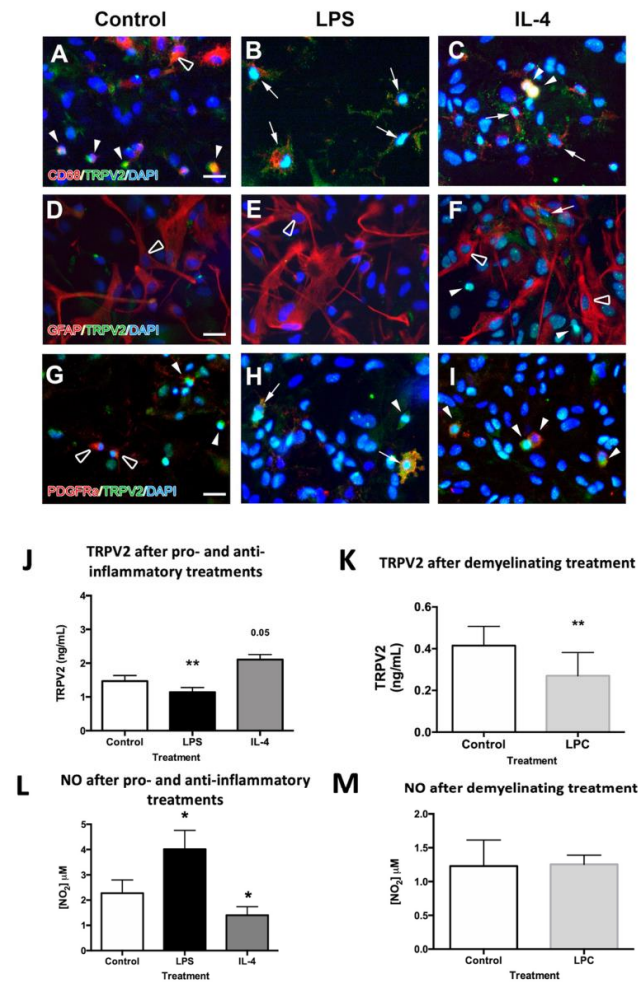


Figure 2. TRPV2 expression in mixed glia cultures of mice after pro-inflammatory (LPS), anti-inflammatory (IL-4) and demyelinating (LPC) treatments. (A–I) Double immunohistochemical staining allowed for the determination of whether TRPV2 was expressed in microglia (A–C), astrocytes (D–F) or oligodendrocyte cells (G–I). TRPV2 was highly expressed in the cell body of some microglia (full arrowheads) but not all of them (empty arrowheads) in control conditions, and TRPV2 was spread afterwards through the cell body of activated microglia cells, with an expression pattern highly coincident with CD68+ lysosomes (arrows). While no expression of TRPV2 was found in astrocytes (empty arrowheads), OPCs showed either low or absent expression in control conditions (full and empty arrowheads, respectively) and increased expression throughout the cell body (arrows)

and the principal soma (arrowheads) after both pro-inflammatory and anti-inflammatory treatments. (J,K) Quantification of TRPV2 protein (ng/mL) by ELISA in secondary mixed glial cultures in control conditions, and after LPS and IL-4 treatments (J) and in quaternary mixed glial cultures, containing myelin-binding protein (MBP)+ oligodendrocytes, in demyelinating conditions (K). Determination of TRPV2 showed a significant decrease in TRPV2 after LPS and LPC treatments (J,K), and an increase after IL-4 treatment ($p = 0.05$) compared to control conditions (J). (L,M) Quantification of NO secondary mixed glial cultures in control conditions, and after LPS and IL-4 treatments (L) and in quaternary mixed glial cultures in demyelinating conditions (M). An increase in NO concentration was observed in cell cultures after LPS treatment compared to control conditions, while a significant decrease was observed after IL-4 treatment. After LPC treatment, NO remained stable compared to the control. Statistical analysis was performed by one-way ANOVA followed by Dunnett's multiple comparison compared to the control in the LPS and IL-4 treated cultures (* $p < 0.05$, ** $p < 0.01$), and a paired Student's *t*-test for LPC treatment (** $p < 0.01$). Scale bar (A–I) = 25 μ m.

In basal conditions, TRPV2 expression in GM was mainly located in the cell body of spinal cord neurons, while in WM, it was in the soma of cells, putatively oligodendrocytes (Figure 3D,d,d'). In the hypomyelinating jimpy mutant mice, TRPV2 expression was significantly reduced in both neurons and oligodendrocytes (Figure 3E,e,e',F, $p = 0.0062$).

We additionally evaluated Opalin expression in jimpy mice as an oligodendrocyte marker, but also as a TRPV2 interactor. Opalin is localized in WM-rich regions of the CNS and shows similar expression to the myelin marker MBP [13]. In the spinal cord of 21-day-old control mice we observed that Opalin was mainly distributed in WM, and located in cell bodies of oligodendrocytes and in the neuropil (Figure 3G,g). In GM, Opalin expression showed low expression, and was mainly located to some myelinated projections. As observed before for TRPV2 and MBP, Opalin was importantly reduced in both GM and WM (Figure 3H,h,h') in the spinal cord of jimpy mice ($p = 0.0092$) in comparison with control animals (Figure 3I).

Since TRPV2 is activated through Met oxidation, which can easily be oxidized by reactive oxygen species (ROS) [20], we explored the expression of the Met reducing enzyme MSRA, a counteracting enzyme that partially reverses TRPV2 endogenous activation [2]. Immunostaining showed that MSRA was found in the GM and WM of both control and jimpy mutant mice (Figure 3J,K). In control mice, this enzyme was expressed mainly in glial cells, putatively oligodendrocytes, in WM, and in glial cells and neurons in GM. Similar observations were made in jimpy mutant mice (Figure 3j,k,j',k'). Despite an apparent reduction of MSRA in jimpy mutant mice compared to control mice (Figure 3K), the quantitative analysis did not show significant differences between them (Figure 3L).

2.5. TRPV2 and MSRA Expression Are Modulated in the Experimental Mouse Models of MS: The Cuprizone and the EAE Models

To investigate TRPV2 and MSRA roles in demyelination, we used two experimental models of demyelination: the cuprizone-induced model and the EAE model. The effects of cuprizone intoxication on myelination were observed after MBP immunodetection: after a 5-week treatment, a substantial demyelination of specific WM areas, such as the corpus callosum (CC), was observed compared to basal conditions (Figure 4A,B), and cuprizone withdrawal allowed CC remyelination one week after (Figure 4C), as already quantified in previous work [22]. In the CC of control mice, TRPV2 and MSRA showed very low to undetectable levels (Figure 4D,G). After a 5-week cuprizone treatment, demyelinated CC showed a slight qualitative increase in TRPV2 (Figure 4E,H) that was mainly located in cell bodies of the CC, putatively oligodendrocytes (Figure 4E). In the caudal CC area, known to be resistant to myelination, TRPV2 increase was more visible (Figure 4D–F). After one week of remyelination, TRPV2 expression was significantly increased in mature oligodendrocytes of the CC when compared to control groups ($p < 0.01$) (Figure 4F, inset, J,K), as we confirmed with a double immunostaining against adenomatous polyposis coli (APC), and its levels were almost duplicated compared to demyelinated animals (Figure 4L). In the case of MSRA, a significant increase of this protein was observed after demyelination

($p < 0.01$) (Figure 4H,K), since most cells in the CC expressed low levels of MSRA. Later, after one week of remyelination, MSRA levels decreased, and only some MSRA+ cells were observed in the CC (Figure 4I,K).

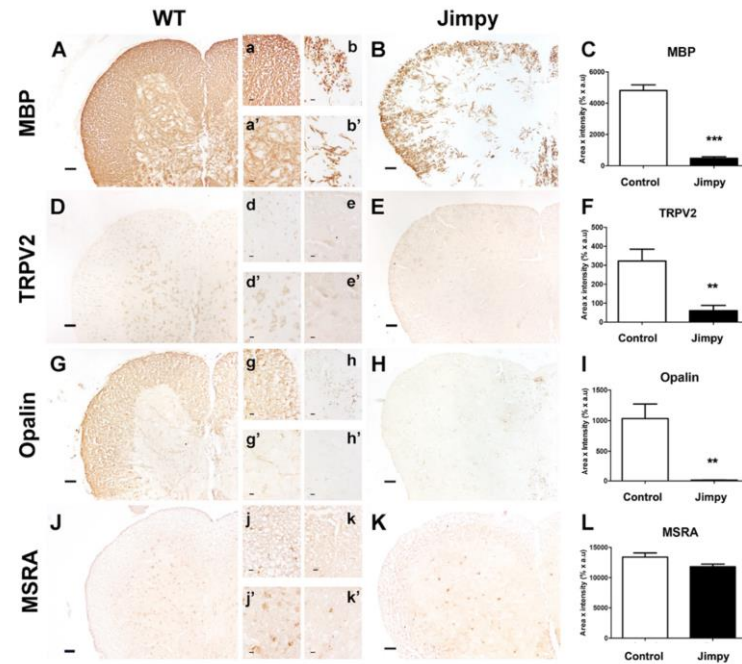


Figure 3. TRPV2, Opalin and MSRA expression in spinal cord of wild-type (WT) and hypomyelination jimpy mice. Immunohistochemical staining against MBP (A,B), TRPV2 (D,E), Opalin (G,H) and MSRA (J,K) were performed in spinal cord sections of 21-day-old WT and jimpy mice, and immunoreactivity was quantified and analyzed as Area x Intensity. Results show that MBP was importantly reduced in both GM (a,b) and WM (a',b') of jimpy mice compared to WT (A–C). TRPV2 expression was mainly located in neurons in GM (d') and glial cells, putatively oligodendrocytes, and in WM (d) of WT. A significant decrease in TRPV2 expression in the spinal cord of jimpy mice was observed compared to WT (E,F,e,e'). Opalin expression was importantly found in WM of WT mice (G,g), and to a lesser extent also in GM (g'), but showed a marked decrease in WM and GM of jimpy mice (H–L,h,h'). MSRA was the only molecule that did not suffer an important reduction of its expression in both WM (j,k) and GM (j',k') in jimpy mice (L). Results were expressed as mean \pm SEM. Statistical analysis of the results were performed with an unpaired Student's *t*-test (** $p < 0.01$, *** $p < 0.001$). Scale bar (A–K) = 50 μ m; (a–k,a'–k') = 20 μ m.

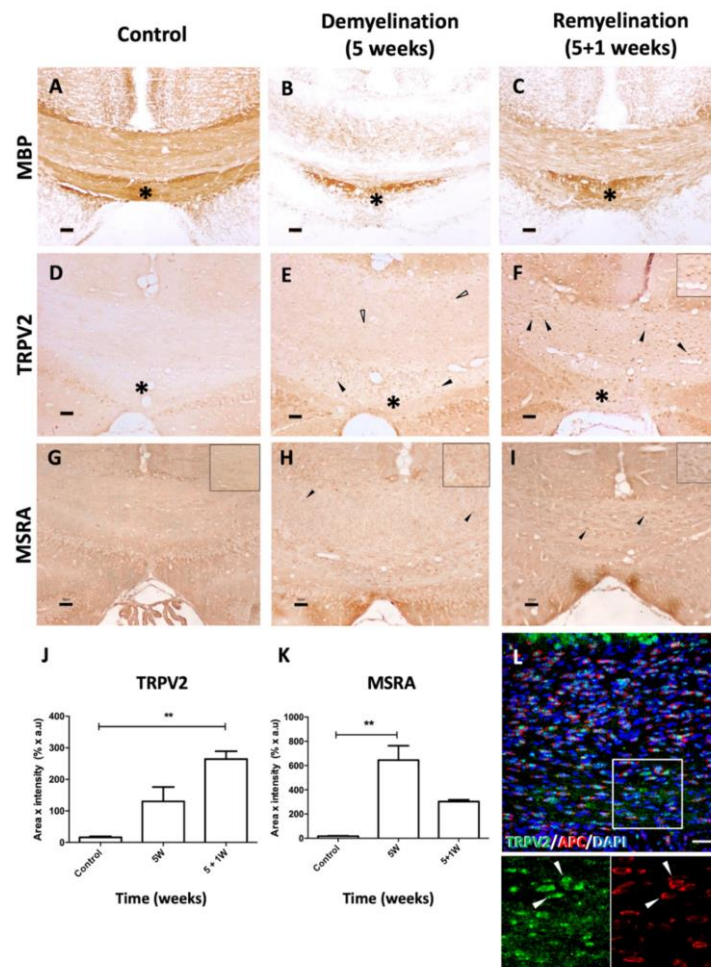


Figure 4. TRPV2 and MSRA expression in WM of cuprizone-induced demyelination and remyelination in mice. (A–I) Representative images of immunohistochemical staining directed against MBP, TRPV2 and MSRA in the CC of control mice (A,D,G) and cuprizone-intoxicated mice after demyelination (B,E,H, 5 weeks of treatment) and during remyelination (C,F,I, 5 weeks of treatment + 1 week of normal diet). (A–C) MBP immunostaining shows the myelinated CC of WT mice in basal conditions (A). At 5 weeks of cuprizone treatment, the CC is largely demyelinated (B) with a myelination-resistant area (*), and after one week of normal diet, the CC is mostly remyelinated (C). Control mice show undetectable levels of TRPV2 and MSRA in the CC (D and G). After demyelination, variably low and high levels of TRPV2 were observed in cell bodies (empty arrowheads and arrowheads, respectively in E,F). High levels of TRPV2 were clearly observed at remyelination (inset in F). During remyelination, most TRPV2+ cells co-expressed APC (full arrowheads in L), a marker for mature oligodendrocytes. In the CC area resistant to demyelination (* in E,F), TRPV2+ cells showed high levels of expression in both conditions. An increase in MSRA levels of expression were also observed in cell bodies after demyelination and remyelination (arrowheads in H and I).

In demyelination, most cells expressed low levels of MSRA in the CC (inset in H), while during remyelination, a lower number of MSRA+ cells expressing higher levels of MSRA were observed (inset in I). (J–K) Quantification of TRPV2 and MSRA expression after cuprizone treatment. (J) Quantitative analysis of TRPV2 immunoreactivity in the CC confirmed the progressive increase of TRPV2 expression in demyelinating and remyelinating conditions compared to control mice, which was statistically significant in the latter. (K) Quantitative analysis of MSRA immunoreactivity in the CC showed that the increase of MSRA expression during demyelination was statistically significant when compared to control mice. Data are shown as \pm SEM. Statistical analysis was performed by one-way ANOVA followed by Tukey's multiple comparison test (** $p < 0.01$). Scale bar (A–I) = 50 μ m; (L) = 100 μ m.

In the EAE model, in which demyelination foci are developed in the spinal cord accompanied by clinical symptoms of paralysis, we analyzed TRPV2 expression in spinal cord sections. In control mice, TRPV2 was mainly expressed in neurons in GM and oligodendrocyte-like cells in the WM (Figure 5A). After EAE induction, in the onset of clinical symptomatology, similar patterns of TRPV2 expression were observed, but later, at the peak of clinical symptomatology, TRPV2 was mainly located in WM, in the inflammatory foci and in infiltrated cells (Figure 5A). During the chronic phase of EAE, in the remission of clinical symptomatology, TRPV2 expression was still found in neurons in GM, and in oligodendrocyte-like cells and inflammatory foci in WM. However, at this time point, an important loss of intensity was found in comparison to TRPV2 levels of expression observed in the peak (Figure 5A). Quantification of TRPV2 by western blot analysis (Figure 5B) confirmed the important increase of TRPV2 protein expression in the spinal cord of EAE mice at 14 days post-immunization (Figure 5B, $p = 0.0014$) compared to control mice. Later, at 21 and 28 days post-immunization, TRPV2 expression levels decreased and were maintained constant (Figure 5B). Evaluation of MSRA expression levels after EAE induction in mice showed an immediate significant increase when compared to the control complete Freund's adjuvant (CFA)-injected mice (Figure 5B). Then, MSRA levels increased progressively until 21 days post-immunization (Figure 5B). At 28 days post-immunization, MSRA expression was significantly reduced when compared to 21 days post-immunization mice, and almost reverted to basal levels (CFA in Figure 5B).

2.6. MSRA and TRPV2 Gene and Protein Expression Are Modified in Frontal Cortex Samples of MS Patients

Gene and protein expression of TRPV2 and MSRA was explored in frontal cortex tissue samples of healthy ($n = 4$) and MS subjects ($n = 6$). In MS subjects, a non-significant tendency to decrease of TRPV2 mRNA levels was observed when compared to healthy subjects (Figure 6A). On the contrary, MSRA mRNA expression in MS subjects was found to be significantly upregulated ($p = 0.0014$) when compared to healthy subjects (Figure 6B). TRPV2 and MSRA protein levels were also determined by western blot (Figure 6C). Protein levels of both MSRA and TRPV2 showed the same tendency as the mRNA expression analysis (Figure 6A–C): while a significant decrease of TRPV2 protein levels was observed in MS patients when compared to the control ($p = 0.0232$) (Figure 6C), MSRA protein expression levels were also significantly increased in MS patients compared to healthy subjects ($p = 0.0124$) (Figure 6C).

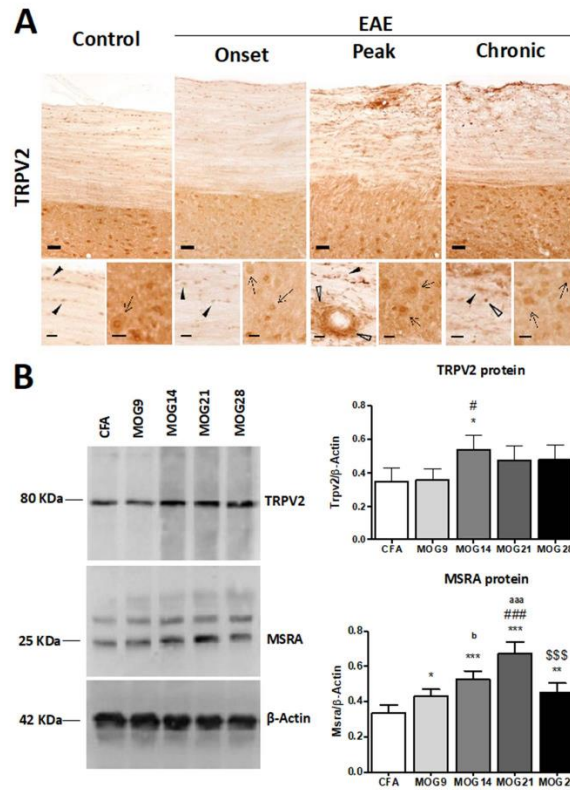


Figure 5. TRPV2 expression in spinal cord samples from WT and EAE mice. (A) Immunohistochemical staining of TRPV2 in spinal cord of control and EAE-induced mice in the onset, peak and in the chronic phase, during remission. In control conditions, TRPV2 is expressed in neurons in GM (inset, arrows), and in oligodendrocytes in WM (inset, arrowheads). After EAE induction, an increase in TRPV2 expression is mainly located in inflammatory foci at the peak clinical symptomatology in WM (empty arrowheads). (B) MSRA and TRPV2 protein expression in thoracic spinal cord samples from CFA and MOG mice (9, 14, 21 and 28 days post-immunization). (B) A significant increase in TRPV2 protein levels ($\#$, $p = 0.0014$) is determined in MOG14 mice when compared with CFA ($p < 0.05$) and when compared with MOG9 ($p < 0.05$). A significant increase ($p < 0.05$) in MSRA protein levels is observed in all groups of mice treated with MOG when compared with CFA mice, as well as between different groups treated with MOG: MOG9 vs. MOG21 (###, $p < 0.001$), MOG9 vs. MOG14 (b , $p < 0.05$), MOG21 vs. MOG28 ($^{\$ \$ \$}$, $p < 0.001$), MOG14 vs. MOG21 ($^{\text{aaa}}$, $p < 0.001$). Bars show mean \pm SEM; * $p < 0.05$, ** $p < 0.01$ and *** $p < 0.001$ vs. CFA using one-way ANOVA and Newman–Keuls post-test. Scale bars = 50 μm ; (insets) = 20 μm .

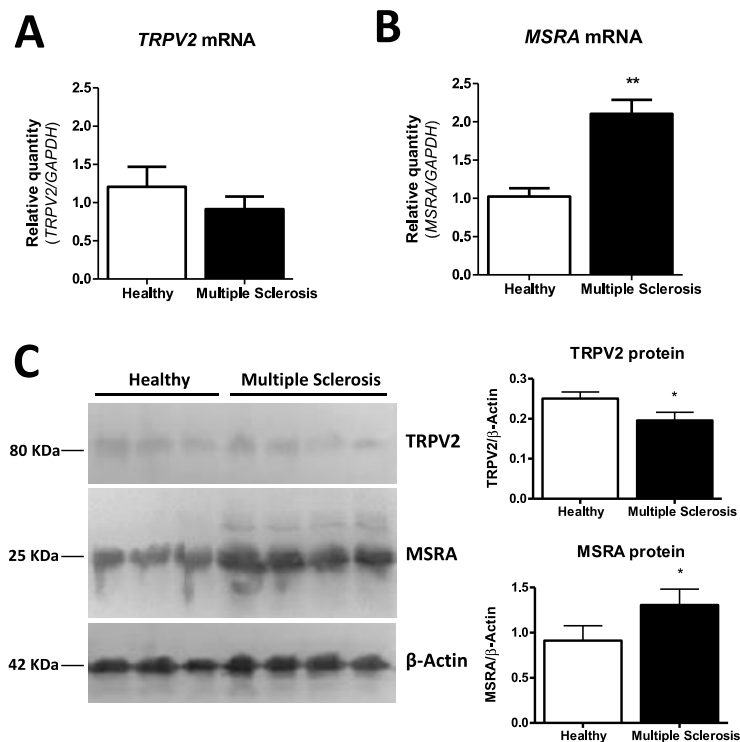


Figure 6. MSRA and TRPV2 expression in frontal cortex samples from healthy subjects ($n = 4$) and MS ($n = 6$) patients. (A) TRPV2 mRNA ($p = 0.3314$) is not changed between MS and healthy samples. (B) A significant upregulation in MSRA mRNA ($p = 0.0014$) is found in MS; (C) A significant decrease in TRPV2 protein levels ($p = 0.0232$) and a significant increase in MSRA protein levels ($p = 0.0124$) were determined in MS samples by western blot. Bars show mean \pm SEM; * $p < 0.05$, ** $p < 0.01$ using unpaired Student's t -test.

3. Discussion

In this study we aimed to explore the role and expression of TRPV2 in the context of myelination disorders of the CNS, taking advantage of previous work indicating the potential role of TRPV2 and its interactors in myelination processes [11]. Opalin has been found in mature myelinating oligodendrocytes [23–25], but also at early stages of OPCs [26]. Opalin has not been found in microglia, astrocytes or neurons [23], and could be used as an oligodendrocyte lineage cell marker. Opalin and TRPV2 co-expression allowed for the identification of TRPV2+ oligodendrocyte-like cells. In physiological conditions, TRPV2 mRNA expression has been determined in OPCs, but not in oligodendrocytes [7]. Our results showed TRPV2 expression in mature oligodendrocytes of WM areas in the mouse spinal cord and brain in basal and inflammatory conditions. To the best of our knowledge, this is the first evidence describing TRPV2 expression in oligodendrocytes, together with the validation of the TRPV2–Opalin interaction pair. Although the physiological relevance of this interaction remains to be elucidated, the fact that TRPV2 is expressed in both microglia and oligodendrocytes opens the question of what the role of this channel is in microglia–oligodendrocyte cross-talk, and potentially in myelination.

The role of TRPV2 in microglia and phagocytosis under oxidative stress is slightly better understood so far. NO promotes TRPV2 translocation to the membrane which results in a higher microglia phagocytic capacity [5] and attenuated microglia proliferation [5]. In *in vitro* experiments, we have positively identified TRPV2+ microglia cells. In basal conditions, TRPV2 was found in the cell body of microglia and oligodendrocytes. Upon pro-inflammatory treatment with LPS, TRPV2 was translocated to the plasma membrane of both microglia and oligodendrocytes, and also colocalized with CD68+ intracellular compartments, in agreement with what has been previously shown in macrophages [27]. We measured the concentration of NO released in the cell media after all treatments; elevated levels of NO were especially found after LPS treatment. Indeed, TRPV2 is expected to be highly active after a pro-inflammatory stimulus, since several molecules produced by microglia, such as NO, or LPC-treatment and oxidative stress, may activate TRPV2 directly or indirectly [2,5,21]. Interestingly, we show that total TRPV2 levels decrease under pro-inflammatory conditions (LPS and LPC treatment) and increase under anti-inflammatory conditions (IL-4 treatment), where a decrease in NO concentration is found. Regardless of the mRNA levels derived from inflammatory conditions, TRPV2 protein was at the plasmatic cell membrane, and not in intracellular compartments, indicating that TRPV2 was ready to promote the TRPV2 NO-induced slow-onset calcium influx, leading to enhanced microglia phagocytic capacity, which is supported by previously published results [28].

NGF-dependent activation of endosomal TRPV2 in neurite outgrowth showed that TRPV2 can be active both at the plasma membrane and in intracellular compartments [7]. The neuronal TRPV2 role in axon and neurite outgrowth [8,9] has already been established, but there is no knowledge regarding TRPV2's role in the oligodendrocyte–microglia crosstalk during myelination. Studies from Hainz et al. [14–16] using the pannexin-1 antagonist probenecid showed protective effects on MS murine models, such as preventing and arresting the progression of clinical symptoms in an EAE mouse model and diminishing demyelination in the cuprizone mouse model of demyelination/remyelination. Beyond being a pannexin-1 antagonist, probenecid is a known agonist for TRPV2 [1]. In addition, previous EAE results using tranilast, a well-known and specific TRPV2 antagonist [1], showed reduced mice paralysis when administered orally in an EAE mouse model [29]. *In vitro* experiments in this study, together with the bibliographic evidence above, bolster a strong argument to focus on the characterization of TRPV2 as a key player in myelination disorders.

The jimpy mouse model, a pathophysiological model for PMD [17–19], shows a strong hypomyelination derived from X-linked deleterious mutations in the PLP gene. TRPV2 and PLP1 are putative interactors derived from our results in a yeast two-hybrid experiment [11], showing interaction at the biochemical level using purified TRPV2 (Figure 1A). Jimpy mice show severe hypomyelination, as we have seen in the current study with significantly decreased MBP expression (Figure 3A–C), failure in oligodendrocyte maturation, oligodendrocyte death, astrogliosis and microgliosis [30]. Observation of TRPV2 and Opalin expression in WT and jimpy mice reinforces a possible interaction of both proteins, since its expression was identified in the cell body of oligodendrocyte-like cells located in the WM of the spinal cord (Figure 3D–I). In jimpy mice, both TRPV2 and Opalin showed a significant reduction in WM. Taking into account the massive oligodendrocyte cell death observed in these animals [30], it is expected that an important reduction of both proteins would be found in hypomyelinating jimpy mice. Additionally in agreement with our previous results on cell cultures, the highly pro-inflammatory tissue environment found in hypomyelinating mice [31] may promote the reduction of TRPV2 levels, as observed in cell cultures (Figures 1 and 2). In addition, other factors that could influence TRPV2 expression are the mutation in the PLP gene, a candidate that putatively interacts with TRPV2, and the oligodendrocyte maturation arrest, since, as we hypothesized based on previous evidence (and also supported by our results in the cuprizone model, discussed below), TRPV2 could be involved in myelination. At this point, it is worthwhile to highlight the choice of MSRA

staining as an indirect measure of TRPV2 activity. As discussed earlier, endogenous activation of TRPV2 results from Met528 and Met607 oxidation in rat TRPV2 [2]. MSRA is in charge of reducing methionine-S-sulfoxide (Met-SO) to Met to protect cells from oxidative stress [32]. Thus, MSRA activity should be required to revert, at least partially, TRPV2 activation. In the jimpy mice, where TRPV2 is significantly reduced (Figure 3J–L), MSRA activity may not be affected due to the fact that the jimpy phenotype is not derived from an acute inflammatory process, as it happens in the cuprizone and EAE experimental models discussed below.

In the experimental models of demyelination, the loss of myelin integrity was produced by oligodendrocyte cell death in the cuprizone model [33], or by an autoimmune reaction against CNS myelin proteins through the activation of autoreactive T cells in the EAE model [34,35]. Study of TRPV2 expression in the CC of mice with cuprizone-induced demyelination showed that TRPV2 progressively increased its expression, mainly in oligodendrocytes, in the peak of demyelination and in the first week of remyelination (Figure 4A–C). Since at those timepoints the main occurring event was the initiation of myelination of migrated OPCs [36], we could infer that TRPV2 is playing a role in the maturation of oligodendrocytes and myelination. Although a role for microglia should not be excluded, microgliosis and phagocytic activity reaches its peak of activity around 3–4 weeks [37], and taking into account that during remyelination of the CC, microglial activation and numbers decrease, a main role for TRPV2 in those microglial functions may not be expected at these timepoints. Interestingly, in remyelination, an anti-inflammatory micro-environment is found [38]. On the contrary, our results on TRPV2 expression in EAE support an important role for this ion channel in microglia and infiltrated immune cells, and as a result, in the pathology of this mouse model. TRPV2 was importantly upregulated in the inflammatory lesions, which are observed in the peak of symptomatology and are attenuated at the chronic phase [39]. Inflammatory lesions are mainly composed of microglia/macrophages, T cells, B cells and reactive astrocytes [40], all cells with previous reported expression on TRPV2 [5,6,10,41], and therefore, TRPV2 may be related to phagocytosis [5], proliferation or other unreported functions executed by those cells in the peak of EAE. In this acute phase, OPCs also proliferate as an attempt to react to demyelination, contrarily to mature oligodendrocytes that are reduced [42]. However, at the chronic phase, OPCs and mature oligodendrocytes are severely decreased, and only pre-myelinating oligodendrocytes remain stable [42]. Therefore, the stability in TRPV2 levels in chronic phases may be explained by the remaining pre-myelinating OPCs present in this chronic phase, since immunostainings also supported elevated TRPV2 expression in those cells.

Indeed, the positive results in the reduction of demyelination in the cuprizone model and the amelioration of the EAE clinical symptoms after probenecid administration [14–16] may be explained by TRPV2 activation at several cellular levels: an increase of the phagocytic activity of microglia [5], which favors the elimination of cell debris and repair of the demyelinated area or other functions in infiltrating immune cells, and the enhancement of oligodendrocyte maturation and promotion of remyelination in TRPV2+ oligodendrocytes. Because of these multiple levels of activation in diverse cells, TRPV2 could be an interesting therapeutic target, as will be discussed later.

Evaluation of MSRA levels in our experimental models showed an expression pattern linked to inflammation and resolution. Oxidative stress is known to be elevated in all three models [31,43,44] and therefore the activation of MSRA is to be expected in those contexts. In the cuprizone and EAE models, MSRA was increased, coinciding with the peak of demyelination in the CC, and after the immune cell infiltration in the spinal cord, respectively. It should be taken into account that infiltrating and immune cells produce important amounts of free radical species that drive oxidative stress once they are activated. This increase in MSRA may be linked to a protection mechanism to reduce Met-SO to Met, since Met residues, which are easily oxidized by ROS [20], are capable of protecting cells from oxidative stress [45]. Furthermore, oligodendrocytes are the most sensitive CNS cells to oxidative stress [46,47] and MSRA may play an important counteracting and

protective effect in these cells, as observed in its readily visible increase in oligodendrocytes in cuprizone-demyelinated mice. A different scenario was observed in hypomyelinating jimpy mice, as discussed earlier. Despite elevated levels of oxidative stress in mutant jimpy mice due to the inflammatory process, no modifications in MSRA levels were found in those animals. This could be the result of the important loss of cells observed in jimpy mice [30], which compensates for a possible increase on MSRA cell expression, and/or the inability of hypomyelinating mice to counterbalance oxidative stress effects by increasing MSRA.

To focus on TRPV2 and human myelin pathophysiology, we evaluated mRNA and protein expression of TRPV2 and MSRA in frontal cortex samples from MS patients compared to control subjects. In this case, a decrease in TRPV2 protein, which was non-significant in TRPV2 mRNA, was observed for MS patients compared to controls, while MSRA mRNA and protein expression were significantly increased in MS patients. Owing to the fact that ROS involvement has been described in MS pathogenesis [48,49], the increase in MSRA may respond to an attempt to protect cells from oxidative stress. These results support our previous findings in the experimental mouse models for MS: cuprizone and EAE. Unexpectedly, a downregulation of TRPV2 into the protein level was observed in the frontal cortex of MS patients compared to control subject samples. TRPV2 downregulation does not match with the upregulation of this protein observed in our results on the cuprizone and EAE models. However, it should also be considered that TRPV2 increase was observed in the acute inflammatory phase and during remyelination, while our MS patient samples should be contextualized in the chronic phase of this disease where inflammation is ameliorated and remyelination is absent. Therefore, this downregulation could be interpreted as the result of cell death observed in MS patients [50,51], or as the failure of oligodendrocytes to promote remyelination, thus approaching a scenario—with their respective important and characteristic pathological differences—similar to that observed in TRPV2 expression in the chronic inflammation of jimpy mice. Indeed, the downregulation of TRPV2 observed in MS patients suggests that TRPV2 may be playing a role, either as a cause or consequence, in this disease, and that promoting its specific activation/inhibition could be an interesting therapeutic target to be explored. Further studies on the expression of TRPV2 and its role in MS and other demyelinating diseases may unravel this question.

4. Materials and Methods

4.1. Animals

C57BL/6 males aged 8–10 weeks and females aged 2–4 months were used. Jimpy mutant male mice (jp/Y) were obtained and distinguished from normal control animals (+/Y) as described in Vela et al. [19]. Male jimpy mice aged 21 days and their corresponding male littermates ($n = 6$ /group) were used. Animals were maintained with food and water ad libitum, in a 12 h light/dark cycle, at 22 ± 2 °C and 50–60% humidity. All experimental work was conducted according to Spanish regulations (Ley 32/2007, Real Decreto 1201/2005, Ley 9/2003, y Real Decreto 178/2004) in agreement with European Union directives (86/609/ CEE, 91/628/CEE i 92/65/CEE) and was approved by the Ethical Committee of the Autonomous University of Barcelona, Spain.

4.2. Cuprizone-Induced Demyelination and Remyelination in Mice

C57BL/6 males were fed with 0.2% (*w/w*) cuprizone (bis-cyclohexanone-oxalldihydrazone, Sigma-Aldrich, Missouri, MO, USA), as described in Petkovic et al. [22]. Three experimental groups were used: a control group fed with standard chow ($n = 6$), a demyelination group fed for 5 weeks with cuprizone ($n = 7$) and a remyelination group fed for one additional week with standard powdered chow ($n = 6$).

4.3. Experimental Autoimmune Encephalomyelitis in Mice

C57BL/6 female mice were immunized with a subcutaneous injection emulsion containing 100 µg/mouse of myelin oligodendrocyte glycoprotein (2) peptide 35-55 (MOG₃₅₋₅₅, Espikem, Italy or M4939; Sigma-Aldrich, Missouri, MO, USA) and 1 mg/mouse of H37R

M. tuberculosis (Difco, USA) in 200 µL of CFA (Sigma-Aldrich). Control sham-treated mice were injected with a similar emulsion without MOG35-55. All mice were injected intraperitoneally with toxin from *B. pertussis* (500 ng/mouse, Sigma-Aldrich) at 1 and 48 h after immunization. Clinical EAE symptoms were evaluated daily according to the following score: 0 = no symptoms; 0.5 = tail weakness; 1 = tail completely flaccid; 1.5 = mild difficulty in righting; 2 = great difficulty in righting; 2.5 = unsteady gait and paraparesis (mild paralysis of one or two hind limbs); 3 = complete paralysis of one hind limb; 3.5 = complete paralysis of one hind limb and mild paralysis of the other hind limb; 4 = paraplegia (complete paralysis of two hind limbs) and incontinence; 4.5 = paraplegia and mild paralysis of one or two forelimbs; and 5 = moribund or dead. CFA and MOG-EAE mice were killed at the following timepoints: 9 DPI (presymptomatic phase), 14 DPI (symptomatic phase), 21 DPI (EAE peak), 28 DPI and 40 DPI (chronic phase) and processed for immunohistochemistry ($n = 2-3$ /group) or western blot ($n = 4-5$ /group).

4.4. Human Samples

Human frontal cortex samples were obtained from the Tissue Bank at the Hospital Clinic (Barcelona, Spain). The whole procedure was performed in accordance with the Helsinki Declaration, the Convention of the Council of Europe on Human Rights and Biomedicine, and approved by the Ethical Committee of the University of Barcelona. Postmortem histological frontal cortex samples were obtained from control subjects and MS patients, as shown in Table 1.

Table 1. Post-mortem human samples of frontal cortex obtained from healthy and MS patients.

Human Sample	Gender	Age (Years Old)	Post-Mortem Time (h)	Multiple Sclerosis Type	Neurological/Histopathological Evaluation
Control #1	Male	66	7	-	Absence of histological lesions; Absence of neurological disease
Control #2	Male	70	n.d.	-	Absence of histological lesions; Absence of neurological disease
Control #3	Female	74	3.33	-	Absence of histological lesions; Absence of neurological disease
Control #4	Female	81	23.5	-	Few Aβ-plaques in entorhinal area; Absence of neurological disease
Multiple Sclerosis #1	Female	65	8	Secondary progressive	Some chronic active lesions; Many chronic inactive lesions
Multiple Sclerosis #2	Female	48	8.25	Secondary progressive	Few chronic active lesions; Many chronic inactive lesions
Multiple Sclerosis #3	Male	46	3.25	Primary progressive	Many chronic active lesions; Few chronic inactive lesions
Multiple Sclerosis #4	Male	68	7	Secondary progressive	Few chronic active lesions; Many chronic inactive lesions
Multiple Sclerosis #5	Female	52	3.5	Secondary progressive	Very few chronic active lesions; Many chronic inactive lesions

4.5. FL and ARD TRPV2 Fragment Purification

Rat TRPV2 FL tagged with a C-terminal GFP and a 8xHis tag was overexpressed in yeast *Pichia pastoris* following our lab protocol as described in Suades et al. [52]. Yeast carrying the construct of interest was grown in YPD Zeocin at 30 °C. Cells were harvested and cultured in Minimal Glycerol Yeast media (MGY) for 48 h, till an OD600 of 10. Protein expression was induced by methanol, culturing the cells in Minimal Methanol media at 30 °C for 24 h. Cells were lysed using a bead beater. Lysates were centrifuged and pellet was solubilized for 1 h at 4 °C in 1% DDM, 0.2% cholesterol 50 mM Tris-HCl (pH 7.4) and 150 mM NaCl buffer complemented with EDTA-free protease inhibitor.

ARD of rat TRPV2 tagged with GFP and 8xHis tag in the C-terminus were heterologously expressed in *Escherichia coli* BL-21 strain, as described previously [53,54]. Expression of the protein was induced with 200 µM IPTG when the culture reached an OD600 of 0.6. After 5–6 h at 37 °C, cells were collected and lysed using a sonicator in 50 mM Tris-HCl (pH 7.4), 150 mM NaCl, 10% glycerol and EDTA-free protease inhibitors.

All lysates were centrifuged for 45 min at $25,000 \times g$ and supernatant was collected and purified using Ni-NTA resin (30210, Qiagen, Hilden, Germany). See Supplementary Figure S4 for Rat TRPV2 FL.

4.6. Slot Blot

FL rat TRPV2 and ARD TRPV2 domain were purified and placed at specific protein concentrations (see Figure 1 for details) into nitrocellulose membranes using a slot blot device. Membranes were dried for 30 min at room temperature (RT) and kept at 4°C . For the interaction screen, TRPV2 membranes were blocked with blocking buffer (2% bovine serum albumin, BSA, in 0.1 M phosphate-buffered saline, PBS, pH 7.4) and incubated with a lysate from rat brain tissue at $1\ \mu\text{g}/\text{mL}$ in blocking buffer for 1 h at RT. Then, membranes were washed in 0.1 M Tris-buffered saline (TBS, pH 7.4) + 0.1% Tween and analyzed by immunoblot against Opalin, Neurotrimin and proteolipid-1 proteins.

4.7. Cell Cultures

Secondary and quaternary cortical mixed glial cultures enriched in oligodendrocytes were obtained from 0- to 3-day-old WT C57BL/6 pups ($n = 5$), following the protocol described by Marignier et al. [55] with some modifications. Briefly, mice neocortices were dissected and digested with 0.25% trypsin (Gibco #25200-072) for 10 min at 37°C . Trypsinization was stopped by adding an equal volume of culture medium composed of Dulbecco's Modified Eagle Medium (DMEM) containing 4.5 g/l glucose (Gibco #41965-039), supplemented with 20% non-heat inactivated fetal bovine serum (FBS) (Gibco #10270106) and 0.1% penicillin/streptomycin with 0.02% deoxyribonuclease I (Sigma-Aldrich #D-5025). The solution was centrifuged at $200 \times g$ and the pellet obtained was resuspended in complete medium described above and brought to a single cell suspension by repeated pipetting followed by passage through a $100\ \mu\text{m}$ pore mesh. Glial cells were seeded at a density of 2.0×10^5 cells/mL in T25 cell culture flasks and were kept at 37°C in humidified 5% $\text{CO}_2/95\%$ air. After three days, a first medium replacement was performed with DMEM-High glucose-20% FBS. The medium was replaced every 5–6 days until the confluence of the cell culture was reached (after 14–16 days in vitro (DIV)). Once primary cultures were confluent, cells were washed for 5 min with 0.1 M PBS (pH 7.4—Gibco #14190094) and 2 mL of 0.125% trypsin-EDTA solution was added. After 5 min at 37°C in humidified 5% $\text{CO}_2/95\%$ air, trypsinization was stopped by adding 2 mL of complete medium. Cells were centrifuged for 7 min at $200 \times g$, and the pellet was resuspended with a 1000 μL pipette for 3–5 steps. For secondary glial cultures, the cells were seeded at a density of 1.5×10^5 cells/mL in T25 cell culture flasks and incubated at 37°C in humidified 5% $\text{CO}_2/95\%$ air. The medium was replaced every 5–6 days until cell confluence was reached (after 28–32 DIV). Quaternary cell cultures were obtained by repeating this process twice. For treatments, cells were seeded in 96- or 48-well culture plates (Falcon #353072, #353078) coated with poly-L-lysine (Sigma-Aldrich).

4.8. Cell Culture Treatments

Cultures were treated for 24 h with 100 ng/mL of LPS from *E. Coli* (Sigma-Aldrich #L2654), 48 h with LPS+IFN γ (100 ng/mL LPS + 4 ng/mL IFN γ —Sigma-Aldrich #I4777), or 24 h with 20 ng/mL IL-4 (BioLegend #57430). LPC (4 ng/mL) was assayed for 24 h with quaternary cell cultures. Control cells were treated with an equivalent volume of culture medium. After treatment, conditioned media were removed and frozen. For immunocytochemistry, cells were fixed with 4% paraformaldehyde (PFA, Sigma-Aldrich #158127) in 0.1 M PBS for 20 min at RT. For ELISA, cells were removed and frozen.

4.9. Nitrite Assay

Nitric oxide (NO) production in the conditioned medium of cultures was assessed by the colorimetric Griess reaction. Twenty-five μL of conditioned medium from each culture and treatment were mixed with 50 μL of a 1% sulfanilamide solution (Sigma-

Aldrich # S9251) and 5% phosphoric acid (PanReac AppliChem #131032) for 5 min. Then, 50 μ L of 0.1% N-(1-Naphthyl)ethylenediamine dihydrochloride solution (Sigma-Aldrich #222488) was added and incubated for 5 min at RT. Sodium nitrite (PanReac AppliChem #131703) was used to generate a standard curve (1.56–100 μ M). Optical density at 530 nm was determined using a Varioskan™ LUX microplate reader (Thermo Scientific, Roskilde, Denmark). Triplicates were performed for each sample and treatment.

4.10. Immunocytochemistry

Cells were permeated with 25% methanol solution for 1 min, and washed afterwards with TBS. To block inspecificities, cells were treated for 15 min with TBS + 5% FBS (Biowest, Nuaille, France, #S181H) and then incubated overnight at 4 °C with primary antibodies diluted in TBS + 5% FBS (Table 2). After several washes with PBS, cells were incubated for 1 h at RT with secondary antibodies diluted in TBS+5%FBS (Table 2) and nuclei counterstained with DAPI (1:10,000; Sigma-Aldrich #D9542). Microscopy images were obtained with an epifluorescence inverted microscope (Nikon ECLIPSE TE2000-E) at 20X with a digital camera connected to the microscope (Hamamatsu ORCA-ER monochrome microscope camera). Image collection was performed with MetaMorph Microscopy Automation and ImageJ Software (NIH, Bethesda, MD, USA).

Table 2. List of antibodies and reagents used in the slot blot, immunocytochemistry (ICC), immunohistochemistry (IHC), double immunofluorescence (IF) and western blot (WB).

Primary Antibody	Host	Dilution	Reference Manufacturer	Secondary Antibody	Dilution	Reference, Manufacturer
<i>Slot blot</i>						
Opalin	Goat	1:1000	sc-163187, SantaCruz Biotechnology	Donkey anti-goat IgG-HRP	1:2000	sc-2033, SantaCruz Biotechnology
NTM	Rabbit	1:1000	sc-98979, SantaCruz Biotechnology	Goat anti-rabbit IgG-HRP	1:2000	sc-2030, SantaCruz Biotechnology
PLP	Rabbit	1:1000	sc-98781, SantaCruz Biotechnology	Goat anti-rabbit IgG-HRP	1:2000	sc-2030, SantaCruz Biotechnology
<i>ICC</i>						
GFAP	Mouse	1:1000	G3893, Sigma-Aldrich	Alexa 555 donkey anti-mouse	1:1000	A31570, Invitrogen
CD68	Rat	1:250	MCA1957, AbD Serotec	Alexa 555 goat anti-rat	1:1000	A21434, Invitrogen
PDGFR α	Rat	1:100	558774, BD Biosciences	Alexa 555 goat anti-rat	1:1000	A21434, Invitrogen
TRPV2	Rabbit	1:200	sc-31155, SantaCruz Biotechnology	Alexa 488 donkey anti-rabbit	1:1000	A21206, Invitrogen
Opalin	Goat	1:50	sc-163187, SantaCruz Biotechnology	Biotinylated horse anti-goat	1:500	BA-9500, Vector Laboratories
<i>IHC</i>						
TRPV2	Rabbit	1:200	ACC-032, Alomone	Biotinylated horse anti-rabbit	1:500	BA-1100, Vector Laboratories
MBP	Rabbit	1:200	A-623, Dako	Biotinylated horse anti-rabbit	1:500	BA-1100, Vector Laboratories
MSRA	Rabbit	1:200	ab16803, abcam	Biotinylated horse anti-rabbit	1:500	BA-1100, Vector Laboratories
Opalin	Goat	1:50	sc-163187, SantaCruz Biotechnology	Biotinylated horse anti-goat	1:500	BA-9500, Vector Laboratories
<i>Double IF</i>						
TRPV2	Rabbit	1:100	ACC-032, Alomone	Biotinylated horse anti-rabbit	1:500	BA-1100, Vector Laboratories
APC	Mouse	1:200	Calbiochem (#OP80)	Alexa 555 donkey anti-mouse	1:500	A31570, Invitrogen
<i>WB</i>						
TRPV2	Goat	1:500	PA5-18989, ThermoFisher	Mouse anti-goat IgG-HRP	1:2000	AP186P, Sigma-Aldrich
MSRA	Rabbit	1:1000	ab16803, abcam	Donkey anti-rabbit IgG-HRP	1:5000	A16035, ThermoFisher
β -actin	Mouse	1:100,000	A1978, Sigma-Aldrich	Goat anti-mouse IgG-HRP	1:2000	62-6520, ThermoFisher

4.11. Colocalization Studies of Opalin and TRPV2 in Cell Cultures

At least four images were taken from cell cultures stained for TRPV2 (green) and Opalin (red) with and without LPS + IFN γ . Colocalization was evaluated using ImageJ and the JACoP plugin [56], which provided Pearson's and Mander's coefficient values (0 = no overlap; 1 = total overlap). The M1 (M_{Opalin}) coefficient estimates the degree of red signal overlapping green, the M2 (M_{TRPV2}) coefficient and vice versa.

4.12. Quantification of TRPV2 in Glial Cell Cultures by Enzyme-Linked Immunosorbent Assay

After washing with 0.1 M PBS, proteins were extracted using a RIPA buffer (1% NP40, 0.5% NA-deoxycholate, 0.1% SDS and one complete protease inhibitor cocktail tablet (Roche Diagnostics GmbH #11697498001) and quantified using BCA Assay (Pierce™ BCA Protein Assay Kit, ThermoFisher #23227). Samples were stored at $-20\text{ }^{\circ}\text{C}$ until use. TRPV2 was quantified using the Mouse Transient Receptor Potential Cation Channel Subfamily V, Member 2 (TRPV2) ELISA Kit (ELISAGENIE, #MODL01340) following the manufacturer's protocol. Briefly, 100 μL of blank, standards (0.16 ng/mL–10.00 ng/mL) and samples (0.3 μg protein/ μL) were added to wells and incubated for 2 h at $37\text{ }^{\circ}\text{C}$. After incubating the detection reagents and washing, the Substrate Solution was added for 15 min at $37\text{ }^{\circ}\text{C}$. Finally, 50 μL of Stop Solution was added and measurements were performed at 450 nm with an iMark™ Microplate Reader (Bio-Rad, Munich, Germany), using Microplate Manager Software 6 (Bio-Rad).

4.13. Tissue Fixation and Processing for Immunohistochemistry

Following anesthesia of ketamine (80 mg/kg) and xylazine (20 mg/kg), animals were perfused intracardially for 10 min with 4% PFA in 0.1 M phosphate buffer (PB, pH 7.4). Brain samples of cuprizone-treated mice and spinal cords of jimpy mice were dissected and included in paraffin blocks, as previously described [22]. Ten- μm -thick coronal brain sections of cuprizone-treated mice and transversal spinal cord sections of jimpy mice were cut with a microtome. For EAE-induced mice and another group of cuprizone-treated mice, samples were prepared for cryostat sectioning. After spinal cord or brain dissection, samples were post-fixed with 4% PFA for 4 h at $4\text{ }^{\circ}\text{C}$, cryoprotected in 30% sucrose in 0.1 M PB for 48 h at $4\text{ }^{\circ}\text{C}$ and frozen in ice-cold methylbutane (320404, Sigma-Aldrich). Thirty- μm -thick longitudinal spinal cord sections or coronal brain sections were obtained using a CM3050s Leica cryostat, and stored at $-20\text{ }^{\circ}\text{C}$ in antifreeze solution.

4.14. Immunohistochemistry

Brain and spinal cord paraffin sections and cryostat spinal cord sections were processed for immunohistochemistry. Paraffin sections were first deparaffined with xylol and hydrated with decreasing graded ethanol solutions, followed by an antigen retrieval step with sodium citrate buffer with 0.1% Triton (pH 6, 40 min at $95\text{ }^{\circ}\text{C}$). After washing with 0.1 M TBS, paraffin or cryostat sections were inactivated for endogenous peroxidase for either 5 or 10 min, respectively, with 2% H_2O_2 in a 70% methanol solution. Sections were washed with TBS+0.1% Triton (TBS-0.1%T) or TBS-1%T for cryostat sections, and incubated for 1 h with blocking buffer solution (BB; 0.05 M TBS, pH 7.4, containing 10% fetal calf serum, 3% BSA and 0.1% Triton X-100). Sections were incubated with the primary antibody diluted in BB overnight at $4\text{ }^{\circ}\text{C}$ followed by 1 h at RT (Table 2). After washing, sections were incubated with the secondary antibody diluted in BB for 1 h at RT (Table 2). Then, sections were washed and incubated for 1 h at RT with horseradish peroxidase-conjugated streptavidin (1:500; SA-5004, Vector Laboratories, Burlingame, CA, USA), and reaction was visualized using a DAB Substrate Kit (SK4100, Vector Laboratories). Sections were dehydrated, treated with xylene and coverslipped with DPX. Sections incubated in BB without primary antibody were used as negative controls, and for MSRA staining, cerebellum sections were used as positive controls.

4.15. Quantification of Immunohistochemical Stainings

Quantitative analysis was performed on sections stained for MBP, TRPV2, Opalin and MSRA. Two to four sections per animal were analyzed. In spinal cord sections of jimpy mice, two photographs per section were taken at $10\times$ magnification for MBP, Opalin and MSRA analysis, and at $20\times$ magnification for TRPV2 analysis. In brain sections of cuprizone-treated mice ($n = 3\text{--}4$ /experimental group), one photograph of the CC was taken at $10\times$ magnification per section. All images were obtained using a DXM 1200F Nikon digital camera joined to a brightfield Nikon Eclipse 80i microscope and the corresponding

ACT-1 2.20 software (Nikon Corporation, Tokyo, Japan). Quantification was performed using AnalySIS software (Soft Imaging System, Münster, Germany), manually setting the threshold for the staining. Analysis resulted in the percentage of area (% Area) and the intensity of the immunoreaction (Mean Gray Value Mean). AI index was calculated by multiplying the percentage of the immunolabeled area and the Mean Gray Value Mean [57]. Results of the AI index and intensity were expressed in arbitrary units.

4.16. Double Immunohistochemistry

Brain cryostat sections were processed for double immunohistochemistry for TRPV2 and APC ($n = 3$ /group). After washes with 0.1 M TBS, sections were incubated for 1 h with BB, and then, overnight with rabbit anti-TRPV2 (1:100, Alomone) diluted in BB at 4 °C and 1 h at RT (Table 2). After washing with TBS-1%T, sections were incubated with an anti-rabbit secondary biotinylated antibody in BB for 1 h at RT (Table 2). Then, sections were washed and incubated for 1 h at RT with streptavidin conjugated to AF488 (1:500, S11223, Invitrogen). After washes, sections were blocked with BB for 1 h and incubated with the primary antibody mouse anti-APC (1:200) overnight at 4 °C and for 1 h at RT. After washes, an anti-mouse IgG secondary antibody conjugated to AF555 was incubated for 1 h at RT, and sections were counterstained with DAPI (1:10,000). Sections were mounted and coverslipped using Fluoromount G™ (0100-01, SouthernBiotech, Birmingham, AL, USA). Sections incubated in BB without primary antibody were used as negative controls. Stained sections were observed and photographed using a Zeiss LSM700 confocal microscope. Images were processed for the maximal intensity projection using Fiji software and merged using Adobe PhotoShop CS6 software.

4.17. Isolation of Total Proteins

Thoracic spinal cords from control (CFA) and EAE (MOG) mice were dissected and quickly frozen in dry ice. Tissues were first sonicated at 4 °C in RIPA buffer (PBS, 10 µL/mL; Igepal, 5 mg/mL; sodium deoxycholate 1 mg/mL SDS) containing protease and phosphatase inhibitor cocktails (Sigma-Aldrich). One mL of ice-cold RIPA buffer was used per gram of tissue. After 30 min of incubation at 4 °C, samples were centrifuged at 5000× g rpm for 10 min at 4 °C and the supernatants were collected. For human samples, total protein extracts were obtained from the powder of frontal cortex samples using a mortar cooled with liquid nitrogen and 100 mg tissue homogenized in 1 mL of Laemmli buffer (0.125 M Tris-HCl pH 6.8, 2% SDS, 10% glycerol, 0.001% bromophenol blue and 5% 2-mercaptoethanol) [58,59] using a vortex. After that, samples were incubated for 10 min at 70 °C, centrifuged at 16,000× g for 10 min at RT and the supernatant was collected.

Protein quantification was determined by Bradford assay (Bio-Rad Laboratories, Madrid, Spain). Samples were stored at −20 °C to be used for western blot analysis.

4.18. Quantification of TRPV2 and MSRA in EAE Mouse and Human Samples by Western Blot

Western blots were performed as previously described by Valente et al. [60]. Briefly, 30 µg of total protein was resolved on 10% SDS-PAGE gels (using the Bio-Rad Mini-PROTEAN 3 system) and transferred to a PVDF membrane (IPVH00010, Millipore, Darmstadt, Germany) for 90 min at 1 mA/cm². Membranes were incubated overnight at 4 °C with primary antibodies (Table 2) diluted in immunoblot buffer (TBS containing 0.05% Tween-20 and 5% non-fat dry milk). After washing with immunoblot buffer, membranes were incubated for 1 h at RT with horseradish peroxidase-labeled secondary antibodies (Table 2). Membranes were developed with ECL-Plus (GE Healthcare, Little Chalfont, UK) and images were obtained using a VersaDoc System camera (Bio-Rad Laboratories). Data are expressed as the ratio between the band intensity of the protein of interest and the loading control protein (β-actin).

4.19. RNA Extraction, cDNA Synthesis and Expression Analyses in Human Samples

Total RNA was extracted from 4 healthy subjects and 5 MS patients as previously described in [60]. Briefly, total RNA was isolated from frozen tissue samples using the Trizol method (Tri[®] Reagent, Sigma-Aldrich). One microgram of RNA was reverse-transcribed with random primers using Transcriptor Reverse Transcriptase (Roche Diagnostics Scheiwz AG, Rotkreuz, Switzerland). Then, cDNA was diluted 1/10 to perform quantitative real-time polymerase chain reaction (qRT-PCR) of MSRA, TRPV2 and GAPDH (housekeeping) mRNA with iTaq[™] Universal SYBR[®] Green Supermix (Bio-Rad #1725121) by qPCR in a Bio-Rad CFX384 RT-PCR System. Reaction mixtures totaling 15 μ L contained 5 ng of cDNA, 7.5 μ L of iTaq[™] Universal SYBR[®] Green Supermix, 500 nM of primer forward and 500 nM of primer reverse (Table 3). Conditions for a thermal cycling test consisted of one 3 min cycle at 95 °C, followed by 49 cycles of 10 s at 95 °C and 49 cycles of 30 s at 60 °C. Melting curves were completed at the end of the amplification with 1 cycle at 95 °C for 10 s, followed by a rate of increase of 0.5 °C/cycle from 65 to 95 °C. Primers were checked by melting curve analysis and no-template control reactions. The GAPDH gene was chosen as an internal reference. Expression levels were calculated using $2^{-\Delta\Delta Ct}$.

Table 3. Primers used for quantitative polymerase chain reaction (qPCR).

Target Gene	Primer Sequences (5'→3')	Annealing Temp. (°C)
MSRA	F: GGC CAT CTA CCC GAC CTC T	60
	R: GCC ATT GGG GTT CTT GCT CA	
TRPV2	F: TCA GGT TGG AGA CAT TAG ATG GA	60
	R: TCG GTA GTT GAG GTT GAC TCT T	
GAPDH	F: CAT GAG AAG TAT GAC AAC AGC CT	60
	R: AGT CCT TCC ACG ATA CCA AAG T	

4.20. Statistical Analysis

Statistics was performed using Graph Pad Prism[®] (Graph Pad Software Inc., San Diego, CA, USA) and results were expressed as mean \pm Standard Error of the Mean (SEM). The statistical tests used were: for cell culture treatments, one-way ANOVA followed by Dunnett's post hoc test (for LPS/IL-4 treatments) and paired Student's *t*-test (for LPC treatment); for time-course experiments (cuprizone, EAE), one-way ANOVA with either Tukey's or Newman–Keuls post hoc test, respectively; and for TRPV2–Opalin colocalization, jimpy mouse and MS human samples compared to controls, unpaired Student's *t*-test.

5. Conclusions

Previous studies have shown that TRPV2 is expressed mainly in neurons at developmental stages (Figure 7). In this work, we first identified TRPV2 expression in oligodendrocytes, and its regulation during pro-inflammatory and anti-inflammatory conditions *in vitro*. This regulation was also observed in deleterious myelination disorders in mice, such as hypomyelination and de-/remyelination, suggesting the involvement of TRPV2 in the cross-talk between neurons, microglia and oligodendrocytes. TRPV2 regulation was predominantly found during inflammation in microglia and immune cells, and during remyelination in oligodendrocytes (Figure 7). Finally, we also identified TRPV2 as an altered protein in the pathology of MS, which points out TRPV2 as an interesting clinical target in myelination disorders' therapy. Further studies are needed to better understand the role of TRPV2 in myelination diseases and how TRPV2 modulation could affect the phenotype of these diseases.

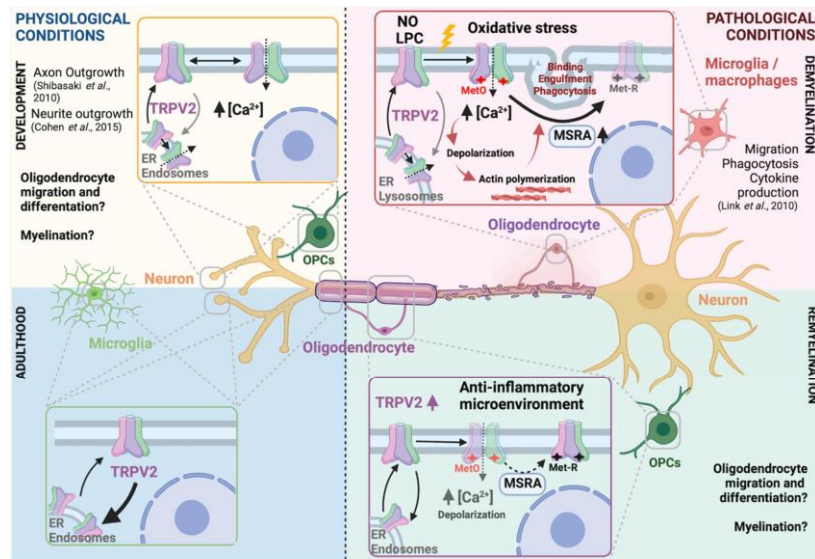


Figure 7. TRPV2-centered cellular cross-talk model in physiological and pathophysiological myelination. During embryonic development, TRPV2 develops an essential role in neurite and axon outgrowth. In that period, TRPV2 is known to be expressed and activated in neurons, and putatively in OPCs, where possible cross-talk between both cells might be triggered through TRPV2 activation. In adulthood, TRPV2 expression is found in microglia, neurons and oligodendrocytes. Upon an insult such as demyelination, TRPV2, as a non-selective ion channel, is activated. Some known triggering stimuli are NO, LPC or oxidative stress, the latter causing methionine oxidation which facilitates TRPV2 sensitization. TRPV2 activation promotes a sodium/calcium inward influx from extracellular media and/or ER or endosomes. Consequently, cells are depolarized, which initiate processes such as actin polymerization or phagocytosis in microglia or innate immune cells. In those cells, TRPV2 has been involved in migration, phagocytosis or cytokine production. TRPV2 inactivation is promoted by MSRA enzyme, by reducing oxidized methionine. In our results, we observed both an increase of TRPV2 and MSRA in demyelinating scenarios. During remyelination, OPCs proliferate and migrate to the demyelinated area, where they differentiate through several stages to mature oligodendrocytes, and start myelination. Our results showed increased TRPV2 expression during this period. Overall, ubiquitous TRPV2 expression and activation in de- and remyelinating processes suggest a multicellular cross-talk that promotes myelin repair at all levels. TRPV2 is relevant in development and demyelination, making this model suitable for the recapitulation hypotheses. Created with [BioRender.com](https://www.biorender.com) (accessed on 10 January 2022) [8–10].

Supplementary Materials: The following supporting information can be downloaded at: <https://www.mdpi.com/article/10.3390/ijms23073617/s1>.

Author Contributions: Conceptualization, G.M. and A.P.-M.; Methodology, J.E.-B., G.M., B.A., P.S.-M. and T.V.; Formal analysis, J.E.-B., G.M., B.A., P.S.-M. and T.V.; Resources, C.S., J.S., B.G., B.C. and A.P.-M.; Writing—original draft preparation, J.E.-B., G.M. and A.P.-M.; Funding acquisition, B.C. and A.P.-M. All authors have read and agreed to the published version of the manuscript.

Funding: The authors acknowledge financial support from the Spanish Government MCIN/AEI/10.13039/501100011033 (Project BFU2017-87843-R- to B.C. and A.P.-M.; Project PID2020-120222GB-I00 to A.P.-M.).

Institutional Review Board Statement: Animals were maintained in conventional plastic cages with food and water ad libitum, in a 12 h light/dark cycle, at 22 ± 2 °C and 50–60% humidity. All experimental work was conducted according to Spanish regulations (Ley 32/2007, Real Decreto 1201/2005, Ley 9/2003, y Real Decreto 178/2004) in agreement with European Union directives (86/609/CEE, 91/628/CEE i 92/65/CEE) and was approved by the Ethical and Scientific Committees of the Autonomous University of Barcelona, the Spanish National Research Council (CSIC) and the University of Barcelona (Spain).

Informed Consent Statement: Post-mortem human brain samples used in this study were supplied by the human neurological tissue bank at the Hospital Clinic (Barcelona, Spain; REF. HCB/2014/1027) and granted by consent from next-of-kin or family. The whole procedure was performed in accordance with the Helsinki Declaration in its latest version and with the Convention of the Council of Europe on Human Rights and Biomedicine, and was approved by the Ethical Committees of the University of Barcelona and Spanish National Research Council-CSIC (REF. 711/14).

Data Availability Statement: Not applicable.

Acknowledgments: We are grateful to the Tissue Bank at the Hospital Clinic (Barcelona, Spain) for the provision of human brain tissue. The authors want to acknowledge the skillful assistance of Elodia Serrano, Pau Doñate-Macian, Miguel Ángel Martil, Virginia Luque Fernández, Núria Munné Rodríguez and Álex Gascón Saperas. We would like to also thank also Marc Cerrada-Giménez for critical reading of the manuscript, R. López-Vales for kindly providing LPC reagent and M.J. Barallobre, for the PDGFR α antibody.

Conflicts of Interest: The authors declare no conflict of interest.

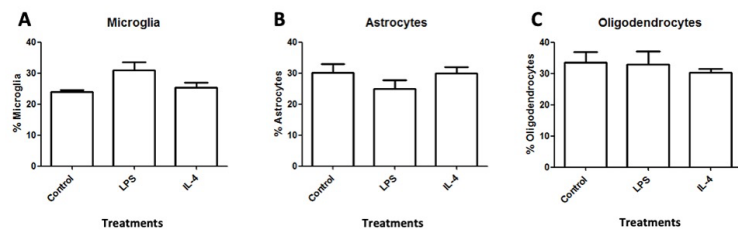
References

1. Perálvarez-Marín, A.; Doñate-Macian, P.; Gaudet, R. What do we know about the transient receptor potential vanilloid 2 (TRPV2) ion channel? *FEBS J.* **2013**, *280*, 5471–5487. [[CrossRef](#)] [[PubMed](#)]
2. Fricke, T.C.; Echtermeyer, F.; Zielke, J.; de la Roche, J.; Filipovic, M.R.; Claverol, S.; Herzog, C.; Tominaga, M.; Pumroy, R.A.; Moiseenkova-Bell, V.Y.; et al. Oxidation of methionine residues activates the high-threshold heat-sensitive ion channel TRPV2. *Proc. Natl. Acad. Sci. USA* **2019**, *116*, 24359–24365. [[CrossRef](#)] [[PubMed](#)]
3. Kojima, I.; Nagasawa, M. TRPV2. *Handb. Exp. Pharmacol.* **2014**, *222*, 247–272. [[CrossRef](#)] [[PubMed](#)]
4. Caterina, M.J.; Rosen, T.A.; Tominaga, M.; Brake, A.J.; Julius, D. A capsaicin-receptor homologue with a high threshold for noxious heat. *Nature* **1999**, *398*, 436–441. [[CrossRef](#)] [[PubMed](#)]
5. Maksoud, M.J.E.; Tellios, V.; An, D.; Xiang, Y.; Lu, W. Nitric oxide upregulates microglia phagocytosis and increases transient receptor potential vanilloid type 2 channel expression on the plasma membrane. *Glia* **2019**, *67*, 2294–2311. [[CrossRef](#)]
6. Shibasaki, K.; Ishizaki, Y.; Mandadi, S. Astrocytes express functional TRPV2 ion channels. *Biochem. Biophys. Res. Commun.* **2013**, *441*, 327–332. [[CrossRef](#)]
7. Cahoy, J.D.; Emery, B.; Kaushal, A.; Foo, L.C.; Zamanian, J.L.; Christopherson, K.S.; Xing, Y.; Lubischer, J.L.; Krieg, P.A.; Krupenko, S.A.; et al. A Transcriptome Database for Astrocytes, Neurons, and Oligodendrocytes: A New Resource for Understanding Brain Development and Function. *J. Neurosci.* **2008**, *28*, 264–278. [[CrossRef](#)]
8. Cohen, M.R.; Johnson, W.M.; Pilat, J.M.; Kiselar, J.; DeFrancesco-Lisowitz, A.; Zigmond, R.E.; Moiseenkova-Bell, V.Y. Nerve Growth Factor Regulates Transient Receptor Potential Vanilloid 2 via Extracellular Signal-Regulated Kinase Signaling to Enhance Neurite Outgrowth in Developing Neurons. *Mol. Cell. Biol.* **2015**, *35*, 4238–4252. [[CrossRef](#)]
9. Shibasaki, K.; Murayama, N.; Ono, K.; Ishizaki, Y.; Tominaga, M. TRPV2 Enhances Axon Outgrowth through Its Activation by Membrane Stretch in Developing Sensory and Motor Neurons. *J. Neurosci.* **2010**, *30*, 4601–4612. [[CrossRef](#)]
10. Link, T.M.; Park, U.; Vonakis, B.M.; Raben, D.M.; Soloski, M.J.; Caterina, M.J. TRPV2 has a pivotal role in macrophage particle binding and phagocytosis. *Nat. Immunol.* **2010**, *11*, 232–239. [[CrossRef](#)]
11. Doñate-Macian, P.; Gómez, A.; Dégano, I.R.; Perálvarez-Marín, A. A TRPV2 interactome-based signature for prognosis in glioblastoma patients. *Oncotarget* **2018**, *9*, 18400–18409. [[CrossRef](#)] [[PubMed](#)]
12. Santoni, G.; Amantini, C. The Transient Receptor Potential Vanilloid Type-2 (TRPV2) Ion Channels in Neurogenesis and Gliomagenesis: Cross-Talk between Transcription Factors and Signaling Molecules. *Cancers* **2019**, *11*, 322. [[CrossRef](#)] [[PubMed](#)]
13. Yoshikawa, F.; Sato, Y.; Tohyama, K.; Akagi, T.; Hashikawa, T.; Nagakura-Takagi, Y.; Sekine, Y.; Morita, N.; Baba, H.; Suzuki, Y.; et al. Opalin, a Transmembrane Sialoglycoprotein Located in the Central Nervous System Myelin Paranodal Loop Membrane. *J. Biol. Chem.* **2008**, *283*, 20830–20840. [[CrossRef](#)] [[PubMed](#)]
14. Hainz, N.; Wolf, S.; Tschernig, T.; Meier, C. Probenecid Application Prevents Clinical Symptoms and Inflammation in Experimental Autoimmune Encephalomyelitis. *Inflammation* **2016**, *39*, 123–128. [[CrossRef](#)]
15. Hainz, N.; Wolf, S.; Beck, A.; Wagenpfeil, S.; Tschernig, T.; Meier, C. Probenecid arrests the progression of pronounced clinical symptoms in a mouse model of multiple sclerosis. *Sci. Rep.* **2017**, *7*, 17214. [[CrossRef](#)]

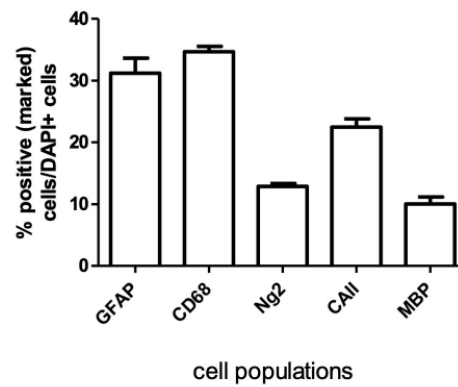
16. Hainz, N.; Becker, P.; Rapp, D.; Wagenpfeil, S.; Wonnenberg, B.; Beisswenger, C.; Tschernig, T.; Meier, C. Probenecid-treatment reduces demyelination induced by cuprizone feeding. *J. Chem. Neuroanat.* **2017**, *85*, 21–26. [\[CrossRef\]](#)
17. Nave, K.A.; Lai, C.; Bloom, F.E.; Milner, R.J. Jimpy mutant mouse: A 74-base deletion in the mRNA for myelin proteolipid protein and evidence for a primary defect in RNA splicing. *Proc. Natl. Acad. Sci. USA* **1986**, *83*, 9264–9268. [\[CrossRef\]](#)
18. Koepfen, A.H.; Barron, K.D.; Csiza, C.K.; Greenfield, E.A. Comparative immunocytochemistry of Pelizaeus-Merzbacher disease, the jimpy mouse, and the myelin-deficient rat. *J. Neurol. Sci.* **1988**, *84*, 315–327. [\[CrossRef\]](#)
19. Vela, J.M.; González, B.; Castellano, B. Understanding glial abnormalities associated with myelin deficiency in the jimpy mutant mouse. *Brain Res. Rev.* **1998**, *26*, 29–42. [\[CrossRef\]](#)
20. Lee, B.C.; Le, D.T.; Gladyshev, V.N. Mammals Reduce Methionine-S-sulfoxide with MsrA and Are Unable to Reduce Methionine-R-sulfoxide, and This Function Can Be Restored with a Yeast Reductase. *J. Biol. Chem.* **2008**, *283*, 28361–28369. [\[CrossRef\]](#)
21. Monet, M.; Gkika, D.; Lehen'Ky, V.; Pourtier, A.; Abeele, F.V.; Bidaux, G.; Juvin, V.; Rassendren, F.; Humez, S.; Prevarsakaya, N. Lysophospholipids stimulate prostate cancer cell migration via TRPV2 channel activation. *Biochim. Biophys. Acta* **2009**, *1793*, 528–539. [\[CrossRef\]](#) [\[PubMed\]](#)
22. Petković, F.; Campbell, I.L.; Gonzalez, B.; Castellano, B. Astrocyte-targeted production of interleukin-6 reduces astroglial and microglial activation in the cuprizone demyelination model: Implications for myelin clearance and oligodendrocyte maturation. *Glia* **2016**, *64*, 2104–2119. [\[CrossRef\]](#) [\[PubMed\]](#)
23. Golan, N.; Adamsky, K.; Kartvelishvili, E.; Brockschneider, D.; Möbius, W.; Spiegel, I.; Roth, A.; Thomson, C.E.; Rechavi, G.; Peles, E. Identification of Tmem10/Opalinas an oligodendrocyte enriched gene using expression profiling combined with genetic cell ablation. *Glia* **2008**, *56*, 1176–1186. [\[CrossRef\]](#) [\[PubMed\]](#)
24. Jiang, W.; Yang, W.; Zhang, J.; Pang, D.; Gan, L.; Luo, L.; Fan, Y.; Liu, Y.; Chen, M. Identification of Tmem10 as a Novel Late-stage Oligodendrocytes Marker for Detecting Hypomyelination. *Int. J. Biol. Sci.* **2013**, *10*, 33–42. [\[CrossRef\]](#)
25. Kippert, A.; Trajkovic, K.; Fitzner, D.; Opitz, L.; Simons, M. Identification of Tmem10/Opalin as a novel marker for oligodendrocytes using gene expression profiling. *BMC Neurosci.* **2008**, *9*, 40. [\[CrossRef\]](#)
26. De Faria, O.; Dhaunchak, A.S.; Kamen, Y.; Roth, A.D.; Kuhlmann, T.; Colman, D.R.; Kennedy, T.E. TMEM10 Promotes Oligodendrocyte Differentiation and is Expressed by Oligodendrocytes in Human Remyelinating Multiple Sclerosis Plaques. *Sci. Rep.* **2019**, *9*, 3606. [\[CrossRef\]](#)
27. Sulik, M.; Seeliger, S.; Aubert, J.; Schwab, V.D.; Cevikbas, F.; Rivier, M.; Nowak, P.; Voegel, J.J.; Buddenkotte, J.; Steinhoff, M. Distribution and Expression of Non-Neuronal Transient Receptor Potential (TRPV) Ion Channels in Rosacea. *J. Investig. Dermatol.* **2012**, *132*, 1253–1262. [\[CrossRef\]](#)
28. Maksoud, M.J.; Tellios, V.; Xiang, Y.-Y.; Lu, W.-Y. Nitric oxide displays a biphasic effect on calcium dynamics in microglia. *Nitric Oxide* **2021**, *108*, 28–39. [\[CrossRef\]](#)
29. Platten, M.; Ho, P.P.; Youssef, S.; Fontoura, P.; Garren, H.; Hur, E.M.; Gupta, R.; Lee, L.Y.; Kidd, B.A.; Robinson, W.H.; et al. Treatment of Autoimmune Neuroinflammation with a Synthetic Tryptophan Metabolite. *Science* **2005**, *310*, 850–855. [\[CrossRef\]](#)
30. Thomson, C.; Anderson, T.; McCulloch, M.; Dickinson, P.; Vouyiouklis, D.; Griffiths, I. The early phenotype associated with the jimpy mutation of the proteolipid protein gene. *J. Neurocytol.* **1999**, *28*, 207–221. [\[CrossRef\]](#)
31. Ruiz, M.; Bégou, M.; Launay, N.; Ranea-Robles, P.; Bianchi, P.; López-Erauskin, J.; Morató, L.; Guilera, C.; Petit, B.; Vours-Barrière, C.; et al. Oxidative stress and mitochondrial dynamics malfunction are linked in Pelizaeus-Merzbacher disease. *Brain Pathol.* **2018**, *28*, 611–630. [\[CrossRef\]](#) [\[PubMed\]](#)
32. Zhang, C.; Jia, P.; Jia, Y.; Weissbach, H.; Webster, K.A.; Huang, X.; Lemanski, S.L.; Achary, M.; Lemanski, L.F. Methionine sulfoxide reductase A (MsrA) protects cultured mouse embryonic stem cells from H₂O₂-mediated oxidative stress. *J. Cell. Biochem.* **2010**, *111*, 94–103. [\[CrossRef\]](#) [\[PubMed\]](#)
33. Torkildsen, Ø.; Brunborg, L.A.; Myhr, K.-M.; Bø, L. The cuprizone model for demyelination. *Acta Neurol. Scand.* **2008**, *117*, 72–76. [\[CrossRef\]](#) [\[PubMed\]](#)
34. Van Der Star, B.J.; Vogel, D.Y.; Kipp, M.; Puentes, F.; Baker, D.; Amor, S. In Vitro and In Vivo Models of Multiple Sclerosis. *CNS Neurol. Disord. Drug Targets* **2012**, *11*, 570–588. [\[CrossRef\]](#) [\[PubMed\]](#)
35. Baker, D. Mouse Models of Multiple Sclerosis: Lost in Translation? *Curr. Pharm. Des.* **2015**, *21*, 2440–2452. [\[CrossRef\]](#)
36. Yamate-Morgan, H.; Lauderdale, K.; Horeczko, J.; Merchant, U.; Tiwari-Woodruff, S.K. Functional Effects of Cuprizone-Induced Demyelination in the Presence of the mTOR-Inhibitor Rapamycin. *Neuroscience* **2019**, *406*, 667–683. [\[CrossRef\]](#)
37. Plastini, M.J.; Desu, H.L.; Brambilla, R. Dynamic Responses of Microglia in Animal Models of Multiple Sclerosis. *Front. Cell. Neurosci.* **2020**, *14*, 269. [\[CrossRef\]](#)
38. Gudi, V.; Gingele, S.; Skripuletz, T.; Stangel, M. Glial response during cuprizone-induced de- and remyelination in the CNS: Lessons learned. *Front. Cell. Neurosci.* **2014**, *8*, 73. [\[CrossRef\]](#)
39. Zorzella-Pezavento, S.F.G.; Chiuso-Minicucci, F.; França, T.G.D.; Ishikawa, L.L.W.; da Rosa, L.C.; Marques, C.; Ikoma, M.R.V.; Sartori, A. Persistent Inflammation in the CNS during Chronic EAE Despite Local Absence of IL-17 Production. *Mediat. Inflamm.* **2013**, *2013*, 519627. [\[CrossRef\]](#)
40. Mangiardi, M.; Crawford, D.K.; Xia, X.; Du, S.; Simon-Freeman, R.; Voskuhl, R.R.; Tiwari-Woodruff, S.K. An Animal Model of Cortical and Callosal Pathology in Multiple Sclerosis. *Brain Pathol.* **2011**, *21*, 263–278. [\[CrossRef\]](#)
41. Saunders, C.I.; Kunde, D.; Crawford, A.; Geraghty, D.P. Expression of transient receptor potential vanilloid 1 (TRPV1) and 2 (TRPV2) in human peripheral blood. *Mol. Immunol.* **2007**, *44*, 1429–1435. [\[CrossRef\]](#) [\[PubMed\]](#)

42. Girolamo, F.; Ferrara, G.; Strippoli, M.; Rizzi, M.; Errede, M.; Trojano, M.; Perris, R.; Roncali, L.; Svelto, M.; Mennini, T.; et al. Cerebral cortex demyelination and oligodendrocyte precursor response to experimental autoimmune encephalomyelitis. *Neurobiol. Dis.* **2011**, *43*, 678–689. [[CrossRef](#)] [[PubMed](#)]
43. Kashani, I.R.; Chavoshi, H.; Pasbakhsh, P.; Hassani, M.; Omid, A.; Mahmoudi, R.; Beyer, C.; Zendedel, A. Protective effects of erythropoietin against cuprizone-induced oxidative stress and demyelination in the mouse corpus callosum. *Iran. J. Basic Med. Sci.* **2017**, *20*, 886–893. [[CrossRef](#)] [[PubMed](#)]
44. Packialakshmi, B.; Zhou, X. Experimental autoimmune encephalomyelitis (EAE) up-regulates the mitochondrial activity and manganese superoxide dismutase (MnSOD) in the mouse renal cortex. *PLoS ONE* **2018**, *13*, e0196277. [[CrossRef](#)]
45. Luo, S.; Levine, R.L. Methionine in proteins defends against oxidative stress. *FASEB J.* **2009**, *23*, 464–472. [[CrossRef](#)]
46. Noble, P.G.; Antel, J.P.; Yong, V.W. Astrocytes and catalase prevent the toxicity of catecholamines to oligodendrocytes. *Brain Res.* **1994**, *633*, 83–90. [[CrossRef](#)]
47. Thorburne, S.K.; Juurlink, B.H.J. Low Glutathione and High Iron Govern the Susceptibility of Oligodendroglial Precursors to Oxidative Stress. *J. Neurochem.* **1996**, *67*, 1014–1022. [[CrossRef](#)]
48. Ohl, K.; Tenbrock, K.; Kipp, M. Oxidative stress in multiple sclerosis: Central and peripheral mode of action. *Exp. Neurol.* **2016**, *277*, 58–67. [[CrossRef](#)]
49. Offen, D.; Gilgun-Sherki, Y.; Melamed, E. The role of oxidative stress in the pathogenesis of multiple sclerosis: The need for effective antioxidant therapy. *J. Neurol.* **2004**, *251*, 261–268. [[CrossRef](#)]
50. Dowling, P.; Husar, W.; Menonna, J.; Donnenfeld, H.; Cook, S.; Sidhu, M. Cell death and birth in multiple sclerosis brain. *J. Neurol. Sci.* **1997**, *149*, 1–11. [[CrossRef](#)]
51. Zipp, F. Apoptosis in multiple sclerosis. *Cell Tissue Res.* **2000**, *301*, 163–171. [[CrossRef](#)] [[PubMed](#)]
52. Suades, A.; Alcaraz, A.; Cruz, E.; Marimon, E.A.; Whitelegge, J.P.; Manyosa, J.; Cladera, J.; Perálvarez-Marín, A. Structural biology workflow for the expression and characterization of functional human sodium glucose transporter type 1 in *Pichia pastoris*. *Sci. Rep.* **2019**, *9*, 1203. [[CrossRef](#)] [[PubMed](#)]
53. Jin, X.; Touhey, J.; Gaudet, R. Structure of the N-terminal Ankyrin Repeat Domain of the TRPV2 Ion Channel. *J. Biol. Chem.* **2006**, *281*, 25006–25010. [[CrossRef](#)] [[PubMed](#)]
54. Doñate-Macián, P.; Álvarez-Marimon, E.; Sepulcre, F.; Vázquez-Ibar, J.L.; Perálvarez-Marín, A. The Membrane Proximal Domain of TRPV1 and TRPV2 Channels Mediates Protein–Protein Interactions and Lipid Binding In Vitro. *Int. J. Mol. Sci.* **2019**, *20*, 682. [[CrossRef](#)] [[PubMed](#)]
55. Marignier, R.; Nicolle, A.; Watrin, C.; Touret, M.; Cavagna, S.; Varrin-Doyer, M.; Cavillon, G.; Rogemond, V.; Confavreux, C.; Honnorat, J.; et al. Oligodendrocytes are damaged by neuromyelitis optica immunoglobulin G via astrocyte injury. *Brain* **2010**, *133*, 2578–2591. [[CrossRef](#)]
56. Bolte, S.; Cordelières, F.P. A guided tour into subcellular colocalization analysis in light microscopy. *J. Microsc.* **2006**, *224*, 213–232. [[CrossRef](#)]
57. Acarin, L.; González, B.; Castellano, B.; Castro, A.J. Quantitative Analysis of Microglial Reaction to a Cortical Excitotoxic Lesion in the Early Postnatal Brain. *Exp. Neurol.* **1997**, *147*, 410–417. [[CrossRef](#)]
58. Laemmli, U.K. Cleavage of Structural Proteins during the Assembly of the Head of Bacteriophage T4. *Nature* **1970**, *227*, 680–685. [[CrossRef](#)]
59. Laemmli, U.; Favre, M. Maturation of the head of bacteriophage T4: I. DNA packaging events. *J. Mol. Biol.* **1973**, *80*, 575–599. [[CrossRef](#)]
60. Valente, T.; Mancera, P.; Tusell, J.M.; Serratos, J.; Saura, J. C/EBP β expression in activated microglia in amyotrophic lateral sclerosis. *Neurobiol. Aging* **2012**, *33*, 2186–2199. [[CrossRef](#)]

Supplementary information

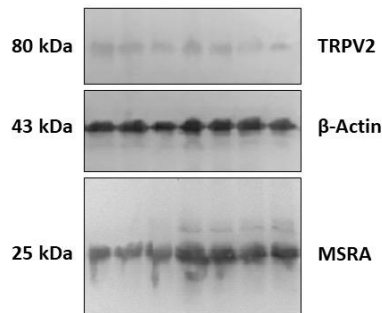


Supplementary Figure S1. Determination of glial populations in mixed glial secondary cell cultures in basal conditions and after pro-inflammatory LPS and anti-inflammatory IL-4 treatments.

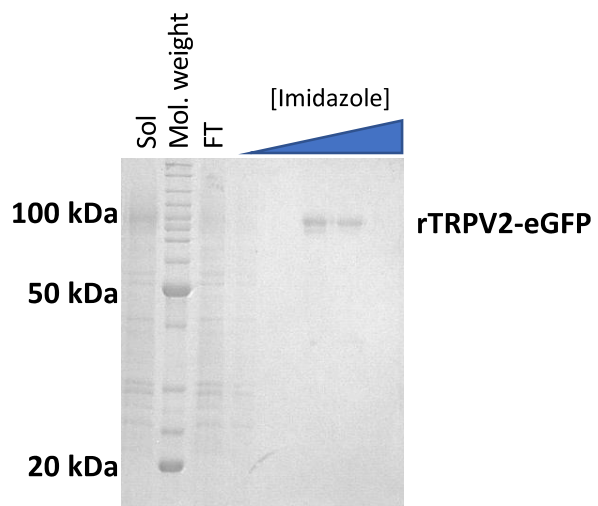


Supplementary Figure S2. Characterization of mixed glial cultures under basal conditions.

Western Blot Quantification	Healthy (H)				Multiple Sclerosis (MS)					Unpaired t test (H vs MS)
	H1	H2	H3	MEAN	MS1	MS2	MS3	MS4	MEAN	
MSRA	0,878	0,873	1,016		1,277	1,344	1,246	1,290		
TRPV2	0,280	0,263	0,227		0,238	0,221	0,176	0,152		
Correction Factor (β-Actin)	1,027	1,063	0,946		1,067	1,026	1,008	0,863		
MSRA β-Actin-Normalized	0,856	0,821	1,074	0,917±0,137	1,196	1,309	1,236	1,495	1,309±0,133	*, p = 0,0124
TRPV2 β-Actin-Normalized	0,273	0,248	0,240	0,253±0,017	0,223	0,216	0,175	0,176	0,197±0,026	*, p = 0,0232



Supplementary Figure S3. Protein determination and data analysis of immunoblot in Figure 6C.



Supplementary Figure S4. Coomassie blue staining of Ni-NTA FL-TRPV2 enrichment and imidazole elution resolved in a 12% SDS-PAGE electrophoresis. Sol; detergent solubilized fraction loaded in the chromatography column. FT; Flow through fraction.

Chapter III

Deciphering the genetic crosstalk between microglia and oligodendrocyte precursor cells during demyelination and remyelination using transcriptomic data

Deciphering the genetic crosstalk between microglia and oligodendrocyte precursor cells during demyelination and remyelination using transcriptomic data

Enrich-Bengoa J^{1,2,†}, Manich G^{2,3,†}, Décano IR^{4-6,*}, Perálvarez-Marín A^{1,2,*}.

¹ Biophysics Unit, Department of Biochemistry and Molecular Biology, School of Medicine, Universitat Autònoma de Barcelona, 08193 Cerdanyola del Vallès, Catalonia, Spain

² Institut de Neurociències, Universitat Autònoma de Barcelona, 08193 Cerdanyola del Vallès, Catalonia, Spain

³ Medical Histology Unit, Department of Cell Biology, Physiology and Immunology, School of Medicine, Universitat Autònoma de Barcelona, 08193 Cerdanyola del Vallès, Catalonia, Spain

⁴ Centro de Investigación Biomédica en Red of Cardiovascular diseases (CIBERCV), Instituto de Salud Carlos III, Madrid, Spain

⁵ *Registre Gironí del Cor* (REGICOR) Study Group, *Hospital del Mar* Medical Research Institute (IMIM), Barcelona, Spain

⁶ Faculty of Medicine, University of Vic-Central University of Catalonia, Vic, Spain

† Equally contributing authors

Correspondence: Irene R. Décano (irene.roman@umedicina.cat; Tel.: +34-93-881-55-37) & Alex Perálvarez Marín (alex.peralvarez@uab.cat; Tel.: +34-93-581-4504)

KEYWORDS: *corpus callosum*, cuprizone, demyelination, oligodendrocytes, microglia, crosstalk

Abstract

Demyelinating disorders are characterized by impaired remyelination due to failure of differentiation from oligodendrocyte progenitor cells (OPCs) to mature-myelin-forming oligodendrocytes driven but the crosstalk between microglia and OPCs. Using a transcriptomic analysis of microarray studies in the cuprizone demyelination-remyelination mouse model we identify molecules involved in this crosstalk. We used GEO transcriptomic raw data after cuprizone treatment. DEGs were identified in each region/cell type followed by functional analysis of DEGs by over-representation of GO terms and WikiPathways. Microglia ligands, OPC receptors and target genes involved in the microglia-OPC crosstalk were examined with the NicheNet model. We identified 108 and 166 DEGs in CC after 2 and 4 weeks of cuprizone treatment; 427 and 355 DEGs in CC after remyelination compared to 2 and 4 weeks of cuprizone treatment; and 2730 and 12 DEGs in OPC and microglia after 4 weeks of cuprizone treatment. After 4 weeks of cuprizone treatment, we found 95 common DEGs in CC and OPCs, and 1 common DEGs in microglia and OPCs. DEGs identified associated to myelin and lipid metabolism. Crosstalk analysis identified 47 microglia ligands, 43 OPC receptors and 115 OPC target genes. Identified ligands, receptors and targets genes, were differentially expressed in cuprizone treated samples and are associated with myelination. Our differential expression pipeline succeeded to identify transcriptomic biomarkers associated to demyelination/remyelination in studies using different platforms and cell types/tissues. The cellular crosstalk analysis yields already described markers as well as novel microglia ligands, and OPC receptors and target genes.

1. Introduction

Multiple sclerosis (MS) is the most common demyelinating disorder of the central nervous system (CNS), with 3.0 million patients worldwide. MS is more common in women than in men, and has a great impact on patients quality of life [1]. MS is considered as a multifactorial disease which is triggered by genetic predisposition and environmental factors leading to neurological impairment and disabling symptoms [2, 3]. MS and current treatments are disease-modifying therapies mainly focused on treating attacks, ameliorating the symptoms and suppressing or modulating inflammation [4, 5]. Therefore, a better understanding of the molecules that are involved in this pathology would be key to discover novel therapies.

MS and most demyelinating disorders are characterized by a neuroinflammation that leads to demyelination, oligodendrocytes death and axonal injury. In the CNS, myelin is produced by myelinating oligodendrocytes that are originated by oligodendrocyte precursor cells (OPCs), which can proliferate, migrate and differentiate into these mature oligodendrocytes capable to generate myelin. Different studies suggest that these different steps from OPCs to mature oligodendrocytes are orchestrated by microglia, astrocytes and OPCs [6–9]. In this crosstalk, microglia can play a dual role, being beneficial or detrimental for (re)myelination. Beneficial roles of microglia promote OPCs survival and maturation, foster OPC differentiation (i.e. via galectin-3), and contribute to myelin formation during development and remyelination [10–14]. However, the complete role of microglia in (re)myelination is poorly understood.

The objectives of this study were: i) to identify transcriptomic markers of demyelination and remyelination in CC, microglia and OPCs using a common pipeline, and ii) to study the microglia ligands as well as the OPC receptors and target genes involved in the microglia-OPC crosstalk in demyelination using available transcriptomic data from cuprizone demyelination-remyelination mouse model experiments.

2. Material and methods

2.1. Data

A search in GEO/ArrayExpress was performed to identify all studies that analyzed gene expression by microarray in mice treated or not with cuprizone (Supplementary Table 1). Raw data for the 4 studies identified were obtained from GEO. There were 2 studies in microglia, 1 in *corpus callosum* (CC) and 1 in OPCs.

2.2. Identification of demyelination/remyelination biomarkers

The pipeline to identify demyelination/remyelination differentially expressed genes (DEGs) included data preprocessing, annotation, gene filtering, DEGs analysis, and functional analysis (Supplementary Figure 1). Demyelination DEGs were examined in the CC, microglia and OPC studies. Remyelination DEGs were only examined in CC as the studies in microglia and OPCs had not analyzed remyelination.

Quality control of raw data was performed with boxplots and density plots of log-intensities and with MA plots. In Affymetrix studies, we also inspected images and plots of relative log expression values and of normalized unscaled standard errors. Preprocessing was performed as follows. Background correction was done with convolution of normal and exponential distributions, then, quantile normalization was used. Finally, summarization was performed with the median-polish method for Affymetrix studies and by replacing array replicates with their average for Agilent studies. For the microglia analysis, normalized data of the 2 available studies was combined using quantile normalization. Normalized data was examined with boxplots.

After preprocessing, data was annotated and filtered. We excluded probes with no symbol and probes with low expression defined as within the 30th percentile of lower intensity in a number of arrays as the smallest experimental group. Agilent studies included also gene filtering for control and negative flagged probes. Sample clustering by treatment and scan date was analyzed with hierarchical clustering and principal component analysis. There was no scan date clustering. Treatment clustering was clear in microglia and OPC data, and moderate in CC data. We excluded the 1/2 most different samples in the CC analyses based on sample clustering. For the microglia analysis, clustering by study was identified and corrected with the ComBat method.

Differential expression was analyzed with moderated t-tests including an intensity trend for prior variance and robustifying for outlier sample variances. p-values were adjusted for multiple comparisons using the Benjamini-Hochberg (BH) method. Duplicated assigned genes were removed by selecting the one with the lowest p-value. DEGs were visualized with volcano plots. Sample clustering by gene expression of all DEGs and by gene expression of the most DEGs was visualized with heatmaps (Supplementary Figure 2).

Functional analysis of DEGs was performed in the 3 cell types/regions separately and in the DEGs identified in more than 1 cell type/region. In OPCs, due to the large number of DEGs, functional analysis was undertaken with the DEGs with an adjusted p-value < 0.001. We did over-representation analyses of gene ontology (GO) molecular-level functions and WikiPathways. p-values were obtained with the hypergeometric test and adjusted with the BH method. Significant GO molecular functions and pathways were visualized with dotplots.

2.3. Microglia and OPC crosstalk

We applied the NicheNet model [15] to examine the intercellular communication between microglia (sender cells) and OPCs (receiver cells). The expressed genes in microglia and OPCs was the expression data after normalization, annotation, and gene filtering. Gene filtering for low expression included genes below the 60th (microglia) and the 75th (OPCs) percentile of intensity. The gene set of interest was defined as the OPC DEGs with a p-value<0.01. The background of OPC genes were all genes expressed by OPCs except for the gene set of interest. As potential microglia ligands we selected those expressed by microglia that could bind a putative OPC receptor. Potential OPC receptors were those expressed by OPCs that could bind a putative microglia ligand. Putative associations between ligands and receptors were restricted to those described in curated databases.

Ligand activity was examined by how well the ligands predicted the observed changes in gene expression in the gene set of interest compared to the background genes. Ligand activity was ranked according to the Pearson correlation coefficient. We analyzed OPC target genes as those expressed by OPCs that belonged to the 100 most strongly predicted target genes of the top ranked microglia ligands. Ligands and receptors were ordered with hierarchical clustering. Association between microglia ligands and OPC receptors/target genes was visualized with heatmaps. Expression of the identified microglia ligands and OPC receptor/target genes was compared between cuprizone samples and controls using t-tests. p-values were adjusted for multiple comparisons with the BH method.

Analyses were done in R version 4.0.4.

3. Results

3.1. Identification of demyelination marker genes in the cuprizone model

3.1.1. DEGs in CC

After 2 weeks of demyelination treatment there were 108 DEGs in CC, 45 downregulated and 63 upregulated (Figure 1 and Supplementary Table 2 and Supplementary Figure 2). The 10 most DEGs between 2-week cuprizone-treated mice and control were: *Serpinb1a*, *Gdf15*, *Pigz*, *Tgm1*, *B230206H07Rik*, *Ninj2*, *Eif4ebp1*, *Slc34a3*, *Trib3* and *Cdkn1a*. Among these genes, *Gdf15*, *Tgm1*, *Eif4ebp1*, *Trib3* and *Cdkn1a* were downregulated in the CC of cuprizone treated mice, while *Serpinb1a*, *Pigz*, *B230206H07Rik*, *Ninj2* and *Slc34a3* were upregulated. There were 3 Wikipathways associated with the DEGs (p53 signaling, white fat cell differentiation and hypertrophy model) (Figure 2E) but no GO molecular functions.

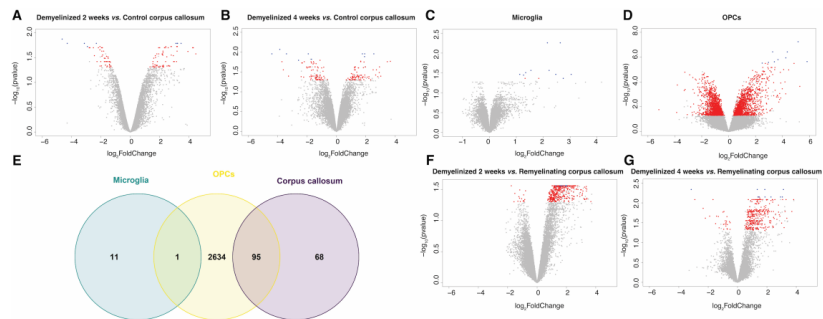


Figure 1. DEGs in CC, OPCs and microglia. Volcano plots of $-\log_{10}$ of adjusted p-values and log fold changes in the CC analysis at early (2-week-cuprizone-treatment) (A) and late (4-week-cuprizone-treatment) (B) demyelination. Significant DEGs are shown in red and the 10 most DEGs are shown in blue. (C) Volcano plot of $-\log_{10}$ of adjusted p-values and log fold changes in the microglia. (D) Volcano plot of $-\log_{10}$ of adjusted p-values and log fold changes in OPCs. (E) The Venn diagram shows the number of common DEGs between the CC, OPCs and microglia. Volcano plots of $-\log_{10}$ of adjusted p-values and log fold changes in CC of early (F) and late (G) demyelination when compared to remyelinating CC.

After 4 weeks of demyelination treatment we identified 166 DEGs in CC: 80 downregulated and 86 upregulated (Figure 1A and Supplementary Table 3). The 10 most DEGs between 4-week cuprizone-treated mice and control were: *Moxd1*, *Gdf15*, *Ddit3*, *Cngl1*, *Atf15*, *Trib3*, *Slc34a3*, *Pigz*, *Xrcc3* and *Ninj2*. Of those, *Moxd1*, *Gdf15*, *Ddit3*, *Cngl1*, *Atf15* and *Trib3* were significantly downregulated in the CC of cuprizone-treated mice while *Slc34a3*, *Pigz*, *Xrcc3* and *Ninj2* were significantly upregulated (Figure 3). There were six significant GO molecular functions associated with the DEGs identified such as structural constituent of myelin sheath (Figure 2A). Four Wikipathways were associated to the DEGs including cholesterol biosynthesis and metabolism (Figure 2E).

There were 75 common DEGs at 2 and 4 weeks of demyelination, all downregulated/upregulated at both time points. Among the 10 most DEGs, 5 genes were present at 2 and 4 weeks: *Gdf15*, *Atf5* and *Trib3* were downregulated compared to control, while *Sc34a3* and *Ninj2* were upregulated.

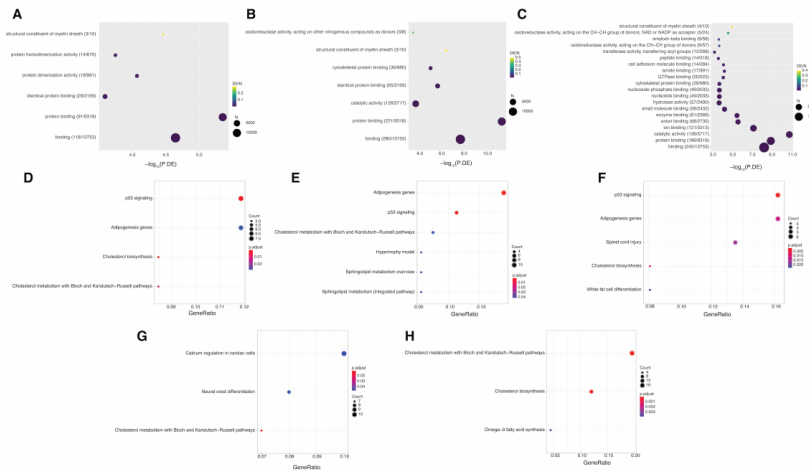


Figure 2. GO annotation and WikiPathways analysis of DEGs (A) Dot plots of the 20 most significant GO molecular functions associated with the DEGs identified in the CC analysis when comparing controls to 4 week treated mice. The x-axis represents the $-\log_{10}$ of the p-value for over-expression of the GO term in the set. The color scale represents the number of DEGs in the differential expression set divided by the number of genes in the GO term. The dot size represents the number of genes in the GO term. Dot plots of the 20 most significant GO molecular functions associated with the DEGs identified in the CC analysis at early (B) and late demyelination (C) when compared to controls. (D) Dot plot of the significant WikiPathways in CC associated with the DEGs identified in late demyelination when compared to remyelinating CC. In dot plot the x-axis represents the number of DEGs in the differential expression set divided by the number of genes in the pathway. The color scale represents the adjusted p-value. The dot size represents the number of genes in the pathway. (E) Dot plot of the significant WikiPathways linked to the identified DEGs in the OPC analysis. (F) WikiPathways in common associated with the 95 DEGs identified in CC and OPC analyses. Dot plots of the 20 most significant GO molecular functions associated with the DEGs identified in the CC analysis at early (G) and late (H) demyelination when compared to remyelinating CC.

3.1.2. DEGs in microglia

There were 12 DEGs when comparing microglia from 4-week-cuprizone treated and control mice. All DEGs were upregulated: *Olr1*, *Cd69*, *Itgax*, *Clic4*, *Lpl*, *Clec7a*, *Gas2l3*, *Fam20c*, *Mmp12*, *Lgals3*, *Rab7* and *Cxcr4* (Figure 1B, Supplementary Table 4 and Supplementary Figure 2C). There was 1 GO molecular function associated to these DEGs (carbohydrate binding), but no WikiPathways.

3.1.3. DEGs in OPCs

Analysis of DEGs of OPCs between 4-week cuprizone treated and control mice revealed 2730 DEGs (those with a p-value <0.001 are presented in Supplementary Table 5). Of the DEGs, 1372 were downregulated and 1358 were upregulated (Figure 1C). The 10 most significant DEGs were all upregulated: *Slc7a1*, *Tagln2*, *Atf5*, *Trib3*, *Cdkn1a*, *Col5a3*, *Gadd45b*, *Egr1*, *Ppp1r15a* and *Ccnd1* (Figure 3). There were 226 GO biological processes associated with the DEGs, such as regulation of axon extension, neurogenesis, and neuron projection development. Associated WikiPathways included cholesterol and sphingolipid metabolism (Figure 2F).

3.1.4. Common DEGs in CC, microglia and OPCs

There were no DEGs in the three tissue/cell types (CC, microglia and OPCs) between 4-week cuprizone-treated and control mice. However, there was 1 common DEGs in microglia and OPCs (*Lgls3*), and 95 common DEGs in CC and OPCs (Supplementary Table 6 and Figure 1D). The 95 common DEGs were associated with 86 GO biological processes including gliogenesis, oligodendrocyte development, and nervous system development among others. These common 95 DEGs were also associated with 5 Wikipathways such as spinal cord injury (Figure 2G).

3.2. Identification of remyelination marker genes in CC in the cuprizone model

After 2-week of demyelination treatment, CC had 415 DEGs compared to remyelinating CC, including 15 downregulated and 400 upregulated. The 10 most DEGs were all upregulated: *D16Ert472e*, *Aoc1*, *Krt15*, *Serpib1c*, *Stain1*, *Cxcl10*, *Sntn*, *Lrig3*, *Ppfbp2* and *Dusp15* (Figure 1E and Supplementary Table 7). These DEGs were associated with 7 GO molecular functions such as structural constituent of myelin sheath (Figure 2D), and with 3 WikiPathways including cholesterol metabolism (Figure 2H).

When comparing the CC of 4-weeks of demyelination and remyelinating CC, there were 355 DEGs, 27 were downregulated and 328 were upregulated (Figure 1E and Supplementary Table 8). The 10 most DEGs in this case were *Ninj2*, *Mog*, *Cyp3a13*, *Trib3*, *Gm5067*, *Shgl3*, *Msmo1*, *E330037M01Rik*, *Plekhh1* and *Insig1*. From those, the only downregulated DEG was *Trib3*, while the rest were upregulated. There were 23 GO molecular functions associated with the DEGs including structural constituent of myelin sheath and amyloid-beta binding (Figure 2D and Supplementary Table 9). Three WikiPathways were associated with the DEGs, cholesterol biosynthesis and metabolism and omega-9 fatty acid synthesis (Figure 2H).

There were 159 common DEGs in remyelinating CC compared to 2 or 4 weeks of demyelination. All up or downregulated in both analysis.

3.3. Microglia-oligodendrocyte interaction in cuprizone-induced demyelination-remyelination: potential receptor-ligand pairs to promote remyelination

We identified 47 potential ligands in microglia that could affect the expression of the gene set of interest in OPCs after cuprizone treatment (Figure 3, Figure 4A and Supplementary Table 10). All ligands had a similar potential to regulate the gene set of interest. All potential ligands had active target links with OPC genes differentially expressed after cuprizone treatment. Expression of microglia ligands in microglia samples is presented in Figure 3A. Ligands showed similar expression in cuprizone-treated and control samples except for *Spp1* (Secreted Phosphoprotein 1) and *Plau* (Plasminogen Activator, Urokinase), which had borderline significant differences in expression (Supplementary Table 11, adjusted p-value=0.052).

Expression of both ligands was higher in microglia from cuprizone-treated mice than in control mice.

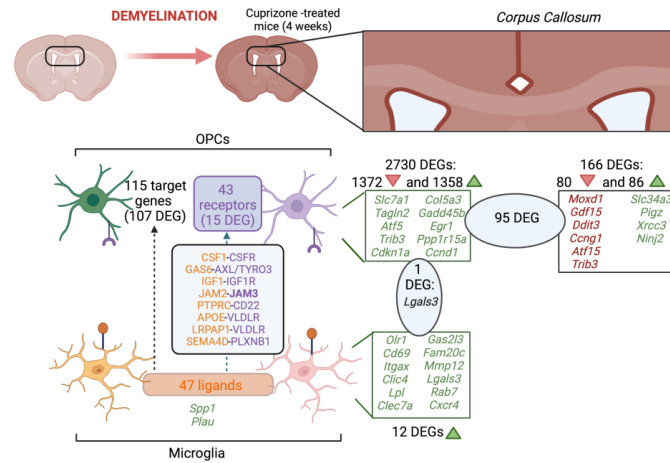


Figure 3. Demyelinating markers genes and microglia-OPCs interactions in cuprizone model. In this study different datasets comparing control to 4-week-cuprizone treated mice are analyzed leading to the discovery of 166 DEGs in CC, 12 in microglia and 2730 in OPCs. Among the identified DEGs, upregulated genes are shown in green and downregulated genes are shown in red. 95 DEGs were found in common between both CC and in OPCs, and 1 DEGs was found expressed in both microglia and OPCs. In the microglia-OPC crosstalk we found 47 ligands in microglia, 43 OPC receptors and 115 target genes in OPCs. Microglia ligands are found in orange and OPC receptors are found in purple.

Analysis of ligand-receptor interaction yielded 43 potential receptors of identified ligands expressed by OPCs after cuprizone treatment (Figure 3 and Figure 4B). The maximum interaction potential was found for the following microglia ligand – OPC receptor pairs: CSF1-CSFR, GAS6-AXL/TYRO3, IGF1-IGF1R, JAM2-JAM3, PTPRC-CD22, APOE-VLDLR, LRPAP1-VLDLR, SMAD4D-PLXNB1. Out of 43 receptors, 15 were differentially expressed between OPCs from cuprizone treated and control mice (Supplementary Table 12). The most differentially expressed was Jam3, which was downregulated in OPCs from cuprizone-treated mice compared to control (Figure 4C).

We identified 115 DEGs in OPCs that were predicted targets of the identified ligands (Figure 3 and Figure 4D). Of those, 107 were differentially expressed between OPCs from cuprizone treated and from control mice (Figure 4E and Supplementary Table 13). The most differentially expressed targets were *Bbc3*, *Gadd45b* and *Hist1h3d*, all of them were upregulated in OPCs after cuprizone treatment.

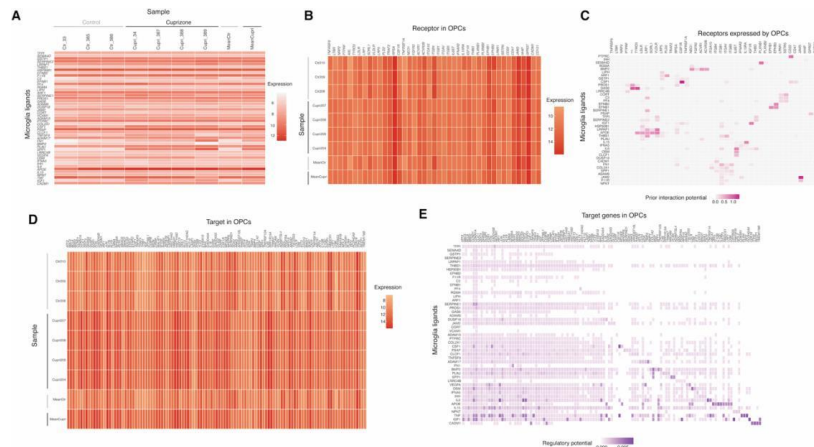


Figure 4. Identification of interacting microglia ligands, OPC receptors and OPC target genes using the NicheNet model. (A) Expression of microglia ligands in microglia samples from cuprizone treated mice (Cupri) and from control mice (Ctr). The darker the red color the higher the expression. (B) Expression of OPC receptors in OPC samples from cuprizone-treated and from control mice. (C) Predicted interactions between identified microglia ligands and OPC receptors. The darker the purple color the higher the regulatory potential of the microglia ligands on the OPC receptors. (D) Expression of OPC target genes in OPC samples from cuprizone-treated and from control mice. OPC: oligodendrocyte progenitor cell. (E) Predicted interactions between microglia ligands and OPC target genes.

4. Discussion

In this *in silico* study, we analyzed demyelination/remyelination transcriptomic markers in CC, microglia and OPCs, and we examined the crosstalk between microglia and OPCs during demyelination. In demyelination, we identified 166 DEGs in CC, 12 in microglia and 2730 in OPCs. Ninety-five genes were differentially expressed in both CC and in OPCs, and 1 gene was differentially expressed in both microglia and OPCs. In remyelinating comparing to demyelinating CC, there were 611 DEGs. These demyelination/remyelination markers were associated with molecular functions and pathways related to myelin, central nervous system cell populations, and lipid metabolism. Regarding the microglia-OPC crosstalk during demyelination, we identified 47 ligands in microglia, 43 OPC receptors and 115 target genes in OPCs (Figure 3).

There were common genes among the 10 most DEGs in early and late demyelinating CC among which *Gdf15*, *Ninj2* and *Trib3* were previously associated with myelination. *Gdf15* was downregulated in demyelinating CC in our study. *Gdf15* is found in oligodendrocytes of CC and it is overexpressed in patients with stabilized MS [16], and also in functional recovery after traumatic spinal cord injury (SCI) [17]. It could be possible that the observed downregulation is linked to the severe decrease of oligodendrocytes in CC. *Ninj2* was found upregulated during early and late demyelination, and also when comparing late demyelination-remyelination. *Ninj2* is associated with neurite outgrowth and myelination networks [18, 19]. Therefore, the observed *Ninj2* upregulation during demyelination may indicate a feedback loop to restore myelin in CC.

Trib3 was downregulated in early and late demyelination, and also during remyelination when compared to late demyelination. *Trib3* has been associated with myelin destruction [20, 21].

The 12 DEGs identified in microglia included *Lpl* [22] and *Olr1* [23] that have been previously associated with myelination. In addition, the common DEG in demyelinating microglia and OPCs, *Lgals3*, has been consistently identified in microglia and oligodendrocytes in the cuprizone demyelination-remyelination model [24, 25].

Three of the 10 most DEGs in demyelinating OPCs have been associated with demyelination and were also found among the most DEGs in CC: *Atf5*, *Trib3* and *Cdkn1a*. *Atf5* was downregulated in CC but upregulated in OPCs. *Atf5* downregulation is necessary for differentiation of neurons, astrocytes and OPCs. While *Atf5* is not expressed in mature oligodendrocytes [26]. One explanation for being downregulated in CC and upregulated OPCs could be that during demyelination OPCs are not capable of differentiating due to overexpression of *Atf5*. However, other cell types may be trying to counterbalance this effect by downregulation of *Atf5*. *Trib3* was also downregulated in CC but upregulated in OPCs. *Trib3* overexpression is linked to myelin destruction and cuprizone has been described to stimulate *Trib3* expression. Our results in OPCs agree with the available bibliography [20, 21]. The observed downregulation in CC could be related to the different cell types present in CC in addition to oligodendrocytes and OPCs. On the other hand, *Cdkn1a* has been found expressed in the majority of oligodendrocytes in demyelinated lesions [27].

GO term analysis showed that DEGs were associated to different biological and molecular processes related to CNS such as to constituents of myelin, axon extension and neurogenesis. While associated pathways included cholesterol and sphingolipid metabolism. Cholesterol and sphingolipids are major components of myelin and their altered metabolism is linked to different neurological and neurodegenerative disorders [28, 29]. The association of most DEGs with demyelination/remyelination, as well as the whole DEGs with myelin-related functions and pathways, argues for the robustness of the method for DEG analysis.

Among the 47 potential microglia ligands, *Spp1* and *Plau* expression we higher in cuprizone-treated compared to control mice. *Spp1* upregulation has been observed in response to injury in different animal models of CNS trauma [30, 31], in experimental autoimmune encephalomyelitis (EAE) [32], and in microglia/macrophages and astrocytes during cuprizone-induced demyelination [33]. *Spp1* has also been related to enhanced myelin formation [33]. Our results are in line with previous results published in cuprizone model [33], showing that that *Spp1* is upregulated during cuprizone-induced demyelination. In addition, *Plau* has been associated with conditioned-injury axon outgrowth in myelin [34].

Regarding the identified OPC target genes, the most differentially expressed were *Bbc3*, *Gadd45b* and *Hist1h3d*. *Bbc3* is a pro-apoptotic gene that promotes premyelinating oligodendrocytes cell death [35]. Our results indicated that *Bbc3* is upregulated in cuprizone treated compared to control mice. These results could indicate that *Bbc3* overexpression in cuprizone treated mice could be linked to fostering programmed cell death in OPCs. Moreover, *Gadd45b*, which was upregulated in cuprizone treated OPCs, downregulates JNK signaling [36], a signaling that is necessary for OPCs proliferation [37].

The performed analysis also revealed that among the 43 identified receptors in OPCs, 15 were differentially expressed. Some of them of them upregulated (PLXNB2, TNFRSF1A, ACVR1, LRPI, ITGB5 and AXL) or downregulated (JAM3, HHIP, LDLR, FGFR2, ITGB4, EPHB1,

LPAR1, TYRO3 and SORL1), after cuprizone treatment. Most of these OPC receptors have been associated with CNS myelin, related pathologies and oligodendrocytes. Regarding upregulated receptors, mutated *Tnfrsf1a* is a risk factor for MS by interfering in the TNF- α signaling pathway leading to an increase of pro-inflammatory signals [38]. In addition, TNF has been associated with an accelerated onset of EAE [39]. Therefore, the increase of *Tnfrsf1a* after cuprizone treatment could modulate TNF signaling pathway and contribute to the observed demyelinating phenotype in the cuprizone model. Mutations in *Acvr1* gene arrest oligodendrocytes differentiation [40], and *Acvr1* can regulate OPCs differentiation and myelin production [41]. Our results reinforce the role of *Acvr1* during demyelination by inhibiting oligodendrocytes differentiation. *Lrp1* is a negative regulator of OPCs differentiation and its deletion is associated to OPCs proliferation and generation of new mature oligodendrocytes [42]. Therefore, *Lrp1* increase in cuprizone model would reduce the number of newborn mature oligodendrocytes and OPCs would not differentiate into oligodendrocytes. *Igfb5* is a member of the integrins family, which is necessary for oligodendrocyte proliferation, survival, and maturation [43]. Upregulation of *Igfb5* after cuprizone treatment could promote OPCs functioning. Finally, *Axl* is necessary for the maintenance of axonal integrity and remyelination. *Axl* increase after cuprizone treatment could be an attempt to protect cells from injury.

Regarding the identified downregulated OPC receptors, *Jam3* has been reported as *Jam2* counter-receptor [44, 45]. *Jam2* inhibits oligodendrocytes wrapping but does not affect OPCs differentiation, proliferation or migration. Therefore, downregulation of *Jam3* could contribute to the loss of myelin integrity that occurs in cuprizone induced demyelination. *Hhip* interacts with Sonic Hedgehog (*shh*) and it has been described that *Shh* signaling protects from demyelination and favors remyelination by OPC proliferation [46]. *Ldlr* has been related to correct myelination, directly [47], and through cholesterol metabolism. In addition, low levels of *Ldlr* have been associated to failure in OPCs differentiation [48], consistent to the observed behavior at 4 weeks of cuprizone treatment. *Fgfr2* is necessary for upregulating myelin gene expression, regulate myelin thickness, OPCs differentiation and foster myelin growth during developmental myelination [49]. Also, *Fgfr2* promotes remyelination in chronic demyelinated lesions but not in acute lesions [49]. *Igfb4* has been related to OPCs proliferation [50] and its deletion leads to delayed peripheral nerve regeneration in the peripheral nervous system (PNS) [51]. *Ephb1* has been described as implicated in T cell differentiation and migration to inflammatory sites in both EAE and MS [52] and also stimulates myelin sheath formation [53]. *Lpar1* expression has been reported as necessary for oligodendrocytes differentiation and myelination [54] and its deletion has been correlated with myelin alterations and oligodendrocytes death [54]. The observed downregulation of *Lpar1* in cuprizone treated mice are in line with published data, contributing to oligodendrocytes death during demyelination. Finally, *Tyro3* expression occurs at the onset of remyelination and enhances myelination [55].

Our results in the microglia-OPC crosstalk analysis showed that most of the identified microglia ligands, and OPC receptors and target genes play important roles in myelination. These results point to ligands, receptors and target genes that have not been associated to myelination so far could also be involved in this process. In addition, our results highlight the potential of the NicheNet model to study cellular crosstalk not only in co-cultured cell types, but also with transcriptomic data of independent studies where cell types have received the same treatment. This observation may open the possibility of analyzing the crosstalk between cell types that cannot be co-cultured or for which transcriptomic data is available.

We combined all the available studies in CC, microglia and OPCs in mice treated with cuprizone analyzed with microarrays, and used the same pipeline to obtain DEGs. DEGs were associated with molecular functions and pathways related to myelination. We conducted a crosstalk analysis between 2 microglia studies and 1 OPCs study with independent transcriptomic data. And the results from the crosstalk analysis are in accordance with the demyelination/remyelination processes. There are, however, limitations that should be taken into account. First, the number of samples in the available studies was small and this could affect the number of DEGs after cuprizone treatment, the common DEGs between cell types and tissues, and the crosstalk analysis. However, taking into account that most of the identified DEGs, ligands, targets and receptors were associated with myelination processes we believe that our study yielded robust results. Second, microglia and OPC samples could include other cell populations, and it is not known which cell types are present in the *corpus callosum* samples.

Conclusion

We developed a strategy to select genes associated with demyelination/remyelination in different cell types/tissues after cuprizone treatment in mice. The identified genes were related with molecular functions and pathways associated with myelination. These genes could be used in subsequent experiments to evaluate demyelination in cuprizone treated mice and this strategy could be applied to other cell types and demyelination treatments. We also performed an *in silico* analysis to identify ligands, receptors, and target genes involved in the crosstalk between microglia and OPCs. Some of the ligands, receptors, and target genes identified were associated with demyelination and were differentially expressed in samples from cuprizone treated compared to control mice. This result suggests that crosstalk analysis, at least in cuprizone induced demyelination, can be studied using data from different experiments. We found novel demyelination biomarkers as well as novel ligands, receptors and target genes in the crosstalk between microglia and OPCs, which warrants further validation studies.

Acknowledgements

Authors acknowledge financial support by the Spanish Government MCIN/AEI/10.13039/501100011033 (Project BFU2017-87843-R- and Project PID2020-120222GB-I00 to A.P.-M.) and by the Carlos III Health Institute and the European Regional Development Fund (CIBERCV CB16/11/00229 and FIS PI21/00163 to I.R.D.), and by the Marató TV3 Foundation (202119-33 to I.R.D.).

References

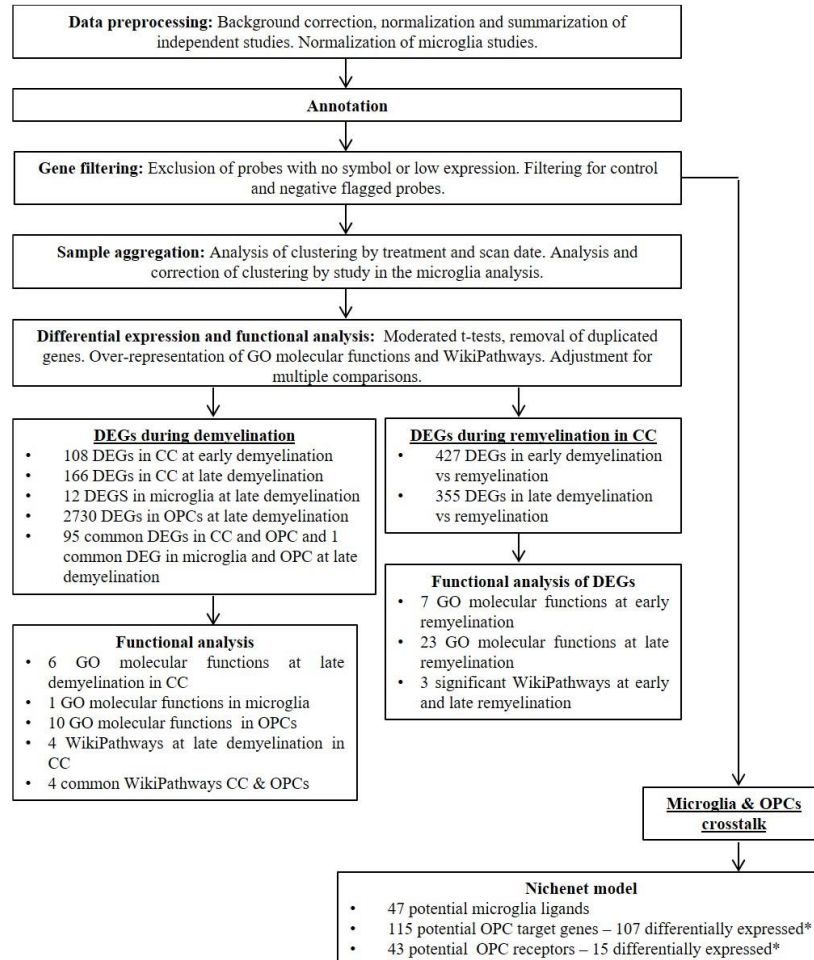
- [1] C. Walton *et al.*, "Rising prevalence of multiple sclerosis worldwide: Insights from the Atlas of MS, third edition," *Mult. Scler. Houndmills Basingstoke Engl.*, vol. 26, no. 14, pp. 1816–1821, Dec. 2020, doi: 10.1177/1352458520970841.
- [2] N. Ghasemi, S. Razavi, and E. Nikzad, "Multiple Sclerosis: Pathogenesis, Symptoms, Diagnoses and Cell-Based Therapy," *Cell J.*, vol. 19, no. 1, pp. 1–10, Jun. 2017.
- [3] J. M. Gelfand, "Multiple sclerosis: diagnosis, differential diagnosis, and clinical presentation," *Handb. Clin. Neurol.*, vol. 122, pp. 269–290, 2014, doi: 10.1016/B978-0-444-52001-2.00011-X.
- [4] S. L. Hauser and B. A. C. Cree, "Treatment of Multiple Sclerosis: A Review," *Am. J. Med.*, vol. 133, no. 12, pp. 1380-1390.e2, Dec. 2020, doi: 10.1016/j.amjmed.2020.05.049.
- [5] R. Dobson and G. Giovannoni, "Multiple sclerosis - a review," *Eur. J. Neurol.*, vol. 26, no. 1, pp. 27–40, Jan. 2019, doi: 10.1111/ene.13819.

- [6] Y. Pang, Z. Cai, and P. G. Rhodes, "Effects of lipopolysaccharide on oligodendrocyte progenitor cells are mediated by astrocytes and microglia," *J. Neurosci. Res.*, vol. 62, no. 4, pp. 510–520, Nov. 2000, doi: 10.1002/1097-4547(20001115)62:4<510::AID-JNRS>3.0.CO;2-F.
- [7] Z. Liu *et al.*, "Astrocytes induce proliferation of oligodendrocyte progenitor cells via connexin 47-mediated activation of the ERK/Id4 pathway," *Cell Cycle Georget. Tex.*, vol. 16, no. 7, pp. 714–722, Apr. 2017, doi: 10.1080/15384101.2017.1295183.
- [8] C. M. Willis *et al.*, "Astrocyte Support for Oligodendrocyte Differentiation can be Conveyed via Extracellular Vesicles but Diminishes with Age," *Sci. Rep.*, vol. 10, Jan. 2020, doi: 10.1038/s41598-020-57663-x.
- [9] O. Schnüdelbach and J. W. Fawcett, "Astrocyte influences on oligodendrocyte progenitor migration," in *Progress in Brain Research*, vol. 132, Elsevier, 2001, pp. 97–102. doi: 10.1016/S0079-6123(01)32068-X.
- [10] I. Kalafatakis and D. Karageorgos, "Oligodendrocytes and Microglia: Key Players in Myelin Development, Damage and Repair," *Biomolecules*, vol. 11, no. 7, p. 1058, Jul. 2021, doi: 10.3390/biom11071058.
- [11] E. N. Santos and R. D. Fields, "Regulation of myelination by microglia," *Sci. Adv.*, vol. 7, no. 50, p. eabk1131, doi: 10.1126/sciadv.abk1131.
- [12] V. E. Miron *et al.*, "M2 microglia and macrophages drive oligodendrocyte differentiation during CNS remyelination," *Nat. Neurosci.*, vol. 16, no. 9, pp. 1211–1218, Sep. 2013, doi: 10.1038/nn.3469.
- [13] E. Traiffort, A. Kassoussi, A. Zahaf, and Y. Laouarem, "Astrocytes and Microglia as Major Players of Myelin Production in Normal and Pathological Conditions," *Front. Cell. Neurosci.*, vol. 14, p. 79, 2020, doi: 10.3389/fncel.2020.00079.
- [14] H. S. Domingues, C. C. Portugal, R. Socodato, and J. B. Relvas, "Oligodendrocyte, Astrocyte, and Microglia Crosstalk in Myelin Development, Damage, and Repair," *Front. Cell Dev. Biol.*, vol. 4, Jun. 2016, doi: 10.3389/fcell.2016.00071.
- [15] R. Browaeys, W. Saelens, and Y. Saeys, "NicheNet: modeling intercellular communication by linking ligands to target genes," *Nat. Methods*, vol. 17, no. 2, pp. 159–162, Feb. 2020, doi: 10.1038/s41592-019-0667-5.
- [16] A. Amstad *et al.*, "Growth differentiation factor 15 is increased in stable MS," *Neurol. Neuroimmunol. Neuroinflammation*, vol. 7, no. 2, p. e675, Feb. 2020, doi: 10.1212/NXI.0000000000000675.
- [17] M. Hassanpour Golakani *et al.*, "MIC-1/GDF15 Overexpression Is Associated with Increased Functional Recovery in Traumatic Spinal Cord Injury," *J. Neurotrauma*, vol. 36, no. 24, pp. 3410–3421, Dec. 2019, doi: 10.1089/neu.2019.6421.
- [18] T. Araki and J. Milbrandt, "Ninjurin2, a novel homophilic adhesion molecule, is expressed in mature sensory and enteric neurons and promotes neurite outgrowth," *J. Neurosci. Off. J. Soc. Neurosci.*, vol. 20, no. 1, pp. 187–195, Jan. 2000.
- [19] M. Allen *et al.*, "Conserved brain myelination networks are altered in Alzheimer's and other neurodegenerative diseases," *Alzheimers Dement. J. Alzheimers Assoc.*, vol. 14, no. 3, pp. 352–366, Mar. 2018, doi: 10.1016/j.jalz.2017.09.012.
- [20] Y. Shimotsuna, M. Tanaka, T. Izawa, J. Yamate, and M. Kuwamura, "Enhanced Expression of Trib3 during the Development of Myelin Breakdown in dmy Myelin Mutant Rats," *PLoS ONE*, vol. 11, no. 12, Dec. 2016, doi: 10.1371/journal.pone.0168250.
- [21] H. Abe *et al.*, "Cuprizone decreases intermediate and late-stage progenitor cells in hippocampal neurogenesis of rats in a framework of 28-day oral dose toxicity study," *Toxicol. Appl. Pharmacol.*, vol. 287, no. 3, pp. 210–221, Sep. 2015, doi: 10.1016/j.taap.2015.06.005.
- [22] K. D. Bruce *et al.*, "Lipoprotein Lipase Is a Feature of Alternatively-Activated Microglia and May Facilitate Lipid Uptake in the CNS During Demyelination," *Front. Mol. Neurosci.*, vol. 11, p. 57, 2018, doi: 10.3389/fnmol.2018.00057.
- [23] A. Gaultier *et al.*, "Low-density lipoprotein receptor-related protein 1 is an essential receptor for myelin phagocytosis," *J. Cell Sci.*, vol. 122, no. Pt 8, pp. 1155–1162, Apr. 2009, doi: 10.1242/jcs.040717.
- [24] H. C. Hoyos *et al.*, "Galectin-3 controls the response of microglial cells to limit cuprizone-induced demyelination," *Neurobiol. Dis.*, vol. 62, pp. 441–455, Feb. 2014, doi: 10.1016/j.nbd.2013.10.023.
- [25] A. Deczkowska, H. Keren-Shaul, A. Weiner, M. Colonna, M. Schwartz, and I. Amit, "Disease-Associated Microglia: A Universal Immune Sensor of Neurodegeneration," *Cell*, vol. 173, no. 5, pp. 1073–1081, May 2018, doi: 10.1016/j.cell.2018.05.003.
- [26] J. L. Mason *et al.*, "ATF5 regulates the proliferation and differentiation of oligodendrocytes," *Mol. Cell. Neurosci.*, vol. 29, no. 3, pp. 372–380, Jul. 2005, doi: 10.1016/j.mcn.2005.03.004.
- [27] K. Shen *et al.*, "Multiple sclerosis risk gene Mertk is required for microglial activation and subsequent remyelination," *Cell Rep.*, vol. 34, no. 10, p. 108835, Mar. 2021, doi: 10.1016/j.celrep.2021.108835.
- [28] B. B. Raddatz *et al.*, "Central Nervous System Demyelination and Remyelination is Independent from Systemic Cholesterol Level in Theiler's Murine Encephalomyelitis," *Brain Pathol. Zurich Switz.*, vol. 26, no. 1, pp. 102–119, Jan. 2016, doi: 10.1111/bpa.12266.
- [29] Y. Li *et al.*, "Genetic variation in the leukotriene pathway is associated with myocardial infarction in the Chinese population," *Lipids Health Dis.*, vol. 18, p. 25, Jan. 2019, doi: 10.1186/s12944-019-0968-9.
- [30] J. A. Ellison, F. C. Barone, and G. Z. Feuerstein, "Matrix remodeling after stroke. De novo expression of matrix proteins and integrin receptors," *Ann. N. Y. Acad. Sci.*, vol. 890, pp. 204–222, 1999, doi: 10.1111/j.1749-6632.1999.tb07996.x.
- [31] X. Wang *et al.*, "Delayed expression of osteopontin after focal stroke in the rat," *J. Neurosci. Off. J. Soc. Neurosci.*, vol. 18, no. 6, pp. 2075–2083, Mar. 1998.

- [32] D. Chabas *et al.*, "The influence of the proinflammatory cytokine, osteopontin, on autoimmune demyelinating disease," *Science*, vol. 294, no. 5547, pp. 1731–1735, Nov. 2001, doi: 10.1126/science.1062960.
- [33] R. Selvaraju *et al.*, "Osteopontin is upregulated during in vivo demyelination and remyelination and enhances myelin formation in vitro," *Mol. Cell. Neurosci.*, vol. 25, no. 4, pp. 707–721, Apr. 2004, doi: 10.1016/j.mcn.2003.12.014.
- [34] K. Minor, J. Phillips, and N. W. Seeds, "Tissue plasminogen activator promotes axonal outgrowth on CNS myelin after conditioned injury," *J. Neurochem.*, vol. 109, no. 3, pp. 706–715, May 2009, doi: 10.1111/j.1471-4159.2009.05977.x.
- [35] L. O. Sun *et al.*, "Spatiotemporal Control of CNS Myelination by Oligodendrocyte Programmed Cell Death through the TFEB-PUMA Axis," *Cell*, vol. 175, no. 7, pp. 1811–1826.e21, Dec. 2018, doi: 10.1016/j.cell.2018.10.044.
- [36] E. De Smaele *et al.*, "Induction of gadd45beta by NF-kappaB downregulates pro-apoptotic JNK signalling," *Nature*, vol. 414, no. 6861, pp. 308–313, Nov. 2001, doi: 10.1038/35104560.
- [37] J.-X. Zhang *et al.*, "JNK is necessary for oligodendrocyte precursor cell proliferation induced by the conditioned medium from B104 neuroblastoma cells," *J. Mol. Neurosci.*, vol. 52, no. 2, pp. 269–276, Feb. 2014, doi: 10.1007/s12031-013-0135-0.
- [38] A. Caminero, M. Comabella, and X. Montalban, "Role of tumour necrosis factor (TNF)- α and TNFRSF1A R92Q mutation in the pathogenesis of TNF receptor-associated periodic syndrome and multiple sclerosis," *Clin. Exp. Immunol.*, vol. 166, no. 3, pp. 338–345, Dec. 2011, doi: 10.1111/j.1365-2249.2011.04484.x.
- [39] G. Kassiotis, M. Pasparakis, G. Kollias, and L. Probert, "TNF accelerates the onset but does not alter the incidence and severity of myelin basic protein-induced experimental autoimmune encephalomyelitis," *Eur. J. Immunol.*, vol. 29, no. 3, pp. 774–780, Mar. 1999, doi: 10.1002/(SICI)1521-4141(199903)29:03<774::AID-IMMU774>3.0.CO;2-T.
- [40] J. Fortin *et al.*, "Mutant ACVR1 Arrests Glial Cell Differentiation to Drive Tumorigenesis in Pediatric Gliomas," *Cancer Cell*, vol. 37, no. 3, pp. 308–323.e12, Mar. 2020, doi: 10.1016/j.ccell.2020.02.002.
- [41] L. Quan, A. Uyeda, and R. Muramatsu, "Central nervous system regeneration: the roles of glial cells in the potential molecular mechanism underlying remyelination," *Inflamm. Regen.*, vol. 42, no. 1, p. 7, Mar. 2022, doi: 10.1186/s41232-022-00193-y.
- [42] L. Auderset *et al.*, "Low-Density Lipoprotein Receptor-Related Protein 1 (LRP1) Is a Negative Regulator of Oligodendrocyte Progenitor Cell Differentiation in the Adult Mouse Brain," *Front. Cell Dev. Biol.*, vol. 8, p. 1067, 2020, doi: 10.3389/fcell.2020.564351.
- [43] R. W. O'Meara, J.-P. Michalski, and R. Kothary, "Integrin Signaling in Oligodendrocytes and Its Importance in CNS Myelination," *J. Signal Transduct.*, vol. 2011, p. 354091, 2011, doi: 10.1155/2011/354091.
- [44] M. P. Arrate, J. M. Rodriguez, T. M. Tran, T. A. Brock, and S. A. Cunningham, "Cloning of human junctional adhesion molecule 3 (JAM3) and its identification as the JAM2 counter-receptor," *J. Biol. Chem.*, vol. 276, no. 49, pp. 45826–45832, Dec. 2001, doi: 10.1074/jbc.M105972200.
- [45] T. W. Liang *et al.*, "Vascular endothelial-junctional adhesion molecule (VE-JAM)/JAM 2 interacts with T, NK, and dendritic cells through JAM 3," *J. Immunol. Baltim. Md 1950*, vol. 168, no. 4, pp. 1618–1626, Feb. 2002, doi: 10.4049/jimmunol.168.4.1618.
- [46] J. Ferent, C. Zimmer, P. Durbec, M. Ruat, and E. Traiffort, "Sonic Hedgehog Signaling Is a Positive Oligodendrocyte Regulator during Demyelination," *J. Neurosci.*, vol. 33, no. 5, pp. 1759–1772, Jan. 2013, doi: 10.1523/JNEUROSCI.3334-12.2013.
- [47] Y. Xie *et al.*, "Aberrant oligodendroglial LDL receptor orchestrates demyelination in chronic cerebral ischemia," *J. Clin. Invest.*, vol. 131, no. 1, doi: 10.1172/JCI128114.
- [48] V. Pietiäinen *et al.*, "NDRG1 functions in LDL receptor trafficking by regulating endosomal recycling and degradation," *J. Cell Sci.*, vol. 126, no. Pt 17, pp. 3961–3971, Sep. 2013, doi: 10.1242/jcs.128132.
- [49] M. Furusho, J. L. Dupree, K.-A. Nave, and R. Bansal, "Fibroblast Growth Factor Receptor Signaling in Oligodendrocytes Regulates Myelin Sheath Thickness," *J. Neurosci.*, vol. 32, no. 19, pp. 6631–6641, May 2012, doi: 10.1523/JNEUROSCI.6005-11.2012.
- [50] W. Zhang *et al.*, "Astrocytes increase exosomal secretion of oligodendrocyte precursor cells to promote their proliferation via integrin β 4-mediated cell adhesion," *Biochem. Biophys. Res. Commun.*, vol. 526, no. 2, pp. 341–348, May 2020, doi: 10.1016/j.bbrc.2020.03.092.
- [51] C. E. M. Van der Zee, M. Kreft, G. Beckers, A. Kuipers, and A. Sonnenberg, "Conditional Deletion of the Itgb4 Integrin Gene in Schwann Cells Leads to Delayed Peripheral Nerve Regeneration," *J. Neurosci.*, vol. 28, no. 44, pp. 11292–11303, Oct. 2008, doi: 10.1523/JNEUROSCI.3068-08.2008.
- [52] T. K. Darling and T. J. Lamb, "Emerging Roles for Eph Receptors and Ephrin Ligands in Immunity," *Front. Immunol.*, vol. 10, p. 1473, 2019, doi: 10.3389/fimmu.2019.01473.
- [53] C. Linneberg, M. Harboe, and L. S. Laursen, "Axo-Glia Interaction Preceding CNS Myelination Is Regulated by Bidirectional Eph-Ephrin Signaling," *ASN NEURO*, vol. 7, no. 5, p. 1759091415602859, Sep. 2015, doi: 10.1177/1759091415602859.
- [54] B. Garcia-Diaz *et al.*, "Loss of lysophosphatidic acid receptor LPA1 alters oligodendrocyte differentiation and myelination in the mouse cerebral cortex," *Brain Struct. Funct.*, vol. 220, no. 6, pp. 3701–3720, Nov. 2015, doi: 10.1007/s00429-014-0885-7.
- [55] R. Akkermann *et al.*, "The TAM receptor Tyro3 regulates myelination in the central nervous system," *Glia*, vol. 65, no. 4, pp. 581–591, 2017, doi: 10.1002/glia.23113.

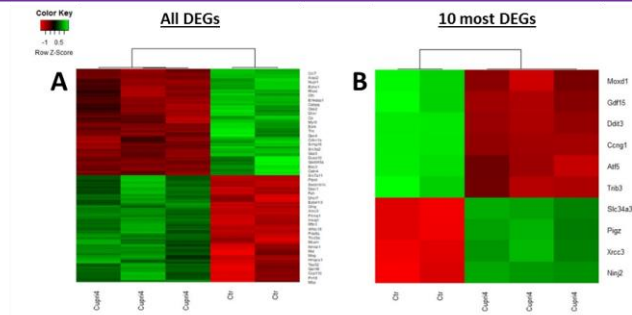
Supplementary information

Supplementary Figures

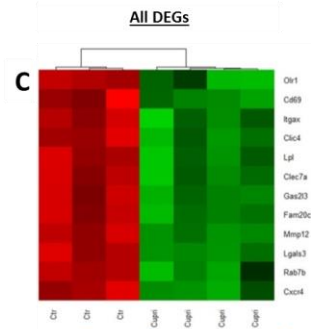


Supplementary Figure 1. Methodology workflow and summary of results. *in OPCs from cuprizone-treated mice compared to OPCs from control mice. CC: corpus callosum; DEGs: differentially expressed genes; GO: gene ontology; OPC: oligodendrocyte progenitor cell.

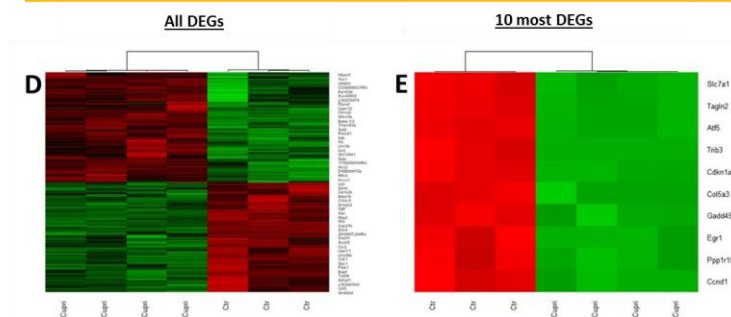
DEGs in CC in 4-week-cuprizone treated and control mice



DEGs in microglia in 4-week-cuprizone treated and control mice



DEGs in OPCs in 4-week-cuprizone treated and control mice



Supplementary Figure 2. Sample clustering by expression of DEGs in CC, microglia and OPCs between control mice and 4-week cuprizone treated mice. (A-B) Heatmap and hierarchical clustering performed with the normalized and filtered expression data and the samples included at late demyelination in the CC analysis, using all DEGs and the 10 most DEGs. Color key indicates the relative expression level of genes across all samples: red color represents an expression level below mean, green color represents expression higher than the mean. (C) Heatmap and hierarchical clustering performed with the normalized and filtered expression data and the samples included in the microglia using all DEGs. (D-E) Heatmap and hierarchical clustering performed with the normalized and filtered expression data and the samples included in the OPCs analysis, using all DEGs and the 10 most DEGs.

Supplementary Tables

Supplementary Table 1. GEO/Array express studies in brain samples/cells from control and cuprizone-treated mice where gene expression has been analyzed with microarrays.

GEO Study	Platform	Cell type/brain region	Length of cuprizone treatment	Remyelination	Number of samples in control group	Number of samples in treatment group
GSE100663	Agilent whole mouse 4x44k	Corpus callosum	2/4 weeks	4 weeks of cuprizone treatment + 1week normal diet	3	3 (2 weeks)/4 (4 weeks)
GSE84113	Affymetrix Mouse Gene 1.0 ST	Microglia	4 weeks		2	3
GSE66926	Affymetrix Mouse Gene 1.0 ST	Microglia	4 weeks		1	1
GSE48872	Agilent whole mouse 4x44k	OPCs	5 weeks		3	4

Supplementary Table 2. DEGS in CC in mice treated with cuprizone for 2 weeks compared to control.

Probe ID	Symbol	Gene Name	logFC	p-value	adj.p-value
A_51_P363947	Cdkn1a	cyclin-dependent kinase inhibitor 1A (P21)	-4.32	1.89E-07	4.55E-03
A_51_P331570	Trib3	tribbles pseudokinase 3	-4.64	1.11E-06	1.34E-02
A_52_P532982	Gdf15	growth differentiation factor 15	-4.3	2.79E-06	1.63E-02
A_51_P285669	Pigz	phosphatidylinositol glycan anchor biosynthesis, class Z	3.1	2.98E-06	1.63E-02
A_52_P627816	Tgm1	transglutaminase 1, K polypeptide	-3.13	3.43E-06	1.63E-02
A_52_P634098	B230206H07Rik	RIKEN cDNA B230206H07 gene	3.46	4.86E-06	1.63E-02
A_51_P329975	Ninj2	ninjurin 2	3.22	5.13E-06	1.63E-02
A_51_P330428	Eif4ebp1	eukaryotic translation initiation factor 4E binding protein 1	-2.31	5.88E-06	1.63E-02
A_51_P230734	Slc34a3	solute carrier family 34 (sodium phosphate), member 3	3.19	6.11E-06	1.63E-02
A_51_P269216	Atf5	activating transcription factor 5	-2.92	8.27E-06	1.89E-02
A_52_P154710	Sesn2	sestrin 2	-2.07	9.95E-06	1.89E-02
A_51_P199494	Caena2d4	calcium channel, voltage-dependent, alpha 2/delta subunit 4	3.16	1.06E-05	1.89E-02
A_51_P516741	Tmprss5	transmembrane protease, serine 5 (spinesin)	2.79	1.08E-05	1.89E-02
A_51_P197043	Xrcc3	X-ray repair complementing defective repair in Chinese hamster cells 3	2.77	1.13E-05	1.89E-02
A_51_P497937	Gjc2	gap junction protein, gamma 2	3.2	1.25E-05	1.89E-02
A_51_P181297	Serpinb1a	serine (or cysteine) peptidase inhibitor, clade B, member 1a	2.42	1.26E-05	1.89E-02
A_51_P411694	Carns1	carnosine synthase 1	2.58	1.52E-05	2.00E-02
A_51_P432460	Ppp1r14a	protein phosphatase 1, regulatory inhibitor subunit 14A	4.29	1.60E-05	2.00E-02
A_52_P427024	Ldlr	low density lipoprotein receptor	2.33	1.81E-05	2.00E-02
A_51_P161612	Ccng1	cyclin G1	-1.9	1.81E-05	2.00E-02
A_51_P370034	Muc11	mucin-like 1	2.41	1.90E-05	2.00E-02
A_51_P219918	Tmem125	transmembrane protein 125	4.25	1.88E-05	2.00E-02
A_52_P329207	Wfdc18	WAP four-disulfide core domain 18	1.93	1.95E-05	2.00E-02
A_52_P452689	Atf3	activating transcription factor 3	-2.17	2.23E-05	2.00E-02
A_51_P519251	Nupr1	nuclear protein transcription regulator 1	-2.8	2.26E-05	2.00E-02
A_52_P608322	Maff	v-maf musculoaponeurotic fibrosarcoma oncogene family, protein F (avian)	-2.75	2.29E-05	2.00E-02
A_51_P493987	Moxd1	monooxygenase, DBH-like 1	-2.51	2.33E-05	2.00E-02
A_51_P444447	Cebpd	CCAAT/enhancer binding protein (C/EBP), delta	-1.96	2.37E-05	2.00E-02
A_51_P246166	Wfdc18	WAP four-disulfide core domain 18	2	2.42E-05	2.00E-02

A_51_P421140	Tubb6	tubulin, beta 6 class V	-2.07	2.75E-05	2.20E-02
A_51_P213544	Klf4	Kruppel-like factor 4 (gut)	-1.81	3.07E-05	2.34E-02
A_52_P395149	Smtnl2	smoothelin-like 2	3.19	3.26E-05	2.34E-02
A_51_P190740	Adssl1	adenylosuccinate synthetase like 1	2.23	3.31E-05	2.34E-02
A_52_P481493	Fkbp5	FK506 binding protein 5	-1.94	3.31E-05	2.34E-02
A_51_P384230	Sgk2	serum/glucocorticoid regulated kinase 2	3.93	3.46E-05	2.38E-02
A_51_P193832	Rtkn2	rhotekin 2	2.23	3.79E-05	2.53E-02
A_52_P448648	Rab37	RAB37, member RAS oncogene family	2.18	4.38E-05	2.66E-02
A_52_P416499	Enpp2	ectonucleotide pyrophosphatase/phosphodiesterase 2	1.94	4.57E-05	2.66E-02
A_52_P344160	Ccp110	centriolar coiled coil protein 110	2.17	4.58E-05	2.66E-02
A_51_P258570	Klk6	kallikrein related-peptidase 6	4.47	4.59E-05	2.66E-02
A_51_P146941	Hmgcs1	3-hydroxy-3-methylglutaryl-Coenzyme A synthase 1	1.81	4.64E-05	2.66E-02
A_51_P212057	Serpinb1c	serine (or cysteine) peptidase inhibitor, clade B, member 1c	2.17	4.88E-05	2.73E-02
A_51_P273639	Slc7a5	solute carrier family 7 (cationic amino acid transporter, y+ system), member 5	-1.88	5.11E-05	2.79E-02
A_51_P484869	Gamt	guanidinoacetate methyltransferase	2.79	5.35E-05	2.81E-02
A_51_P480233	Nmr11	NmrA-like family domain containing 1	2.22	5.38E-05	2.81E-02
A_52_P207163	Eda2r	ectodysplasin A2 receptor	-2.45	5.73E-05	2.90E-02
A_51_P336070	Lctl	lactase-like	2.93	5.88E-05	2.90E-02
A_51_P174996	Slc17a6	solute carrier family 17 (sodium-dependent inorganic phosphate cotransporter), member 6	1.7	5.90E-05	2.90E-02
A_51_P111612	Arrdc4	arrestin domain containing 4	-1.93	6.31E-05	2.97E-02
A_52_P533146	Ddit3	DNA-damage inducible transcript 3	-1.62	6.36E-05	2.97E-02
A_51_P354354	Gal3st1	galactose-3-O-sulfotransferase 1	2.49	6.81E-05	3.05E-02
A_51_P319460	Osmr	oncostatin M receptor	-1.52	6.84E-05	3.05E-02
A_52_P690855	Fndc11	fibronectin type III domain containing 11	1.72	7.33E-05	3.15E-02
A_52_P161495	Bcl6	B cell leukemia/lymphoma 6	-1.51	7.93E-05	3.25E-02
A_51_P237307	Plekhg1	pleckstrin homology domain containing, family G (with RhoGef domain) member 1	1.6	7.94E-05	3.25E-02
A_51_P170807	Map3k6	mitogen-activated protein kinase kinase kinase 6	-1.77	7.96E-05	3.25E-02
A_51_P195153	Gtse1	G two S phase expressed protein 1	-1.71	8.34E-05	3.27E-02
A_52_P63553	Cebpb	CCAAT/enhancer binding protein (C/EBP), beta	-1.51	8.38E-05	3.27E-02
A_51_P452323	Nes	nestin	-1.69	1.02E-04	3.80E-02
A_51_P263965	Hmox1	heme oxygenase 1	-1.77	1.02E-04	3.80E-02

A_51_P282896	Mast4	microtubule associated serine/threonine kinase family member 4	1.55	1.03E-04	3.80E-02
A_51_P206585	Runx1	runt related transcription factor 1	-1.62	1.05E-04	3.80E-02
A_52_P24835	Nectin4	nectin cell adhesion molecule 4	2.95	1.07E-04	3.80E-02
A_51_P129502	Slc7a11	solute carrier family 7 (cationic amino acid transporter, y+ system), member 11	-2.01	1.09E-04	3.80E-02
A_51_P275905	Fgl1	fibrinogen-like protein 1	-1.46	1.11E-04	3.80E-02
A_51_P472726	Pdlim2	PDZ and LIM domain 2	3.15	1.14E-04	3.80E-02
A_51_P117457	Dcaf12l2	DDB1 and CUL4 associated factor 12-like 2	-1.57	1.15E-04	3.80E-02
A_51_P366867	Gas5	growth arrest specific 5	-1.43	1.16E-04	3.80E-02
A_51_P367060	Ifrd1	interferon-related developmental regulator 1	-1.41	1.19E-04	3.80E-02
A_52_P630673	Gpr62	G protein-coupled receptor 62	2.99	1.22E-04	3.80E-02
A_52_P628702	Cntn2	contactin 2	2.41	1.22E-04	3.80E-02
A_51_P340027	Pappa	pregnancy-associated plasma protein A	-2.27	1.23E-04	3.80E-02
A_52_P430348	Serpib1b	serine (or cysteine) peptidase inhibitor, clade B, member 1b	1.84	1.23E-04	3.80E-02
A_51_P117666	Snhg16	small nucleolar RNA host gene 16	-1.36	1.28E-04	3.91E-02
A_52_P142154	Pcyt2	phosphate cytidylyltransferase 2, ethanolamine	1.54	1.40E-04	4.21E-02
A_51_P246903	Rps27l	ribosomal protein S27-like	-1.42	1.45E-04	4.32E-02
A_52_P45616	Emilin3	elastin microfibril interfacier 3	1.67	1.51E-04	4.42E-02
A_51_P248122	Bbc3	BCL2 binding component 3	-1.69	1.54E-04	4.46E-02
A_51_P348183	Tmem141	transmembrane protein 141	1.76	1.58E-04	4.51E-02
A_52_P245648	Slc3a2	solute carrier family 3 (activators of dibasic and neutral amino acid transport), member 2	-1.4	1.60E-04	4.51E-02
A_52_P335606	Prima1	proline rich membrane anchor 1	2.24	1.65E-04	4.51E-02
A_51_P315411	Epb41l3	erythrocyte membrane protein band 4.1 like 3	1.82	1.64E-04	4.51E-02
A_52_P494168	Prr18	proline rich 18	2.61	1.69E-04	4.58E-02
A_52_P563375	Lgals2	lectin, galactose-binding, soluble 2	1.81	1.76E-04	4.65E-02
A_51_P482990	Arid5a	AT rich interactive domain 5A (MRF1-like)	-1.97	1.78E-04	4.65E-02
A_51_P186552	Hid1	HID1 domain containing	1.55	1.81E-04	4.68E-02
A_52_P500027	Nfil3	nuclear factor, interleukin 3, regulated	-1.32	1.83E-04	4.68E-02
A_51_P110341	Scgb3a1	secretoglobin, family 3A, member 1	-1.57	1.87E-04	4.68E-02
A_52_P391000	Pde8a	phosphodiesterase 8A	2.26	1.92E-04	4.68E-02
A_52_P355169	Tnc	tenascin C	-2.06	1.93E-04	4.68E-02
A_51_P219109	Il12rb1	interleukin 12 receptor, beta 1	2.63	1.95E-04	4.68E-02

A_51_P356967	Lgi3	leucine-rich repeat LGI family, member 3	2.18	1.96E-04	4.68E-02
A_52_P384465	Mobp	myelin-associated oligodendrocytic basic protein	2.5	1.98E-04	4.68E-02
A_51_P104710	Sspo	SCO-spondin	2.69	1.98E-04	4.68E-02
A_52_P515620	5033421B08Rik	RIKEN cDNA 5033421B08 gene	2.04	2.02E-04	4.73E-02
A_51_P420415	Srd5a1	steroid 5 alpha-reductase 1	1.54	2.09E-04	4.84E-02
A_52_P377160	Galnt6	polypeptide N-acetylgalactosaminyltransferase 6	2.22	2.18E-04	4.87E-02
A_52_P72587	Prkcq	protein kinase C, theta	1.62	2.20E-04	4.87E-02
A_51_P212068	Aoc1	amine oxidase, copper-containing 1	1.96	2.22E-04	4.87E-02
A_52_P31814	1110038B12Rik	RIKEN cDNA 1110038B12 gene	-1.33	2.25E-04	4.87E-02
A_51_P117581	Cables1	CDK5 and Abl enzyme substrate 1	-1.6	2.27E-04	4.87E-02
A_51_P379798	Fdps	farnesyl diphosphate synthetase	1.34	2.29E-04	4.87E-02
A_51_P246317	Mt2	metallothionein 2	-1.43	2.31E-04	4.87E-02
A_51_P125725	Sh3gl3	SH3-domain GRB2-like 3	1.65	2.31E-04	4.87E-02
A_51_P303749	Depdc1b	DEP domain containing 1B	2.25	2.38E-04	4.87E-02
A_52_P302496	Fah	fumarylacetoacetate hydrolase	1.72	2.35E-04	4.87E-02
A_52_P121502	Plip	plasma membrane proteolipid	2.27	2.39E-04	4.87E-02
A_51_P438752	Gm4221	predicted gene 4221	1.92	2.39E-04	4.87E-02

Supplementary Table 3. DEGs identified in the CC of mice treated with cuprizone for 4 weeks compared to corpus callosum from control mice.

ProbeID	Symbol	Gene name	Log2 fold change	p-value	Adjusted p-value
A_52_P532982	Gdf15	growth differentiation factor 15	-3.86	3.37e-07	8.51e-03
A_51_P285669	Pigz	phosphatidylinositol glycan anchor biosynthesis, class Z	2.54	1.35e-06	1.10e-02
A_51_P331570	Trib3	tribbles pseudokinase 3	-4.40	1.77e-06	1.10e-02
A_51_P329975	Ninj2	ninjurin 2	1.92	2.01e-06	1.10e-02
A_51_P161612	Ccng1	cyclin G1	-1.93	2.41e-06	1.10e-02
A_51_P230734	Slc34a3	solute carrier family 34 (sodium phosphate), member 3	1.76	2.78e-06	1.10e-02
A_51_P269216	Atf5	activating transcription factor 5	-3.41	3.05e-06	1.10e-02
A_51_P197043	Xrcc3	X-ray repair complementing defective repair in Chinese hamster cells 3	1.91	4.10e-06	1.29e-02
A_52_P533146	Ddit3	DNA-damage inducible transcript 3	-1.70	5.40e-06	1.51e-02
A_51_P493987	Moxd1	monooxygenase, DBH-like 1	-2.59	7.51e-06	1.60e-02
A_52_P207163	Eda2r	ectodysplasin A2 receptor	-1.12	7.61e-06	1.60e-02
A_52_P395149	Smtnl2	smoothelin-like 2	1.65	8.68e-06	1.69e-02
A_51_P432460	Ppp1r14a	protein phosphatase 1, regulatory inhibitor subunit 14A	3.67	9.42e-06	1.70e-02
A_52_P154710	Sesn2	sestrin 2	-2.20	1.05e-05	1.74e-02
A_51_P363947	Cdkn1a	cyclin-dependent kinase inhibitor 1A (P21)	-3.72	1.13e-05	1.74e-02
A_51_P219918	Tmem125	transmembrane protein 125	3.46	1.21e-05	1.74e-02
A_51_P479230	Nat8	N-acetyltransferase 8 (GCN5-related)	-1.57	1.24e-05	1.74e-02
A_51_P516741	Tmprss5	transmembrane protease, serine 5 (spinesin)	1.65	1.34e-05	1.74e-02
A_51_P273639	Slc7a5	solute carrier family 7 (cationic amino	-1.73	1.38e-05	1.74e-02

		acid transporter, y+ system), member 5			
A_52_P329207	Wfdc18	WAP four-disulfide core domain 18	1.87	1.47e-05	1.77e-02
A_51_P129502	Slc7a11	solute carrier family 7 (cationic amino acid transporter, y+ system), member 11	-2.37	1.75e-05	1.87e-02
A_51_P283473	Fibin	fin bud initiation factor homolog (zebrafish)	-1.70	1.82e-05	1.87e-02
A_51_P213544	Klf4	Kruppel-like factor 4 (gut)	-1.71	1.84e-05	1.87e-02
A_51_P330428	Eif4ebp1	eukaryotic translation initiation factor 4E binding protein 1	-2.33	1.85e-05	1.87e-02
A_51_P472901	Slc3a2	solute carrier family 3 (activators of dibasic and neutral amino acid transport), member 2	-1.54	1.94e-05	1.89e-02
A_51_P241407	Arap2	ArfGAP with RhoGAP domain, ankyrin repeat and PH domain 2	-1.39	2.08e-05	1.95e-02
A_51_P337925	Gzmm	granzyme M (lymphocyte met-ase 1)	-1.60	2.20e-05	1.98e-02
A_51_P384230	Sgk2	serum/glucocorticoid regulated kinase 2	2.93	2.78e-05	2.35e-02
A_51_P248122	Bbc3	BCL2 binding component 3	-1.77	3.04e-05	2.35e-02
A_51_P340027	Pappa	pregnancy-associated plasma protein A	-2.02	3.26e-05	2.35e-02
A_51_P452323	Nes	nestin	-1.85	3.28e-05	2.35e-02
A_51_P366867	Gas5	growth arrest specific 5	-1.46	3.29e-05	2.35e-02
A_51_P379798	Fdps	farnesyl diphosphate synthetase	1.28	3.37e-05	2.35e-02
A_52_P335606	Prima1	proline rich membrane anchor 1	1.25	3.40e-05	2.35e-02
A_51_P181297	Serpinb1a	serine (or cysteine) peptidase inhibitor, clade B, member 1a	1.98	3.59e-05	2.35e-02
A_52_P506217	Rhod	ras homolog family member D	-1.28	3.63e-05	2.35e-02
A_52_P208763	Ccl7	chemokine (C-C motif) ligand 7	-0.87	3.80e-05	2.39e-02
A_51_P493234	Cp	ceruloplasmin	-1.89	3.88e-05	2.39e-02
A_51_P355943	Mvd	mevalonate (diphospho) decarboxylase	1.23	4.04e-05	2.43e-02
A_52_P427024	Ldlr	low density lipoprotein receptor	1.83	4.19e-05	2.46e-02
A_51_P497937	Gjc2	gap junction protein, gamma 2	1.49	4.42e-05	2.49e-02
A_51_P508289	Ephx1	epoxide hydrolase 1, microsomal	-2.01	4.64e-05	2.49e-02
A_52_P416072	Ephx1	epoxide hydrolase 1, microsomal	-1.99	4.80e-05	2.49e-02
A_52_P634098	B230206H07Rik	RIKEN cDNA B230206H07 gene	1.50	4.81e-05	2.49e-02
A_51_P195153	Gtse1	G two S phase expressed protein 1	-1.01	4.83e-05	2.49e-02
A_52_P388072	Hmgcs1	3-hydroxy-3-methylglutaryl-Coenzyme A synthase 1	1.23	4.84e-05	2.49e-02
A_51_P117666	Snhg16	small nucleolar RNA host gene 16	-1.25	4.93e-05	2.49e-02
A_52_P111715	Galnt6	polypeptide N-acetylgalactosaminyltransferase 6	2.72	5.88e-05	2.79e-02
A_52_P630673	Gpr62	G protein-coupled receptor 62	2.50	5.98e-05	2.79e-02
A_52_P377160	Galnt6	polypeptide N-acetylgalactosaminyltransferase 6	1.22	6.01e-05	2.79e-02
A_51_P519251	Nupr1	nuclear protein transcription regulator 1	-3.63	6.02e-05	2.79e-02
A_52_P489295	Adams1	a disintegrin-like and metallopeptidase (repolyisin type) with thrombospondin type 1 motif, 1	-1.59	6.07e-05	2.79e-02
A_52_P142154	Pcyt2	phosphate cytidyltransferase 2, ethanolamine	1.28	6.19e-05	2.79e-02
A_51_P500984	Gadd45b	growth arrest and DNA-damage-inducible 45 beta	-1.31	6.43e-05	2.85e-02
A_52_P355169	Tnc	tenascin C	-1.71	6.56e-05	2.86e-02
A_51_P110341	Scgb3a1	secretoglobin, family 3A, member 1	-0.92	7.29e-05	3.02e-02
A_52_P406181	Nacad	NAC alpha domain containing	1.38	7.82e-05	3.19e-02
A_51_P258570	Klk6	kallikrein related-peptidase 6	2.91	8.19e-05	3.27e-02
A_52_P255849	Tlcd3a	TLC domain containing 3A	1.01	8.97e-05	3.47e-02
A_51_P222381	Tmeff1	transmembrane protein with EGF-like and two follistatin-like domains 1	1.11	9.49e-05	3.58e-02
A_51_P186703	Fbln5	fibulin 5	-1.34	1.04e-04	3.77e-02
A_51_P181312	Dcxr	dicarbonyl L-xylulose reductase	-1.37	1.06e-04	3.77e-02
A_52_P85040	Mog	myelin oligodendrocyte glycoprotein	2.67	1.06e-04	3.77e-02
A_52_P443705	Aen	apoptosis enhancing nuclease	-1.37	1.08e-04	3.77e-02
A_51_P480233	Nmral1	Nmra-like family domain containing 1	1.92	1.08e-04	3.77e-02
A_52_P633597	Rftn1	raftlin lipid raft linker 1	1.20	1.09e-04	3.77e-02
A_51_P411694	Carns1	carnosine synthase 1	1.40	1.13e-04	3.81e-02

A_52_P344160	Ccp110	centriolar coiled coil protein 110	1.70	1.13e-04	3.81e-02
A_52_P653684	Eprs	glutamyl-prolyl-tRNA synthetase	-1.11	1.15e-04	3.82e-02
A_52_P2710	Nat8f5	N-acetyltransferase 8 (GCN5-related) family member 5	-1.40	1.19e-04	3.82e-02
A_52_P670978	Nkain1	Na ⁺ /K ⁺ transporting ATPase interacting 1	1.65	1.20e-04	3.82e-02
A_52_P597634	Fzd1	frizzled class receptor 1	-1.74	1.25e-04	3.82e-02
A_51_P225186	Calcr1	calcitonin receptor-like	-1.31	1.27e-04	3.82e-02
A_52_P326502	Sox21	SRY (sex determining region Y)-box 21	-1.13	1.27e-04	3.82e-02
A_51_P315411	Epb41f3	erythrocyte membrane protein band 4.1 like 3	1.44	1.28e-04	3.82e-02
A_52_P391000	Pde8a	phosphodiesterase 8A	1.53	1.41e-04	4.01e-02
A_51_P104418	Dusp10	dual specificity phosphatase 10	-1.54	1.42e-04	4.01e-02
A_51_P246903	Rps27l	ribosomal protein S27-like	-1.64	1.43e-04	4.01e-02
A_52_P627816	Tgm1	transglutaminase 1, K polypeptide	-3.27	1.44e-04	4.01e-02
A_52_P263068	Rhog	ras homolog family member G	1.12	1.45e-04	4.01e-02
A_51_P111612	Arrdc4	arrestin domain containing 4	-1.54	1.46e-04	4.01e-02
A_52_P624415	Opalin	oligodendrocytic myelin paranodal and inner loop protein	3.02	1.48e-04	4.03e-02
A_51_P381618	Pla1a	phospholipase A1 member A	-0.87	1.52e-04	4.05e-02
A_51_P252947	Mapk8ip1	mitogen-activated protein kinase 8 interacting protein 1	1.49	1.52e-04	4.05e-02
A_51_P482990	Arid5a	AT rich interactive domain 5A (MRF1-like)	-1.72	1.56e-04	4.09e-02
A_52_P503387	Trp53inp1	transformation related protein 53 inducible nuclear protein 1	-1.28	1.58e-04	4.09e-02
A_52_P512955	Anln	anillin, actin binding protein	1.45	1.59e-04	4.09e-02
A_51_P290921	Syt12	synaptotagmin-like 2	1.22	1.66e-04	4.15e-02
A_51_P286737	Ccl2	chemokine (C-C motif) ligand 2	-2.41	1.66e-04	4.15e-02
A_51_P296608	Gadd45a	growth arrest and DNA-damage-inducible 45 alpha	-1.81	1.67e-04	4.15e-02
A_51_P209372	Msmo1	methylsterol monooxygenase 1	1.08	1.68e-04	4.15e-02
A_51_P499071	Mal	myelin and lymphocyte protein, T cell differentiation protein	2.81	1.71e-04	4.15e-02
A_52_P494168	Prr18	proline rich 18	2.21	1.71e-04	4.15e-02
A_52_P188172	Synj2	synaptojanin 2	1.37	1.73e-04	4.15e-02
A_51_P367060	Ifrd1	interferon-related developmental regulator 1	-1.28	1.74e-04	4.15e-02
A_51_P190740	Adssl1	adenylosuccinate synthetase like 1	1.81	1.78e-04	4.17e-02
A_51_P331805	Kctd15	potassium channel tetramerisation domain containing 15	-1.13	1.82e-04	4.20e-02
A_52_P641367	Desi1	desumoylating isopeptidase 1	1.52	1.83e-04	4.20e-02
A_51_P302503	Ppp1r15a	protein phosphatase 1, regulatory subunit 15A	-1.37	1.86e-04	4.24e-02
A_51_P107686	Foxc1	forkhead box C1	-1.14	1.90e-04	4.25e-02
A_51_P354354	Gal3st1	galactose-3-O-sulfotransferase 1	1.77	1.91e-04	4.25e-02
A_51_P108990	Cetn4	centrin 4	-1.40	1.93e-04	4.25e-02
A_52_P608322	Maff	v-maf musculoaponeurotic fibrosarcoma oncogene family, protein F (avian)	-2.24	1.95e-04	4.25e-02
A_52_P628702	Cntn2	contactin 2	1.94	1.96e-04	4.25e-02
A_52_P577329	Tmem88b	transmembrane protein 88B	2.10	1.97e-04	4.25e-02
A_51_P202857	Cdca7	cell division cycle associated 7	1.13	2.03e-04	4.33e-02
A_51_P406846	Nipal4	NIPA-like domain containing 4	1.10	2.04e-04	4.33e-02
A_51_P431737	Cth	cystathionase (cystathionine gamma-lyase)	-1.02	2.07e-04	4.33e-02
A_52_P393392	Insig1	insulin induced gene 1	0.96	2.09e-04	4.33e-02
A_51_P504863	Cdk18	cyclin-dependent kinase 18	1.32	2.10e-04	4.33e-02
A_51_P436269	Grin2c	glutamate receptor, ionotropic, NMDA2C (epsilon 3)	1.19	2.11e-04	4.33e-02
A_51_P426270	Mgp	matrix Gla protein	-1.46	2.23e-04	4.47e-02
A_52_P605266	Ptprd	protein tyrosine phosphatase, receptor type, D	1.49	2.24e-04	4.47e-02
A_51_P356967	Lgi3	leucine-rich repeat LGI family, member 3	1.76	2.25e-04	4.47e-02
A_52_P164709	Poc1a	POC1 centriolar protein A	1.10	2.30e-04	4.47e-02
A_51_P277994	Oas2	2'-5' oligoadenylate synthetase 2	-1.20	2.32e-04	4.47e-02

A_51_P201187	Pllp	plasma membrane proteolipid	1.65	2.33e-04	4.47e-02
A_52_P52357	Tor3a	torsin family 3, member A	-1.37	2.33e-04	4.47e-02
A_51_P268439	Mcam	melanoma cell adhesion molecule	1.29	2.34e-04	4.47e-02
A_52_P302496	Fah	fumarylacetoacetate hydrolase	1.30	2.36e-04	4.47e-02
A_51_P345975	Lpin3	lipin 3	-0.81	2.41e-04	4.48e-02
A_52_P268852	Helt	helt bHLH transcription factor	0.78	2.49e-04	4.56e-02
A_51_P252725	Gpc4	glypican 4	-1.73	2.49e-04	4.56e-02
A_51_P438527	Cyb5r1	cytochrome b5 reductase 1	-1.42	2.51e-04	4.56e-02
A_51_P211980	Rgs3	regulator of G-protein signaling 3	1.04	2.56e-04	4.57e-02
A_51_P111492	Nfil3	nuclear factor, interleukin 3, regulated	-1.05	2.57e-04	4.57e-02
A_51_P349205	Mbp	myelin basic protein	2.20	2.60e-04	4.59e-02
A_51_P480202	Dlx2	distal-less homeobox 2	1.21	2.81e-04	4.84e-02
A_51_P290986	Dhcr7	7-dehydrocholesterol reductase	1.23	2.83e-04	4.84e-02
A_52_P20977	Ldlrad4	low density lipoprotein receptor class A domain containing 4	1.12	2.87e-04	4.84e-02
A_51_P442501	Ano4	anoctamin 4	0.86	2.88e-04	4.84e-02
A_51_P175858	Cyb5r2	cytochrome b5 reductase 2	-0.63	2.89e-04	4.84e-02
A_52_P421344	Paqr5	progesterin and adipoQ receptor family member V	-1.17	2.89e-04	4.84e-02
A_52_P193022	Hfe	homeostatic iron regulator	-1.41	2.90e-04	4.84e-02
A_51_P104710	Sspo	SCO-spondin	1.22	2.91e-04	4.84e-02
A_51_P117457	Dcaf12l2	DDB1 and CUL4 associated factor 12-like 2	-1.27	2.94e-04	4.86e-02
A_52_P384574	Stard4	StAR-related lipid transfer (START) domain containing 4	1.23	3.02e-04	4.92e-02
A_52_P598309	Zfas1	zinc finger, NFX1-type containing 1, antisense RNA 1	-1.17	3.07e-04	4.92e-02
A_52_P119997	Rhbdd1	rhomboid domain containing 1	-1.12	3.12e-04	4.92e-02
A_51_P424709	Nxph4	neurexophilin 4	0.93	3.13e-04	4.92e-02
A_51_P287617	Plekhh1	pleckstrin homology domain containing, family H (with MyTH4 domain) member 1	1.86	3.13e-04	4.92e-02
A_51_P325173	Tpm1	tropomyosin 1, alpha	0.92	3.14e-04	4.92e-02
A_51_P329928	Phlda3	pleckstrin homology like domain, family A, member 3	-1.33	3.19e-04	4.93e-02
A_52_P690855	Fndc11	fibronectin type III domain containing 11	1.31	3.20e-04	4.93e-02
A_51_P257282	Ttll7	tubulin tyrosine ligase-like family, member 7	1.07	3.24e-04	4.96e-02
A_51_P206585	Runx1	runt related transcription factor 1	-1.06	3.28e-04	4.97e-02
A_52_P493477	Serpinb1c	serine (or cysteine) peptidase inhibitor, clade B, member 1c	0.90	3.34e-04	4.97e-02
A_52_P7041	Odc1	ornithine decarboxylase, structural 1	-0.92	3.34e-04	4.97e-02
A_51_P486971	Tex52	testis expressed 52	0.91	3.35e-04	4.97e-02
A_51_P185575	Adamtsl4	ADAMTS-like 4	0.92	3.38e-04	4.97e-02
A_51_P308290	Cerox1	cytoplasmic endogenous regulator of oxidative phosphorylation 1	0.66	3.44e-04	4.97e-02
A_51_P484869	Gamt	guanidinoacetate methyltransferase	2.33	3.44e-04	4.97e-02
A_52_P198435	Rasgrp3	RAS, guanyl releasing protein 3	1.08	3.48e-04	4.97e-02
A_51_P308298	MyI9	myosin, light polypeptide 9, regulatory	-1.26	3.49e-04	4.97e-02
A_52_P121675	Cebpg	CCAAT/enhancer binding protein (C/EBP), gamma	-1.13	3.49e-04	4.97e-02
A_52_P31814	1110038B12Rik	RIKEN cDNA 1110038B12 gene	-1.36	3.53e-04	4.97e-02
A_52_P335478	Pole4	polymerase (DNA-directed), epsilon 4 (p12 subunit)	-0.95	3.58e-04	4.97e-02
A_52_P63553	Cebpb	CCAAT/enhancer binding protein (C/EBP), beta	-1.33	3.59e-04	4.97e-02
A_52_P485007	Abca2	ATP-binding cassette, sub-family A (ABC1), member 2	1.57	3.63e-04	4.97e-02
A_51_P255832	Omg	oligodendrocyte myelin glycoprotein	0.92	3.63e-04	4.97e-02
A_51_P432380	Aplp1	amyloid beta (A4) precursor-like protein 1	1.21	3.68e-04	4.97e-02
A_51_P398260	Tppp	tubulin polymerization promoting protein	0.94	3.68e-04	4.97e-02
A_52_P517683	Tagln	transgelin	-1.76	3.73e-04	4.97e-02
A_51_P282896	Mast4	microtubule associated serine/threonine	1.53	3.75e-04	4.97e-02

		kinase family member 4			
A_51_P105927	Ras12	RAS-like, family 12	0.89	3.77e-04	4.97e-02
A_51_P212057	Serpinb1c	serine (or cysteine) peptidase inhibitor, clade B, member 1c	1.65	3.77e-04	4.97e-02

Supplementary Table 4. DEGs identified in the microglia obtained from mice treated with cuprizone for 4 weeks compared with microglia obtained from control mice.

ProbeID	Symbol	Gene name	Log2 fold change	p-value	Adjusted p-value
10583056	Mmp12	matrix metalloproteinase 12	2.63	3.14E-07	5.52E-03
10414360	Lgals3	lectin, galactose binding, soluble 3	2.15	6.23E-07	5.52E-03
10526853	Fam20c	family with sequence similarity 20, member C	2.22	5.16E-06	2.73E-02
10371770	Gas2l3	growth arrest-specific 2 like 3	1.54	6.17E-06	2.73E-02
10357472	Cxcr4	chemokine (C-X-C motif) receptor 4	1.35	8.77E-06	3.11E-02
10517336	Clic4	chloride intracellular channel 4 (mitochondrial)	1.13	1.19E-05	3.43E-02
10548375	Clec7a	C-type lectin domain family 7, member a	2.47	1.44E-05	3.43E-02
10572130	Lpl	lipoprotein lipase	3.04	1.55E-05	3.43E-02
10548333	Cd69	CD69 antigen	1.27	1.82E-05	3.58E-02
10557895	Itgax	integrin alpha X	2.74	2.52E-05	4.34E-02
10249661	Rab7b	RAB7B, member RAS oncogene family	1.33	2.78E-05	4.34E-02
10548385	Olr1	oxidized low density lipoprotein (lectin-like) receptor 1	1.83	2.94E-05	4.34E-02

Supplementary Table 5. DEGs identified in the OPCs obtained from mice treated with cuprizone for 4 weeks compared with OPCs obtained from control mice. Due to the large number of DEGs only those with an adjusted p-value<0.001 are presented.

ProbeID	Symbol	Gene name	Log2 fold change	p-value	Adjusted p-value
A_55_P1986296	Tagln2	Mus musculus transgelin 2 (Tagln2), mRNA [NM_178598]	5.16	1.79e-12	5.74e-08
A_55_P2105858	Atf5	Mus musculus activating transcription factor 5 (Atf5), transcript variant 1, mRNA [NM_030693]	3.27	2.35e-11	3.76e-07
A_66_P106661	Slc7a1	Mus musculus solute carrier family 7 (cationic amino acid transporter, y+ system), member 1 (Slc7a1), mRNA [NM_007513]	4.35	3.56e-11	3.80e-07
A_51_P241995	Col5a3	Mus musculus collagen, type V, alpha 3 (Col5a3), mRNA [NM_016919]	4.25	1.43e-10	1.15e-06
A_52_P1197913	Gadd45b	Mus musculus growth arrest and DNA-damage-inducible 45 beta (Gadd45b), mRNA [NM_008655]	3.67	2.49e-10	1.60e-06
A_51_P363947	Cdkn1a	Mus musculus cyclin-dependent kinase inhibitor 1A (P21) (Cdkn1a), transcript variant 1, mRNA [NM_007669]	5.83	4.29e-10	2.29e-06
A_66_P111562	Ccnd1	Mus musculus cyclin D1 (Ccnd1), mRNA [NM_007631]	3.40	5.58e-10	2.38e-06
A_55_P2009988	Trib3	Mus musculus tribbles homolog 3 (Drosophila) (Trib3), mRNA [NM_175093]	7.23	5.93e-10	2.38e-06
A_55_P2136880	Ppp1r15a	Mus musculus protein phosphatase 1, regulatory (inhibitor) subunit 15A (Ppp1r15a), mRNA [NM_008654]	2.96	7.51e-10	2.67e-06
A_51_P367866	Egr1	Mus musculus early growth response 1 (Egr1), mRNA [NM_007913]	2.49	9.52e-10	3.05e-06
A_51_P519251	Nupr1	Mus musculus nuclear protein 1 (Nupr1), mRNA [NM_019738]	4.86	1.13e-09	3.22e-06
A_51_P403536	Ltbp4	Mus musculus latent transforming growth factor beta binding protein 4 (Ltbp4), transcript variant 1, mRNA [NM_175641]	2.73	1.21e-09	3.22e-06

A_51_P248122	Bbc3	Mus musculus BCL2 binding component 3 (Bbc3), mRNA [NM_133234]	2.91	1.48e-09	3.64e-06
A_55_P2113051	Fosb	Mus musculus FBJ osteosarcoma oncogene B (Fosb), mRNA [NM_008036]	2.54	3.51e-09	6.85e-06
A_55_P2034864	Tubb2b	Mus musculus tubulin, beta 2B (Tubb2b), mRNA [NM_023716]	2.92	3.64e-09	6.85e-06
A_51_P474459	Socs3	Mus musculus suppressor of cytokine signaling 3 (Socs3), mRNA [NM_007707]	3.16	3.85e-09	6.85e-06
A_51_P392687	Vim	Mus musculus vimentin (Vim), mRNA [NM_011701]	3.44	3.21e-09	6.85e-06
A_55_P2121608	Sox4	Transcription factor SOX-4 [Source:UniProtKB/Swiss-Prot;Acc:Q06831] [ENSMUST00000067230]	3.21	3.84e-09	6.85e-06
A_55_P2162204	Kctd15	Mus musculus potassium channel tetramerisation domain containing 15 (Kctd15), mRNA [NM_146188]	2.95	5.25e-09	8.85e-06
A_51_P315904	Gadd45g	Mus musculus growth arrest and DNA-damage-inducible 45 gamma (Gadd45g), mRNA [NM_011817]	4.09	6.27e-09	1.01e-05
A_51_P131408	Tnfrsf12a	Mus musculus tumor necrosis factor receptor superfamily, member 12a (Tnfrsf12a), transcript variant 1, mRNA [NM_013749]	3.42	6.65e-09	1.01e-05
A_55_P1959748	Asns	Mus musculus asparagine synthetase (Asns), mRNA [NM_012055]	4.47	7.35e-09	1.07e-05
A_55_P2127139	Hist1h3d	Mus musculus histone cluster 1, H3d (Hist1h3d), mRNA [NM_178204]	1.78	8.52e-09	1.19e-05
A_55_P2122020	Klf4	Mus musculus Kruppel-like factor 4 (gut) (Klf4), mRNA [NM_010637]	3.07	9.31e-09	1.24e-05
A_51_P394190	Lmo4	Mus musculus LIM domain only 4 (Lmo4), transcript variant 1, mRNA [NM_010723]	2.61	1.06e-08	1.35e-05
A_51_P490023	Tubb2a	Mus musculus tubulin, beta 2A (Tubb2a), mRNA [NM_009450]	2.52	1.10e-08	1.35e-05
A_51_P483118	Hmga1	Mus musculus high mobility group AT-hook 1 (Hmga1), transcript variant 1, mRNA [NM_016660]	2.66	1.20e-08	1.43e-05
A_51_P206405	Ptprz1	Mus musculus protein tyrosine phosphatase, receptor type Z, polypeptide 1 (Ptprz1), mRNA [NM_001081306]	2.62	1.41e-08	1.52e-05
A_55_P2076273	Gm12260	PREDICTED: Mus musculus similar to histone H3 (LOC382523), mRNA [XM_905850]	2.01	1.46e-08	1.52e-05
A_55_P2162910	Rtn1	Mus musculus reticulon 1 (Rtn1), transcript variant 1, mRNA [NM_153457]	3.15	1.47e-08	1.52e-05
A_55_P1955869	Gm9315	PREDICTED: Mus musculus predicted gene, EG668714 (EG668714), mRNA [XM_001003263]	-3.25	1.69e-08	1.64e-05
A_51_P352968	Marcks	Mus musculus myristoylated alanine rich protein kinase C substrate (Marcks), mRNA [NM_008538]	3.84	1.79e-08	1.68e-05
A_55_P2035320	Nfil3	Mus musculus nuclear factor, interleukin 3, regulated (Nfil3), mRNA [NM_017373]	2.10	1.86e-08	1.70e-05
A_55_P1964960	Il33	Mus musculus interleukin 33 (Il33), transcript variant 1, mRNA [NM_001164724]	-1.81	2.24e-08	1.99e-05
A_55_P2141860	Aen	Mus musculus apoptosis enhancing nuclease (Aen), transcript variant 1, mRNA [NM_026531]	2.47	2.59e-08	2.24e-05
A_55_P2003541	Nrcam	Mus musculus neuron-glia-CAM-related cell adhesion molecule (Nrcam),	2.55	2.81e-08	2.35e-05

		transcript variant 1, mRNA [NM_176930]			
A_51_P258690	Scrg1	Mus musculus scrapie responsive gene 1 (Scrg1), mRNA [NM_009136]	2.72	2.86e-08	2.35e-05
A_55_P2006008	Serpinb1a	Mus musculus serine (or cysteine) peptidase inhibitor, clade B, member 1a (Serpinb1a), mRNA [NM_025429]	-1.88	3.04e-08	2.43e-05
A_55_P1971599	Bcan	Mus musculus brevican (Bcan), transcript variant 1, mRNA [NM_007529]	3.27	3.35e-08	2.54e-05
A_51_P314397	Crip2	Mus musculus cysteine rich protein 2 (Crip2), mRNA [NM_024223]	2.10	3.41e-08	2.54e-05
A_52_P76034	Rcc2	Mus musculus regulator of chromosome condensation 2 (Rcc2), mRNA [NM_173867]	2.24	3.57e-08	2.60e-05
A_55_P1959485	LOC634933	PREDICTED: Mus musculus similar to protein phosphatase 1, catalytic subunit (LOC634933), mRNA [XM_909811]	-2.90	3.81e-08	2.68e-05
A_51_P439612	Dnajb2	Mus musculus Dnaj (Hsp40) homolog, subfamily B, member 2 (Dnajb2), transcript variant 1, mRNA [NM_020266]	-1.85	3.85e-08	2.68e-05
A_55_P2080860	Cmtm5	Mus musculus CKLF-like MARVEL transmembrane domain containing 5 (Cmtm5), mRNA [NM_026066]	-1.96	3.94e-08	2.68e-05
A_51_P501844	Cyp26b1	Mus musculus cytochrome P450, family 26, subfamily b, polypeptide 1 (Cyp26b1), mRNA [NM_175475]	2.50	4.13e-08	2.75e-05
A_66_P129048	2610002J02Rik	Mus musculus RIKEN cDNA 2610002J02 gene (2610002J02Rik), mRNA [NM_001033134]	1.98	4.86e-08	3.18e-05
A_52_P262219	Fos	Mus musculus FBJ osteosarcoma oncogene (Fos), mRNA [NM_010234]	2.36	4.97e-08	3.19e-05
A_52_P665675	Abca1	Mus musculus ATP-binding cassette, sub-family A (ABC1), member 1 (Abca1), mRNA [NM_013454]	2.24	5.28e-08	3.26e-05
A_55_P2117710	Snhg1	Mus musculus small nucleolar RNA host gene (non-protein coding) 1 (Snhg1), non-coding RNA [NR_002896]	1.93	5.34e-08	3.26e-05
A_66_P105032	Gm13889	Mus musculus predicted gene 13889 (Gm13889), mRNA [NM_001145034]	2.15	5.74e-08	3.38e-05
A_55_P2008061	Itp2	Mus musculus inositol 1,4,5-triphosphate receptor 2 (Itp2), transcript variant 1, mRNA [NM_019923]	2.36	5.80e-08	3.38e-05
A_55_P2098598	Btg1	Mus musculus B-cell translocation gene 1, anti-proliferative (Btg1), mRNA [NM_007569]	3.03	6.03e-08	3.45e-05
A_51_P242414	Mical1	Mus musculus microtubule associated monooxygenase, calponin and LIM domain containing -like 1 (Mical1), mRNA [NM_177461]	-1.59	6.50e-08	3.65e-05
A_51_P398260	Tppp	Mus musculus tubulin polymerization promoting protein (Tppp), mRNA [NM_182839]	-1.53	6.77e-08	3.74e-05
A_55_P2024704	Cpe	Mus musculus carboxypeptidase E (Cpe), mRNA [NM_013494]	1.88	6.99e-08	3.80e-05
A_51_P198434	H2-K1	Mus musculus histocompatibility 2, K1, K region (H2-K1), transcript variant 1, mRNA [NM_001001892]	2.11	7.26e-08	3.87e-05
A_55_P1986998	Enoph1	Mus musculus enolase-phosphatase 1 (Enoph1), transcript variant 1, mRNA [NM_026421]	-1.63	7.37e-08	3.87e-05
A_51_P355151	Camk2n2	Mus musculus calcium/calmodulin-dependent protein kinase II inhibitor 2 (Camk2n2), mRNA [NM_028420]	2.32	8.05e-08	4.11e-05
A_65_P19395	H2-D1	Mus musculus histocompatibility 2, D region locus 1 (H2-D1), mRNA	2.84	8.08e-08	4.11e-05

A_55_P2042923	Sgk2	[NM_010380] Mus musculus serum/glucocorticoid regulated kinase 2 (Sgk2), mRNA [NM_013731]	-2.66	9.13e-08	4.47e-05
A_52_P439263	Ugt8a	Mus musculus UDP galactosyltransferase 8A (Ugt8a), mRNA [NM_011674]	-1.83	9.19e-08	4.47e-05
A_55_P2047559	6330503K22Rik	Mus musculus RIKEN cDNA 6330503K22 gene (6330503K22Rik), mRNA [NM_182995]	-1.97	9.22e-08	4.47e-05
A_55_P2072373	Msn	Mus musculus moesin (Msn), mRNA [NM_010833]	2.27	9.44e-08	4.51e-05
A_51_P170463	Gpr17	Mus musculus G protein-coupled receptor 17 (Gpr17), mRNA [NM_001025381]	2.93	9.61e-08	4.53e-05
A_55_P2059164	H3f3b	Mus musculus H3 histone, family 3B (H3f3b), mRNA [NM_008211]	1.49	1.01e-07	4.55e-05
A_66_P134542	Anln	Mus musculus anillin, actin binding protein (Anln), mRNA [NM_028390]	-1.82	1.01e-07	4.55e-05
A_55_P1972575	Tmeff1	Mus musculus transmembrane protein with EGF-like and two follistatin-like domains 1 (Tmeff1), mRNA [NM_021436]	-1.77	1.02e-07	4.55e-05
A_55_P2130388	Mical1	Mus musculus microtubule associated monooxygenase, calponin and LIM domain containing 1 (Mical1), transcript variant 1, mRNA [NM_138315]	2.04	1.00e-07	4.55e-05
A_55_P2075070	S1pr5	Mus musculus sphingosine-1-phosphate receptor 5 (S1pr5), mRNA [NM_053190]	-1.79	1.13e-07	4.91e-05
A_51_P472901	Slc3a2	Mus musculus solute carrier family 3 (activators of dibasic and neutral amino acid transport), member 2 (Slc3a2), transcript variant 2, mRNA [NM_008577]	1.76	1.25e-07	5.35e-05
A_55_P2002578	Ephx1	Mus musculus epoxide hydrolase 1, microsomal (Ephx1), mRNA [NM_010145]	2.66	1.30e-07	5.48e-05
A_66_P111430	2410006H16Rik	Mus musculus RIKEN cDNA 2410006H16 gene (2410006H16Rik), non-coding RNA [NR_030738]	2.56	1.34e-07	5.48e-05
A_51_P269084	Chchd10	Mus musculus coiled-coil-helix-coiled-coil-helix domain containing 10 (Chchd10), mRNA [NM_175329]	2.85	1.35e-07	5.48e-05
A_51_P502614	Dusp6	Mus musculus dual specificity phosphatase 6 (Dusp6), mRNA [NM_026268]	2.49	1.35e-07	5.48e-05
A_55_P2136501	Midn	Mus musculus midnolin (Midn), mRNA [NM_021565]	2.56	1.43e-07	5.53e-05
A_55_P2126448	1810032O08Rik	Mus musculus RIKEN cDNA 1810032O08 gene (1810032O08Rik), transcript variant 3, non-coding RNA [NR_027821]	1.93	1.45e-07	5.53e-05
A_55_P2066697	Trim47	Mus musculus tripartite motif-containing 47 (Trim47), mRNA [NM_172570]	2.15	1.42e-07	5.53e-05
A_55_P2345853	3830612M24	Mus musculus 18 days pregnant adult female placenta and extra embryonic tissue cDNA, RIKEN full-length enriched library, clone:3830612M24 product:unclassifiable, full insert sequence. [AK028406]	2.88	1.43e-07	5.53e-05
A_51_P106059	Traf4	Mus musculus TNF receptor associated factor 4 (Traf4), mRNA [NM_009423]	2.47	1.44e-07	5.53e-05
A_51_P451346	Klf6	Mus musculus Kruppel-like factor 6 (Klf6), mRNA [NM_011803]	1.65	1.51e-07	5.71e-05
A_55_P2006525	Adamts14	Mus musculus ADAMTS-like 4 (Adamts14), mRNA [NM_144899]	-2.48	1.59e-07	5.90e-05
A_55_P1983999	Pppde2	Mus musculus PPPDE peptidase domain containing 2 (Pppde2), mRNA	-2.17	1.60e-07	5.90e-05

A_52_P137765	Lmna	[NM_134095] Mus musculus lamin A (Lmna), transcript variant 2, mRNA [NM_019390]	1.91	1.64e-07	5.90e-05
A_52_P598309	1500012F01Rik	Mus musculus RIKEN cDNA 1500012F01 gene (1500012F01Rik), mRNA [NM_001081005]	1.68	1.65e-07	5.90e-05
A_55_P2078633	C4b	Mus musculus complement component 4B (Childo blood group) (C4b), mRNA [NM_009780]	2.09	1.66e-07	5.90e-05
A_52_P497188	Prrg1	Mus musculus proline rich Gla (G-carboxyglutamic acid) 1 (Prrg1), transcript variant 1, mRNA [NM_027322]	-1.95	1.68e-07	5.90e-05
A_55_P2117119	Efhf1	Mus musculus EF hand domain containing 1 (Efhf1), mRNA [NM_028889]	-1.93	1.75e-07	6.08e-05
A_66_P126332	Zfp703	Mus musculus zinc finger protein 703 (Zfp703), transcript variant 2, mRNA [NM_001110508]	2.88	1.79e-07	6.17e-05
A_51_P409429	Aars	Mus musculus alanyl-tRNA synthetase (Aars), mRNA [NM_146217]	1.83	1.82e-07	6.22e-05
A_51_P200561	4930506M07Rik	Mus musculus RIKEN cDNA 4930506M07 gene (4930506M07Rik), transcript variant 2, mRNA [NM_175172]	-2.42	2.15e-07	7.10e-05
A_52_P533146	Ddit3	Mus musculus DNA-damage inducible transcript 3 (Ddit3), mRNA [NM_007837]	2.26	2.15e-07	7.10e-05
A_55_P2150757	Gzmm	Mus musculus granzyme M (lymphocyte met-ase 1) (Gzmm), mRNA [NM_008504]	1.78	2.35e-07	7.67e-05
A_52_P452689	Atf3	Mus musculus activating transcription factor 3 (Atf3), mRNA [NM_007498]	2.99	2.45e-07	7.92e-05
A_55_P2083889	Pea15a	Mus musculus phosphoprotein enriched in astrocytes 15A (Pea15a), transcript variant 2, mRNA [NM_011063]	-1.57	2.48e-07	7.92e-05
A_55_P2012389	Sfxn3	Mus musculus sideroflexin 3 (Sfxn3), mRNA [NM_053197]	1.61	2.50e-07	7.92e-05
A_51_P225793	Prr5l	Mus musculus proline rich 5 like (Prr5l), transcript variant 2, mRNA [NM_175181]	-1.10	2.57e-07	8.06e-05
A_51_P140690	Stmn3	Mus musculus stathmin-like 3 (Stmn3), mRNA [NM_009133]	2.06	2.69e-07	8.38e-05
A_55_P2091359	Padi2	Mus musculus peptidyl arginine deiminase, type II (Padi2), mRNA [NM_008812]	-1.75	2.74e-07	8.42e-05
A_55_P2142072	Synj2	Mus musculus synaptojanin 2 (Synj2), transcript variant 3, mRNA [NM_011523]	-2.01	2.76e-07	8.42e-05
A_55_P2017645	Tap2	Mus musculus transporter 2, ATP-binding cassette, sub-family B (MDR/TAP) (Tap2), mRNA [NM_011530]	2.09	3.10e-07	9.37e-05
A_51_P129012	B2m	Mus musculus beta-2 microglobulin (B2m), mRNA [NM_009735]	2.18	3.14e-07	9.39e-05
A_55_P1955393	Sept7	Mus musculus septin 7 (Sept7), mRNA [NM_009859]	-1.23	3.30e-07	9.61e-05
A_55_P2033376	1810041L15Rik	Mus musculus RIKEN cDNA 1810041L15 gene (1810041L15Rik), mRNA [NM_001163145]	2.79	3.38e-07	9.76e-05
A_55_P2149931	Arap2	Mus musculus ArfGAP with RhoGAP domain, ankyrin repeat and PH domain 2 (Arap2), mRNA [NM_178407]	1.73	3.54e-07	1.00e-04
A_66_P135106	Slco3a1	Mus musculus solute carrier organic anion transporter family, member 3a1 (Slco3a1), transcript variant 2, mRNA	-1.58	3.59e-07	1.00e-04

		[NM_001038643]			
A_55_P2033362	Egr2	Mus musculus early growth response 2 (Egr2), mRNA [NM_010118]	2.47	3.64e-07	1.00e-04
A_55_P1958678	Brd2	Mus musculus bromodomain containing 2 (Brd2), transcript variant 2, mRNA [NM_001025387]	1.30	3.64e-07	1.00e-04
A_51_P110759	Slc1a1	Mus musculus solute carrier family 1 (neuronal/epithelial high affinity glutamate transporter, system Xag), member 1 (Slc1a1), mRNA [NM_009199]	2.43	3.65e-07	1.00e-04
A_51_P493987	Moxd1	Mus musculus monooxygenase, DBH-like 1 (Moxd1), mRNA [NM_021509]	4.18	3.58e-07	1.00e-04
A_55_P1961461	Bnip3l	Mus musculus BCL2/adenovirus E1B interacting protein 3-like (Bnip3l), mRNA [NM_009761]	-1.14	3.69e-07	1.00e-04
A_55_P1960097	Epb4.113	Mus musculus erythrocyte protein band 4.1-like 3 (Epb4.113), mRNA [NM_013813]	-1.74	4.05e-07	1.08e-04
A_51_P246317	Mt2	Mus musculus metallothionein 2 (Mt2), mRNA [NM_008630]	3.35	4.37e-07	1.15e-04
A_55_P2067942	D16Ert472e	Mus musculus DNA segment, Chr 16, ERATO Doi 472, expressed (D16Ert472e), mRNA [NM_025967]	-1.33	4.61e-07	1.19e-04
A_55_P2032966	Hmgcs1	Mus musculus 3-hydroxy-3-methylglutaryl-Coenzyme A synthase 1 (Hmgcs1), mRNA [NM_145942]	-1.74	4.75e-07	1.22e-04
A_55_P2108988	Kcnip3	Mus musculus Kv channel interacting protein 3, calsenilin (Kcnip3), transcript variant 2, mRNA [NM_001111331]	2.78	4.89e-07	1.23e-04
A_55_P2118268	Chpf	Mus musculus chondroitin polymerizing factor (Chpf), transcript variant 2, mRNA [NM_001001565]	1.59	4.93e-07	1.23e-04
A_51_P330428	Eif4ebp1	Mus musculus eukaryotic translation initiation factor 4E binding protein 1 (Eif4ebp1), mRNA [NM_007918]	3.88	4.94e-07	1.23e-04
A_55_P2101088	Slc5a11	Mus musculus solute carrier family 5 (sodium/glucose cotransporter), member 11 (Slc5a11), mRNA [NM_146198]	-1.96	5.27e-07	1.29e-04
A_51_P507053	Slc38a1	Mus musculus solute carrier family 38, member 1 (Slc38a1), transcript variant 1, mRNA [NM_134086]	2.12	5.50e-07	1.33e-04
A_52_P590396	Sort1	Mus musculus sortilin 1 (Sort1), mRNA [NM_019972]	-1.43	5.55e-07	1.34e-04
A_51_P259975	Aspa	Mus musculus aspartoacylase (Aspa), mRNA [NM_023113]	-1.49	5.68e-07	1.34e-04
A_55_P1998651	Entpd5	Mus musculus ectionucleoside triphosphate diphosphohydrolase 5 (Entpd5), transcript variant 2, mRNA [NM_001026214]	-1.66	5.67e-07	1.34e-04
A_55_P2227321	Ptprd	Mus musculus protein tyrosine phosphatase, receptor type, D (Ptprd), transcript variant b, mRNA [NM_011211]	-2.27	5.68e-07	1.34e-04
A_55_P1978511	H2-Q7	Mus musculus histocompatibility 2, Q region locus 7 (H2-Q7), mRNA [NM_010394]	2.33	6.04e-07	1.39e-04
A_55_P2051334	Gm7035	Mus musculus predicted gene 7035 (Gm7035), non-coding RNA [NR_004446]	1.51	6.26e-07	1.43e-04
A_55_P2045802	Nelf	Mus musculus nasal embryonic LHRH factor (Nelf), transcript variant 1, mRNA [NM_001039386]	-1.15	7.13e-07	1.61e-04
A_55_P1985793	Dock6	Mus musculus dedicator of cytokinesis 6 (Dock6), mRNA [NM_177030]	1.59	7.26e-07	1.62e-04
A_55_P2165869	Cebpb	Mus musculus CCAAT/enhancer binding	2.33	7.27e-07	1.62e-04

		protein (C/EBP), beta (Cebpb), mRNA [NM_009883]			
A_51_P464300	Gdf1	Mus musculus growth differentiation factor 1 (Gdf1), transcript variant 2, mRNA [NM_008107]	1.61	7.42e-07	1.64e-04
A_51_P426739	Gpt	Mus musculus glutamic pyruvic transaminase, soluble (Gpt), mRNA [NM_182805]	-1.77	7.75e-07	1.70e-04
A_55_P2018847	Crif2	Mus musculus cytokine receptor-like factor 2 (Crif2), transcript variant 1, mRNA [NM_001164735]	1.81	7.87e-07	1.72e-04
A_66_P100249	Snhg12	Mus musculus small nucleolar RNA host gene 12 (Snhg12), non-coding RNA [NR_029468]	1.80	8.03e-07	1.74e-04
A_52_P373694	Jph4	Mus musculus junctophilin 4 (Jph4), transcript variant a, mRNA [NM_177049]	-3.81	8.19e-07	1.76e-04
A_51_P237754	H2-T23	Mus musculus histocompatibility 2, T region locus 23 (H2-T23), mRNA [NM_010398]	1.92	8.49e-07	1.81e-04
A_55_P1999361	Dip2a	Mus musculus DIP2 disco-interacting protein 2 homolog A (Drosophila) (Dip2a), mRNA [NM_001081419]	-1.40	8.52e-07	1.81e-04
A_51_P172344	Foxn3	Mus musculus forkhead box N3 (Foxn3), mRNA [NM_183186]	-1.41	8.97e-07	1.89e-04
A_55_P1971963	Tmem176b	Mus musculus transmembrane protein 176B (Tmem176b), transcript variant 1, mRNA [NM_023056]	2.76	9.23e-07	1.93e-04
A_66_P121369	Gars	Mus musculus glycyl-tRNA synthetase (Gars), mRNA [NM_180678]	1.05	9.83e-07	2.05e-04
A_51_P358354	Jam3	Mus musculus junction adhesion molecule 3 (Jam3), mRNA [NM_023277]	-0.98	1.07e-06	2.20e-04
A_51_P520384	Atp1b3	Mus musculus ATPase, Na ⁺ /K ⁺ transporting, beta 3 polypeptide (Atp1b3), mRNA [NM_007502]	-1.27	1.07e-06	2.20e-04
A_52_P597634	Fzd1	Mus musculus frizzled homolog 1 (Drosophila) (Fzd1), mRNA [NM_021457]	2.26	1.12e-06	2.28e-04
A_55_P1960735	Gdf15	Mus musculus growth differentiation factor 15 (Gdf15), mRNA [NM_011819]	5.28	1.12e-06	2.28e-04
A_55_P1956672	Rab34	Mus musculus RAB34, member of RAS oncogene family (Rab34), transcript variant 1, mRNA [NM_033475]	1.69	1.13e-06	2.28e-04
A_55_P1989921	Eml2	Mus musculus echinoderm microtubule associated protein like 2 (Eml2), transcript variant 1, mRNA [NM_028153]	-1.66	1.19e-06	2.39e-04
A_51_P105927	Rasl12	Mus musculus RAS-like, family 12 (Rasl12), transcript variant 1, mRNA [NM_001033158]	-1.93	1.21e-06	2.40e-04
A_55_P1979684	Rhoc	Mus musculus ras homolog gene family, member C (Rhoc), mRNA [NM_007484]	1.44	1.23e-06	2.42e-04
A_55_P1996674	Itih3	Mus musculus inter-alpha trypsin inhibitor, heavy chain 3 (Itih3), mRNA [NM_008407]	-2.29	1.32e-06	2.57e-04
A_51_P122035	Nipa1	Mus musculus non imprinted in Prader-Willi/Angelman syndrome 1 homolog (human) (Nipa1), mRNA [NM_153578]	-1.76	1.31e-06	2.57e-04
A_55_P2099358	Cars	Mus musculus cysteinyl-tRNA synthetase (Cars), mRNA [NM_013742]	1.43	1.35e-06	2.60e-04
A_55_P2102515	Daam1	Mus musculus dishevelled associated activator of morphogenesis 1 (Daam1), transcript variant 1, mRNA [NM_026102]	-1.85	1.36e-06	2.60e-04
A_55_P2256163	4930506C21Rik	Mus musculus adult male testis cDNA, RIKEN full-length enriched library,	-2.15	1.43e-06	2.72e-04

		clone:4930506C21 product:unclassifiable, full insert sequence. [AK015714]			
A_51_P438841	Ctnna2	Mus musculus catenin (cadherin associated protein), alpha 2 (Ctnna2), transcript variant 2, mRNA [NM_009819]	-1.29	1.46e-06	2.76e-04
A_51_P444447	Cebpd	Mus musculus CCAAT/enhancer binding protein (C/EBP), delta (Cebpd), mRNA [NM_007679]	2.49	1.49e-06	2.77e-04
A_52_P624415	Opalin	Mus musculus oligodendrocytic myelin paranodal and inner loop protein (Opalin), mRNA [NM_153520]	-1.99	1.50e-06	2.77e-04
A_51_P492125	Ciapin1	Mus musculus cytokine induced apoptosis inhibitor 1 (Ciapin1), mRNA [NM_134141]	1.38	1.50e-06	2.77e-04
A_55_P2227355	Ptpro	Mus musculus protein tyrosine phosphatase, receptor type, O (Ptpro), transcript variant 1, mRNA [NM_011216]	1.77	1.52e-06	2.77e-04
A_55_P2030938	Trim59	Mus musculus tripartite motif-containing 59 (Trim59), mRNA [NM_025863]	-1.11	1.52e-06	2.77e-04
A_51_P296608	Gadd45a	Mus musculus growth arrest and DNA- damage-inducible 45 alpha (Gadd45a), mRNA [NM_007836]	2.07	1.53e-06	2.77e-04
A_51_P339540	Cdkn1c	Mus musculus cyclin-dependent kinase inhibitor 1C (P57) (Cdkn1c), transcript variant 2, mRNA [NM_009876]	1.62	1.58e-06	2.84e-04
A_65_P02958	Rnf13	Mus musculus ring finger protein 13 (Rnf13), transcript variant 1, mRNA [NM_001113413]	-1.09	1.62e-06	2.88e-04
A_55_P2032818	Trim2	Mus musculus tripartite motif-containing 2 (Trim2), mRNA [NM_030706]	-0.91	1.61e-06	2.88e-04
A_52_P489295	Adams1	Mus musculus a disintegrin-like and metallopeptidase (reprolysin type) with thrombospondin type 1 motif, 1 (Adams1), mRNA [NM_009621]	1.36	1.63e-06	2.88e-04
A_51_P297336	Chmp7	Mus musculus CHMP family, member 7 (Chmp7), mRNA [NM_134078]	-1.27	1.64e-06	2.89e-04
A_55_P2086128	Fa2h	Mus musculus fatty acid 2-hydroxylase (Fa2h), mRNA [NM_178086]	-1.43	1.69e-06	2.96e-04
A_51_P436817	Dos	Mus musculus downstream of Stk11 (Dos), mRNA [NM_015761]	1.52	1.80e-06	3.14e-04
A_52_P541833	Vps37b	Mus musculus vacuolar protein sorting 37B (yeast) (Vps37b), mRNA [NM_177876]	1.52	1.83e-06	3.17e-04
A_55_P2014224	Sema5a	Mus musculus sema domain, seven thrombospondin repeats (type 1 and type 1-like), transmembrane domain (TM) and short cytoplasmic domain, (semaphorin) 5A (Sema5a), mRNA [NM_009154]	2.11	1.84e-06	3.17e-04
A_55_P2040170	Pmp22	Mus musculus peripheral myelin protein 22 (Pmp22), mRNA [NM_008885]	-1.34	1.87e-06	3.20e-04
A_55_P2031496	Rufy3	Mus musculus RUN and FYVE domain containing 3 (Rufy3), mRNA [NM_027530]	-1.05	1.88e-06	3.20e-04
A_55_P2121856	Ier5l	Mus musculus immediate early response 5-like (Ier5l), mRNA [NM_030244]	2.96	1.89e-06	3.21e-04
A_51_P251352	Slc25a13	Mus musculus solute carrier family 25 (mitochondrial carrier, adenine nucleotide translocator), member 13 (Slc25a13), nuclear gene encoding mitochondrial protein, mRNA [NM_015829]	-1.83	1.93e-06	3.24e-04
A_55_P2167999	Ldlr	Mus musculus low density lipoprotein receptor (Ldlr), mRNA [NM_010700]	-1.61	2.00e-06	3.34e-04
A_55_P1977633	6430527G	Mus musculus RIKEN cDNA	1.53	2.08e-06	3.45e-04

	18Rik	6430527G18 gene (6430527G18Rik), mRNA [NM_145836]			
A_51_P463765	Timp3	Mus musculus tissue inhibitor of metalloproteinase 3 (Timp3), mRNA [NM_011595]	2.30	2.09e-06	3.45e-04
A_55_P2094896	Phyh1	Mus musculus phytanoyl-CoA dioxygenase domain containing 1 (Phyh1), mRNA [NM_172267]	2.29	2.11e-06	3.47e-04
A_66_P105046	Il18	Mus musculus interleukin 18 (Il18), mRNA [NM_008360]	-1.21	2.13e-06	3.48e-04
A_55_P1961863	Pcdhga9	Mus musculus protocadherin gamma subfamily A, 9 (Pcdhga9), mRNA [NM_033592]	1.25	2.17e-06	3.53e-04
A_55_P2058942	Aldh3b1	Mus musculus aldehyde dehydrogenase 3 family, member B1 (Aldh3b1), mRNA [NM_026316]	-1.37	2.20e-06	3.57e-04
A_55_P1979575	Shroom2	Mus musculus shroom family member 2 (Shroom2), mRNA [NM_172441]	-1.24	2.24e-06	3.57e-04
A_55_P1956130	LOC68395	PREDICTED: Mus musculus RIKEN cDNA 0610037M15 gene, transcript variant 2 (0610037M15Rik), mRNA [XM_903697]	2.30	2.24e-06	3.57e-04
A_51_P161354	Sesn2	Mus musculus sestrin 2 (Sesn2), mRNA [NM_144907]	1.34	2.25e-06	3.57e-04
A_51_P134812	Chac1	Mus musculus ChaC, cation transport regulator-like 1 (E. coli) (Chac1), mRNA [NM_026929]	3.98	2.23e-06	3.57e-04
A_66_P138915	Fyn	Mus musculus Fyn proto-oncogene (Fyn), transcript variant 1, mRNA [NM_001122893]	1.63	2.32e-06	3.65e-04
A_51_P436878	Sertad1	Mus musculus SERTA domain containing 1 (Sertad1), mRNA [NM_018820]	2.02	2.37e-06	3.69e-04
A_55_P2063266	Piga	Mus musculus phosphatidylinositol glycan anchor biosynthesis, class A (Piga), mRNA [NM_011081]	-1.72	2.38e-06	3.69e-04
A_66_P127969	Bcat1	Mus musculus branched chain aminotransferase 1, cytosolic (Bcat1), transcript variant 2, mRNA [NM_007532]	1.47	2.40e-06	3.70e-04
A_55_P1987839	Erb2ip	Mus musculus ErbB2 interacting protein (Erb2ip), transcript variant 1, mRNA [NM_001005868]	-1.28	2.44e-06	3.72e-04
A_51_P323620	Thyn1	Mus musculus thymocyte nuclear protein 1 (Thyn1), mRNA [NM_144543]	1.09	2.44e-06	3.72e-04
A_55_P1960351	Cntn1	Mus musculus contactin 1 (Cntn1), transcript variant 1, mRNA [NM_001159647]	1.33	2.51e-06	3.80e-04
A_55_P1983209	Rcctb1	Mus musculus regulator of chromosome condensation (RCC1) and BTB (POZ) domain containing protein 1 (Rcctb1), mRNA [NM_027764]	-1.34	2.52e-06	3.80e-04
A_55_P2043122	Arsg	Mus musculus arylsulfatase G (Arsg), transcript variant 1, mRNA [NM_028710]	-0.95	2.52e-06	3.80e-04
A_55_P1970033	Per1	Mus musculus period homolog 1 (Drosophila) (Per1), transcript variant 1, mRNA [NM_011065]	2.21	2.56e-06	3.84e-04
A_55_P2121352	Cdk5	Mus musculus cyclin-dependent kinase 5 (Cdk5), mRNA [NM_007668]	-2.21	2.57e-06	3.84e-04
A_51_P242166	Lap3	Mus musculus leucine aminopeptidase 3 (Lap3), mRNA [NM_024434]	-1.06	2.60e-06	3.86e-04
A_55_P1995173	Odc1	Mus musculus ornithine decarboxylase, structural 1 (Odc1), mRNA [NM_013614]	1.65	2.65e-06	3.91e-04
A_55_P2096395	Cdc42bpa	Mus musculus CDC42 binding protein	-1.27	2.70e-06	3.98e-04

		kinase alpha (Cdc42bpa), mRNA [NM_001033285]			
A_55_P2149942	Ninj2	Mus musculus ninjurin 2 (Ninj2), mRNA [NM_016718]	-2.65	2.73e-06	4.00e-04
A_51_P494675	Cot1l	Mus musculus coactosin-like 1 (Dictyostelium) (Cot1l), mRNA [NM_028071]	2.14	2.75e-06	4.00e-04
A_55_P2146520	Atpgd1	Mus musculus ATP-grasp domain containing 1 (Atpgd1), mRNA [NM_134148]	-3.23	2.80e-06	4.04e-04
A_51_P430900	Dusp1	Mus musculus dual specificity phosphatase 1 (Dusp1), mRNA [NM_013642]	1.81	2.80e-06	4.04e-04
A_55_P2108837	Tuba1c	Mus musculus tubulin, alpha 1C (Tuba1c), mRNA [NM_009448]	2.25	2.85e-06	4.07e-04
A_55_P1969276	Hhip	Mus musculus Hedgehog-interacting protein (Hhip), mRNA [NM_020259]	-1.39	2.84e-06	4.07e-04
A_55_P1962771	Cyfp2	Mus musculus cytoplasmic FMR1 interacting protein 2 (Cyfp2), mRNA [NM_133769]	1.48	2.87e-06	4.08e-04
A_55_P2154387	Bmp4	Mus musculus bone morphogenetic protein 4 (Bmp4), mRNA [NM_007554]	2.32	2.88e-06	4.08e-04
A_51_P348397	Hexim1	Mus musculus hexamethylene bis-acetamide inducible 1 (Hexim1), mRNA [NM_138753]	1.55	2.94e-06	4.13e-04
A_55_P2070347	Rps2	Mus musculus ribosomal protein S2 (Rps2), mRNA [NM_008503]	0.96	3.02e-06	4.22e-04
A_55_P2139027	Plec1	Mus musculus plectin 1 (Plec1), transcript variant 13, mRNA [NM_001163540]	2.19	3.09e-06	4.26e-04
A_52_P184149	Mthfd2	Mus musculus methylenetetrahydrofolate dehydrogenase (NAD+ dependent), methylenetetrahydrofolate cyclohydrolase (Mthfd2), nuclear gene encoding mitochondrial protein, mRNA [NM_008638]	1.50	3.07e-06	4.26e-04
A_51_P184728	Cnksr3	Mus musculus Cnksr family member 3 (Cnksr3), mRNA [NM_172546]	1.79	3.10e-06	4.26e-04
A_55_P2111855	Gale	Mus musculus galactose-4-epimerase, UDP (Gale), mRNA [NM_178389]	1.37	3.09e-06	4.26e-04
A_55_P2032558	Gm7159	PREDICTED: Mus musculus predicted gene, EG635497 (EG635497), misc RNA [XR_002030]	1.19	3.13e-06	4.26e-04
A_55_P1987730	5730469M10Rik	Mus musculus RIKEN cDNA 5730469M10 gene (5730469M10Rik), mRNA [NM_027464]	-1.59	3.13e-06	4.26e-04
A_55_P1999349	Nudt4	Mus musculus nudix (nucleoside diphosphate linked moiety X)-type motif 4 (Nudt4), mRNA [NM_027722]	-1.40	3.14e-06	4.26e-04
A_55_P2147736	Dpysl4	Mus musculus dihydropyrimidinase-like 4 (Dpysl4), mRNA [NM_011993]	2.78	3.16e-06	4.28e-04
A_55_P2135331	Evl	Mus musculus Ena-vasodilator stimulated phosphoprotein (Evl), transcript variant 1, mRNA [NM_001163394]	1.41	3.29e-06	4.41e-04
A_55_P2374381	A230001M10Rik	Mus musculus adult male hypothalamus cDNA, RIKEN full-length enriched library, clone:A230012K17 product:unclassifiable, full insert sequence. [AK038444]	-1.58	3.37e-06	4.49e-04
A_55_P2011286	Hopx	Mus musculus HOP homeobox (Hopx), transcript variant 1, mRNA [NM_175606]	-1.64	3.41e-06	4.51e-04
A_55_P2110713	Anxa2	Mus musculus annexin A2 (Anxa2), mRNA [NM_007585]	2.48	3.40e-06	4.51e-04
A_51_P279712	Rel1	Mus musculus RELT-like 1 (Rel1), mRNA [NM_145923]	1.24	3.44e-06	4.53e-04

A_55_P2023727	Limch1	Mus musculus LIM and calponin homology domains 1 (Limch1), mRNA [NM_001001980]	-1.36	3.50e-06	4.55e-04
A_55_P2123502	Jam2	Mus musculus junction adhesion molecule 2 (Jam2), mRNA [NM_023844]	1.41	3.49e-06	4.55e-04
A_66_P133413	Gm4892	PREDICTED: Mus musculus similar to QM protein (LOC638133), mRNA [XM_914040]	0.78	3.54e-06	4.59e-04
A_51_P473229	Zbtb7b	Mus musculus zinc finger and BTB domain containing 7B (Zbtb7b), mRNA [NM_009565]	1.24	3.57e-06	4.61e-04
A_55_P1984655	Smtnl2	Mus musculus smoothelin-like 2 (Smtnl2), mRNA [NM_177776]	-2.17	3.59e-06	4.61e-04
A_55_P2032727	Gm8432	PREDICTED: Mus musculus predicted gene, EG667040 (EG667040), misc RNA [XR_001962]	1.62	3.65e-06	4.68e-04
A_51_P321886	Cmtm3	Mus musculus CKLF-like MARVEL transmembrane domain containing 3 (Cmtm3), mRNA [NM_024217]	1.64	3.67e-06	4.68e-04
A_55_P1954221	Emp1	Mus musculus epithelial membrane protein 1 (Emp1), mRNA [NM_010128]	3.45	3.68e-06	4.68e-04
A_55_P2111416	LOC100047340	PREDICTED: Mus musculus hypothetical protein LOC100047340 (LOC100047340), mRNA [XM_001477942]	1.77	3.74e-06	4.68e-04
A_66_P135173	9630013A20Rik	Mus musculus RIKEN cDNA 9630013A20 gene (9630013A20Rik), non-coding RNA [NR_015539]	2.60	3.74e-06	4.68e-04
A_51_P438805	Txnip	Mus musculus thioredoxin interacting protein (Txnip), transcript variant 1, mRNA [NM_001009935]	1.58	3.71e-06	4.68e-04
A_55_P2090880	Stk40	Mus musculus serine/threonine kinase 40 (Stk40), transcript variant 1, mRNA [NM_001145827]	1.56	3.74e-06	4.68e-04
A_51_P265869	Hspa9	Mus musculus heat shock protein 9 (Hspa9), nuclear gene encoding mitochondrial protein, mRNA [NM_010481]	1.05	3.77e-06	4.70e-04
A_51_P173709	Gprc5b	Mus musculus G protein-coupled receptor, family C, group 5, member B (Gprc5b), mRNA [NM_022420]	-0.97	3.80e-06	4.72e-04
A_55_P1979252	Glod4	Mus musculus glyoxalase domain containing 4 (Glod4), mRNA [NM_026029]	-1.23	3.83e-06	4.73e-04
A_51_P480233	Nmral1	Mus musculus NmrA-like family domain containing 1 (Nmral1), mRNA [NM_026393]	-1.65	3.85e-06	4.73e-04
A_55_P2139992	Mrps18b	Mus musculus mitochondrial ribosomal protein S18B (Mrps18b), nuclear gene encoding mitochondrial protein, mRNA [NM_025878]	1.24	3.85e-06	4.73e-04
A_51_P486543	Grm3	Mus musculus glutamate receptor, metabotropic 3 (Grm3), mRNA [NM_181850]	-1.79	3.87e-06	4.73e-04
A_51_P159453	Serpina3n	Mus musculus serine (or cysteine) peptidase inhibitor, clade A, member 3N (Serpina3n), mRNA [NM_009252]	2.30	3.90e-06	4.74e-04
A_55_P2109263	Ppp1r14b	Mus musculus protein phosphatase 1, regulatory (inhibitor) subunit 14B (Ppp1r14b), mRNA [NM_008889]	1.74	3.91e-06	4.74e-04
A_55_P2069251	Prr18	Mus musculus proline rich region 18 (Prr18), transcript variant 1, mRNA [NM_178774]	-1.02	3.95e-06	4.75e-04
A_55_P2000062	Irf1	Mus musculus interferon regulatory factor 1 (Irf1), transcript variant 1, mRNA [NM_008390]	1.82	3.98e-06	4.77e-04

A_51_P368591	Tle6	Mus musculus transducin-like enhancer of split 6, homolog of Drosophila E(spl) (Tle6), mRNA [NM_053254]	1.45	3.99e-06	4.77e-04
A_51_P259571	Angptl6	Mus musculus angiopoietin-like 6 (Angptl6), mRNA [NM_145154]	1.76	4.09e-06	4.86e-04
A_51_P281089	S100a6	Mus musculus S100 calcium binding protein A6 (calcyclin) (S100a6), mRNA [NM_011313]	2.33	4.11e-06	4.87e-04
A_55_P2171116	Lgals3	Mus musculus lectin, galactose binding, soluble 3 (Lgals3), transcript variant 1, mRNA [NM_001145953]	2.76	4.16e-06	4.90e-04
A_51_P487228	B9d2	Mus musculus B9 protein domain 2 (B9d2), mRNA [NM_172148]	1.27	4.24e-06	4.96e-04
A_51_P203878	Dynll2	Mus musculus dynein light chain LC8-type 2 (Dynll2), transcript variant 1, mRNA [NM_026556]	1.28	4.29e-06	4.98e-04
A_51_P200667	Clmn	Mus musculus calmin (Clmn), transcript variant 1, mRNA [NM_053155]	-1.73	4.32e-06	4.99e-04
A_52_P540434	Ppp1cc	Mus musculus protein phosphatase 1, catalytic subunit, gamma isoform (Ppp1cc), mRNA [NM_013636]	-3.30	4.33e-06	4.99e-04
A_51_P498257	Rnf141	RING finger protein 141 (Zinc finger protein 230) [Source:UniProtKB/Swiss-Prot;Acc:Q99MB7] [ENSMUST00000106682]	-1.11	4.49e-06	5.15e-04
A_55_P2032258	Pdlim1	Mus musculus PDZ and LIM domain 1 (elfin) (Pdlim1), mRNA [NM_016861]	-1.46	4.55e-06	5.20e-04
A_55_P2144931	Gm5100	PREDICTED: Mus musculus predicted gene, EG329126 (EG329126), misc RNA [XR_001880]	1.13	4.62e-06	5.27e-04
A_52_P202142	Sv2a	Mus musculus synaptic vesicle glycoprotein 2 a (Sv2a), mRNA [NM_022030]	-1.37	4.67e-06	5.29e-04
A_55_P2060158	Ernm	Mus musculus ermin, ERM-like protein (Ernm), mRNA [NM_029972]	-1.39	4.70e-06	5.29e-04
A_55_P2106351	LOC100047749	PREDICTED: Mus musculus similar to cAMP-specific cyclic nucleotide phosphodiesterase PDE8; MMPDE8 (LOC100047749), mRNA [XM_001478817]	-1.25	4.70e-06	5.29e-04
A_55_P2086949	Cntf	Mus musculus ciliary neurotrophic factor (Cntf), mRNA [NM_170786]	1.69	4.74e-06	5.29e-04
A_55_P2065239	Gm11230	PREDICTED: Mus musculus similar to ribosomal protein (LOC100039979), mRNA [XM_001474183]	1.22	4.76e-06	5.29e-04
A_55_P2047962	Gjc2	Mus musculus gap junction protein, gamma 2 (Gjc2), transcript variant 2, mRNA [NM_175452]	-1.80	4.77e-06	5.29e-04
A_55_P2081123	Srcin1	Mus musculus SRC kinase signaling inhibitor 1 (Srcin1), mRNA [NM_018873]	-1.69	4.99e-06	5.52e-04
A_66_P100853	RP23-480B19.10	PREDICTED: Mus musculus similar to histone 2a, transcript variant 2 (Rp23-480b19.10), mRNA [XM_978341]	2.48	5.05e-06	5.56e-04
A_51_P348433	Rasal1	Mus musculus RAS protein activator like 1 (GAP1 like) (Rasal1), mRNA [NM_013832]	-2.13	5.37e-06	5.83e-04
A_55_P2035590	Gm4838	PREDICTED: Mus musculus predicted gene, EG225416 (EG225416), mRNA [XM_140295]	1.57	5.36e-06	5.83e-04
A_52_P31543	Btg2	Mus musculus B-cell translocation gene 2, anti-proliferative (Btg2), mRNA [NM_007570]	1.55	5.36e-06	5.83e-04
A_55_P2181508	Gm10653	Mus musculus predicted gene 10653 (Gm10653), non-coding RNA [NR_003965]	0.97	5.40e-06	5.83e-04

A_55_P1990919	Sepx1	Mus musculus selenoprotein X 1 (Sepx1), mRNA [NM_013759]	-1.07	5.42e-06	5.83e-04
A_55_P2095266	Gm7204	PREDICTED: Mus musculus predicted gene, EG637273, transcript variant 1 (EG637273), mRNA [XM_917437]	-1.36	5.48e-06	5.86e-04
A_55_P1972322	Btg3	Mus musculus B-cell translocation gene 3 (Btg3), mRNA [NM_009770]	1.46	5.49e-06	5.86e-04
A_55_P2141084	Odz4	Mus musculus odd Oz/ten-m homolog 4 (Drosophila) (Odz4), mRNA [NM_011858]	1.68	5.60e-06	5.97e-04
A_55_P2039284	Hspb1	Mus musculus heat shock protein 1 (Hspb1), mRNA [NM_013560]	1.62	5.66e-06	5.99e-04
A_55_P1954393	Susd4	Mus musculus sushi domain containing 4 (Susd4), mRNA [NM_144796]	1.92	5.67e-06	5.99e-04
A_55_P2095688	Sh3bp5l	Mus musculus SH3 binding domain protein 5 like (Sh3bp5l), transcript variant 1, mRNA [NM_001161338]	-1.01	5.72e-06	6.03e-04
A_51_P209372	Sc4mol	Mus musculus sterol-C4-methyl oxidase-like (Sc4mol), mRNA [NM_025436]	-1.43	5.78e-06	6.07e-04
A_55_P2042356	Rftn1	Mus musculus raftlin lipid raft linker 1 (Rftn1), mRNA [NM_181397]	-2.10	5.85e-06	6.12e-04
A_55_P2005691	Gm8420	PREDICTED: Mus musculus similar to ribosomal protein L15 (LOC667014), mRNA [XM_001473655]	0.97	5.89e-06	6.15e-04
A_51_P367060	Ifrd1	Mus musculus interferon-related developmental regulator 1 (Ifrd1), mRNA [NM_013562]	1.19	6.06e-06	6.29e-04
A_51_P368496	Tmem98	Mus musculus transmembrane protein 98 (Tmem98), mRNA [NM_029537]	-1.44	6.07e-06	6.29e-04
A_55_P2098471	Rps19	Mus musculus ribosomal protein S19 (Rps19), mRNA [NM_023133]	1.62	6.12e-06	6.31e-04
A_55_P2044582	Igln5	Mus musculus IgLON family member 5 (Igln5), mRNA [NM_001164518]	2.01	6.39e-06	6.53e-04
A_55_P1997604	Pla2g4a	Mus musculus phospholipase A2, group IVA (cytosolic, calcium-dependent) (Pla2g4a), mRNA [NM_008869]	-1.28	6.40e-06	6.53e-04
A_52_P167278	Mthfd11	Mus musculus methylenetetrahydrofolate dehydrogenase (NADP+ dependent) 1-like (Mthfd11), nuclear gene encoding mitochondrial protein, transcript variant 2, mRNA [NM_172308]	1.39	6.43e-06	6.54e-04
A_51_P277336	Sdpr	Mus musculus serum deprivation response (Sdpr), mRNA [NM_138741]	-1.31	6.45e-06	6.54e-04
A_55_P1990210	Scpep1	Mus musculus serine carboxypeptidase 1 (Scpep1), mRNA [NM_029023]	1.41	6.53e-06	6.60e-04
A_55_P2106916	Kcna1	Mus musculus potassium voltage-gated channel, shaker-related subfamily, member 1 (Kcna1), mRNA [NM_010595]	-1.39	6.67e-06	6.72e-04
A_55_P2131954	Gm2590	PREDICTED: Mus musculus hypothetical protein LOC100040086 (LOC100040086), mRNA [XM_001474060]	-2.04	6.69e-06	6.72e-04
A_55_P2024888	Ctss	Mus musculus cathepsin S (Ctss), mRNA [NM_021281]	2.84	6.84e-06	6.85e-04
A_51_P461779	Ppp2r2c	Mus musculus protein phosphatase 2 (formerly 2A), regulatory subunit B (PR 52), gamma isoform (Ppp2r2c), mRNA [NM_172994]	-1.54	6.91e-06	6.90e-04
A_55_P2150555	Pcgf5	Mus musculus polycomb group ring finger 5 (Pcgf5), mRNA [NM_029508]	1.47	6.96e-06	6.93e-04
A_55_P2123002	Tet1	Mus musculus tet oncogene 1 (Tet1), mRNA [NM_027384]	-1.55	7.00e-06	6.95e-04
A_51_P472829	Aif1l	Mus musculus allograft inflammatory factor 1-like (Aif1l), mRNA [NM_145144]	-1.42	7.03e-06	6.96e-04

A_52_P594768	Aprt	Mus musculus adenine phosphoribosyl transferase (Aprt), mRNA [NM_009698]	1.65	7.15e-06	7.05e-04
A_55_P2059931	Prom1	Mus musculus prominin 1 (Prom1), transcript variant 2, mRNA [NM_001163577]	2.02	7.21e-06	7.09e-04
A_51_P226269	1190002H23Rik	Mus musculus RIKEN cDNA 1190002H23 gene (1190002H23Rik), mRNA [NM_025427]	1.99	7.28e-06	7.13e-04
A_51_P285077	Hhatl	Mus musculus hedgehog acyltransferase-like (Hhatl), transcript variant 1, mRNA [NM_029095]	-2.17	7.46e-06	7.29e-04
A_55_P1989061	Tsc22d3	Mus musculus TSC22 domain family, member 3 (Tsc22d3), transcript variant 1, mRNA [NM_001077364]	-1.56	7.73e-06	7.53e-04
A_66_P106113	Rhoj	Mus musculus ras homolog gene family, member J (Rhoj), mRNA [NM_023275]	1.39	7.77e-06	7.54e-04
A_55_P1978506	H2-Q6	Mus musculus histocompatibility 2, Q region locus 6 (H2-Q6), mRNA [NM_207648]	2.19	7.79e-06	7.54e-04
A_55_P1968295	Pacsin3	Mus musculus protein kinase C and casein kinase substrate in neurons 3 (Pacsin3), mRNA [NM_028733]	-1.67	7.91e-06	7.61e-04
A_55_P2025538	Ano4	Mus musculus anoctamin 4 (Ano4), mRNA [NM_178773]	-1.34	7.93e-06	7.61e-04
A_51_P432460	Ppp1r14a	Mus musculus protein phosphatase 1, regulatory (inhibitor) subunit 14A (Ppp1r14a), mRNA [NM_026731]	-1.34	8.14e-06	7.73e-04
A_55_P2101906	Rpl10a	Mus musculus ribosomal protein L10A (Rpl10a), mRNA [NM_011287]	0.94	8.16e-06	7.73e-04
A_55_P2033282	Cept1	Mus musculus choline/ethanolaminephosphotransferase 1 (Cept1), mRNA [NM_133869]	-0.91	8.18e-06	7.73e-04
A_55_P2094520	Fam171a1	Mus musculus family with sequence similarity 171, member A1 (Fam171a1), mRNA [NM_001081161]	-1.28	8.39e-06	7.87e-04
A_51_P209150	Pcdh10	Mus musculus protocadherin 10 (Pcdh10), transcript variant 2, mRNA [NM_001098172]	1.31	8.40e-06	7.87e-04
A_52_P243391	Sema4f	Mus musculus sema domain, immunoglobulin domain (Ig), TM domain, and short cytoplasmic domain (Sema4f), transcript variant 1, mRNA [NM_011350]	1.42	8.45e-06	7.90e-04
A_55_P1974957	Tnr	Mus musculus tenascin R (Tnr), mRNA [NM_022312]	1.96	8.59e-06	7.98e-04
A_55_P2124498	Il17rb	Mus musculus interleukin 17 receptor B (Il17rb), mRNA [NM_019583]	-1.48	8.67e-06	7.99e-04
A_51_P246166	Expi	Mus musculus extracellular proteinase inhibitor (Expi), mRNA [NM_007969]	-2.55	8.63e-06	7.99e-04
A_55_P2036280	Psen2	Mus musculus presenilin 2 (Psen2), transcript variant 2, mRNA [NM_001128605]	-1.22	8.69e-06	7.99e-04
A_55_P2147427	Prdx1	Mus musculus peroxiredoxin 1 (Prdx1), mRNA [NM_011034]	-1.41	8.72e-06	7.99e-04
A_51_P250058	Epas1	Mus musculus endothelial PAS domain protein 1 (Epas1), mRNA [NM_010137]	-1.16	8.73e-06	7.99e-04
A_66_P122087	Zfp622	Mus musculus zinc finger protein 622 (Zfp622), mRNA [NM_144523]	0.99	8.81e-06	8.04e-04
A_55_P2135631	Rps18	Mus musculus ribosomal protein S18 (Rps18), mRNA [NM_011296]	1.22	8.91e-06	8.11e-04
A_55_P1963529	Abcb10	Mus musculus ATP-binding cassette, sub-family B (MDR/TAP), member 10 (Abcb10), nuclear gene encoding mitochondrial protein, mRNA [NM_019552]	-1.25	8.93e-06	8.11e-04
A_55_P2181341	Ecel1	Mus musculus endothelin converting	2.31	9.09e-06	8.15e-04

		enzyme-like 1 (Ecel1), mRNA [NM_021306]			
A_55_P2153292	Tubb2c	Mus musculus tubulin, beta 2C (Tubb2c), mRNA [NM_146116]	1.05	9.07e-06	8.15e-04
A_52_P163795	Tubb5	Mus musculus tubulin, beta 5 (Tubb5), mRNA [NM_011655]	1.37	9.08e-06	8.15e-04
A_55_P2027087	Plc1l	Mus musculus phospholipase C-like 1 (Plc1l), mRNA [NM_00114663]	-1.26	9.13e-06	8.15e-04
A_55_P2090070	Myh14	Mus musculus myosin, heavy polypeptide 14 (Myh14), mRNA [NM_028021]	-1.41	9.14e-06	8.15e-04
A_55_P2091736	Rassf2	Mus musculus Ras association (RalGDS/AF-6) domain family member 2 (Rassf2), mRNA [NM_175445]	-0.91	9.17e-06	8.16e-04
A_51_P418056	Sc5d	Mus musculus sterol-C5-desaturase (fungal ERG3, delta-5-desaturase) homolog (S. cerevisiae) (Sc5d), mRNA [NM_172769]	-1.36	9.32e-06	8.27e-04
A_55_P2021216	Crif3	Mus musculus cytokine receptor-like factor 3 (Crif3), mRNA [NM_018776]	-1.56	9.54e-06	8.44e-04
A_51_P158678	Fam181b	Mus musculus family with sequence similarity 181, member B (Fam181b), mRNA [NM_021427]	3.79	9.89e-06	8.70e-04
A_55_P2005552	Arhgef10l	Mus musculus Rho guanine nucleotide exchange factor (GEF) 10-like (Arhgef10l), transcript variant 1, mRNA [NM_172415]	1.95	1.01e-05	8.82e-04
A_55_P2064876	Mtvr2	Mus musculus mammary tumor virus receptor 2 (Mtvr2), transcript variant 1, mRNA [NM_181452]	1.23	1.01e-05	8.82e-04
A_55_P1985890	Tiparp	Mus musculus TCDD-inducible poly(ADP-ribose) polymerase (Tiparp), mRNA [NM_178892]	1.21	1.02e-05	8.87e-04
A_52_P88983	Dock5	Mus musculus dedicator of cytokinesis 5 (Dock5), mRNA [NM_177780]	-1.89	1.04e-05	9.01e-04
A_55_P1969745	Pitpnm1	Mus musculus phosphatidylinositol transfer protein, membrane-associated 1 (Pitpnm1), transcript variant 2, mRNA [NM_001136078]	1.47	1.05e-05	9.07e-04
A_55_P2030859	Gm8225	PREDICTED: Mus musculus predicted gene, EG666668 (EG666668), mRNA [XM_985281]	1.05	1.05e-05	9.08e-04
A_51_P155313	Gsto1	Mus musculus glutathione S-transferase omega 1 (Gsto1), mRNA [NM_010362]	2.08	1.06e-05	9.10e-04
A_55_P2125743	Gm8842	PREDICTED: Mus musculus predicted gene, EG667847, transcript variant 2 (EG667847), mRNA [XM_001003664]	0.75	1.06e-05	9.10e-04
A_55_P2020128	Dhrs3	Mus musculus dehydrogenase/reductase (SDR family) member 3 (Dhrs3), mRNA [NM_011303]	1.41	1.06e-05	9.10e-04
A_51_P194306	Lrrc1	Mus musculus leucine rich repeat containing 1 (Lrrc1), transcript variant 2, mRNA [NM_172528]	-1.05	1.06e-05	9.10e-04
A_51_P498890	Degs1	Mus musculus degenerative spermatocyte homolog 1 (Drosophila) (Degs1), mRNA [NM_007853]	-0.96	1.07e-05	9.10e-04
A_55_P1960049	2810408A11Rik	Mus musculus RIKEN cDNA 2810408A11 gene (2810408A11Rik), mRNA [NM_027419]	1.35	1.07e-05	9.10e-04
A_55_P1991770	Pdlim4	Mus musculus PDZ and LIM domain 4 (Pdlim4), mRNA [NM_019417]	4.24	1.08e-05	9.12e-04
A_55_P2165314	Trio	Mus musculus triple functional domain (PTPRF interacting) (Trio), mRNA [NM_001081302]	2.17	1.09e-05	9.21e-04
A_52_P18807	Eif3c	Mus musculus eukaryotic translation initiation factor 3, subunit C (Eif3c), mRNA [NM_146200]	1.05	1.11e-05	9.31e-04

A_51_P193794	Lrp1	Mus musculus low density lipoprotein receptor-related protein 1 (Lrp1), mRNA [NM_008512]	1.57	1.14e-05	9.35e-04
A_55_P2004159	LOC100039646	PREDICTED: Mus musculus similar to polyprotein (LOC100039646), mRNA [XM_001472835]	-1.89	1.12e-05	9.35e-04
A_66_P129893	1700047M11Rik	Mus musculus RIKEN cDNA 1700047M11 gene (1700047M11Rik), non-coding RNA [NR_015458]	-1.36	1.12e-05	9.35e-04
A_55_P1984113	Nup62	Mus musculus nucleoporin 62 (Nup62), mRNA [NM_053074]	1.35	1.12e-05	9.35e-04
A_51_P108901	Ccdc86	Mus musculus coiled-coil domain containing 86 (Ccdc86), mRNA [NM_023731]	1.34	1.13e-05	9.35e-04
A_55_P2009285	Fbxo25	Mus musculus F-box protein 25 (Fbxo25), mRNA [NM_025785]	-1.13	1.13e-05	9.35e-04
A_55_P2028961	Idi1	Mus musculus isopentenyl-diphosphate delta isomerase (Idi1), mRNA [NM_145360]	-1.66	1.14e-05	9.35e-04
A_55_P2005190	Herc4	Mus musculus hect domain and RLD 4 (Herc4), mRNA [NM_026101]	-1.45	1.14e-05	9.35e-04
A_55_P2151609	Sorl1	Mus musculus sortilin-related receptor, LDLR class A repeats-containing (Sorl1), mRNA [NM_011436]	-1.54	1.15e-05	9.35e-04
A_51_P144349	Dtx4	Mus musculus deltex 4 homolog (Drosophila) (Dtx4), mRNA [NM_172442]	1.16	1.15e-05	9.35e-04
A_52_P284889	Prkcz	Mus musculus protein kinase C, zeta (Prkcz), transcript variant 1, mRNA [NM_008860]	-1.26	1.15e-05	9.39e-04
A_51_P237668	Bex2	Mus musculus brain expressed X-linked 2 (Bex2), mRNA [NM_009749]	1.76	1.18e-05	9.56e-04
A_51_P173961	Pdrg1	Mus musculus p53 and DNA damage regulated 1 (Pdrg1), mRNA [NM_178939]	0.90	1.18e-05	9.56e-04
A_55_P2001718	Pex1	Mus musculus peroxisomal biogenesis factor 1 (Pex1), mRNA [NM_027777]	-1.24	1.19e-05	9.62e-04
A_51_P505493	Elov15	Mus musculus ELOVL family member 5, elongation of long chain fatty acids (yeast) (Elov15), mRNA [NM_134255]	-0.98	1.20e-05	9.69e-04
A_55_P2022074	Klf10	Mus musculus Kruppel-like factor 10 (Klf10), mRNA [NM_013692]	1.57	1.23e-05	9.86e-04
A_55_P2052696	Synn	Mus musculus synemin, intermediate filament protein (Synn), transcript variant 1, mRNA [NM_201639]	-1.42	1.23e-05	9.86e-04
A_51_P234113	Nod1	Mus musculus nucleotide-binding oligomerization domain containing 1 (Nod1), mRNA [NM_172729]	-1.35	1.23e-05	9.86e-04
A_51_P341918	Tsc22d1	Mus musculus TSC22 domain family, member 1 (Tsc22d1), transcript variant 2, mRNA [NM_009366]	1.51	1.26e-05	9.96e-04
A_55_P2037524	Rps15	Mus musculus ribosomal protein S15 (Rps15), mRNA [NM_009091]	0.91	1.26e-05	9.96e-04
A_55_P2020577	Pcolce	Mus musculus procollagen C-endopeptidase enhancer protein (Pcolce), mRNA [NM_008788]	1.33	1.26e-05	9.96e-04
A_51_P195958	Phlda1	Mus musculus pleckstrin homology-like domain, family A, member 1 (Phlda1), mRNA [NM_009344]	1.12	1.26e-05	9.96e-04

Supplementary Table 6. Common DEGs identified in the CC and OPC analysis.

Symbol	Gene name
Gdf15	growth differentiation factor 15
Pigz	phosphatidylinositol glycan anchor biosynthesis, class Z

Trib3	tribbles pseudokinase 3
Ninj2	ninjurin 2
Ccng1	cyclin G1
Slc34a3	solute carrier family 34 (sodium phosphate), member 3
Atf5	activating transcription factor 5
Xrcc3	X-ray repair complementing defective repair in Chinese hamster cells 3
Ddit3	DNA-damage inducible transcript 3
Moxd1	monooxygenase, DBH-like 1
Smtnl2	smoothelin-like 2
Ppp1r14a	protein phosphatase 1, regulatory inhibitor subunit 14A
Sesn2	sestrin 2
Cdkn1a	cyclin-dependent kinase inhibitor 1A (P21)
Tmem125	transmembrane protein 125
Tmprss5	transmembrane protease, serine 5 (spinesin)
Slc7a5	solute carrier family 7 (cationic amino acid transporter, y+ system), member 5
Klf4	Kruppel-like factor 4 (gut)
Eif4ebp1	eukaryotic translation initiation factor 4E binding protein 1
Slc3a2	solute carrier family 3 (activators of dibasic and neutral amino acid transport), member 2
Arap2	ArfGAP with RhoGAP domain, ankyrin repeat and PH domain 2
Gzmm	granzyme M (lymphocyte met-ase 1)
Sgk2	serum/glucocorticoid regulated kinase 2
Bbc3	BCL2 binding component 3
Nes	nestin
Gas5	growth arrest specific 5
Fdps	farnesyl diphosphate synthetase
Prima1	proline rich membrane anchor 1
Serpinb1a	serine (or cysteine) peptidase inhibitor, clade B, member 1a
Ldlr	low density lipoprotein receptor
Gjc2	gap junction protein, gamma 2
Ephx1	epoxide hydrolase 1, microsomal
Ephx1	epoxide hydrolase 1, microsomal
B230206H07Rik	RIKEN cDNA B230206H07 gene
Hmgcs1	3-hydroxy-3-methylglutaryl-Coenzyme A synthase 1
Galnt6	polypeptide N-acetylgalactosaminyltransferase 6
Galnt6	polypeptide N-acetylgalactosaminyltransferase 6
Nupr1	nuclear protein transcription regulator 1
Adams1	a disintegrin-like and metallopeptidase (reprolysin type) with thrombospondin type 1 motif, 1
Pcyt2	phosphate cytidylyltransferase 2, ethanolamine
Gadd45b	growth arrest and DNA-damage-inducible 45 beta
Nacad	NAC alpha domain containing
Klk6	kallikrein related-peptidase 6
Tmeff1	transmembrane protein with EGF-like and two follistatin-like domains 1
Mog	myelin oligodendrocyte glycoprotein
Aen	apoptosis enhancing nuclease
Nmral1	NmrA-like family domain containing 1
Rftn1	raftlin lipid raft linker 1
Eprs	glutamyl-prolyl-tRNA synthetase
Nkain1	Na+/K+ transporting ATPase interacting 1
Fzd1	frizzled class receptor 1
Rps27l	ribosomal protein S27-like
Rhog	ras homolog family member G
Aradc4	arrestin domain containing 4
Opalin	oligodendrocytic myelin paranodal and inner loop protein
Anln	anillin, actin binding protein
Syt12	synaptotagmin-like 2
Ccl2	chemokine (C-C motif) ligand 2
Gadd45a	growth arrest and DNA-damage-inducible 45 alpha
Prr18	proline rich 18
Synj2	synaptojanin 2
Ifrd1	interferon-related developmental regulator 1
Adssl1	adenylosuccinate synthetase like 1
Kctd15	potassium channel tetramerisation domain containing 15
Ppp1r15a	protein phosphatase 1, regulatory subunit 15A
Gal3st1	galactose-3-O-sulfotransferase 1

Maff	v-maf musculoaponeurotic fibrosarcoma oncogene family, protein F (avian)
Cntn2	contactin 2
Nipal4	NIPA-like domain containing 4
Cdk18	cyclin-dependent kinase 18
Mgp	matrix Gla protein
Ptprd	protein tyrosine phosphatase, receptor type, D
Lgi3	leucine-rich repeat LGI family, member 3
Tor3a	torsin family 3, member A
Mcam	melanoma cell adhesion molecule
Fah	fumarylacetoacetate hydrolase
Rgs3	regulator of G-protein signaling 3
Nfil3	nuclear factor, interleukin 3, regulated
Mbp	myelin basic protein
Dhcr7	7-dehydrocholesterol reductase
Ano4	anoctamin 4
Cyb5r2	cytochrome b5 reductase 2
Plekhh1	pleckstrin homology domain containing, family H (with MyTH4 domain) member 1
Ttl7	tubulin tyrosine ligase-like family, member 7
Runx1	runt related transcription factor 1
Odc1	ornithine decarboxylase, structural 1
Adamts14	ADAMTS-like 4
Gamt	guanidinoacetate methyltransferase
Rasgrp3	RAS, guanyl releasing protein 3
Cebpg	CCAAT/enhancer binding protein (C/EBP), gamma
1110038B12Rik	RIKEN cDNA 1110038B12 gene
Cebpb	CCAAT/enhancer binding protein (C/EBP), beta
Abca2	ATP-binding cassette, sub-family A (ABC1), member 2
Omg	oligodendrocyte myelin glycoprotein
Tppp	tubulin polymerization promoting protein
Mast4	microtubule associated serine/threonine kinase family member 4
Rasl12	RAS-like, family 12

Supplementary Table 7. DEGs in CC from mice which underwent remyelination compared to mice treated with cuprizone for 2 weeks.

Probe ID	Symbol	Gene Name	logFC	p-value	adj.p-value
A_52_P244463	D16Erd472e	DNA segment, Chr 16, ERATO Doi 472, expressed	1.97	4.11E-06	2.74E-02
A_51_P212068	Aoc1	amine oxidase, copper-containing 1	1.66	4.95E-06	2.74E-02
A_51_P482128	Krt15	keratin 15	1.76	6.14E-06	2.74E-02
A_52_P493477	Serp1b1c	serine (or cysteine) peptidase inhibitor, clade B, member 1c	1.92	7.42E-06	2.74E-02
A_51_P147284	Slain1	SLAIN motif family, member 1	2.02	1.05E-05	2.74E-02
A_51_P432641	Cxcl10	chemokine (C-X-C motif) ligand 10	1.3	1.35E-05	2.74E-02
A_52_P345471	Sntn	sentan, cilia apical structure protein	1.63	1.36E-05	2.74E-02
A_51_P428134	Lrig3	leucine-rich repeats and immunoglobulin-like domains 3	1.56	1.39E-05	2.74E-02
A_51_P230439	Ppfbp2	PTPRF interacting protein, binding protein 2 (liprin beta 2)	1.95	1.58E-05	2.74E-02
A_52_P272175	Dusp15	dual specificity phosphatase-like 15	1.29	1.65E-05	2.74E-02
A_51_P136355	Gng11	guanine nucleotide binding protein (G protein), gamma 11	2.07	1.65E-05	2.74E-02
A_51_P154867	Plp	plasma membrane proteolipid	1.34	1.71E-05	2.74E-02
A_52_P361534	Wnt3	wingless-type MMTV integration site family, member 3	2.03	1.73E-05	2.74E-02

A_52_P268206	Mcam	melanoma cell adhesion molecule	1.47	1.74E-05	2.74E-02
A_51_P412732	D16Ert472e	DNA segment, Chr 16, ERATO Doi 472, expressed	1.96	1.77E-05	2.74E-02
A_52_P137529	Creb5	cAMP responsive element binding protein 5	1.47	1.97E-05	2.74E-02
A_52_P233411	Insc	INSC spindle orientation adaptor protein	2.11	2.33E-05	2.74E-02
A_52_P530082	Bfsp2	beaded filament structural protein 2, phakinin	2.08	2.43E-05	2.74E-02
A_51_P101347	Pls1	plastin 1 (I-isoform)	2.26	2.74E-05	2.74E-02
A_52_P266916	Otud7b	OTU domain containing 7B	1.56	2.93E-05	2.74E-02
A_52_P451355	St6galnac3	ST6 (alpha-N-acetyl-neuraminyl-2,3-beta-galactosyl-1,3)-N-acetylgalactosaminide alpha-2,6-sialyltransferase 3	1.74	3.07E-05	2.74E-02
A_52_P328304	Plekhh3	pleckstrin homology domain containing, family G (with RhoGef domain) member 3	2.64	3.90E-05	2.74E-02
A_51_P450955	P3h4	prolyl 3-hydroxylase family member 4 (non-enzymatic)	1.95	4.06E-05	2.74E-02
A_51_P450952	P3h4	prolyl 3-hydroxylase family member 4 (non-enzymatic)	1.61	4.07E-05	2.74E-02
A_51_P172542	Slc4a2	solute carrier family 4 (anion exchanger), member 2	1.78	4.13E-05	2.74E-02
A_51_P359570	Ifit3	interferon-induced protein with tetratricopeptide repeats 3	1.15	4.40E-05	2.74E-02
A_52_P269672	Sox8	SRY (sex determining region Y)-box 8	1.49	4.55E-05	2.74E-02
A_52_P154800	Plaat3	phospholipase A and acyltransferase 3	2.05	4.58E-05	2.74E-02
A_52_P192625	Sox10	SRY (sex determining region Y)-box 10	1.38	4.64E-05	2.74E-02
A_51_P346704	Sox10	SRY (sex determining region Y)-box 10	1.96	4.71E-05	2.74E-02
A_52_P354682	Elovl7	ELOVL family member 7, elongation of long chain fatty acids (yeast)	2.22	4.71E-05	2.74E-02
A_52_P125954	Plekhh1	pleckstrin homology domain containing, family H (with MyTH4 domain) member 1	1.63	4.81E-05	2.74E-02
A_52_P347764	Lrrc74b	leucine rich repeat containing 74B	1.62	4.85E-05	2.74E-02
A_52_P45616	Emilin3	elastin microfibril interfacier 3	1.58	4.90E-05	2.74E-02
A_51_P338935	Prkcq	protein kinase C, theta	1.7	5.07E-05	2.74E-02
A_51_P315785	Tnfaip6	tumor necrosis factor alpha induced protein 6	2.38	5.08E-05	2.74E-02
A_52_P417437	Gab1	growth factor receptor bound protein 2-associated protein 1	1.58	5.21E-05	2.74E-02
A_51_P298802	Bfsp2	beaded filament structural protein 2, phakinin	1.82	5.32E-05	2.74E-02
A_51_P205385	Uox	urate oxidase	1.53	5.34E-05	2.74E-02
A_51_P219109	Il12rb1	interleukin 12 receptor, beta 1	2.51	5.37E-05	2.74E-02
A_51_P462422	Gjb1	gap junction protein, beta 1	1.84	5.50E-05	2.74E-02
A_52_P622641	Ppfbp2	PTPRF interacting protein, binding protein 2 (liprin beta 2)	1.85	5.69E-05	2.74E-02

A_51_P189594	Elov17	ELOVL family member 7, elongation of long chain fatty acids (yeast)	2.35	6.07E-05	2.74E-02
A_51_P223025	Dock5	dedicator of cytokinesis 5	2.27	6.21E-05	2.74E-02
A_52_P30328	Tmem163	transmembrane protein 163	1.69	6.27E-05	2.74E-02
A_52_P481493	Fkbp5	FK506 binding protein 5	-1.76	6.39E-05	2.74E-02
A_51_P241465	Gsn	gelsolin	2.45	6.54E-05	2.74E-02
A_51_P206203	Mrgprf	MAS-related GPR, member F	1.36	6.66E-05	2.74E-02
A_51_P352245	Sema6a	sema domain, transmembrane domain (TM), and cytoplasmic domain, (semaphorin) 6A	1.9	6.77E-05	2.74E-02
A_51_P389864	B3gnt9	UDP-GlcNAc:betaGal beta-1,3-N-acetylglucosaminyltransferase 9	2.35	6.83E-05	2.74E-02
A_51_P305770	Emilin2	elastin microfibril interfacier 2	1.34	6.83E-05	2.74E-02
A_52_P72587	Prkceq	protein kinase C, theta	2.15	6.84E-05	2.74E-02
A_51_P184728	Cnksr3	Cnksr family member 3	1.37	7.29E-05	2.74E-02
A_51_P150433	Cd8b1	CD8 antigen, beta chain 1	1.55	7.33E-05	2.74E-02
A_51_P142896	Cd59a	CD59a antigen	1.51	7.37E-05	2.74E-02
A_51_P455647	Car2	carbonic anhydrase 2	2.57	7.44E-05	2.74E-02
A_51_P387239	Iigg1	interferon inducible GTPase 1	1.21	7.50E-05	2.74E-02
A_51_P211980	Rgs3	regulator of G-protein signaling 3	1.67	7.56E-05	2.74E-02
A_51_P128336	Serinc5	serine incorporator 5	1.57	7.80E-05	2.74E-02
A_51_P223583	Rgs3	regulator of G-protein signaling 3	1.14	7.89E-05	2.74E-02
A_51_P337101	Rnf43	ring finger protein 43	1.62	8.05E-05	2.74E-02
A_52_P68087	Enpp6	ectonucleotide pyrophosphatase/phosphodiesterase 6	1.67	8.07E-05	2.74E-02
A_51_P149906	Kif13a	kinesin family member 13A	1.02	8.08E-05	2.74E-02
A_52_P282430	D16Ert472e	DNA segment, Chr 16, ERATO Doi 472, expressed	1.56	8.13E-05	2.74E-02
A_52_P379277	Enpp3	ectonucleotide pyrophosphatase/phosphodiesterase 3	1.04	8.15E-05	2.74E-02
A_51_P294535	Unc5b	unc-5 netrin receptor B	2.39	8.25E-05	2.74E-02
A_51_P224424	Klhl4	kelch-like 4	1.65	8.27E-05	2.74E-02
A_51_P275808	Trim59	tripartite motif-containing 59	2.54	8.30E-05	2.74E-02
A_52_P62121	Gpr37	G protein-coupled receptor 37	2.48	8.40E-05	2.74E-02
A_51_P225781	Insc	INSC spindle orientation adaptor protein	2.39	8.40E-05	2.74E-02
A_51_P251964	E330034G19Rik	RIKEN cDNA E330034G19 gene	1.26	8.43E-05	2.74E-02
A_52_P639223	Behe	butyrylcholinesterase	1.78	8.56E-05	2.74E-02
A_52_P619738	Gramd3	GRAM domain containing 3	1.3	8.67E-05	2.74E-02
A_52_P507802	Lpar1	lysophosphatidic acid receptor 1	2.77	8.76E-05	2.74E-02
A_51_P451632	5031410I06Rik	RIKEN cDNA 5031410I06 gene	1.27	9.25E-05	2.74E-02
A_52_P439502	Plekhh1	pleckstrin homology domain containing, family H (with MyTH4 domain) member 1	2.56	9.36E-05	2.74E-02
A_51_P432403	Fgfr2	fibroblast growth factor receptor 2	1.37	9.34E-05	2.74E-02
A_52_P348720	Rhobtb3	Rho-related BTB domain containing 3	1.44	9.44E-05	2.74E-02
A_51_P406846	Nipal4	NIPA-like domain containing 4	2.22	9.46E-05	2.74E-02

A_51_P292550	Chdh	choline dehydrogenase	1.45	9.47E-05	2.74E-02
A_52_P488501	Gtsf11	gametocyte specific factor 1-like	1.38	9.48E-05	2.74E-02
A_52_P642662	Efh1	EF hand domain containing 1	1.89	9.53E-05	2.74E-02
A_52_P24951	Ado	2-aminoethanethiol (cysteamine) dioxygenase	1.36	9.55E-05	2.74E-02
A_51_P363564	Trp53bp2	transformation related protein 53 binding protein 2	1.25	9.61E-05	2.74E-02
A_52_P563375	Lgals2	lectin, galactose-binding, soluble 2	1.3	9.63E-05	2.74E-02
A_51_P472829	Aif11	allograft inflammatory factor 1-like	1.85	9.70E-05	2.74E-02
A_51_P401659	Sspn	sarcospan	1.55	9.77E-05	2.74E-02
A_51_P368496	Tmem98	transmembrane protein 98	2.61	9.88E-05	2.74E-02
A_52_P169764	E030046B03Rik	RIKEN cDNA E030046B03 gene	1.2	1.00E-04	2.75E-02
A_52_P106482	Cryab	crystallin, alpha B	2.2	1.04E-04	2.81E-02
A_51_P265151	Arhgef10	Rho guanine nucleotide exchange factor (GEF) 10	1.63	1.09E-04	2.81E-02
A_51_P421279	Eml1	echinoderm microtubule associated protein like 1	1.4	1.10E-04	2.81E-02
A_51_P413721	Gjc3	gap junction protein, gamma 3	1.96	1.11E-04	2.81E-02
A_51_P499195	Nkg7	natural killer cell group 7 sequence	1.22	1.14E-04	2.81E-02
A_51_P196158	Btd	biotinidase	1.18	1.14E-04	2.81E-02
A_51_P173709	Gpre5b	G protein-coupled receptor, family C, group 5, member B	1.54	1.14E-04	2.81E-02
A_52_P164136	Arrdc3	arrestin domain containing 3	1.49	1.17E-04	2.81E-02
A_52_P16877	Tmcc3	transmembrane and coiled coil domains 3	1.76	1.18E-04	2.81E-02
A_51_P490867	Enpp4	ectonucleotide pyrophosphatase/phosphodiesterase 4	1.55	1.19E-04	2.81E-02
A_52_P401504	Thbs4	thrombospondin 4	1.56	1.20E-04	2.81E-02
A_52_P610965	St18	suppression of tumorigenicity 18	1.58	1.20E-04	2.81E-02
A_51_P451588	Plekhh1	pleckstrin homology domain containing, family B (evectins) member 1	2.38	1.24E-04	2.81E-02
A_51_P234944	Adams4	a disintegrin-like and metallopeptidase (reprolysin type) with thrombospondin type 1 motif, 4	2.2	1.24E-04	2.81E-02
A_51_P278464	Fam183b	family with sequence similarity 183, member B	1.72	1.25E-04	2.81E-02
A_51_P412027	Cxcr6	chemokine (C-X-C motif) receptor 6	1.19	1.26E-04	2.81E-02
A_51_P477692	Fa2h	fatty acid 2-hydroxylase	3.35	1.28E-04	2.81E-02
A_52_P618745	Ermp1	endoplasmic reticulum metallopeptidase 1	1.34	1.28E-04	2.81E-02
A_52_P497188	Prrg1	proline rich Gla (G-carboxyglutamic acid) 1	2.07	1.30E-04	2.81E-02
A_51_P110068	Sirt2	sirtuin 2	1.33	1.35E-04	2.84E-02
A_52_P681456	Rftn2	raftlin family member 2	1.16	1.36E-04	2.84E-02
A_51_P395546	Phldb1	pleckstrin homology like domain, family B, member 1	2.5	1.38E-04	2.85E-02
A_52_P636742	Rnf122	ring finger protein 122	1.77	1.41E-04	2.87E-02
A_52_P470150	Ddc	dopa decarboxylase	1.98	1.41E-04	2.87E-02
A_52_P27871	Fnbp1	formin binding protein 1	1.59	1.45E-04	2.88E-02

A_52_P84901	Slc44a1	solute carrier family 44, member 1	2.5	1.49E-04	2.88E-02
A_52_P461378	Tmbim1	transmembrane BAX inhibitor motif containing 1	1.51	1.49E-04	2.88E-02
A_52_P391639	1600029114Rik	RIKEN cDNA 1600029114 gene	2.31	1.52E-04	2.88E-02
A_51_P378381	Crnde	colorectal neoplasia differentially expressed (non-protein coding)	1.23	1.53E-04	2.88E-02
A_51_P129464	Scd2	stearoyl-Coenzyme A desaturase 2	1.2	1.53E-04	2.88E-02
A_52_P439263	Ugt8a	UDP galactosyltransferase 8A	3.24	1.54E-04	2.88E-02
A_52_P561671	Msx1	msh homeobox 1	1.3	1.56E-04	2.88E-02
A_52_P868419	Fbxo32	F-box protein 32	1.47	1.56E-04	2.88E-02
A_51_P246924	Tppp3	tubulin polymerization-promoting protein family member 3	2.41	1.57E-04	2.88E-02
A_51_P194306	Lrrc1	leucine rich repeat containing 1	1.22	1.58E-04	2.88E-02
A_51_P358484	Ephb1	Eph receptor B1	1.15	1.58E-04	2.88E-02
A_51_P163444	Carhsp1	calcium regulated heat stable protein 1	1.92	1.59E-04	2.88E-02
A_51_P435704	Tnni1	troponin I, skeletal, slow 1	1.86	1.61E-04	2.88E-02
A_52_P302496	Fah	fumarylacetoacetate hydrolase	1.84	1.62E-04	2.88E-02
A_52_P607674	Plpp2	phospholipid phosphatase 2	1.19	1.70E-04	2.98E-02
A_51_P202596	Sh3tc2	SH3 domain and tetratricopeptide repeats 2	1.58	1.71E-04	2.98E-02
A_52_P391000	Pde8a	phosphodiesterase 8A	2.51	1.73E-04	2.98E-02
A_51_P342031	Mkm3	makorin, ring finger protein, 3	1.23	1.73E-04	2.98E-02
A_51_P275527	Slc12a2	solute carrier family 12, member 2	1.76	1.75E-04	2.98E-02
A_51_P189959	Oxsr1	oxidative-stress responsive 1	1.24	1.76E-04	2.98E-02
A_51_P133381	Dbnnd2	dysbindin (dystrobrevin binding protein 1) domain containing 2	1.67	1.83E-04	2.98E-02
A_52_P52946	Erich3	glutamate rich 3	1.5	1.84E-04	2.98E-02
A_51_P282940	Fam216b	family with sequence similarity 216, member B	1.76	1.84E-04	2.98E-02
A_52_P603038	Olig1	oligodendrocyte transcription factor 1	1.86	1.84E-04	2.98E-02
A_52_P255849	Tlcd3a	TLC domain containing 3A	1.34	1.87E-04	2.98E-02
A_51_P362959	Fbxo36	F-box protein 36	1.57	1.87E-04	2.98E-02
A_52_P199237	Fam166b	family with sequence similarity 166, member B	1.74	1.90E-04	2.98E-02
A_51_P358354	Jam3	junction adhesion molecule 3	1.68	1.90E-04	2.98E-02
A_52_P211737	Myo1d	myosin ID	1.7	1.91E-04	2.98E-02
A_52_P389324	Sox2ot	SOX2 overlapping transcript (non-protein coding)	2.1	1.93E-04	2.98E-02
A_51_P438924	Cmtm5	CKLF-like MARVEL transmembrane domain containing 5	1.99	1.93E-04	2.98E-02
A_52_P382754	Ncam1	neural cell adhesion molecule 1	1.57	1.92E-04	2.98E-02
A_51_P354354	Gal3st1	galactose-3-O-sulfotransferase 1	2.44	1.95E-04	2.99E-02
A_51_P289380	Olfrl341	olfactory receptor 1341	3.32	1.96E-04	2.99E-02
A_51_P114714	Trim13	tripartite motif-containing 13	1.62	2.01E-04	2.99E-02
A_52_P586851	Efs	embryonal Fyn-associated substrate	1.12	2.01E-04	2.99E-02
A_52_P430348	Serp1b1b	serine (or cysteine) peptidase inhibitor, clade B, member 1b	2.13	2.01E-04	2.99E-02

A_51_P464838	Il17rb	interleukin 17 receptor B	1.86	2.01E-04	2.99E-02
A_51_P255805	Fhdc1	FH2 domain containing 1	1.18	2.03E-04	2.99E-02
A_51_P221263	Arsg	arylsulfatase G	2.34	2.06E-04	2.99E-02
A_51_P342773	Vipr2	vasoactive intestinal peptide receptor 2	1.47	2.05E-04	2.99E-02
A_51_P261931	A930003A15Rik	RIKEN cDNA A930003A15 gene	1.53	2.05E-04	2.99E-02
A_51_P468140	Serpind1	serine (or cysteine) peptidase inhibitor, clade D, member 1	2.69	2.18E-04	3.09E-02
A_51_P176661	Tprn	taperin	2.07	2.17E-04	3.09E-02
A_52_P254237	Tmem229a	transmembrane protein 229A	1.29	2.17E-04	3.09E-02
A_51_P167763	Kenk13	potassium channel, subfamily K, member 13	1.52	2.21E-04	3.10E-02
A_51_P187226	1500015L24Rik	RIKEN cDNA 1500015L24 gene	1.45	2.22E-04	3.10E-02
A_51_P291224	Mobp	myelin-associated oligodendrocytic basic protein	3.39	2.26E-04	3.10E-02
A_51_P285206	Cd3d	CD3 antigen, delta polypeptide	1.28	2.24E-04	3.10E-02
A_52_P201912	Smim1	small integral membrane protein 1	1.28	2.26E-04	3.10E-02
A_51_P175424	Car14	carbonic anhydrase 14	2.66	2.29E-04	3.12E-02
A_52_P171178	Ccdc33	coiled-coil domain containing 33	1.56	2.36E-04	3.15E-02
A_51_P244092	Nkain1	Na ⁺ /K ⁺ transporting ATPase interacting 1	1.29	2.37E-04	3.15E-02
A_52_P596592	Rassf9	Ras association (RalGDS/AF-6) domain family (N-terminal) member 9	1.32	2.38E-04	3.15E-02
A_51_P416822	Hhip	Hedgehog-interacting protein	1.23	2.38E-04	3.15E-02
A_51_P366811	Apod	apolipoprotein D	2.21	2.40E-04	3.15E-02
A_51_P285077	Hhat1	hedgehog acyltransferase-like	1.6	2.39E-04	3.15E-02
A_52_P630673	Gpr62	G protein-coupled receptor 62	2.79	2.41E-04	3.15E-02
A_52_P209184	Csrp1	cysteine and glycine-rich protein 1	2.08	2.46E-04	3.17E-02
A_52_P679101	Tjp2	tight junction protein 2	1.23	2.50E-04	3.17E-02
A_51_P232901	Cnp	2',3'-cyclic nucleotide 3' phosphodiesterase	2.97	2.54E-04	3.17E-02
A_51_P476879	Olfml1	olfactomedin-like 1	1.62	2.52E-04	3.17E-02
A_51_P200586	Marchf8	membrane associated ring-CH-type finger 8	1.4	2.53E-04	3.17E-02
A_52_P399175	Rffl	ring finger and FYVE like domain containing protein	1.84	2.53E-04	3.17E-02
A_52_P540072	Edil3	EGF-like repeats and discoidin I-like domains 3	1.35	2.58E-04	3.18E-02
A_51_P497937	Gjc2	gap junction protein, gamma 2	2.24	2.61E-04	3.18E-02
A_52_P358860	Gss	glutathione synthetase	1.31	2.61E-04	3.18E-02
A_52_P577329	Tmem88b	transmembrane protein 88B	3.02	2.63E-04	3.18E-02
A_52_P494982	Dhx40	DEAH (Asp-Glu-Ala-His) box polypeptide 40	0.99	2.63E-04	3.18E-02
A_52_P690855	Fndc11	fibronectin type III domain containing 11	1.41	2.63E-04	3.18E-02
A_51_P195825	Tsnax1p	translin-associated factor X (Tsnax) interacting protein 1	0.94	2.66E-04	3.19E-02
A_52_P486774	Cobl1l	Cobl-like 1	1.27	2.67E-04	3.19E-02
A_52_P42231	Nol3	nucleolar protein 3 (apoptosis repressor with CARD domain)	1.16	2.69E-04	3.19E-02

A_51_P409694	Psrl1	proline/serine-rich coiled-coil 1	-1.18	2.70E-04	3.19E-02
A_51_P180974	Cavin3	caveolae associated 3	1.02	2.72E-04	3.20E-02
A_51_P257258	Cpox	coproporphyrinogen oxidase	1.42	2.75E-04	3.22E-02
A_51_P375543	Myb	myeloblastosis oncogene	1.48	2.75E-04	3.22E-02
A_51_P414166	Rnf7	ring finger protein 7	1	2.77E-04	3.22E-02
A_51_P164219	Usp18	ubiquitin specific peptidase 18	1.5	2.79E-04	3.22E-02
A_51_P136294	Ms4a4b	membrane-spanning 4-domains, subfamily A, member 4B	1.46	2.85E-04	3.27E-02
A_51_P359603	Itgb7	integrin beta 7	1	2.87E-04	3.28E-02
A_51_P161582	Ddr1	discoidin domain receptor family, member 1	1.62	2.92E-04	3.29E-02
A_52_P335606	Prima1	proline rich membrane anchor 1	1.81	2.92E-04	3.29E-02
A_51_P245789	Pcolce2	procollagen C-endopeptidase enhancer 2	1.52	2.96E-04	3.30E-02
A_51_P262757	Plin5	perilipin 5	1.88	3.00E-04	3.30E-02
A_51_P494825	Mfhas1	malignant fibrous histiocytoma amplified sequence 1	-0.79	3.00E-04	3.30E-02
A_52_P62284	Apln	apelin	1.04	3.00E-04	3.30E-02
A_52_P246703	Ak7	adenylate kinase 7	1.4	3.06E-04	3.33E-02
A_51_P435428	Mag	myelin-associated glycoprotein	3.13	3.10E-04	3.33E-02
A_51_P384230	Sgk2	serum/glucocorticoid regulated kinase 2	3.36	3.11E-04	3.33E-02
A_51_P338705	Kank1	KN motif and ankyrin repeat domains 1	1.15	3.09E-04	3.33E-02
A_52_P657376	Tspan15	tetraspanin 15	1.73	3.09E-04	3.33E-02
A_51_P383991	Septin4	septin 4	2.34	3.16E-04	3.33E-02
A_51_P225948	Snx33	sorting nexin 33	1.77	3.14E-04	3.33E-02
A_51_P478942	Golga7	golgi autoantigen, golgin subfamily a, 7	1.29	3.20E-04	3.35E-02
A_52_P12590	Ly6g6d	lymphocyte antigen 6 complex, locus G6D	1.51	3.22E-04	3.35E-02
A_52_P229044	Slc20a2	solute carrier family 20, member 2	1.08	3.23E-04	3.35E-02
A_52_P566741	Tcf7l2	transcription factor 7 like 2, T cell specific, HMG box	1.1	3.24E-04	3.35E-02
A_51_P406020	Abhd4	abhydrolase domain containing 4	0.88	3.28E-04	3.38E-02
A_51_P257762	Kat2b	K(lysine) acetyltransferase 2B	0.98	3.34E-04	3.43E-02
A_51_P506513	Qdpr	quinoid dihydropteridine reductase	2.48	3.38E-04	3.44E-02
A_51_P273556	Fam83d	family with sequence similarity 83, member D	1.04	3.37E-04	3.44E-02
A_51_P439612	Dnajb2	DnaJ heat shock protein family (Hsp40) member B2	1.7	3.41E-04	3.46E-02
A_52_P568257	Sort1	sortilin 1	1.04	3.44E-04	3.46E-02
A_52_P562054	Cilk1	ciliogenesis associated kinase 1	1.37	3.47E-04	3.46E-02
A_52_P265965	Trim36	tripartite motif-containing 36	2	3.48E-04	3.46E-02
A_51_P448236	Ctsk	cathepsin K	1.13	3.49E-04	3.47E-02
A_51_P124285	Nkd1	naked cuticle 1	1.61	3.51E-04	3.47E-02
A_51_P138952	Cep97	centrosomal protein 97	1.35	3.58E-04	3.51E-02
A_51_P162773	Sccpdh	saccharopine dehydrogenase (putative)	1.37	3.60E-04	3.51E-02
A_51_P358462	Ppp1r32	protein phosphatase 1, regulatory	1.71	3.62E-04	3.51E-02

		subunit 32			
A_52_P348031	Syt9	synaptotagmin IX	1.18	3.67E-04	3.51E-02
A_51_P222936	Fmnl2	formin-like 2	0.82	3.68E-04	3.51E-02
A_51_P501145	Lef1	lymphoid enhancer binding factor 1	1.05	3.70E-04	3.52E-02
A_51_P394394	Tspan2	tetraspanin 2	2.94	3.72E-04	3.52E-02
A_51_P114002	Gstm7	glutathione S-transferase, mu 7	1.42	3.81E-04	3.59E-02
A_51_P397876	En2	engrailed 2	1.13	3.82E-04	3.59E-02
A_51_P394269	Spg20	spastic paraplegia 20, spartin (Troyer syndrome) homolog (human)	1.3	3.85E-04	3.60E-02
A_51_P349495	Mboat1	membrane bound O-acyltransferase domain containing 1	2.2	3.88E-04	3.61E-02
A_51_P454696	Mtarc1	mitochondrial amidoxime reducing component 1	1.39	3.89E-04	3.61E-02
A_51_P423085	Cyp2j11	cytochrome P450, family 2, subfamily j, polypeptide 11	1.09	3.90E-04	3.61E-02
A_51_P480169	S1pr5	sphingosine-1-phosphate receptor 5	3.1	3.95E-04	3.61E-02
A_51_P370975	Ptp4a1	protein tyrosine phosphatase 4a1	0.81	3.94E-04	3.61E-02
A_51_P273489	Acap1	ArfGAP with coiled-coil, ankyrin repeat and PH domains 1	0.86	4.00E-04	3.61E-02
A_51_P365152	Hs3st1	heparan sulfate (glucosamine) 3-O-sulfotransferase 1	1.38	4.01E-04	3.61E-02
A_51_P327751	Ifit1	interferon-induced protein with tetratricopeptide repeats 1	1.06	4.01E-04	3.61E-02
A_52_P401640	Bpgm	2,3-bisphosphoglycerate mutase	1.36	4.01E-04	3.61E-02
A_51_P280117	Padi2	peptidyl arginine deiminase, type II	2.11	4.03E-04	3.62E-02
A_52_P684647	Ptk2b	PTK2 protein tyrosine kinase 2 beta	-1.51	4.07E-04	3.63E-02
A_51_P259029	Dusp26	dual specificity phosphatase 26 (putative)	1.09	4.11E-04	3.66E-02
A_51_P465445	Map4	microtubule-associated protein 4	1.2	4.14E-04	3.67E-02
A_51_P503822	Slitrk6	SLIT and NTRK-like family, member 6	1.33	4.27E-04	3.72E-02
A_51_P304469	Stxbp3	syntaxin binding protein 3	1.25	4.29E-04	3.72E-02
A_52_P467814	Il1rap	interleukin 1 receptor accessory protein	1.57	4.30E-04	3.72E-02
A_52_P1100511	Gm10791	predicted gene 10791	1.28	4.32E-04	3.72E-02
A_51_P311476	Rgma	repulsive guidance molecule family member A	0.85	4.43E-04	3.76E-02
A_51_P232617	Spag17	sperm associated antigen 17	1.16	4.44E-04	3.76E-02
A_51_P502026	Rab33b	RAB33B, member RAS oncogene family	0.92	4.44E-04	3.76E-02
A_51_P146633	Bicc1	BicC family RNA binding protein 1	1.3	4.45E-04	3.76E-02
A_51_P224263	Adi1	acireductone dioxygenase 1	1.14	4.46E-04	3.76E-02
A_52_P565427	Myo6	myosin VI	1	4.52E-04	3.77E-02
A_52_P174346	Mia	melanoma inhibitory activity	1.97	4.56E-04	3.79E-02
A_51_P151862	Lims2	LIM and senescent cell antigen like domains 2	1.01	4.55E-04	3.79E-02
A_51_P240476	Dnah11	dynein, axonemal, heavy chain 11	1.37	4.62E-04	3.81E-02
A_51_P181297	Serp1b1a	serine (or cysteine) peptidase inhibitor, clade B, member 1a	3.08	4.72E-04	3.84E-02

A_52_P224844	Cfap61	cilia and flagella associated protein 61	1.21	4.70E-04	3.84E-02
A_52_P219266	Frmd8	FERM domain containing 8	1.82	4.74E-04	3.84E-02
A_51_P431018	Selenbp2	selenium binding protein 2	0.97	4.73E-04	3.84E-02
A_51_P403636	Smad7	SMAD family member 7	1.2	4.74E-04	3.84E-02
A_52_P134228	Lsm11	U7 snRNP-specific Sm-like protein LSM11	-0.91	4.76E-04	3.84E-02
A_52_P676510	Tgtp1	T cell specific GTPase 1	1.47	4.78E-04	3.84E-02
A_51_P127681	Clic4	chloride intracellular channel 4 (mitochondrial)	1.46	4.78E-04	3.84E-02
A_51_P455866	Elf5	E74-like factor 5	1.26	4.81E-04	3.85E-02
A_51_P376883	Ift43	intraflagellar transport 43	0.96	4.83E-04	3.85E-02
A_51_P500002	Sema6d	sema domain, transmembrane domain (TM), and cytoplasmic domain, (semaphorin) 6D	1.17	4.85E-04	3.86E-02
A_51_P458008	Wscd1	WSC domain containing 1	1.1	4.91E-04	3.89E-02
A_51_P135832	Fermt2	fermitin family member 2	0.92	4.99E-04	3.91E-02
A_52_P581390	Kif1c	kinesin family member 1C	1.13	4.99E-04	3.91E-02
A_52_P329451	Mbp	myelin basic protein	3.06	5.07E-04	3.92E-02
A_51_P409101	Cdhr4	cadherin-related family member 4	2.38	5.08E-04	3.92E-02
A_51_P430950	Rdx	radixin	1.44	5.04E-04	3.92E-02
A_51_P237307	Plekhh1	pleckstrin homology domain containing, family G (with RhoGef domain) member 1	1.83	5.05E-04	3.92E-02
A_52_P458806	5430414B12Rik	RIKEN cDNA 5430414B12 gene	1.25	5.05E-04	3.92E-02
A_52_P252305	Fam177a	family with sequence similarity 177, member A	0.98	5.10E-04	3.92E-02
A_51_P286172	Lzts2	leucine zipper, putative tumor suppressor 2	1.23	5.14E-04	3.94E-02
A_51_P401974	Enpp2	ectonucleotide pyrophosphatase/phosphodiesterase 2	2.75	5.19E-04	3.96E-02
A_51_P422369	Odf3b	outer dense fiber of sperm tails 3B	1.79	5.28E-04	4.02E-02
A_52_P597618	Acs11	acyl-CoA synthetase long-chain family member 1	1.12	5.33E-04	4.04E-02
A_52_P423222	Nfe2l3	nuclear factor, erythroid derived 2, like 3	1.85	5.37E-04	4.05E-02
A_51_P502964	Tmem63a	transmembrane protein 63a	2.47	5.42E-04	4.05E-02
A_51_P194853	Sec14l4	SEC14-like lipid binding 4	1.21	5.39E-04	4.05E-02
A_52_P682382	Scd1	stearoyl-Coenzyme A desaturase 1	1.77	5.42E-04	4.05E-02
A_52_P241751	2700046A07Rik	RIKEN cDNA 2700046A07 gene	1.73	5.47E-04	4.06E-02
A_51_P135012	Rhpn2	rhophilin, Rho GTPase binding protein 2	1.35	5.48E-04	4.06E-02
A_52_P628702	Cntn2	contactin 2	2.06	5.57E-04	4.08E-02
A_51_P390446	Pacs2	phosphofurin acidic cluster sorting protein 2	1.88	5.63E-04	4.08E-02
A_51_P313896	Anln	anillin, actin binding protein	2.54	5.63E-04	4.08E-02
A_51_P325491	Josd2	Josephin domain containing 2	1.5	5.62E-04	4.08E-02
A_51_P217695	Cfap157	cilia and flagella associated protein 157	1.31	5.63E-04	4.08E-02
A_51_P402617	Nkx6-2	NK6 homeobox 2	2.92	5.69E-04	4.08E-02
A_51_P170536	Mycbpap	MYCBP associated protein	1.48	5.67E-04	4.08E-02
A_51_P377856	Gstt3	glutathione S-transferase, theta 3	1.48	5.68E-04	4.08E-02
A_52_P573255	Cdc42ep1	CDC42 effector protein (Rho)	1.56	5.69E-04	4.08E-02

		GTPase binding) 1			
A_51_P325173	Tpm1	tropomyosin 1, alpha	0.99	5.71E-04	4.09E-02
A_52_P94516	Camk4	calcium/calmodulin-dependent protein kinase IV	-1.24	5.75E-04	4.10E-02
A_51_P105589	Eci1	enoyl-Coenzyme A delta isomerase 1	0.81	5.77E-04	4.11E-02
A_51_P376959	Tmeff2	transmembrane protein with EGF-like and two follistatin-like domains 2	1.49	5.80E-04	4.11E-02
A_51_P234044	I190005I06Rik	RIKEN cDNA 1190005I06 gene	1.22	5.81E-04	4.11E-02
A_51_P338208	Pde1c	phosphodiesterase 1C	0.85	5.84E-04	4.12E-02
A_51_P255657	Misp3	MISP family member 3	1.88	5.86E-04	4.12E-02
A_52_P377160	Galnt6	polypeptide N-acetylgalactosaminyltransferase 6	1.63	5.88E-04	4.12E-02
A_51_P266683	Efna1	ephrin A1	0.92	5.92E-04	4.14E-02
A_51_P479618	Rdh5	retinol dehydrogenase 5	1.59	6.01E-04	4.19E-02
A_51_P296487	Lss	lanosterol synthase	0.93	6.03E-04	4.19E-02
A_51_P433192	Bcas1	breast carcinoma amplified sequence 1	2.15	6.10E-04	4.20E-02
A_51_P294643	Cdr2	cerebellar degeneration-related 2	1.42	6.08E-04	4.20E-02
A_51_P367136	Foxn3	forkhead box N3	1.38	6.09E-04	4.20E-02
A_51_P238523	Shisa4	shisa family member 4	0.99	6.15E-04	4.22E-02
A_52_P308542	Ywhaq	tyrosine 3-monooxygenase/tryptophan 5-monooxygenase activation protein theta	0.89	6.22E-04	4.25E-02
A_51_P390285	Larp6	La ribonucleoprotein domain family, member 6	1.11	6.25E-04	4.25E-02
A_51_P393567	I110017D15Rik	RIKEN cDNA 1110017D15 gene	1.5	6.25E-04	4.25E-02
A_52_P663686	Ifit3b	interferon-induced protein with tetratricopeptide repeats 3B	1.07	6.30E-04	4.26E-02
A_51_P430033	Ccdc13	coiled-coil domain containing 13	1.66	6.31E-04	4.26E-02
A_51_P109541	E130308A19Rik	RIKEN cDNA E130308A19 gene	1.15	6.32E-04	4.26E-02
A_51_P470205	Mob3b	MOB kinase activator 3B	1.48	6.37E-04	4.27E-02
A_51_P413005	Chn2	chimerin 2	1.24	6.37E-04	4.27E-02
A_52_P164161	Cyp51	cytochrome P450, family 51	1.06	6.45E-04	4.32E-02
A_51_P308446	I700094D03Rik	RIKEN cDNA 1700094D03 gene	1.09	6.50E-04	4.33E-02
A_51_P326942	Nsdhl	NAD(P) dependent steroid dehydrogenase-like	0.93	6.57E-04	4.33E-02
A_51_P242634	Dusp16	dual specificity phosphatase 16	1.09	6.60E-04	4.33E-02
A_51_P285669	Pigz	phosphatidylinositol glycan anchor biosynthesis, class Z	2.39	6.67E-04	4.33E-02
A_51_P282760	Per2	period circadian clock 2	-1.19	6.67E-04	4.33E-02
A_52_P271140	Dnaaf1	dynein, axonemal assembly factor 1	1.13	6.68E-04	4.33E-02
A_51_P203955	Gbp2	guanylate binding protein 2	1.29	6.69E-04	4.33E-02
A_51_P393934	Cd82	CD82 antigen	2.41	6.74E-04	4.33E-02
A_51_P457187	Tnfrsf13c	tumor necrosis factor receptor superfamily, member 13c	1.03	6.75E-04	4.33E-02
A_52_P390345	Efcab14	EF-hand calcium binding domain 14	1.16	6.75E-04	4.33E-02
A_51_P201137	Lbr	lamin B receptor	0.87	6.76E-04	4.33E-02

A_52_P271085	Slc5a11	solute carrier family 5 (sodium/glucose cotransporter), member 11	2.03	6.80E-04	4.34E-02
A_52_P497534	Wipi1	WD repeat domain, phosphoinositide interacting 1	1.19	6.82E-04	4.34E-02
A_52_P321978	Cldn34c1	claudin 34C1	1.07	6.83E-04	4.34E-02
A_51_P476481	Cyp2j13	cytochrome P450, family 2, subfamily j, polypeptide 13	0.97	6.84E-04	4.34E-02
A_51_P480233	Nmr11	NmrA-like family domain containing 1	1.98	6.88E-04	4.35E-02
A_51_P219918	Tmem125	transmembrane protein 125	3.39	6.98E-04	4.35E-02
A_51_P329975	Ninj2	ninjurin 2	2.21	7.02E-04	4.35E-02
A_52_P300500	Gphn	gephyrin	1.02	6.96E-04	4.35E-02
A_51_P461319	Gatm	glycine amidinotransferase (L-arginine:glycine amidinotransferase)	1.9	7.04E-04	4.35E-02
A_51_P304397	Cpm	carboxypeptidase M	2.04	7.06E-04	4.35E-02
A_51_P517381	Cers2	ceramide synthase 2	2.01	7.22E-04	4.40E-02
A_51_P327405	Gbp8	guanylate-binding protein 8	0.87	7.21E-04	4.40E-02
A_52_P38436	Baiap2	brain-specific angiogenesis inhibitor 1-associated protein 2	-1.05	7.29E-04	4.43E-02
A_51_P293307	Hepacam	hepatocyte cell adhesion molecule	0.79	7.36E-04	4.43E-02
A_52_P151974	Clcn5	chloride channel, voltage-sensitive 5	0.93	7.36E-04	4.43E-02
A_52_P436564	Cdh20	cadherin 20	1.12	7.37E-04	4.43E-02
A_51_P259975	Aspa	aspartoacylase	3.21	7.40E-04	4.44E-02
A_51_P240136	Gng8	guanine nucleotide binding protein (G protein), gamma 8	2.5	7.43E-04	4.44E-02
A_51_P351872	Slc6a9	solute carrier family 6 (neurotransmitter transporter, glycine), member 9	1.54	7.45E-04	4.44E-02
A_52_P559957	MacroD1	mono-ADP ribosylhydrolase 1	0.94	7.49E-04	4.45E-02
A_52_P445239	Plp1	proteolipid protein (myelin) 1	3.38	7.71E-04	4.50E-02
A_51_P202980	Ernm	ermin, ERM-like protein	2.48	7.75E-04	4.50E-02
A_51_P135389	Zfp474	zinc finger protein 474	1.63	7.69E-04	4.50E-02
A_52_P591740	Usp54	ubiquitin specific peptidase 54	1.08	7.69E-04	4.50E-02
A_51_P287001	Fxyd1	FXYD domain-containing ion transport regulator 1	1.42	7.74E-04	4.50E-02
A_51_P118246	Fam161a	family with sequence similarity 161, member A	1.15	7.75E-04	4.50E-02
A_51_P162232	Slc35a2	solute carrier family 35 (UDP-galactose transporter), member A2	0.91	7.78E-04	4.51E-02
A_52_P85040	Mog	myelin oligodendrocyte glycoprotein	3.27	7.82E-04	4.52E-02
A_51_P112912	Rras2	related RAS viral (r-ras) oncogene 2	0.74	7.86E-04	4.54E-02
A_52_P223626	Olig2	oligodendrocyte transcription factor 2	1.45	7.93E-04	4.56E-02
A_52_P494168	Prr18	proline rich 18	3.24	7.98E-04	4.56E-02
A_51_P478569	Adamts11	ADAMTS-like 1	1.19	7.99E-04	4.56E-02
A_51_P412966	Lrrn1	leucine rich repeat protein 1, neuronal	1.43	8.00E-04	4.56E-02
A_52_P421357	Clip1	CAP-GLY domain containing	-0.84	8.01E-04	4.56E-02

		linker protein 1			
A_51_P420415	Srd5a1	steroid 5 alpha-reductase 1	1.61	8.09E-04	4.57E-02
A_52_P670026	Rsad2	radical S-adenosyl methionine domain containing 2	1.14	8.11E-04	4.57E-02
A_52_P51548	Pard3	par-3 family cell polarity regulator	1	8.11E-04	4.57E-02
A_52_P1083765	Gm16124	predicted gene 16124	0.82	8.18E-04	4.59E-02
A_51_P308290	Cerox1	cytoplasmic endogenous regulator of oxidative phosphorylation 1	1.05	8.20E-04	4.59E-02
A_51_P115526	Ccdc146	coiled-coil domain containing 146	1.1	8.21E-04	4.59E-02
A_51_P228295	Mpz11	myelin protein zero-like 1	0.93	8.22E-04	4.59E-02
A_52_P557265	Cyp39a1	cytochrome P450, family 39, subfamily a, polypeptide 1	1.11	8.32E-04	4.63E-02
A_52_P698715	Lhx1os	LIM homeobox 1, opposite strand	1.46	8.34E-04	4.63E-02
A_51_P425232	Rcbtb1	regulator of chromosome condensation (RCC1) and BTB (POZ) domain containing protein 1	1.38	8.35E-04	4.63E-02
A_51_P188135	Fbxo7	F-box protein 7	1.16	8.38E-04	4.64E-02
A_52_P495565	Efnb3	ephrin B3	2.39	8.45E-04	4.66E-02
A_51_P249286	Rgs16	regulator of G-protein signaling 16	0.91	8.44E-04	4.66E-02
A_52_P639751	Akap14	A kinase (PRKA) anchor protein 14	1.39	8.50E-04	4.67E-02
A_51_P208361	Ak3	adenylate kinase 3	0.73	8.54E-04	4.69E-02
A_52_P623053	Add2	adducin 2 (beta)	-0.91	8.69E-04	4.75E-02
A_52_P210893	Litaf	LPS-induced TN factor	1.86	8.76E-04	4.76E-02
A_51_P119760	H2-Aa	histocompatibility 2, class II antigen A, alpha	1.22	8.76E-04	4.76E-02
A_51_P297388	Spat24	spermatogenesis associated 24	1.05	8.77E-04	4.76E-02
A_52_P561690	BC034090	cDNA sequence BC034090	1.19	8.79E-04	4.76E-02
A_52_P590339	Kazn	kazrin, periplakin interacting protein	1.24	8.85E-04	4.78E-02
A_52_P557249	Fam107b	family with sequence similarity 107, member B	1.2	8.86E-04	4.78E-02
A_51_P284608	Cd74	CD74 antigen (invariant polypeptide of major histocompatibility complex, class II antigen-associated)	1.24	8.92E-04	4.78E-02
A_51_P516741	Tmprss5	transmembrane protease, serine 5 (spinesin)	2.14	9.02E-04	4.80E-02
A_51_P505823	Endod1	endonuclease domain containing 1	1.07	8.97E-04	4.80E-02
A_51_P386344	Mtmr10	myotubularin related protein 10	1.03	9.02E-04	4.80E-02
A_51_P458839	Piga	phosphatidylinositol glycan anchor biosynthesis, class A	1.52	9.03E-04	4.80E-02
A_52_P521122	Lyst	lysosomal trafficking regulator	-0.88	9.14E-04	4.85E-02
A_52_P431662	Lap3	leucine aminopeptidase 3	1.05	9.18E-04	4.85E-02
A_52_P188423	Lrrfip1	leucine rich repeat (in FLII) interacting protein 1	-0.94	9.18E-04	4.85E-02
A_52_P273821	Abhd5	abhydrolase domain containing 5	0.86	9.21E-04	4.85E-02
A_52_P48767	Rassf8	Ras association (RalGDS/AF-6) domain family (N-terminal) member 8	0.99	9.24E-04	4.86E-02
A_51_P174696	Casq2	calsequestrin 2	0.9	9.28E-04	4.86E-02

A_51_P270960	Ppp2r3a	protein phosphatase 2, regulatory subunit B", alpha	1.06	9.30E-04	4.86E-02
A_52_P2745	2010001K21Rik	RIKEN cDNA 2010001K21 gene	1.31	9.34E-04	4.86E-02
A_51_P178392	Cfap70	cilia and flagella associated protein 70	1.26	9.35E-04	4.86E-02
A_51_P254045	Traip	TRAF-interacting protein	-1.31	9.39E-04	4.86E-02
A_51_P270005	Lrguk	leucine-rich repeats and guanylate kinase domain containing	0.92	9.40E-04	4.86E-02
A_51_P221291	Sntb2	syntrophin, basic 2	-1.14	9.54E-04	4.92E-02
A_51_P252677	Card19	caspase recruitment domain family, member 19	1.28	9.58E-04	4.92E-02
A_51_P230734	Slc34a3	solute carrier family 34 (sodium phosphate), member 3	2.15	9.61E-04	4.93E-02
A_52_P8197	Slc17a6	solute carrier family 17 (sodium-dependent inorganic phosphate cotransporter), member 6	1.22	9.67E-04	4.93E-02
A_52_P466147	Rarres2	retinoic acid receptor responder (tazarotene induced) 2	1.84	9.75E-04	4.93E-02
A_51_P499071	Mal	myelin and lymphocyte protein, T cell differentiation protein	3.67	9.75E-04	4.93E-02
A_51_P234407	Tjp3	tight junction protein 3	1.26	9.70E-04	4.93E-02
A_51_P459320	Gkap1	G kinase anchoring protein 1	0.83	9.76E-04	4.93E-02
A_51_P414762	Pkp4	plakophilin 4	1.3	9.78E-04	4.93E-02
A_52_P714957	Slit3	slit guidance ligand 3	-1.57	9.85E-04	4.96E-02
A_52_P316474	St3gal4	ST3 beta-galactoside alpha-2,3-sialyltransferase 4	1	9.91E-04	4.97E-02

Supplementary Table 8. DEGs in CC from mice which underwent remyelination compared to mice treated with cuprizone for 4 weeks.

Probe ID	Symbol	Gene Name	logFC	p-value	adj.p-value
A_51_P329975	Ninj2	ninjurin 2	1.86	6.35E-07	4.60E-03
A_52_P169614	Mog	myelin oligodendrocyte glycoprotein	3.13	7.39E-07	4.60E-03
A_51_P114941	Cyp3a13	cytochrome P450, family 3, subfamily a, polypeptide 13	1.34	7.49E-07	4.60E-03
A_51_P331570	Trib3	tribbles pseudokinase 3	-3.16	7.56E-07	4.60E-03
A_52_P652729	Gm5067	ribosome biogenesis regulatory protein homolog	2.93	1.52E-06	7.10E-03
A_51_P125725	Sh3gl3	SH3-domain GRB2-like 3	1.87	2.47E-06	7.10E-03
A_51_P209372	Msmo1	methylsterol monooxygenase 1	1.47	2.58E-06	7.10E-03
A_52_P672437	E330037M01Rik	RIKEN cDNA E330037M01 gene	3.05	2.84E-06	7.10E-03
A_52_P439502	Plekhh1	pleckstrin homology domain containing, family H (with MyTH4 domain) member 1	2.28	2.93E-06	7.10E-03
A_52_P393392	Insig1	insulin induced gene 1	1.39	3.13E-06	7.10E-03
A_51_P264666	Col11a2	collagen, type XI, alpha 2	1.42	3.21E-06	7.10E-03
A_52_P479038	Ccp110	centriolar coiled coil protein 110	1.52	3.73E-06	7.58E-03
A_52_P634098	B230206H07Rik	RIKEN cDNA B230206H07 gene	1.6	4.85E-06	8.28E-03

A_52_P39314	Speer4cos	spermatogenesis associated glutamate (E)-rich protein 4C, opposite strand transcript	2.03	5.67E-06	8.28E-03
A_51_P519251	Nupr1	nuclear protein transcription regulator 1	-2.91	6.28E-06	8.28E-03
A_51_P499071	Mal	myelin and lymphocyte protein, T cell differentiation protein	3.82	7.10E-06	8.28E-03
A_51_P384230	Sgk2	serum/glucocorticoid regulated kinase 2	3.07	7.23E-06	8.28E-03
A_51_P458839	Piga	phosphatidylinositol glycan anchor biosynthesis, class A	1.48	7.31E-06	8.28E-03
A_51_P477692	Fa2h	fatty acid 2-hydroxylase	3.3	7.94E-06	8.28E-03
A_52_P299684	Zdhc9	zinc finger, DHHC domain containing 9	1.35	8.24E-06	8.28E-03
A_51_P442497	Ano4	anoctamin 4	0.98	8.30E-06	8.28E-03
A_51_P411694	Carns1	carnosine synthase 1	1.42	8.46E-06	8.28E-03
A_51_P313896	Anln	anillin, actin binding protein	2.54	8.58E-06	8.28E-03
A_52_P328304	Plekhg3	pleckstrin homology domain containing, family G (with RhoGef domain) member 3	2.37	8.70E-06	8.28E-03
A_52_P274287	Nipal4	NIPA-like domain containing 4	0.74	9.31E-06	8.28E-03
A_51_P468140	Serpind1	serine (or cysteine) peptidase inhibitor, clade D, member 1	1.96	1.01E-05	8.28E-03
A_51_P185575	Adamtsl4	ADAMTS-like 4	1.08	1.02E-05	8.28E-03
A_51_P358354	Jam3	junction adhesion molecule 3	1.48	1.05E-05	8.28E-03
A_51_P120305	Elov11	elongation of very long chain fatty acids (FEN1/Elo2, SUR4/Elo3, yeast)-like 1	1.4	1.10E-05	8.28E-03
A_51_P104710	Sspo	SCO-spondin	1.25	1.13E-05	8.28E-03
A_51_P351872	Slc6a9	solute carrier family 6 (neurotransmitter transporter, glycine), member 9	1.53	1.13E-05	8.28E-03
A_51_P327369	Plekhg3	pleckstrin homology domain containing, family G (with RhoGef domain) member 3	1.71	1.24E-05	8.28E-03
A_51_P486971	Tex52	testis expressed 52	1.16	1.26E-05	8.28E-03
A_51_P395546	Phldb1	pleckstrin homology like domain, family B, member 1	2.37	1.27E-05	8.28E-03
A_51_P257258	Cpox	coproporphyrinogen oxidase	1.31	1.32E-05	8.28E-03
A_51_P330428	Eif4ebp1	eukaryotic translation initiation factor 4E binding protein 1	-1.67	1.33E-05	8.28E-03
A_51_P383991	Septin4	septin 4	2.41	1.41E-05	8.48E-03
A_52_P605266	Ptpd	protein tyrosine phosphatase, receptor type, D	1.37	1.44E-05	8.48E-03
A_51_P194181	Dock5	dedicator of cytokinesis 5	1.99	1.46E-05	8.48E-03
A_51_P259968	Aspa	aspartoacylase	2.28	1.54E-05	8.70E-03
A_51_P342050	ErbB3	erb-b2 receptor tyrosine kinase 3	0.89	1.66E-05	8.76E-03
A_51_P381683	Aatk	apoptosis-associated tyrosine kinase	1.34	1.74E-05	9.01E-03
A_51_P374457	Gstp1	glutathione S-transferase, pi 1	0.98	1.92E-05	9.32E-03
A_52_P269672	Sox8	SRY (sex determining region Y)-box 8	1.54	1.94E-05	9.32E-03

A_51_P253527	Rffl	ring finger and FYVE like domain containing protein	1.32	1.95E-05	9.32E-03
A_52_P232763	Map7	microtubule-associated protein 7	1.39	2.06E-05	9.58E-03
A_51_P232748	Plxnb3	plexin B3	2.4	2.09E-05	9.58E-03
A_51_P425232	Rcbt1	regulator of chromosome condensation (RCC1) and BTB (POZ) domain containing protein 1	1.46	2.26E-05	1.02E-02
A_51_P517182	Plaat3	phospholipase A and acyltransferase 3	2.17	2.37E-05	1.05E-02
A_51_P228354	Trp53inp2	transformation related protein 53 inducible nuclear protein 2	1.19	2.40E-05	1.05E-02
A_51_P464838	Il17rb	interleukin 17 receptor B	1.25	2.49E-05	1.05E-02
A_51_P375987	Fign	fidgetin	1.42	2.49E-05	1.05E-02
A_51_P262563	Opalin	oligodendrocytic myelin paranodal and inner loop protein	1.3	2.58E-05	1.06E-02
A_51_P325491	Josd2	Josephin domain containing 2	1.3	2.61E-05	1.06E-02
A_51_P506822	Ugt8a	UDP galactosyltransferase 8A	2.79	2.85E-05	1.14E-02
A_51_P390446	Pacs2	phosphofurin acidic cluster sorting protein 2	1.93	2.98E-05	1.17E-02
A_51_P234944	Adams4	a disintegrin-like and metallopeptidase (reprolysin type) with thrombospondin type 1 motif, 4	1.81	3.20E-05	1.24E-02
A_52_P343916	A730008I21Rik	RIKEN cDNA A730008I21 gene	0.83	3.30E-05	1.25E-02
A_51_P230734	Slc34a3	solute carrier family 34 (sodium phosphate), member 3	1.6	3.47E-05	1.28E-02
A_51_P176661	Tprn	taperin	1.9	3.68E-05	1.32E-02
A_51_P269216	Atf5	activating transcription factor 5	-2.34	3.88E-05	1.37E-02
A_51_P175424	Car14	carbonic anhydrase 14	2.1	4.13E-05	1.43E-02
A_52_P628702	Cntn2	contactin 2	1.82	4.17E-05	1.43E-02
A_51_P376959	Tmeff2	transmembrane protein with EGF-like and two follistatin-like domains 2	1.26	4.23E-05	1.43E-02
A_52_P377160	Galnt6	polypeptide N-acetylgalactosaminyltransferase 6	1.2	4.53E-05	1.50E-02
A_51_P490867	Enpp4	ectonucleotide pyrophosphatase/phosphodiesterase 4	1.33	4.75E-05	1.50E-02
A_51_P187612	Desi1	desumoylating isopeptidase 1	1.5	4.82E-05	1.50E-02
A_52_P271085	Slc5a11	solute carrier family 5 (sodium/glucose cotransporter), member 11	1.54	4.87E-05	1.50E-02
A_51_P105927	Rasl12	RAS-like, family 12	0.95	5.04E-05	1.50E-02
A_52_P68087	Enpp6	ectonucleotide pyrophosphatase/phosphodiesterase 6	1.13	5.06E-05	1.50E-02
A_52_P610872	Speer4b	spermatogenesis associated glutamate (E)-rich protein 4B	0.7	5.11E-05	1.50E-02
A_52_P980644	Gnb4	guanine nucleotide binding protein (G protein), beta 4	0.81	5.12E-05	1.50E-02
A_51_P199494	Cacna2d4	calcium channel, voltage-dependent, alpha 2/delta subunit 4	1.75	5.16E-05	1.50E-02
A_51_P403636	Smad7	SMAD family member 7	1.32	5.24E-05	1.50E-02

A_51_P517381	Cers2	ceramide synthase 2	2	5.25E-05	1.50E-02
A_51_P304397	Cpm	carboxypeptidase M	1.94	5.25E-05	1.50E-02
A_51_P346704	Sox10	SRY (sex determining region Y)-box 10	1.6	5.40E-05	1.50E-02
A_52_P145975	Dync1li2	dynein, cytoplasmic 1 light intermediate chain 2	0.84	5.44E-05	1.50E-02
A_51_P439612	Dnajb2	DnaJ heat shock protein family (Hsp40) member B2	1.5	5.58E-05	1.51E-02
A_51_P367136	Foxn3	forkhead box N3	1.31	5.60E-05	1.51E-02
A_52_P27871	Fnbp1	formin binding protein 1	1.33	5.64E-05	1.51E-02
A_51_P355702	Trpv3	transient receptor potential cation channel, subfamily V, member 3	0.68	5.77E-05	1.51E-02
A_51_P219109	Il12rb1	interleukin 12 receptor, beta 1	1.92	5.81E-05	1.51E-02
A_51_P420415	Srd5a1	steroid 5 alpha-reductase 1	1.5	5.95E-05	1.51E-02
A_52_P427024	Ldlr	low density lipoprotein receptor	1.77	5.95E-05	1.51E-02
A_52_P354682	Elovl7	ELOVL family member 7, elongation of long chain fatty acids (yeast)	1.94	5.96E-05	1.51E-02
A_51_P349495	Mboat1	membrane bound O-acyltransferase domain containing 1	2.1	6.29E-05	1.55E-02
A_51_P138060	Rnf13	ring finger protein 13	0.9	6.43E-05	1.56E-02
A_52_P633597	Rftn1	raftlin lipid raft linker 1	1.42	6.57E-05	1.56E-02
A_52_P149801	Pde4b	phosphodiesterase 4B, cAMP specific	1.48	6.62E-05	1.56E-02
A_52_P266916	Otud7b	OTU domain containing 7B	1.43	6.63E-05	1.56E-02
A_51_P346165	Agpat4	1-acylglycerol-3-phosphate O-acyltransferase 4 (lysophosphatidic acid acyltransferase, delta)	1.08	6.73E-05	1.56E-02
A_52_P690855	Fndc11	fibronectin type III domain containing 11	1.27	6.80E-05	1.56E-02
A_52_P219266	Frmf8	FERM domain containing 8	1.74	6.80E-05	1.56E-02
A_51_P176474	Kndc1	kinase non-catalytic C-lobe domain (KIND) containing 1	1.45	7.19E-05	1.62E-02
A_51_P438752	Gm4221	predicted gene 4221	0.94	7.20E-05	1.62E-02
A_51_P221990	Micall1	microtubule associated monooxygenase, calponin and LIM domain containing -like 1	2.08	7.25E-05	1.62E-02
A_52_P155554	Cdc42ep2	CDC42 effector protein (Rho GTPase binding) 2	1.88	7.42E-05	1.64E-02
A_51_P291224	Mobp	myelin-associated oligodendrocytic basic protein	3.24	7.66E-05	1.65E-02
A_52_P268206	Mcam	melanoma cell adhesion molecule	0.75	7.85E-05	1.65E-02
A_51_P146701	Nsdhl	NAD(P) dependent steroid dehydrogenase-like	1.16	7.92E-05	1.65E-02
A_52_P267600	Mobp	myelin-associated oligodendrocytic basic protein	3.7	7.95E-05	1.65E-02
A_51_P290986	Dhcr7	7-dehydrocholesterol reductase	1.1	8.02E-05	1.65E-02
A_52_P43727	5031439G07Rik	RIKEN cDNA 5031439G07 gene	1.45	8.03E-05	1.65E-02
A_52_P540072	Edil3	EGF-like repeats and discoidin I-like domains 3	0.81	8.05E-05	1.65E-02
A_51_P268439	Mcam	melanoma cell adhesion molecule	2.17	8.15E-05	1.65E-02
A_51_P509518	Ralgds	ral guanine nucleotide dissociation stimulator	1.04	8.31E-05	1.65E-02

A_52_P276748	Daam1	dishevelled associated activator of morphogenesis 1	1	8.31E-05	1.65E-02
A_52_P263068	Rhog	ras homolog family member G	1.69	8.40E-05	1.65E-02
A_52_P331824	Nfasc	neurofascin	1.35	8.42E-05	1.65E-02
A_52_P679101	Tjp2	tight junction protein 2	1.11	8.50E-05	1.65E-02
A_52_P523516	Hapln2	hyaluronan and proteoglycan link protein 2	2.3	8.52E-05	1.65E-02
A_52_P507802	Lpar1	lysophosphatidic acid receptor 1	2.44	8.68E-05	1.65E-02
A_51_P479230	Nat8	N-acetyltransferase 8 (GCN5-related)	-0.92	8.74E-05	1.65E-02
A_52_P244463	D16Erd472e	DNA segment, Chr 16, ERATO Doi 472, expressed	1.73	8.90E-05	1.65E-02
A_51_P516741	Tmprss5	transmembrane protease, serine 5 (spinesin)	1.66	8.91E-05	1.65E-02
A_51_P218953	Zfp536	zinc finger protein 536	1.54	9.02E-05	1.65E-02
A_52_P108243	Pde1c	phosphodiesterase 1C	0.72	9.06E-05	1.65E-02
A_51_P351883	Usp54	ubiquitin specific peptidase 54	1.55	9.07E-05	1.65E-02
A_52_P255849	Tlcd3a	TLC domain containing 3A	0.9	9.10E-05	1.65E-02
A_52_P211737	Myo1d	myosin ID	1.16	9.11E-05	1.65E-02
A_52_P238468	Gipr	gastric inhibitory polypeptide receptor	0.85	9.22E-05	1.65E-02
A_51_P234113	Nod1	nucleotide-binding oligomerization domain containing 1	1.3	9.33E-05	1.65E-02
A_52_P211863	Speer8-ps1	spermatogenesis associated glutamate (E)-rich protein 8, pseudogene 1	0.79	9.38E-05	1.65E-02
A_52_P41520	Nkain2	Na+/K+ transporting ATPase interacting 2	0.88	9.42E-05	1.65E-02
A_51_P432504	Pcyt2	phosphate cytidyltransferase 2, ethanolamine	0.98	9.49E-05	1.65E-02
A_51_P265151	Arhgef10	Rho guanine nucleotide exchange factor (GEF) 10	1.37	9.55E-05	1.65E-02
A_51_P280117	Padi2	peptidyl arginine deiminase, type II	2.03	9.66E-05	1.66E-02
A_51_P350513	Bin1	bridging integrator 1	0.84	1.01E-04	1.69E-02
A_52_P200599	Secisbp2l	SECIS binding protein 2-like	0.98	1.01E-04	1.69E-02
A_51_P101347	Pls1	plastin 1 (I-isoform)	2.03	1.02E-04	1.69E-02
A_52_P156251	Tafa1	TAFA chemokine like family member 1	-0.99	1.04E-04	1.71E-02
A_52_P630964	Tspan2	tetraspanin 2	2.8	1.05E-04	1.71E-02
A_51_P122035	Nipa1	non imprinted in Prader-Willi/Angelman syndrome 1 homolog (human)	1.04	1.06E-04	1.71E-02
A_52_P802856	A1300008O04Rik	RIKEN cDNA A1300008O04 gene	1.83	1.07E-04	1.71E-02
A_51_P321126	Fasn	fatty acid synthase	0.66	1.08E-04	1.71E-02
A_52_P110791	Erbn	ErbB2 interacting protein	1.49	1.11E-04	1.74E-02
A_51_P376501	Stard9	START domain containing 9	0.75	1.11E-04	1.74E-02
A_51_P259029	Dusp26	dual specificity phosphatase 26 (putative)	0.93	1.11E-04	1.74E-02
A_51_P480233	Nmral1	NmrA-like family domain containing 1	2.08	1.15E-04	1.78E-02
A_51_P438924	Cmtm5	CKLF-like MARVEL transmembrane domain containing 5	1.83	1.19E-04	1.82E-02
A_51_P336070	Lct1	lactase-like	0.73	1.20E-04	1.83E-02
A_51_P424709	Nxph4	neurexophilin 4	0.97	1.23E-04	1.87E-02

A_52_P391000	Pde8a	phosphodiesterase 8A	1.89	1.26E-04	1.88E-02
A_51_P230439	Ppfibp2	PTPRF interacting protein, binding protein 2 (liprin beta 2)	1.55	1.26E-04	1.88E-02
A_52_P636752	Cyp51	cytochrome P450, family 51	1.02	1.29E-04	1.90E-02
A_51_P504863	Cdk18	cyclin-dependent kinase 18	1.33	1.30E-04	1.90E-02
A_51_P190740	Adssl1	adenylosuccinate synthetase like 1	1.45	1.35E-04	1.92E-02
A_51_P225793	Prr5l	proline rich 5 like	2.59	1.36E-04	1.92E-02
A_52_P62617	Gm9895	predicted gene 9895	2.05	1.36E-04	1.92E-02
A_51_P210992	4930506C21Rik	RIKEN cDNA 4930506C21 gene	0.91	1.38E-04	1.92E-02
A_51_P216742	Arhgap23	Rho GTPase activating protein 23	1.53	1.38E-04	1.92E-02
A_51_P251245	Pkp4	plakophilin 4	1.29	1.38E-04	1.92E-02
A_51_P200586	Marchf8	membrane associated ring-CH-type finger 8	1.21	1.39E-04	1.92E-02
A_51_P146941	Hmgcs1	3-hydroxy-3-methylglutaryl-Coenzyme A synthase 1	1.19	1.39E-04	1.92E-02
A_51_P418056	Sc5d	sterol-C5-desaturase	0.77	1.40E-04	1.92E-02
A_52_P527800	Emilin2	elastin microfibril interfacier 2	1.61	1.41E-04	1.92E-02
A_51_P450487	Sqle	squalene epoxidase	1.07	1.43E-04	1.95E-02
A_51_P234330	Rtkn	rhotekin	1	1.45E-04	1.97E-02
A_52_P559545	Cercam	cerebral endothelial cell adhesion molecule	0.66	1.49E-04	1.99E-02
A_51_P408382	Itgb4	integrin beta 4	2.84	1.50E-04	1.99E-02
A_52_P417437	Gab1	growth factor receptor bound protein 2-associated protein 1	1.12	1.51E-04	1.99E-02
A_52_P258116	Wnt3	wingless-type MMTV integration site family, member 3	1.79	1.54E-04	2.00E-02
A_52_P485007	Abca2	ATP-binding cassette, sub-family A (ABC1), member 2	1.67	1.57E-04	2.03E-02
A_51_P351948	Rap1a	RAS-related protein 1a	1.01	1.62E-04	2.08E-02
A_52_P390944	Chst3	carbohydrate sulfotransferase 3	1.29	1.64E-04	2.09E-02
A_52_P158800	Fgfr2	fibroblast growth factor receptor 2	1.38	1.67E-04	2.12E-02
A_51_P375862	Srpk3	serine/arginine-rich protein specific kinase 3	1.89	1.71E-04	2.14E-02
A_52_P459288	4930402H24Rik	RIKEN cDNA 4930402H24 gene	0.92	1.72E-04	2.14E-02
A_51_P398260	Tppp	tubulin polymerization promoting protein	0.77	1.74E-04	2.14E-02
A_52_P198435	Rasgrp3	RAS, guanyl releasing protein 3	1.14	1.74E-04	2.14E-02
A_52_P1067686	Dbndd2	dysbindin (dystrobrevin binding protein 1) domain containing 2	1.5	1.75E-04	2.14E-02
A_51_P401958	Taldo1	transaldolase 1	0.99	1.75E-04	2.14E-02
A_51_P468876	Dixdc1	DIX domain containing 1	1.15	1.76E-04	2.14E-02
A_52_P590339	Kazn	kazrin, periplakin interacting protein	1.09	1.79E-04	2.16E-02
A_51_P264835	Epn2	epsin 2	0.71	1.80E-04	2.16E-02
A_51_P458638	Spink8	serine peptidase inhibitor, Kazal type 8	-1.9	1.80E-04	2.16E-02
A_51_P134812	Chac1	ChaC, cation transport regulator 1	-1.43	1.81E-04	2.16E-02
A_51_P409452	Cldn11	claudin 11	2.89	1.82E-04	2.16E-02
A_51_P129464	Scd2	stearoyl-Coenzyme A desaturase 2	1.12	1.84E-04	2.17E-02

A_51_P255805	Fhdc1	FH2 domain containing 1	1.15	1.86E-04	2.19E-02
A_51_P113403	Slc26a11	solute carrier family 26, member 11	1.03	1.87E-04	2.19E-02
A_52_P568257	Sort1	sortilin 1	1.04	1.90E-04	2.20E-02
A_51_P167971	Bace1	beta-site APP cleaving enzyme 1	0.75	1.91E-04	2.20E-02
A_51_P452506	Tmem189	transmembrane protein 189	0.91	1.91E-04	2.20E-02
A_51_P273639	Slc7a5	solute carrier family 7 (cationic amino acid transporter, y+ system), member 5	-1.31	1.92E-04	2.20E-02
A_51_P277536	Ramp2	receptor (calcitonin) activity modifying protein 2	-0.72	1.94E-04	2.22E-02
A_51_P455647	Car2	carbonic anhydrase 2	2.1	1.99E-04	2.27E-02
A_52_P357745	Ypel2	yippee like 2	0.8	2.02E-04	2.29E-02
A_51_P520378	Atp1b3	ATPase, Na+/K+ transporting, beta 3 polypeptide	0.88	2.05E-04	2.31E-02
A_51_P459320	Gkap1	G kinase anchoring protein 1	0.84	2.07E-04	2.31E-02
A_52_P59285	2810410L24Rik	RIKEN cDNA 2810410L24 gene	0.69	2.08E-04	2.31E-02
A_51_P502964	Tmem63a	transmembrane protein 63a	2.45	2.08E-04	2.31E-02
A_52_P210893	Litaf	LPS-induced TN factor	1.74	2.16E-04	2.39E-02
A_51_P227392	Rhou	ras homolog family member U	1.39	2.16E-04	2.39E-02
A_52_P532982	Gdf15	growth differentiation factor 15	-2.19	2.22E-04	2.43E-02
A_52_P445239	Plp1	proteolipid protein (myelin) 1	3.36	2.24E-04	2.43E-02
A_52_P413280	Rhobtb3	Rho-related BTB domain containing 3	1	2.26E-04	2.44E-02
A_51_P193832	Rtkn2	rhotekin 2	1.6	2.28E-04	2.45E-02
A_51_P446315	Cdc37l1	cell division cycle 37-like 1	1.25	2.31E-04	2.47E-02
A_52_P630673	Gpr62	G protein-coupled receptor 62	2.49	2.32E-04	2.47E-02
A_52_P510592	Adams2	a disintegrin-like and metallopeptidase (reprolysin type) with thrombospondin type 1 motif, 2	0.89	2.39E-04	2.53E-02
A_51_P242043	Dhcr24	24-dehydrocholesterol reductase	1.14	2.48E-04	2.60E-02
A_52_P358860	Gss	glutathione synthetase	1.11	2.50E-04	2.61E-02
A_51_P480169	S1pr5	sphingosine-1-phosphate receptor 5	2.68	2.51E-04	2.61E-02
A_51_P200561	Shtn1	shootin 1	1.65	2.56E-04	2.65E-02
A_51_P273556	Fam83d	family with sequence similarity 83, member D	0.81	2.58E-04	2.67E-02
A_51_P378667	Wrap53	WD repeat containing, antisense to Trp53	0.76	2.69E-04	2.77E-02
A_51_P428086	Sptbn1	spectrin beta, non-erythrocytic 1	1.56	2.75E-04	2.79E-02
A_51_P285669	Pigz	phosphatidylinositol glycan anchor biosynthesis, class Z	2.25	2.76E-04	2.79E-02
A_51_P296487	Lss	lanosterol synthase	0.82	2.78E-04	2.79E-02
A_52_P497534	Wipi1	WD repeat domain, phosphoinositide interacting 1	1.03	2.79E-04	2.79E-02
A_51_P197043	Xrcc3	X-ray repair complementing defective repair in Chinese hamster cells 3	1.67	2.80E-04	2.79E-02
A_52_P374053	Jakmip3	janus kinase and microtubule interacting protein 3	0.95	2.84E-04	2.80E-02
A_52_P229278	Limch1	LIM and calponin homology domains 1	0.79	2.85E-04	2.80E-02

A_52_P603038	Olig1	oligodendrocyte transcription factor 1	1.69	2.85E-04	2.80E-02
A_52_P181610	Speer4a	spermatogenesis associated glutamate (E)-rich protein 4A	0.56	2.87E-04	2.80E-02
A_51_P426739	Gpt	glutamic pyruvic transaminase, soluble	1.14	2.89E-04	2.80E-02
A_52_P84315	Chd7	chromodomain helicase DNA binding protein 7	1.07	2.89E-04	2.80E-02
A_52_P515620	5033421B08Rik	RIKEN cDNA 5033421B08 gene	0.62	2.92E-04	2.80E-02
A_52_P234744	Mbnl2	muscleblind like splicing factor 2	0.97	2.92E-04	2.80E-02
A_52_P1075973	Gm35438	predicted gene, 35438	0.66	2.92E-04	2.80E-02
A_51_P466478	Ptpnf	protein tyrosine phosphatase, receptor type, F	1.03	2.96E-04	2.80E-02
A_52_P528996	Mxd4	Max dimerization protein 4	1.29	2.99E-04	2.80E-02
A_52_P27576	Stxbp3	syntaxin binding protein 3	1.33	2.99E-04	2.80E-02
A_52_P249826	Hhip	Hedgehog-interacting protein	1.37	2.99E-04	2.80E-02
A_52_P29583	Hipk2	homeodomain interacting protein kinase 2	0.91	3.01E-04	2.80E-02
A_52_P267564	Creb5	cAMP responsive element binding protein 5	1.34	3.02E-04	2.80E-02
A_52_P550325	Kcnj16	potassium inwardly-rectifying channel, subfamily J, member 16	-0.84	3.06E-04	2.82E-02
A_52_P787919	St6galnac3	ST6 (alpha-N-acetyl-neuraminyl-2,3-beta-galactosyl-1,3)-N-acetylgalactosaminide alpha-2,6-sialyltransferase 3	1.01	3.08E-04	2.83E-02
A_51_P484869	Gamt	guanidinoacetate methyltransferase	2.17	3.11E-04	2.84E-02
A_51_P467668	Cilk1	ciliogenesis associated kinase 1	0.94	3.16E-04	2.87E-02
A_52_P562054	Cilk1	ciliogenesis associated kinase 1	1.31	3.18E-04	2.87E-02
A_52_P241751	2700046A07Rik	RIKEN cDNA 2700046A07 gene	1.49	3.21E-04	2.87E-02
A_51_P451588	Plekhh1	pleckstrin homology domain containing, family B (evectins) member 1	2.27	3.22E-04	2.87E-02
A_51_P428134	Lrig3	leucine-rich repeats and immunoglobulin-like domains 3	1.36	3.26E-04	2.88E-02
A_51_P222381	Tmeff1	transmembrane protein with EGF-like and two follistatin-like domains 1	1.07	3.26E-04	2.88E-02
A_51_P110189	Ttyh2	tweety family member 2	1.54	3.27E-04	2.88E-02
A_51_P494541	Abhd17b	abhydrolase domain containing 17B	0.89	3.28E-04	2.88E-02
A_51_P186735	Tesk2	testis-specific kinase 2	0.95	3.29E-04	2.88E-02
A_52_P421344	Paqr5	progesterin and adipoQ receptor family member V	-0.75	3.30E-04	2.88E-02
A_52_P470150	Ddc	dopa decarboxylase	1.5	3.31E-04	2.88E-02
A_51_P413005	Chn2	chimerin 2	1.19	3.38E-04	2.92E-02
A_52_P370484	Uqcrcq	ubiquinol-cytochrome c reductase, complex III subunit VII	-0.55	3.43E-04	2.95E-02
A_51_P476321	Mindy1	MINDY lysine 48 deubiquitinase 1	0.9	3.44E-04	2.95E-02
A_51_P303749	Depdc1b	DEP domain containing 1B	1.3	3.47E-04	2.97E-02
A_51_P390285	Larp6	La ribonucleoprotein domain family, member 6	0.84	3.51E-04	2.98E-02
A_52_P82209	Wnk1	WNK lysine deficient protein kinase 1	1.04	3.59E-04	3.03E-02

A_52_P329207	Wfdc18	WAP four-disulfide core domain 18	1.47	3.69E-04	3.09E-02
A_52_P385896	Atp8a1	ATPase, aminophospholipid transporter (APLT), class I, type 8A, member 1	0.66	3.70E-04	3.09E-02
A_52_P395149	Smtnl2	smoothelin-like 2	1.2	3.73E-04	3.11E-02
A_51_P431737	Cth	cystathionase (cystathionine gamma-lyase)	-0.79	3.82E-04	3.15E-02
A_52_P1027170	Hsf5	heat shock transcription factor family member 5	0.65	3.82E-04	3.15E-02
A_52_P84901	Slc44a1	solute carrier family 44, member 1	2.2	3.83E-04	3.15E-02
A_51_P369154	Sez6l2	seizure related 6 homolog like 2	0.97	3.85E-04	3.15E-02
A_51_P430033	Ccdc13	coiled-coil domain containing 13	1.37	3.87E-04	3.16E-02
A_52_P650387	Ccnj1	cyclin J-like	1.1	3.91E-04	3.17E-02
A_52_P354844	Eda2r	ectodysplasin A2 receptor	-0.51	3.91E-04	3.17E-02
A_51_P337101	Rnf43	ring finger protein 43	1.11	3.94E-04	3.18E-02
A_51_P258570	Klk6	kallikrein related-peptidase 6	2.25	4.02E-04	3.19E-02
A_52_P593965	Fdps	farnesyl diphosphate synthetase	1.07	4.02E-04	3.19E-02
A_52_P335606	Prima1	proline rich membrane anchor 1	1.21	4.03E-04	3.19E-02
A_51_P157297	Efcab14	EF-hand calcium binding domain 14	0.89	4.03E-04	3.19E-02
A_52_P329451	Mbp	myelin basic protein	3	4.08E-04	3.22E-02
A_51_P355943	Mvd	mevalonate (diphospho) decarboxylase	1.05	4.09E-04	3.22E-02
A_51_P485946	Fdft1	farnesyl diphosphate farnesyl transferase 1	0.86	4.15E-04	3.26E-02
A_52_P78746	Kif13a	kinesin family member 13A	1.19	4.21E-04	3.30E-02
A_52_P497188	Prrg1	proline rich Gla (G-carboxyglutamic acid) 1	1.66	4.23E-04	3.30E-02
A_51_P162773	Scpdp	saccharopine dehydrogenase (putative)	1.11	4.27E-04	3.32E-02
A_52_P164136	Arrdc3	arrestin domain containing 3	1.38	4.29E-04	3.32E-02
A_52_P45616	Emilin3	elastin microfibril interfacier 3	1.05	4.30E-04	3.32E-02
A_51_P238523	Shisa4	shisa family member 4	0.89	4.35E-04	3.33E-02
A_52_P154710	Sesn2	sestrin 2	-1.49	4.37E-04	3.33E-02
A_51_P188772	Arhgef28	Rho guanine nucleotide exchange factor (GEF) 28	0.94	4.45E-04	3.36E-02
A_51_P367734	Plc11	phospholipase C-like 1	1.05	4.45E-04	3.36E-02
A_51_P147284	Slain1	SLAIN motif family, member 1	1.47	4.48E-04	3.36E-02
A_51_P416521	Tmcc3	transmembrane and coiled coil domains 3	1.58	4.60E-04	3.41E-02
A_51_P414166	Rnf7	ring finger protein 7	0.85	4.60E-04	3.41E-02
A_51_P346803	Septin9	septin 9	-0.78	4.61E-04	3.41E-02
A_52_P547447	Sirt2	sirtuin 2	1.32	4.66E-04	3.41E-02
A_51_P260730	Syt11	synaptotagmin XI	0.6	4.66E-04	3.41E-02
A_51_P410260	Pip5k1b	phosphatidylinositol-4-phosphate 5-kinase, type 1 beta	-0.86	4.70E-04	3.41E-02
A_52_P682382	Scd1	stearoyl-Coenzyme A desaturase 1	1.43	4.74E-04	3.43E-02
A_51_P123623	Ptpdc1	protein tyrosine phosphatase domain containing 1	0.94	4.79E-04	3.45E-02
A_51_P250934	Hsd17b7	hydroxysteroid (17-beta) dehydrogenase 7	0.7	4.84E-04	3.47E-02
A_52_P106482	Cryab	crystallin, alpha B	1.85	4.88E-04	3.47E-02

A_51_P190886	Ankrd13a	ankyrin repeat domain 13a	0.94	4.88E-04	3.47E-02
A_51_P432380	Aplp1	amyloid beta (A4) precursor-like protein 1	0.95	4.89E-04	3.47E-02
A_51_P186703	Fbln5	fibulin 5	-0.96	4.92E-04	3.48E-02
A_52_P338530	Zdhhc20	zinc finger, DHHC domain containing 20	0.84	5.00E-04	3.51E-02
A_52_P337899	Fkbp5	FK506 binding protein 5	-0.69	5.02E-04	3.51E-02
A_52_P24835	Nectin4	nectin cell adhesion molecule 4	1.37	5.12E-04	3.56E-02
A_51_P478942	Golga7	golgi autoantigen, golgin subfamily a, 7	1.19	5.16E-04	3.58E-02
A_51_P356967	Lgi3	leucine-rich repeat LGI family, member 3	1.66	5.19E-04	3.59E-02
A_52_P139788	Adamts11	ADAMTS-like 1	0.5	5.38E-04	3.70E-02
A_51_P187226	1500015L24Rik	RIKEN cDNA 1500015L24 gene	1.02	5.39E-04	3.70E-02
A_51_P213781	Ldlrad4	low density lipoprotein receptor class A domain containing 4	0.77	5.50E-04	3.76E-02
A_52_P66226	Rab33a	RAB33A, member RAS oncogene family	0.74	5.55E-04	3.79E-02
A_52_P10622	Emb	embigin	-0.79	5.62E-04	3.83E-02
A_52_P577329	Tmem88b	transmembrane protein 88B	2.4	5.67E-04	3.84E-02
A_52_P483324	D630028G08Rik	RIKEN cDNA D630028G08 gene	0.6	5.68E-04	3.84E-02
A_52_P413448	Vmp1	vacuole membrane protein 1	1.92	5.89E-04	3.97E-02
A_51_P433843	Slc22a23	solute carrier family 22, member 23	0.61	5.97E-04	4.01E-02
A_51_P412846	Efh1	EF hand domain containing 1	2.15	6.01E-04	4.03E-02
A_51_P149562	Apbb2	amyloid beta (A4) precursor protein-binding, family B, member 2	0.56	6.05E-04	4.05E-02
A_52_P357181	Cep97	centrosomal protein 97	0.92	6.07E-04	4.05E-02
A_51_P122321	Il33	interleukin 33	2.42	6.14E-04	4.07E-02
A_51_P506513	Qdpr	quinoid dihydropteridine reductase	2.45	6.20E-04	4.10E-02
A_52_P251623	Fam222a	family with sequence similarity 222, member A	1.56	6.27E-04	4.14E-02
A_51_P246924	Tppp3	tubulin polymerization-promoting protein family member 3	2.06	6.34E-04	4.16E-02
A_51_P497937	Gjc2	gap junction protein, gamma 2	1.34	6.38E-04	4.17E-02
A_52_P618745	Ermp1	endoplasmic reticulum metalloproteinase 1	1.09	6.39E-04	4.17E-02
A_51_P205968	Snx15	sorting nexin 15	0.79	6.48E-04	4.20E-02
A_52_P494168	Prr18	proline rich 18	3.17	6.48E-04	4.20E-02
A_51_P161413	Usp30	ubiquitin specific peptidase 30	0.81	6.53E-04	4.22E-02
A_52_P362772	Sik1	salt inducible kinase 1	0.82	6.56E-04	4.23E-02
A_51_P375201	Plk3	polo like kinase 3	0.84	6.58E-04	4.23E-02
A_52_P350111	Cyth1	cytohesin 1	0.89	6.60E-04	4.23E-02
A_52_P30328	Tmem163	transmembrane protein 163	1.26	6.69E-04	4.25E-02
A_52_P493477	Serp1b1c	serine (or cysteine) peptidase inhibitor, clade B, member 1c	1	6.74E-04	4.25E-02
A_51_P225427	Pkp2	plakophilin 2	-1.26	6.76E-04	4.25E-02
A_51_P365482	Ipo13	importin 13	0.64	6.76E-04	4.25E-02
A_51_P315785	Tnfrsf6	tumor necrosis factor alpha induced protein 6	1.87	6.78E-04	4.25E-02

A_52_P670978	Nkain1	Na+/K+ transporting ATPase interacting 1	1.78	6.79E-04	4.25E-02
A_52_P72587	Prkcq	protein kinase C, theta	1.66	6.80E-04	4.25E-02
A_51_P163444	Carhsp1	calcium regulated heat stable protein 1	1.78	6.88E-04	4.28E-02
A_51_P408666	Sstr3	somatostatin receptor 3	0.54	6.89E-04	4.28E-02
A_52_P423222	Nfe2l3	nuclear factor, erythroid derived 2, like 3	1.03	6.91E-04	4.28E-02
A_51_P451632	5031410I06Rik	RIKEN cDNA 5031410I06 gene	1.02	6.98E-04	4.30E-02
A_52_P1060609	Gm32450	predicted gene, 32450	0.67	7.03E-04	4.32E-02
A_52_P1180449	Rtn4	reticulon 4	0.73	7.07E-04	4.33E-02
A_51_P124388	Slc45a3	solute carrier family 45, member 3	0.61	7.28E-04	4.42E-02
A_51_P412966	Lrn1	leucine rich repeat protein 1, neuronal	1.32	7.30E-04	4.42E-02
A_51_P332201	Cst3	cystatin C	-0.71	7.40E-04	4.45E-02
A_51_P498890	Degs1	delta(4)-desaturase, sphingolipid 1	0.75	7.42E-04	4.45E-02
A_52_P512561	Trim59	tripartite motif-containing 59	1.36	7.43E-04	4.45E-02
A_51_P249627	Bicd2	BICD cargo adaptor 2	0.76	7.45E-04	4.45E-02
A_52_P647393	E130308A19Rik	RIKEN cDNA E130308A19 gene	1.25	7.51E-04	4.47E-02
A_51_P298802	Bfsp2	beaded filament structural protein 2, phakinin	1.41	7.60E-04	4.51E-02
A_51_P128336	Serinc5	serine incorporator 5	1.32	7.62E-04	4.51E-02
A_51_P450952	P3h4	prolyl 3-hydroxylase family member 4 (non-enzymatic)	1.02	7.72E-04	4.56E-02
A_51_P201137	Lbr	lamin B receptor	0.84	7.75E-04	4.57E-02
A_51_P389539	Adgrv1	adhesion G protein-coupled receptor V1	1.06	7.79E-04	4.57E-02
A_52_P416499	Enpp2	ectonucleotide pyrophosphatase/phosphodiesterase 2	0.91	7.80E-04	4.57E-02
A_52_P21659	Pck2	phosphoenolpyruvate carboxykinase 2 (mitochondrial)	-0.7	7.87E-04	4.61E-02
A_52_P413492	Ldlrap1	low density lipoprotein receptor adaptor protein 1	1.08	7.93E-04	4.62E-02
A_51_P148814	Ly6e	lymphocyte antigen 6 complex, locus E	-0.94	7.95E-04	4.62E-02
A_51_P354354	Gal3st1	galactose-3-O-sulfotransferase 1	1.95	8.02E-04	4.63E-02
A_51_P287677	Rps18	ribosomal protein S18	-0.51	8.02E-04	4.63E-02
A_51_P206346	Reep3	receptor accessory protein 3	1	8.18E-04	4.68E-02
A_51_P498257	Rnf141	ring finger protein 141	0.69	8.22E-04	4.69E-02
A_51_P496432	Acs11	acyl-CoA synthetase long-chain family member 1	0.66	8.23E-04	4.69E-02
A_52_P302496	Fah	fumarylacetoacetate hydrolase	1.42	8.26E-04	4.70E-02
A_51_P252677	Card19	caspase recruitment domain family, member 19	1.08	8.62E-04	4.87E-02
A_52_P62121	Gpr37	G protein-coupled receptor 37	1.86	8.75E-04	4.93E-02

Supplementary Table9. GO molecular functions during remyelination compared to treatment with cuprizone for 4 weeks in CC.

GO ID	Term	Ontology	N	DE	P.DE	adj.pvalue
GO:0003824	Catalytic activity	MF	5717	136	1.07E-11	1.58E-08

GO:0005515	Protein binding	MF	9318	186	8.26E-10	5.49E-07
GO:0005488	Binding	MF	13753	245	3.90E-09	2.32E-06
GO:0043167	Ion binding	MF	5513	121	4.81E-08	2.26E-05
GO:0043168	Anion binding	MF	2730	68	1.80E-06	5.80E-04
GO:0019899	Enzyme binding	MF	2366	61	2.30E-06	6.96E-04
GO:0019911	Structural constituent of myelin sheath	MF	10	4	7.51E-06	1.91E-03
GO:0016628	Oxidoreductase activity, acting on the CH-CH group of donors, NAD or NADP as acceptor	MF	24	5	1.81E-05	3.94E-03
GO:0036094	Small molecule binding	MF	2432	58	4.24E-05	7.80E-03
GO:0033218	Amide binding	MF	391	17	4.35E-05	7.91E-03
GO:0050839	Cell adhesion molecule binding	MF	284	14	5.44E-05	9.26E-03
GO:0051020	GTPase binding	MF	523	20	5.74E-05	9.60E-03
GO:0070402	NADPH binding	MF	18	4	1.00E-04	1.48E-02
GO:0000166	Nucleotide binding	MF	2033	49	1.41E-04	1.97E-02
GO:1901265	Nucleoside phosphate binding	MF	2033	49	1.41E-04	1.97E-02
GO:0008092	Cytoskeletal protein binding	MF	980	29	1.41E-04	1.97E-02
GO:0016627	Oxidoreductase activity, acting on the CH-CH group of donors	MF	57	6	1.46E-04	2.01E-02
GO:0016717	Oxidoreductase activity, acting on paired donors, with oxidation of a pair of donors resulting in the reduction of molecular oxygen to two molecules of water	MF	8	3	1.46E-04	2.01E-02
GO:0016787	Hydrolase activity	MF	2490	57	1.51E-04	2.07E-02
GO:0001540	Amyloid-beta binding	MF	58	6	1.61E-04	2.19E-02
GO:0042277	Peptide binding	MF	318	14	1.79E-04	2.37E-02
GO:0004312	Fatty acid synthase activity	MF	11	3	4.17E-04	4.50E-02
GO:0016746	Transferase activity, transferring acyl groups	MF	268	12	4.41E-04	4.67E-02

Abbreviations: MF, molecular function

Supplementary Table 10. Potential ligands in microglia that could affect gene expression after cuprizone treatment in OPCs ordered by the Pearson correlation coefficient.

Symbol	Gene name
TFPI	Tissue factor pathway inhibitor
SEMA4D	Semaphorin 4D
GSTP1	Glutathione S-Transferase Pi
SERPINE2	Serpin Family E Member 2
LRPAP1	Low Density Lipoprotein-Receptor Related Protein Associated Protein 1
THBS1	Thrombospondin 1
HSP90B1	Heat Shock Protein 90 Beta Family Member 1
EFNB2	Ephrin B2
F11R	F11 Receptor
C3	Complement C3
EFNB1	Ephrin B1
PF4	Platelet Factor 4
RGMA	Repulsive Guidance Molecule BMP Co-Receptor A
LIPH	Lipase H
ARF1	ADP Ribosylation Factor 1
SERPINE1	Serpin Family E Member 1
PROS1	Protein S
GAS6	Growth Arrest Specific 6
ADAM9	ADAM Metallopeptidase Domain 9
DUSP18	Dual Specificity Phosphatase 18

JAM2	Junctional Adhesion Molecule 2
CORT	Cortistatin
VCAM1	Vascular Cell Adhesion Molecule 1
ADAM15	ADAM Metallopeptidase Domain 15
PTPRC	Protein Tyrosine Phosphatase Receptor Type C
COL2A1	Collagen Type II Alpha 1 Chain
CSF1	Colony Stimulating Factor 1
PSAP	Prosaposin
CLCF1	Cardiotrophin Like Cytokine Factor 1
TNFSF9	TNF Superfamily Member 9
ADAM17	ADAM Metallopeptidase Domain 17
FN1	Fibronectin 1
BMP2	Bone Morphogenetic Protein 2
PLAU	Plasminogen Activator, Urokinase
SPP1	Secreted Phosphoprotein 1
LRRRC4B	Leucine Rich Repeat Containing 4B
VEGFA	Vascular Endothelial Growth Factor A
OSM	Oncostatin M
IFNA5	Interferon Alpha 5
IHH	Indian Hedgehog Signaling Molecule
IL6	Interleukin 6
APOE	Apolipoprotein E
IL15	Interleukin 15
NPNT	Nephronectin
TNF	Tumor Necrosis Factor
IGF1	Insulin Like Growth Factor 1
CADM1	Cell Adhesion Molecule 1

Supplementary Table 11. Mean expression and adjusted p-value of differential expressed ligands in microglia from control and cuprizone treated mice.

Ligand	Name	Mean expression in microglia from control mice	Mean expression in microglia from cuprizone treated mice	Fold change	Adjusted p-value
PLAU	Plasminogen activator, urokinase	8.69	9.67	1.94	0.052
SPP1	Secreted phosphoprotein 1	5.06	9.84	1.11	0.052

Supplementary Table 12. Mean expression and adjusted p-value of differential expressed receptors in OPCs from control and cuprizone treated mice.

Receptor	Name	Mean expression in OPCs from control mice	Mean expression in OPCs from cuprizone treated mice	Fold change	Adjusted p-value
Jam3	junction adhesion molecule 3	15.63	14.65	0.94	5.69e-05
Plxn2	plexin B2	11.21	12.53	1.12	4.28e-03
Hhip	Hedgehog-interacting protein	14.11	12.72	0.90	4.28e-03
Tnfrsf1a	tumor necrosis factor receptor superfamily, member 1a	9.44	11.09	1.17	6.06e-03
Acvr1	activin A receptor, type 1	12.40	13.27	1.07	6.06e-03
Ldlr	low density lipoprotein receptor	12.66	11.05	0.87	7.19e-03
Fgfr2	fibroblast growth factor receptor 2	11.40	10.09	0.89	8.94e-03
Irgb4	integrin beta 4	14.62	12.61	0.86	8.94e-03
Ephb1	Eph receptor B1	14.38	13.59	0.94	1.23e-02
Lrp1	low density lipoprotein receptor-related protein 1	10.34	12.00	1.16	2.06e-02
Lpar1	lysophosphatidic acid receptor 1	12.06	10.77	0.89	2.12e-02
Tyro3	TYRO3 protein tyrosine kinase 3	11.69	10.51	0.90	3.22e-02
Irgb5	integrin beta 5	11.37	12.11	1.07	3.22e-02
Axl	AXL receptor tyrosine kinase	9.21	11.61	1.26	4.76e-02

Sorl1	sortilin-related receptor, LDLR class A repeats-containing	13.39	11.85	0.88	4.76e-02
-------	--	-------	-------	------	----------

Supplementary Table 13. Mean expression and adjusted p-value of differentially expressed target genes in OPCs from control and cuprizone treated mice.

Target	Name	Mean expression in OPCs from control mice	Mean expression in OPCs from cuprizone treated mice	Fold change	Adjusted p-value
Gadd45b	growth arrest and DNA-damage-inducible 45 beta	10.84	14.51	1.34	3.32e-05
Hist1h3d		13.77	15.55	1.13	3.32e-05
Bbc3	BCL2 binding component 3	11.33	14.24	1.26	3.61e-05
Tnfrsf12a	tumor necrosis factor receptor superfamily, member 12a	9.82	13.34	1.36	7.25e-05
Cdkn1a	cyclin-dependent kinase inhibitor 1A (P21)	9.30	15.17	1.63	1.07e-04
Fosb	FBJ osteosarcoma oncogene B	11.78	14.32	1.22	1.38e-04
Abca1	ATP-binding cassette, sub-family A (ABC1), member 1	11.16	13.40	1.20	2.10e-04
Fam181b	family with sequence similarity 181, member B	8.80	12.59	1.43	2.10e-04
Vgf	VGF nerve growth factor inducible	8.98	11.80	1.31	5.08e-04
Klf4	Kruppel-like factor 4 (gut)	11.08	14.15	1.28	5.08e-04
Kdr	kinase insert domain protein receptor	10.76	8.99	0.84	5.08e-04
Gstp1	glutathione S-transferase, pi 1	15.01	14.19	0.94	6.83e-04
Hexim1	hexamethylene bis-acetamide inducible 1	10.37	11.92	1.15	7.02e-04
Trim47	tripartite motif-containing 47	10.00	12.24	1.22	7.02e-04
Egr2	early growth response 2	10.38	12.85	1.24	7.45e-04
Sgk2	serum/glucocorticoid regulated kinase 2	14.82	12.16	0.82	7.79e-04
Ccnd1	cyclin D1	9.92	13.32	1.34	8.81e-04
Il18	interleukin 18	13.55	12.34	0.91	1.00e-03
Hmgal1	high mobility group AT-hook 1	12.84	15.50	1.21	1.40e-03
Ppp1r15a	protein phosphatase 1, regulatory subunit 15A	12.47	15.43	1.24	1.40e-03
Dusp1	dual specificity phosphatase 1	11.41	13.23	1.16	1.57e-03
Egr1	early growth response 1	13.21	15.70	1.19	1.57e-03
Gadd45g	growth arrest and DNA-damage-inducible 45 gamma	11.15	15.24	1.37	1.57e-03
Chpf	chondroitin polymerizing factor	11.33	12.92	1.14	1.57e-03
Rab37	RAB37, member RAS oncogene family	11.40	10.28	0.90	1.57e-03
Adamts14	ADAMTS-like 4	14.13	11.65	0.82	1.57e-03
Pdgfra	platelet derived growth factor receptor, alpha polypeptide	9.35	10.82	1.16	1.57e-03
Cntf	ciliary neurotrophic factor	10.32	12.01	1.16	1.57e-03
C1qc	complement component 1, q subcomponent, C chain	9.57	12.34	1.29	1.57e-03
Hmgcs1	3-hydroxy-3-methylglutaryl-Coenzyme A synthase 1	15.24	13.50	0.89	1.63e-03
Itih3	inter-alpha trypsin inhibitor, heavy chain 3	13.02	10.49	0.81	1.66e-03
Smad7	SMAD family member 7	13.14	11.94	0.91	1.75e-03
Nfil3	nuclear factor, interleukin 3, regulated	11.65	13.75	1.18	1.85e-03
Midn	midnolin	9.99	12.55	1.26	1.95e-03
Vim	vimentin	10.19	13.81	1.36	1.99e-03
Tnfrsf1a	tumor necrosis factor receptor superfamily, member 1a	9.44	11.09	1.17	2.19e-03
Nrcam	neuronal cell adhesion molecule	10.02	12.56	1.25	2.29e-03
Dhrs3	dehydrogenase/reductase (SDR family) member 3	10.19	11.60	1.14	2.60e-03

Traf4	TNF receptor associated factor 4	9.68	12.26	1.27	2.63e-03
Cdh13	cadherin 13	9.18	12.09	1.32	2.63e-03
Ldlr	low density lipoprotein receptor	12.66	11.05	0.87	2.81e-03
S100a10	S100 calcium binding protein A10 (calpactin)	9.46	12.25	1.30	2.86e-03
Pcdhga9	protocadherin gamma subfamily A, 9	10.71	11.93	1.11	2.96e-03
Klf6	Kruppel-like factor 6	12.88	14.53	1.13	3.03e-03
Atf4	activating transcription factor 4	10.68	12.04	1.13	3.03e-03
Serpind1	serine (or cysteine) peptidase inhibitor, clade D, member 1	12.36	10.60	0.86	3.10e-03
Timp3	tissue inhibitor of metalloproteinase 3	10.82	13.12	1.21	3.10e-03
Hist1h2ag		13.02	15.17	1.16	4.15e-03
Tsc22d3	TSC22 domain family, member 3	14.90	13.33	0.89	4.98e-03
Lmna	lamin A	12.29	14.20	1.16	5.01e-03
Gdf15	growth differentiation factor 15	8.91	14.19	1.59	5.01e-03
Odc1	ornithine decarboxylase, structural 1	11.01	12.66	1.15	5.01e-03
Bax	BCL2-associated X protein	13.11	14.07	1.07	5.01e-03
Rps19	ribosomal protein S19	13.44	15.06	1.12	5.01e-03
Socs3	suppressor of cytokine signaling 3	11.13	14.29	1.28	5.05e-03
Synpo	synaptopodin	12.27	11.25	0.92	5.19e-03
Klf10	Kruppel-like factor 10	10.07	11.65	1.16	6.18e-03
Ddc	dopa decarboxylase	13.71	12.80	0.93	6.18e-03
Cdk5r1	cyclin-dependent kinase 5, regulatory subunit 1 (p35)	10.93	12.01	1.10	8.98e-03
Lrp1	low density lipoprotein receptor-related protein 1	10.34	12.00	1.16	9.07e-03
Plin4	perilipin 4	11.79	13.36	1.13	9.07e-03
Ifit3	interferon-induced protein with tetratricopeptide repeats 3	9.33	11.03	1.18	9.17e-03
Myh9	myosin, heavy polypeptide 9, non-muscle	12.76	13.59	1.06	9.36e-03
Fos	FBJ osteosarcoma oncogene	12.59	14.95	1.19	9.80e-03
Ank3	ankyrin 3, epithelial	11.95	10.80	0.90	9.80e-03
Apln	apelin	12.35	11.03	0.89	9.80e-03
Per1	period circadian clock 1	12.20	14.41	1.18	1.00e-02
Tle3	transducin-like enhancer of split 3	13.65	14.54	1.07	1.00e-02
Tap2	transporter 2, ATP-binding cassette, sub-family B (MDR/TAP)	10.53	12.63	1.20	1.09e-02
Atf3	activating transcription factor 3	9.71	13.05	1.34	1.19e-02
Zfp361l1	zinc finger protein 36, C3H type-like 1	9.79	11.55	1.18	1.19e-02
Csmp1	cysteine-serine-rich nuclear protein 1	11.70	12.93	1.11	1.19e-02
C4b	complement component 4B (Chido blood group)	13.80	15.89	1.15	1.19e-02
Cdk18	cyclin-dependent kinase 18	15.67	14.68	0.94	1.29e-02
Crybg3	beta-gamma crystallin domain containing 3	12.51	11.29	0.90	1.36e-02
Cebpb	CCAAT/enhancer binding protein (C/EBP), beta	9.61	12.35	1.28	1.41e-02
Hist1h4d		11.42	13.42	1.17	1.50e-02
Olig2	oligodendrocyte transcription factor 2	13.02	13.99	1.07	1.50e-02
Stat3	signal transducer and activator of transcription 3	12.83	13.59	1.06	1.76e-02
Sgk1	serum/glucocorticoid regulated kinase 1	13.72	15.42	1.12	1.80e-02
Nfkbia	nuclear factor of kappa light polypeptide gene enhancer in B cells inhibitor, alpha	13.02	14.38	1.10	1.83e-02
Rab34	RAB34, member RAS oncogene family	10.57	12.47	1.18	1.90e-02
Cd44	CD44 antigen	9.51	10.83	1.14	1.90e-02
Anxa2	annexin A2	11.49	14.06	1.22	1.90e-02
Col1a2	collagen, type I, alpha 2	11.44	12.73	1.11	1.94e-02
Gadd45a	growth arrest and DNA-damage-inducible 45 alpha	10.56	12.64	1.20	2.04e-02

C1qb	complement component 1, q subcomponent, beta polypeptide	9.35	11.19	1.20	2.09e-02
Tgif1	TGFB-induced factor homeobox 1	8.84	12.71	1.44	2.14e-02
Spp1	secreted phosphoprotein 1	9.26	10.42	1.13	2.23e-02
Bcl6	B cell leukemia/lymphoma 6	12.51	13.62	1.09	2.30e-02
Mfge8	milk fat globule-EGF factor 8 protein	13.48	14.49	1.07	2.48e-02
Arhgef10l	Rho guanine nucleotide exchange factor (GEF) 10-like	9.48	11.96	1.26	2.59e-02
Reep1	receptor accessory protein 1	9.76	10.99	1.13	2.59e-02
Ddit4	DNA-damage-inducible transcript 4	14.37	15.55	1.08	2.64e-02
Csflr	colony stimulating factor 1 receptor	11.50	13.92	1.21	2.67e-02
Trib1	tribbles pseudokinase 1	8.13	11.74	1.44	2.93e-02
Tnfaip3	tumor necrosis factor, alpha-induced protein 3	8.94	11.00	1.23	2.97e-02
Cirbp	cold inducible RNA binding protein	12.46	14.16	1.14	2.97e-02
Npepps	aminopeptidase puromycin sensitive	14.04	13.24	0.94	2.97e-02
Jun	jun proto-oncogene	14.96	15.97	1.07	3.20e-02
Ly86	lymphocyte antigen 86	7.52	12.08	1.61	3.48e-02
Mgp	matrix Gla protein	12.43	14.42	1.16	3.67e-02
Malat1	metastasis associated lung adenocarcinoma transcript 1 (non-coding RNA)	12.95	14.16	1.09	4.04e-02
Zeb2	zinc finger E-box binding homeobox 2	10.72	9.59	0.89	4.04e-02
Clc1	chloride intracellular channel 1	10.10	12.23	1.21	4.26e-02
Vcan	versican	8.95	11.37	1.27	4.37e-02
Magi1	membrane associated guanylate kinase, WW and PDZ domain containing 1	13.71	12.88	0.94	4.73e-02

Supplementary Table 14. GO terms from DEGS expressed between control and 4-week-treated mice in CC.

GO ID	Term	Ontology	N	DE	P.DE	adj.pvalue
GO:0008610	lipid biosynthetic process	BP	581	45	1.16E-20	2.61E-16
GO:0016126	sterol biosynthetic process	BP	55	15	8.60E-16	4.86E-12
GO:0006695	cholesterol biosynthetic process	BP	49	14	3.86E-15	1.45E-11
GO:1902653	secondary alcohol biosynthetic process	BP	49	14	3.86E-15	1.45E-11
GO:0008203	cholesterol metabolic process	BP	130	18	3.56E-13	1.15E-09
GO:0016125	sterol metabolic process	BP	139	18	1.15E-12	2.89E-09
GO:1902652	secondary alcohol metabolic process	BP	141	18	1.48E-12	3.34E-09
GO:0006629	lipid metabolic process	BP	1311	53	3.72E-12	6.30E-09
GO:0007272	ensheathment of neurons	BP	170	19	3.90E-12	6.30E-09
GO:0008366	axon ensheathment	BP	170	19	3.90E-12	6.30E-09
GO:0046165	alcohol biosynthetic process	BP	138	17	1.12E-11	1.58E-08
GO:0044283	small molecule biosynthetic process	BP	597	33	2.50E-11	3.13E-08
GO:0042552	myelination	BP	167	18	2.68E-11	3.19E-08
GO:0007275	multicellular organism development	BP	5467	130	4.50E-11	4.91E-08
GO:0048731	system development	BP	4878	120	4.56E-11	4.91E-08
GO:0010001	glial cell differentiation	BP	249	21	6.42E-11	6.31E-08
GO:1901617	organic hydroxy compound biosynthetic process	BP	225	20	7.19E-11	6.77E-08
GO:0009987	cellular process	BP	17114	291	8.45E-11	7.34E-08
GO:0042063	gliogenesis	BP	338	24	9.94E-11	8.32E-08
GO:0048856	anatomical structure development	BP	5977	137	1.34E-10	1.04E-07
GO:0051179	localization	BP	6076	137	4.36E-10	3.18E-07
GO:0048709	oligodendrocyte differentiation	BP	110	14	4.86E-10	3.43E-07
GO:0007399	nervous system development	BP	2423	72	6.24E-10	4.27E-07
GO:0006694	steroid biosynthetic process	BP	161	16	1.16E-09	7.46E-07
GO:0032502	developmental process	BP	6449	141	1.80E-09	1.13E-06
GO:0008202	steroid metabolic process	BP	309	21	3.31E-09	2.02E-06
GO:0044255	cellular lipid metabolic process	BP	981	39	5.56E-09	3.22E-06
GO:0035556	intracellular signal transduction	BP	2455	70	6.46E-09	3.56E-06
GO:0016043	cellular component organization	BP	6040	132	9.47E-09	4.98E-06
GO:0006643	membrane lipid metabolic process	BP	174	15	2.67E-08	1.34E-05
GO:0006066	alcohol metabolic process	BP	323	20	3.75E-08	1.84E-05
GO:0014013	regulation of gliogenesis	BP	154	14	4.00E-08	1.92E-05
GO:0071840	cellular component organization or biogenesis	BP	6229	132	6.76E-08	3.12E-05
GO:0022008	neurogenesis	BP	1835	55	7.38E-08	3.33E-05
GO:0021782	glial cell development	BP	118	12	1.09E-07	4.85E-05
GO:0046467	membrane lipid biosynthetic process	BP	121	12	1.45E-07	6.28E-05
GO:1901615	organic hydroxy compound metabolic process	BP	498	24	1.88E-07	7.71E-05
GO:0007010	cytoskeleton organization	BP	1366	44	2.55E-07	0.00010279
GO:0051239	regulation of multicellular organismal process	BP	3366	82	2.80E-07	0.00011101
GO:1901564	organonitrogen compound metabolic	BP	6063	127	2.89E-07	0.00011278

	process					
GO:0006665	sphingolipid metabolic process	BP	131	12	3.46E-07	0.00013018
GO:0007417	central nervous system development	BP	930	34	4.02E-07	0.00014893
GO:0044281	small molecule metabolic process	BP	1701	50	5.64E-07	0.00020562
GO:0032501	multicellular organismal process	BP	8423	162	6.21E-07	0.00022273
GO:0045685	regulation of glial cell differentiation	BP	92	10	6.81E-07	0.00024045
GO:0065007	biological regulation	BP	12806	224	7.38E-07	0.00025654
GO:0007422	peripheral nervous system development	BP	74	9	9.48E-07	0.00032466
GO:0008152	metabolic process	BP	11039	199	1.02E-06	0.00034413
GO:0051128	regulation of cellular component organization	BP	2496	64	1.48E-06	0.00049087
GO:0097435	supramolecular fiber organization	BP	730	28	1.79E-06	0.00057977
GO:0048468	cell development	BP	2461	63	1.92E-06	0.00061065
GO:0007155	cell adhesion	BP	1379	42	2.08E-06	0.00065132
GO:0014003	oligodendrocyte development	BP	43	7	2.12E-06	0.00065488
GO:0030154	cell differentiation	BP	4310	95	2.31E-06	0.00069633
GO:0034613	cellular protein localization	BP	1787	50	2.34E-06	0.00069633
GO:0071704	organic substance metabolic process	BP	10518	190	2.41E-06	0.00070869
GO:0022610	biological adhesion	BP	1392	42	2.63E-06	0.00076121
GO:0070727	cellular macromolecule localization	BP	1798	50	2.78E-06	0.00079643
GO:0032879	regulation of localization	BP	2874	69	5.35E-06	0.00144874
GO:0008654	phospholipid biosynthetic process	BP	172	12	6.17E-06	0.00163911
GO:0048869	cellular developmental process	BP	4418	95	6.74E-06	0.00175656
GO:0006633	fatty acid biosynthetic process	BP	145	11	6.77E-06	0.00175656
GO:0048585	negative regulation of response to stimulus	BP	1607	45	7.81E-06	0.00196123
GO:0051641	cellular localization	BP	2743	66	8.39E-06	0.00208304
GO:0051234	establishment of localization	BP	4571	97	9.09E-06	0.00223149
GO:0048699	generation of neurons	BP	1724	47	9.67E-06	0.00232528
GO:0050793	regulation of developmental process	BP	2813	67	9.86E-06	0.00234464
GO:0051129	negative regulation of cellular component organization	BP	756	27	1.01E-05	0.00237498
GO:0045338	farnesyl diphosphate metabolic process	BP	4	3	1.09E-05	0.00253253
GO:0099612	protein localization to axon	BP	11	4	1.17E-05	0.0026912
GO:0032288	myelin assembly	BP	23	5	1.45E-05	0.00331063
GO:0007264	small GTPase mediated signal transduction	BP	437	19	1.56E-05	0.00351564
GO:0050789	regulation of biological process	BP	12212	210	1.59E-05	0.0035463
GO:0022010	central nervous system myelination	BP	24	5	1.81E-05	0.00393514
GO:0032291	axon ensheathment in central nervous system	BP	24	5	1.81E-05	0.00393514
GO:0009247	glycolipid biosynthetic process	BP	59	7	1.85E-05	0.00397647
GO:0048518	positive regulation of biological process	BP	6358	124	1.99E-05	0.00423719
GO:0006664	glycolipid metabolic process	BP	83	8	2.20E-05	0.00465132
GO:0060284	regulation of cell development	BP	1121	34	2.27E-05	0.00475051
GO:0072330	monocarboxylic acid biosynthetic process	BP	196	12	2.30E-05	0.00476976
GO:0030148	sphingolipid biosynthetic process	BP	84	8	2.41E-05	0.00489583

GO:1903509	liposaccharide metabolic process	BP	84	8	2.41E-05	0.00489583
GO:0044087	regulation of cellular component biogenesis	BP	984	31	2.60E-05	0.00524301
GO:0002175	protein localization to paranode region of axon	BP	5	3	2.69E-05	0.00528461
GO:0048523	negative regulation of cellular process	BP	4950	101	2.95E-05	0.00575593
GO:0044238	primary metabolic process	BP	9716	173	3.55E-05	0.00686474
GO:0007265	Ras protein signal transduction	BP	350	16	4.02E-05	0.00757488
GO:0008104	protein localization	BP	2596	61	4.00E-05	0.00757488
GO:0006810	transport	BP	4431	92	4.06E-05	0.00757695
GO:0044237	cellular metabolic process	BP	9877	175	4.12E-05	0.0076367
GO:0048519	negative regulation of biological process	BP	5500	109	4.37E-05	0.00790763
GO:0050794	regulation of cellular process	BP	11652	200	4.50E-05	0.00806114
GO:0006464	cellular protein modification process	BP	3538	77	4.57E-05	0.00806276
GO:0036211	protein modification process	BP	3538	77	4.57E-05	0.00806276
GO:0048522	positive regulation of cellular process	BP	5834	114	4.95E-05	0.0086769
GO:0030030	cell projection organization	BP	1628	43	5.03E-05	0.00874997
GO:0090118	receptor-mediated endocytosis involved in cholesterol transport	BP	6	3	5.32E-05	0.00918157
GO:0120036	plasma membrane bounded cell projection organization	BP	1581	42	5.45E-05	0.00925824
GO:0050767	regulation of neurogenesis	BP	977	30	5.62E-05	0.00947048
GO:0065009	regulation of molecular function	BP	2574	60	5.90E-05	0.0097944
GO:0030029	actin filament-based process	BP	793	26	6.20E-05	0.01023332
GO:0045595	regulation of cell differentiation	BP	1971	49	6.65E-05	0.01088716
GO:0019538	protein metabolic process	BP	5242	104	6.91E-05	0.01124054
GO:0009058	biosynthetic process	BP	5512	108	7.87E-05	0.01261798
GO:0006796	phosphate-containing compound metabolic process	BP	2946	66	7.84E-05	0.01261798
GO:0022607	cellular component assembly	BP	2663	61	8.33E-05	0.01315699
GO:0048583	regulation of response to stimulus	BP	3972	83	8.94E-05	0.01403148
GO:0051960	regulation of nervous system development	BP	1103	32	9.19E-05	0.01422165
GO:0033036	macromolecule localization	BP	2964	66	9.40E-05	0.01437571
GO:0046394	carboxylic acid biosynthetic process	BP	299	14	9.42E-05	0.01437571
GO:0006793	phosphorus metabolic process	BP	2967	66	9.68E-05	0.01458572
GO:0016053	organic acid biosynthetic process	BP	300	14	9.75E-05	0.01459571
GO:1901576	organic substance biosynthetic process	BP	5414	106	9.83E-05	0.014609
GO:0044267	cellular protein metabolic process	BP	4666	94	0.00010337	0.01516712
GO:0009966	regulation of signal transduction	BP	2874	64	0.00012254	0.01763688
GO:0051240	positive regulation of multicellular organismal process	BP	1975	48	0.0001367	0.01954915
GO:0034330	cell junction organization	BP	740	24	0.00014015	0.01972198
GO:0120035	regulation of plasma membrane bounded cell projection organization	BP	798	25	0.00017385	0.02338289
GO:0030036	actin cytoskeleton organization	BP	705	23	0.00017703	0.02366959
GO:0010648	negative regulation of cell communication	BP	1350	36	0.00017835	0.02367152
GO:0023057	negative regulation of signaling	BP	1353	36	0.00018616	0.02439961
GO:0007009	plasma membrane organization	BP	112	8	0.00018681	0.02439961

GO:0009968	negative regulation of signal transduction	BP	1200	33	0.00019255	0.024969
GO:2000777	positive regulation of proteasomal ubiquitin-dependent protein catabolic process involved in cellular response to hypoxia	BP	2	2	0.00019669	0.024969
GO:0016128	phytosteroid metabolic process	BP	2	2	0.00019669	0.024969
GO:0016129	phytosteroid biosynthetic process	BP	2	2	0.00019669	0.024969
GO:0031106	septin ring organization	BP	2	2	0.00019669	0.024969
GO:0031344	regulation of cell projection organization	BP	807	25	0.00020613	0.025756
GO:1990778	protein localization to cell periphery	BP	363	15	0.00021148	0.02611281
GO:0048708	astrocyte differentiation	BP	86	7	0.00021062	0.02611281
GO:1903364	positive regulation of cellular protein catabolic process	BP	145	9	0.00021777	0.02674357
GO:0048261	negative regulation of receptor-mediated endocytosis	BP	22	4	0.00022897	0.02796606
GO:0046513	ceramide biosynthetic process	BP	62	6	0.00023296	0.02830047
GO:0043412	macromolecule modification	BP	3722	77	0.00023954	0.02894403
GO:2000026	regulation of multicellular organismal development	BP	2254	52	0.00025401	0.03053
GO:0014037	Schwann cell differentiation	BP	41	5	0.00026261	0.03123092
GO:0030162	regulation of proteolysis	BP	727	23	0.0002745	0.0324741
GO:0006644	phospholipid metabolic process	BP	374	15	0.0002908	0.03422299
GO:0008643	carbohydrate transport	BP	151	9	0.00029454	0.03448438
GO:0072659	protein localization to plasma membrane	BP	295	13	0.00029993	0.03475519
GO:0014015	positive regulation of gliogenesis	BP	91	7	0.00029888	0.03475519
GO:0006928	movement of cell or subcellular component	BP	2101	49	0.00030473	0.03513099
GO:0016477	cell migration	BP	1501	38	0.00032904	0.03755004
GO:1902531	regulation of intracellular signal transduction	BP	1613	40	0.00034571	0.03875545
GO:0048513	animal organ development	BP	3587	74	0.00035633	0.03966302
GO:0006497	protein lipidation	BP	94	7	0.00036468	0.0403939
GO:0051493	regulation of cytoskeleton organization	BP	557	19	0.00037333	0.04115019
GO:0034329	cell junction assembly	BP	426	16	0.00038171	0.0418695
GO:0043949	regulation of cAMP-mediated signaling	BP	68	6	0.00038656	0.04219715
GO:0042221	response to chemical	BP	4153	83	0.00039649	0.04307291
GO:0032787	monocarboxylic acid metabolic process	BP	608	20	0.00041862	0.04504334
GO:0065008	regulation of biological quality	BP	4104	82	0.00043832	0.0467385
GO:0042157	lipoprotein metabolic process	BP	127	8	0.0004393	0.0467385
GO:0000910	cytokinesis	BP	160	9	0.00045065	0.04758345

Abbreviations: BP, biological process; N, number of genes; DE, number of DEGs; P.DE, P-value of DEGs

SupplementaryTable 15. GO molecular functions in OPCs.

GO ID	Term	Ontology	N	DE	P.DE	adj.pvalue
GO:0005515	protein binding	MF	9318	93	7.18E-14	5.67E-10
GO:0005488	binding	MF	13753	109	2.07E-10	2.60E-07
GO:0019899	enzyme binding	MF	2366	32	9.51E-07	3.07E-04
GO:0030234	enzyme regulator activity	MF	997	18	7.85E-06	1.74E-03
GO:0044877	protein-containing complex binding	MF	1483	22	1.60E-05	3.07E-03
GO:0004861	cyclin-dependent protein serine/threonine kinase inhibitor activity	MF	12	3	3.33E-05	5.50E-03
GO:0098772	molecular function regulator	MF	3519	37	4.06E-05	6.41E-03
GO:0019207	kinase regulator activity	MF	202	7	1.22E-04	1.59E-02
GO:0042288	MHC class I protein binding	MF	19	3	1.43E-04	1.77E-02
GO:0004486	methylenetetrahydrofolate dehydrogenase [NAD(P)+] activity	MF	4	2	1.75E-04	2.04E-02
GO:0004488	methylenetetrahydrofolate dehydrogenase (NADP+) activity	MF	4	2	1.75E-04	2.04E-02
GO:0019900	kinase binding	MF	832	14	1.80E-04	2.07E-02
GO:0004860	protein kinase inhibitor activity	MF	54	4	2.14E-04	2.42E-02
GO:0019901	protein kinase binding	MF	747	13	2.23E-04	2.47E-02
GO:0004857	enzyme inhibitor activity	MF	392	9	3.01E-04	3.14E-02
GO:0019210	kinase inhibitor activity	MF	59	4	3.01E-04	3.14E-02
GO:0019887	protein kinase regulator activity	MF	170	6	3.41E-04	3.40E-02
GO:0015179	L-amino acid transmembrane transporter activity	MF	61	4	3.43E-04	3.40E-02
GO:0030291	protein serine/threonine kinase inhibitor activity	MF	29	3	5.18E-04	4.48E-02

Abbreviations: MF, molecular function ;N, number of genes; DE, number of DEGs; P.DE, P-value of DEGs

General discussion

DISCUSSION

In this section we are going to discuss the different chapters derived from this work. From all this work there are four main important points of relevance to discuss:

1. Protein-protein interactions of TRPV2 and TRPV4 are related to CNS biological processes and protein trafficking.
2. NO is responsible of TRPV2 activation in glial cells by TRPV2 translocation to the membrane.
3. TRPV2 interaction with important key myelin proteins.
4. TRPV2 involvement in CNS myelin related disorders.
5. Expression of MSRA in association with TRPV2 function.
6. The importance of microglia-oligodendrocytes crosstalk in CNS myelin disorders.

1. Protein-protein interactions of TRPV2 and TRPV4 are related to CNS biological processes and protein trafficking

TRPV2 and TRPV4 are ubiquitously expressed in the whole body but also in the nervous system. TRPV2 is found in in medium-to-large neurons that have myelinated fibers (Caterina et al., 1999), in OPCs (Cahoy et al., 2008) and also in glial cells (Maksoud et al., 2019; Shibasaki et al., 2013). The functions of TRPV2 in the CNS have been related to the axon and neurite outgrowth of motor and sensory neurons (Cohen et al., 2015; Shibasaki et al., 2010) and phagocytosis of cellular debris by microglia and macrophages (Link et al., 2010). In the case of TRPV4, it has been described that it is expressed in DRG, osmosensory and hippocampal neurons (Bourque et al., 2007; Shibasaki et al., 2007) but also in oligodendrocytes and glial cells, being suggested that its expression controls glial cells volume, maturation and activation (Shibasaki et al., 2014). In addition, TRPV4 expression has been associated to different neurodegenerative disorders (Bai and Lipski, 2014; Butenko et al., 2012; Chen et al., 2016; Velilla et al., 2019; Verma et al., 2010). Importantly in the context of this project, TRPV4 activation in cuprizone model leads to oligodendrocyte death and subsequent demyelination (Liu et al., 2018).

As many evidences suggested that TRPV2 and TRPV4 activation are linked to their translocation to the plasma membrane, a PPI analysis of both ion channels was performed in our lab (Pau Doñate-Macián et al., 2018; P. Doñate-Macián et al., 2018) as an attempt to unravel their functions. Interestingly, as shown in **Chapter I** it is possible to observe that some biological common processes for TRPV2 and TRPV4 are related to the nervous system (neural

nucleus development, myelin sheath formation, phospholipid biosynthetic process, modulation of chemical synaptic transmission and cellular lipid metabolic process) but also with protein trafficking (cellular lipid metabolic process, phospholipid biosynthetic process and regulation of vesicle-mediated transport). Phospholipids and lipids are the main components of myelin, being necessary for the correct myelin compaction. In addition, lipids and phosphoinositides, type of phospholipids, are important regulators in protein trafficking (Krauss and Haucke, 2007). Phosphoinositides role has also been associated to protein binding (Krauss and Haucke, 2007). Also, regulation of vesicle-mediated transport seems to be related to TRP channels (Ferrandiz-Huertas et al., 2014). The results obtained by interactomics (Pau Doñate-Macián et al., 2018; P. Doñate-Macián et al., 2018) indicate that TRPV2 and TRPV4 are involved on protein trafficking (**Table 1 in Chapter I**). Interestingly some proteins found on TRPV2 interactome in the CNS (Pau Doñate-Macián et al., 2018) were found related to protein trafficking such as ARF1, ARL15, ABR, SYT-9 and SNAPIN, suggesting the involvement of these proteins on TRPV2 trafficking.

2. NO is responsible of TRPV2 activation in glial cells by TRPV2 translocation to the membrane

TRPV2 activation in the nervous system has been described as necessary for axon and neurite outgrowth (Cohen et al., 2015; Shibasaki et al., 2010). To date, it is known that TRPV2 can be activated by different stimuli such as mechanical stress, elevated temperatures (>52 °C) (Caterina et al., 1999; Perálvarez-Marín et al., 2013), several ligands that include growth factors (Kanzaki et al., 1999), different chemical compounds (Perálvarez-Marín et al., 2013) and oxidative stress (Fricke et al., 2019). Although there is some information available (Perálvarez-Marín et al., 2013), the knowledge of TRPV2 pharmacology is still limited and challenging. There are some compounds that are more specific TRPV2 modulators but are not completely specific for TRPV2, therefore, can activate other ion channels. In addition, these compounds can be species-dependent.

Several studies observed that some ligands activate phosphatidylinositol (PI) 3-kinase pathway resulting in TRPV2 translocation from intracellular compartments to the plasma membrane (Monet et al., 2009; Nagasawa and Kojima, 2012; Penna et al., 2006). Other studies also found that insulin-like growth factor-I translocates TRPV2 from an intracellular compartment to the plasma membrane (Hisanaga et al., 2009; Kanzaki et al., 1999). Besides ligands, membrane stretch has also been reported to be responsible of TRPV2 trafficking (Iwata et al., 2003). Studies performed in vascular smooth cells demonstrated that hypotonic stimulation and membrane stretch are responsible of increased cytoplasmic free Ca²⁺ concentration levels due to TRPV2 activation (Muraki et al., 2003). Interestingly, NO has also been related to TRPV2

activation. *Mihara et al.* (Mihara et al., 2010) found that TRPV2 activation results in intestinal relaxation through NO production. The same team also found that muscle contractions are inhibited by TRPV2 activators, but not in the presence of NO antagonists leading to the conclusion that TRPV2 is activated downstream NO. *Maksoud et al.* (Maksoud et al., 2019) observed that NO promotes TRPV2 trafficking to the plasma membrane and results in increased microglial phagocytosis capacity. Our results in mixed glial cultures (**Figure 2 in Chapter II**) reveal that TRPV2 is present in microglia, as previously said, and in OPCs. At basal conditions TRPV2 is mainly found in the cell body of both microglia and OPCs. However, after pro-inflammatory treatment with LPS, when levels of NO are increased, TRPV2 is translocated to the plasma membrane in both cell types (**Figure 2 in Chapter II**). These results are coincident with the previous studies, suggesting that TRPV2 trafficking to the plasma membrane is necessary for its activation and also that NO is one of the responsible of the TRPV2 translocation and subsequent activation (**Figure 7 in Chapter II**).

3. TRPV2 interaction with important key myelin proteins

Previous work from our lab performed by a MYTH assay (Pau Doñate-Macián et al., 2018) demonstrated that TRPV2 in the CNS interacts with important key myelin proteins such as PLP1, NTM and Opalin. This study also showed that TRPV2 interacts with other proteins involved in neoplasms and diseases of the CNS such as ABR, FGF1, KCNJ10, PEBP1, PLP1 and SCD3. As TRPV2 is widely expressed through the CNS and found in microglia (Maksoud et al., 2019), astrocytes (Shibasaki et al., 2013), medium-to-large neurons of myelinated fibers (Caterina et al., 1999) and also mRNA levels have been detected in OPC (Cahoy et al., 2008), we decide to investigate the relationship between TRPV2 and myelin. In **Chapter II (Figure 1A in Chapter II)** it is biochemically confirmed the capacity of interaction between TRPV2-PLP1, TRPV2-NTM and TRPV2-Opalin as observed in our previous MYHT assay (Pau Doñate-Macián et al., 2018). Also the strength of interaction in MYTH assay seems to be in accordance with the results observed in membranes (**Figure 1A in Chapter II**). Opalin and NTM show higher strength of interaction in both studies, showing strong blue intensity in MYTH assay (Pau Doñate-Macián et al., 2018) and the bands are more remarkable on membranes (**Figure 1A in Chapter II**). Also in the case of Opalin it can be observed that the TRPV2-Opalin interaction takes place thanks to ankyrin repeat domain (ARD) as they are able to bind when this domain is isolated (**Figure 1A in Chapter II**). Among these interactors we decide to go further with TRPV2 and Opalin interaction, because Opalin is specifically found in oligodendroglial cells, mainly in mature myelinating oligodendrocytes (Golan et al., 2008; Jiang et al., 2013; Kippert et al., 2008) but also at some early stages of OPCs (de Faria et al., 2019). However, Opalin is not found in any other glial cell types (Golan et al., 2008). In this work we

check the localization of TRPV2 and Opalin in mouse mixed glial primary cultures that are composed approximately by 25% microglia, 30% astrocytes and 35% oligodendrocytes. Our results reaffirm that TRPV2 and Opalin are interacting because a TRPV2-Opalin colocalization is found (**Figure 1B in Chapter II**), and also both of them share a common cell type; oligodendrocytes. Results obtained in **Chapter II (Figure 3D-I in Chapter II)** reinforce the TRPV2-Opalin interaction and the presence of TRPV2 on oligodendrocytes. In the WM of the spinal cord of these WT and jimpy mutant mice, TRPV2 and Opalin are both found in oligodendrocyte-like cells. Also when there is a severe loss of oligodendrocytes in jimpy mutant mice as already described (Thomson et al., 1999), there is a significant reduction of both TRPV2 and Opalin. Therefore, these results support the TRPV2 expression in oligodendrocytes and also the TRPV2-Opalin interaction.

4. TRPV2 involvement in CNS myelin related disorders

Our results exposed above points out a plausible involvement of TRPV2 in (re)myelination and myelin related disorders. In addition, other studies may indicate the TRPV2 implication in myelin disorders. Some studies performed by *Hainz et al.* (Hainz et al., 2017a, 2017b, 2016) revealed that probenecid, a pannexin-1 antagonist but also one of the most specific TRPV2 agonists, is capable to prevent and arrest the progression of clinical symptoms in EAE mice, and reduce demyelination in the cuprizone model of demyelination/remyelination. Another study performed by *Platten et al.* (Platten et al., 2005) showed that tranilast, a very specific TRPV2 antagonist is capable to ameliorate mice paralysis in EAE mice. All these data and our results lead us to study the TRPV2 expression in the hypomyelinating jimpy mice, the cuprizone and EAE mouse models of MS, and in MS human subjects.

4.1 TRPV2 expression in jimpy mutant mice

Spinal cord is a CNS structure responsible to carry messages from brain to the body and vice versa, being composed of GM and WM. GM is mainly composed by neuronal cell bodies, glial cells and non-myelinated axons. However, WM is mainly composed by myelinated axons. Therefore, it is expected that oligodendrocytes and also important key myelin proteins are found in the WM. Jimpy mutant mice express X-linked deleterious mutations in the PLP1 gene, one of the key myelin proteins interacting with TRPV2. As already said, jimpy mutant mice shows a severe significant decrease of TRPV2 (**Figure 3D-F in Chapter II**). For this decrease of TRPV2 could be different possible explanations. These animals show a severe loss and lack of oligodendrocytes maturation. Therefore, as TRPV2 is observed in oligodendrocytes could be possible that this decrease of TRPV2 reflect the decrease of the number of oligodendrocytes that occurs in jimpy mutant mice. Also, the decrease of TRPV2 levels in jimpy mutant mice are in

agreement with the previous results found in the mixed glial cultures that show a significant decrease of TRPV2 after pro-inflammatory (LPS) and demyelinating (LPC) treatments (**Figure 1J and K in Chapter II**). Jimpy mutant mice have an important loss and lack of oligodendrocytes but also express a pro-inflammatory environment with astrogliosis and microgliosis (Thomson et al., 1999)]. Therefore, may be possible that this pro-inflammatory environment found in jimpy mutant mice leads to decrease of TRPV2 expression although not necessarily affect its activation. Mutations in PLP1, a TRPV2 interactor, could also affect the TRPV2 expression resulting in a severe decrease of TRPV2 in jimpy mutant mice.

4.2 TRPV2 in cuprizone mouse model of MS

The cuprizone mouse model is a toxic model of demyelination in the CNS WM and GM. In this mouse model animals are fed with cuprizone that results in the apoptosis of mature oligodendrocytes leading to a strong demyelination and intense activation of both microglia and astrocytes. However, once cuprizone is withdrawal from the diet remyelination takes place. Therefore, this mouse model is a very used mouse model to study demyelination and remyelination in MS. *Hainz et al.* (Hainz et al., 2017a) demonstrated that probencid; pannexin-1 inhibitor and TRPV2 activator, is capable to reduce demyelination in cuprizone model. For all these reasons we decide to study the TRPV2 expression in cuprizone mice, concretely in CC that is one of the most affected areas with a severe demyelination (Blakemore, 1973b). In this study TRPV2 expression is evaluated in control mice, in the peak of demyelination (5 weeks with cuprizone treatment) and during the first week of remyelination (5 weeks with cuprizone treatment + 1 week with normal diet). Checking **Figure 4 in Chapter II** it can be observed that TRPV2 expression is mainly found in WM oligodendrocyte cell bodies and its expression progressive increases. It means, TRPV2 expression is increased during the peak of demyelination in comparison with control animals, however, the increase of TRPV2 is just significant when comparing control animals with animals at first week of remyelination. It has been described that in cuprizone model during active demyelination by cuprizone feeding there is primary adult oligodendrocyte degeneration but not OPCs (Bénardais et al., 2013; Fischbach et al., 2019). Meanwhile, astrocytes and microglia are activated (Gudi et al., 2014). Around 4-5 weeks of cuprizone diet, coincident with the peak of demyelination, there is a OPCs proliferative peak with the attempt to repopulate the loss of mature oligodendrocytes (Yamate-Morgan et al., 2019). In addition, during cuprizone exposure, microgliosis and phagocytic activity reaches its peak of activity around 3–4 weeks and then is stabilized (Plastini et al., 2020). As a first time to our knowledge, it is the first time that TRPV2 is observed in mature oligodendrocytes. Our results suggest that this increase of TRPV2 expression during demyelinating could be due to the proliferative peak of OPCs at 5 weeks of cuprizone diet, suggesting a plausible role of TRPV2 in oligodendrocytes maturation and myelination. Once,

cuprizone diet is stopped, spontaneously starts the remyelination process. This process of remyelination is accompanied by OPCs proliferation, migration and differentiation to achieve myelin restoration (Gudi et al., 2014). Therefore, the significant increase of TRPV2 during remyelination could be associated to OPCs increase and the presence of new adult oligodendrocytes. Although the most plausible explanation for this progressive increase of TRPV2 seems linked to OPCs and the new adult oligodendrocytes, it should take into account that during demyelination there is a peak of active microglia. Therefore, as TRPV2 is also expressed in microglial cells, the role of TRPV2 in microglia can not be excluded during the peak of demyelination. However, during remyelination microglia presence is rapidly diminished. Therefore, a role of TRPV2 in microglial functions is not expected for remyelinating timepoints.

4.3 TRPV2 in EAE mouse model of MS

EAE mouse model is caused by an autoimmune reaction against CNS myelin proteins through the activation of autoreactive T cells (Baker and Amor, 2015; van der Star et al., 2012). Studies performed by *Hainz et al.* (Hainz et al., 2017b, 2016) in EAE mice demonstrated that probenecid, a pannexin-1 antagonist but also a very specific TRPV2 agonist, is capable to prevent and arrest the progression of clinical symptoms and promotes oligodendrocytes proliferation. Another study performed in EAE mice showed that the very specific antagonist of TRPV2, tranilast, mice paralysis is reduced when administrated to these mice (Platten et al., 2005). In basal conditions and EAE onset, TRPV2 is mainly found in oligodendrocyte-like cells in the WM and in neurons in the GM (**Figure 5A in Chapter II**). However, during the peak of demyelination, there is a significant increase of TRPV2 levels and is mainly found in WM and in inflammatory lesions. These inflammatory lesions are composed by cells in which TRPV2 has already been described; microglia/macrophages, B cells, T cells and reactive astrocytes (Link et al., 2010; Maksoud et al., 2019; Mangiardi et al., 2011; Saunders et al., 2007; Shibasaki et al., 2013). Furthermore, during the peak of demyelination there is an increase of OPCs proliferation and a reduction of oligodendrocytes (Girolamo et al., 2011). Our results suggest that TRPV2 increase during the peak of demyelination could be due to the increase of OPCs and also supports a role of TRPV2 in microglia and infiltrated immune cells. Therefore, TRPV2 activity could be involved with cell phagocytosis, OPCs proliferation and any other function performed by the cells found in inflammatory focuses. During the chronic phase there is a severe decrease of the entire oligodendrocyte lineage; OPCs and mature oligodendrocytes. However, pre-myelinating oligodendrocytes remain stable (Girolamo et al., 2011). Our histological results show that TRPV2 is expressed in oligodendrocyte-like cells and inflammatory focuses. Also, shows that TRPV2 intensity is lower for chronic phase when comparing to samples from EAE at the peak of demyelination (**Figure 5A in Chapter II**).

Histological results are in agreement with TRPV2 quantification, showing a significant increase of TRPV2 expression during the peak of EAE and then there is a decrease during the chronic phase. TRPV2 expression remains stabilized during the different timepoints at the chronic phase (**Figure 5B in Chapter II**). A possible explanation for this TRPV2 constant expression along the chronic phase could be due to the remaining pre-myelinating oligodendrocytes that has been described as stable during the chronic phase (Girolamo et al., 2011).

4.4 How MSRA affects on TRPV2 expression in MS mouse models?

Methionine (Met) is an amino acid present in most organisms with important biological functions such as methylation and sulfur pathways, metabolite synthesis and involved in immune system function (Lee et al., 2008; Martínez et al., 2017). Impairment in the balance of Met oxidation and reduction could affect the correct functioning of the Met biological roles above and lead to different pathological conditions (Ahmadian et al., 2019; Stadtman and Berlett, 1998). Met residues can be easily oxidized by reactive oxygen species (ROS) to methionine-S-sulfoxide (Met-SO) and methionine-R-sulfoxide (Met-RO) (Lee et al., 2008). Methionine sulfoxide reductases are ubiquitously expressed in different organisms and are in charge to reduce Met residues (Tarrago et al., 2009). Concretely, methionine sulfoxide reductase type A (MSRA) is in charge to specifically reduce Met-SO to Met (Weissbach et al., 2005). It has been demonstrated that MSRA protects cells from oxidative stress (Zhang et al., 2010) that is a marker of MS (Choi et al., 2018; Ohl et al., 2016). Also, our used animal models to study TRPV2 in MS, cuprizone and EAE, and PMD patients that we study using jimpy mutant mice show elevated levels of oxidative stress (Kashani et al., 2017; Packialakshmi and Zhou, 2018; Ruiz et al., 2018). In addition, it has been recently found that a methionine-dependent redox pathway plays an important role in TRPV2 sensitization and activation (Fricke et al., 2019). *Fricke et al.* (Fricke et al., 2019) observed that MSRA is capable to partially reverse TRPV2 endogenous activation.

Our obtained results regarding the MSRA expression differ between the hypomyelinating jimpy mutant mice and the MS mouse models of cuprizone and EAE. As oxidative stress is found elevated in all MS mouse models and in PMD patients (Kashani et al., 2017; Packialakshmi and Zhou, 2018; Ruiz et al., 2018) we expected an increase of MSRA levels in our samples of the pathological conditions described above. Surprisingly, our results do not show this increase of MSRA levels in the hypomyelinating jimpy mutant mice. Although high levels of oxidative stress are found in PMD subjects (Ruiz et al., 2018) it is observed a significant reduction of TRPV2 levels in jimpy mice (**Figure 3D-F in Chapter II**). These results suggest that although oxidative stress is found upregulated in PMD patients, there is not a dysregulation of Met metabolic pathway in jimpy mutant mice. Some plausible explanations could be that probably

different amino acids than Met are oxidized in the pathogenesis of jimpy mutant mice or may be that MSRA activity is not affected as jimpy phenotype is not due to an acute inflammatory process. Studies focused on oxidative stress activity in jimpy mice could probably reply this question. Contrary to jimpy mutant mice, MSRA expression levels are increased in cuprizone and EAE models when comparing to controls. In cuprizone model this significant increase of MSRA is coincident with the peak of demyelination in CC (**Figure 4K in Chapter II**). However, in EAE model is more coincident with immune cell infiltration in the spinal cord (**Figure 5 in Chapter II**). It should take into account that immune cell infiltration results in increased levels of oxidative stress and ROS. Therefore, could be possible that MSRA upregulation is produced as an attempt to maintain the balance of Met oxidation and reduction. Met residues are easily oxidized by ROS (Lee et al., 2008) and also oligodendrocytes are the most sensitive CNS cells to oxidative stress (Noble et al., 1994; Thorburne and Juurlink, 1996). Therefore, MSRA increase could be associated to a mechanism to protect cells from oxidative stress by reducing Met-SO to Met. Our results on cuprizone model show an important increase of MSRA during demyelination and decrease during remyelination. These results suggest that MSRA may play a role on reverse TRPV2 activation and also a protective effect on oligodendrocytes, as it is observed an important increase of oligodendrocytes during remyelination.

4.5 TRPV2 and MSRA expression in MS human brains

All the obtained data with animal models leads us to go further and decide to study the TRPV2 and MSRA expression in frontal cortex samples from MS patients. In this case TRPV2 and MSRA expression is evaluated at mRNA and protein levels. TRPV2 mRNA and protein levels show a decrease on MS subject when comparing to controls, however, the decrease is just significant at protein levels. In the case of MSRA there is a significant increase in MS subjects mRNA and protein levels (**Figure 6 in Chapter II**). It has been described that in MS patients ROS production is increased leading to oxidative stress (Gilgun-Sherki et al., 2004; Ohl et al., 2016). Therefore, the observed increased levels of MSRA could be as an attempt to protect cells from oxidative stress by reducing Met-SO to Met. Our results obtained in the MS mouse models of cuprizone (**Figure 4K in Chapter II**) and EAE (**Figure 5B in Chapter II**), are in agreement with the results obtained in human samples. There is an increase of MSRA during the course of the pathology when there is a severe demyelination. Contrary to the obtained results of TRPV2 expression in cuprizone and EAE models, TRPV2 is downregulated in human samples. Importantly, in our used animal models TRPV2 is found upregulated during acute demyelination and remyelination. In cuprizone model we find an increase of TRPV2 when there is a severe demyelination but this increase is significant during remyelination (**Figure 4J in Chapter II**). In the case of EAE, TRPV2 is significantly upregulated during the peak of

symptomatology that courses with severe demyelination. Furthermore, in EAE model, there is a decrease of TRPV2 expression during the chronic phase when inflammation is attenuated (**Figure 5B in Chapter II**). TRPV2 levels in MS patients are evaluated at the chronic phase of the disease. Therefore, these results are in agreement with the obtained results in the chronic phase of EAE. Would be possible that this observed downregulation is a result of the cell death observed in MS patients (Dowling et al., 1997; Zipp, 2000) or due to a failure of oligodendrocytes to promote remyelination. TRPV2 pattern of expression in human samples is also coincident with the pattern of TRPV2 expression in jimpy mice. With all these data it can be said that TRPV2 downregulation in MS subjects indicates a putative involvement of TRPV2, as a cause or consequence, in MS pathology. In this regard, future studies of interest could be focused on TRPV2 activation/inhibition in MS mouse models such as EAE, and in other demyelinating diseases.

4.6 TRPV2 points out oligodendrocytes-microglia cross-talk to achieve (re)myelination

The starting point of our project is TRPV2 that in CNS has been described in medium-to-large neurons that have myelinated fibers (Caterina et al., 1999), astrocytes (Shibasaki et al., 2013), microglia (Maksoud et al., 2019), OPCs (Cahoy et al., 2008) and we also find its expression in mature oligodendrocytes. The function of TRPV2 remains unknown but it has been described that TRPV2 is necessary for axon and neurite outgrowth in motor and sensory neurons (Cohen et al., 2015; Shibasaki et al., 2010). In microglial cells, NO fosters TRPV2 trafficking to the membrane resulting in TRPV2 activation and subsequent increased microglial phagocytic capacity (Maksoud et al., 2019). This higher phagocytic activity of microglia could be very helpful to eliminate cell debris, restore demyelinated areas and other functions in infiltrating immune cells. In addition, studies on MS mouse models demonstrated that probenecid which is a very specific TRPV2 agonist improves the outcome in these experimental models (Hainz et al., 2017a, 2017b, 2016). With all the available data, our team decided to perform a MYTH assay to unravel the potential interactors of TRPV2 in the CNS (Pau Doñate-Macián et al., 2018). PPIs studies such as MYTH assay are very used to decipher a protein function based on the function of interacting proteins. Our team found that many of the TRPV2 interactors are associated with trafficking, neoplasms and other CNS diseases, and key myelin proteins (PLP1, NTM and Opalin). All these evidences point out the involvement of TRPV2 in (re)myelination. Also TRPV2 is expressed in glial cells and oligodendrocytes that are in continuous communication with OPCs, communication that is necessary to achieve (re)myelination. Therefore, with all the available bibliography and our discovery of TRPV2 expression in oligodendrocytes, we decide to go further and study the microglia-OPCs crosstalk in demyelinating disorders.

5. The importance of microglia and OPCs crosstalk during (re)myelination and demyelination

In **Chapter II** we focus in a small subset of players in the microglia-OPCs crosstalk (mainly TRPV2). Trying to obtain a wider perspective in pathophysiological myelination, and still highlighting the importance of the microglia and OPCs communication, we design a strategy to decipher potential demyelination/remyelination transcriptomic markers in a myelination experimental model in microglia and OPCs but also in CC, using data available in public repositories.

In this part of the work we unraveled different genes that could be very important during demyelination and remyelination. Concretely, we were really interested in the DEGs found between CC, microglia and OPCs when compared to their respective controls. In the case of CC, one of the most affected areas in cuprizone model (Blakemore, 1973b), DEGs were analyzed at early (2 weeks of cuprizone treatment) and late demyelination (4 weeks of cuprizone treatment) compared to controls, and also early and late demyelination were compared to remyelinating CC (4 weeks of cuprizone diet + 1 week normal diet). Although we are mainly interested in microglia-OPCs crosstalk, we also decided to check CC as is one of the most affected areas in cuprizone mice and we also found different patterns of expression of the TRPV2, an important key player in CNS disorders, in cuprizone mice (Enrich-Bengoa et al., 2022).

Our results in **Chapter II** demonstrated that TRPV2 expression in CC progressively increases in oligodendrocyte cells at peak of demyelination and in the first week of remyelination when compared to controls. It must be take into account that at these time points there is an important proliferation of OPCs and also during remyelination stage OPCs start to migrate and differentiate into mature oligodendrocytes to restore myelin (Gudi et al., 2014). These results in our previous study (Enrich-Bengoa et al., 2022) indicated that TRPV2 could play a significant role in oligodendrocytes maturation and myelination. However, in CC we must also take into account that in addition of oligodendroglia cells, there are also found astrocytes (Zhang et al., 2019) and microglial (Lee et al., 2019) cells. Although microglia activation severely decreases during remyelination we cannot completely discard the function of some DEGs found in CC as taking part of microglial processes such as phagocytosis Our results in CC show that the majority of the 10 most DEGs found in the four datasets (control-early demyelination, control-late demyelination, early demyelination-remyelination, and late demyelination-remyelination) (**Table3**) were associated to demyelination, neurite outgrowth, myelination networks or oligodendrocytes death. In addition, some of these DEGs were found in common among the datasets in CC.

Table 3. Comparison of the 10 most DEGs found in CC during early and late demyelination, and remyelination in cuprizone model.

<i>Gene</i>	Values	Ct vs 2 weeks	CT vs 4 weeks	2 weeks vs remyelination	4 weeks vs remyelination	Association with CNS
<i>Gdf15</i>	Log2 fold change	-4.3	-3.86			<p>Increase of <i>Gdf15</i> is related to functional recovery after traumatic spinal cord injury (Hassanpour Golakani et al., 2019)</p> <p><i>Gdf15</i> is found increased in mice after eight days of CZ feeding (Pandur et al., 2019).</p> <p><i>Gdf15</i> levels are increased in patients with stable MS, being a possible future marker of stability in MS (Amstad et al., 2020)</p>
	p-value	2.79e-06	3.37e-07			
	Adjusted p-value	1.63e-02	8.51e-03			
<i>Pigz</i>	Log2 fold change	3.1	2.54			<p>Downregulated in 2 day cuprizone mice in myelinating oligodendrocytes (Zhan et al., 2020).</p>
	p-value	2.98e-06	1.35e-06			
	Adjusted p-value	1.63E-02	1.10e-02			
<i>Trib3</i>	Log2 fold change	-4.64	-4.40		-3.16	<p>Overexpression of <i>trib3</i> is associated with myelin destruction in demyelination rats (Shimotsuma et al., 2016)</p> <p>Cuprizone stimulates <i>trib3</i> expression in the dentate gyrus (Abe et al., 2015).</p>
	p-value	1.11e-06	1.77e-06		7.56e-07	
	Adjusted p-value	1.34E-02	1.10e-02		4.60e-03	
<i>Ninj2</i>	Log2 fold change	3.22	1.92		1.86	<p>Promotes neurite outgrowth (Araki and Milbrandt, 2000) and involved in myelination networks (Allen et al., 2018).</p> <p>Downregulated in 2 day cuprizone mice in myelinating oligodendrocytes (Zhan et al., 2020).</p> <p>Lack of <i>Ninj2</i> in oligodendrocytes inhibits oligodendrocytes development and myelination. Also impairs neuronal structure and functions (Sun et al., 2021)</p> <p>Overexpressed in nonactivated adult OPCs when compared to activated adult OPCs (Moyon et al., 2015).</p>
	p-value	5.13e-06	2.01e-06		6.35e-07	
	Adjusted p-value	1.63e-02	1.10e-02		4.60e-03	
<i>Ccng1</i>	Log2 fold change		-1.93			<p>Upregulated during oligodendrocytes differentiation (Dugas et al., 2006)</p>
	p-value		2.41e-06			
	Adjusted p-value		1.10e-02			
<i>Slc34a3</i>	Log2 fold change	3.19	1.76			Not reported
	p-value	6.11e-06	2.78e-06			

	Adjusted p-value	1.63e-02	1.10e-02			
<i>Atf5</i>	Log2 fold change	-2.92	-3.41			Involved in oligodendrocytes proliferation and differentiation (Mason et al., 2005)
	p-value	8.27e-06	3.05e-06			
	Adjusted p-value	1.89e-02	1.10e-02			
<i>Xrcc3</i>	Log2 fold change		1.91			Expressed in cortical MS lesions and experimental demyelination (Martin et al., 2018)
	p-value		4.10e-06			
	Adjusted p-value		1.29e-02			
<i>Ddit3</i>	Log2 fold change		-1.70			Regulator of graded oligodendrocyte vulnerability and demyelination in cuprizone model (Fischbach et al., 2019)
	p-value		5.40e-06			
	Adjusted p-value		1.51e-02			
<i>Moxd1</i>	Log2 fold change		-2.59			Not reported
	p-value		7.51e-06			
	Adjusted p-value		1.60e-02			
<i>Cdkn1a</i>	Log2 fold change	-4.32				Found expressed in the majority of oligodendrocytes in demyelinated lesions, suggested as a possible marker for demyelination (Shen et al., 2021)
	p-value	1.89e-07				
	Adjusted p-value	4.55e-03				
<i>Tgm1</i>	Log2 fold change	-3.13				Upregulated in 2 day cuprizone mice in microglia/macrophages (Zhan et al., 2020). Tgm1 expression is severely increased at the lesion site after one and two weeks post-SCI (Kisucká et al., 2021)
	p-value	3.43e-06				
	Adjusted p-value	1.63e-02				
<i>B23007Rik</i>	Log2 fold change	3.46				Overexpressed in nonactivated adult OPCs when compared to activated adult OPCs (Moyon et al., 2015)
	p-value	4.86e-06				
	Adjusted p-value	1.63e-02				
<i>Eif4ebp1</i>	Log2 fold change	-2.31				Upregulated in blood MS patients and an mTOR downstream target. mTOR involved in oligodendrocytes differentiation (Akbarian et al., 2020)
	p-value	5.88e-06				
	Adjusted p-value	1.63e-02				
<i>D16Ert472e</i>	Log2 fold change			1.97		<i>D16Ert472e</i> is found severely expressed in myelinating oligodendrocytes (Reiche et al., 2021)
	p-value			4.11e-06		
	Adjusted p-value			2.74e-02		
<i>Aoc1</i>	Log2 fold change			1.66		Not reported
	p-value			4.95e-06		
	Adjusted p-value			2.74e-02		
<i>Krt15</i>	Log2 fold change			1.76		Not reported

	p-value			6.14e-06		
	Adjusted p-value			2.74e-02		
<i>Serpinb1c</i>	Log2 fold change			1.92		Overexpressed in nonactivated adult OPCs when compared to activated adults OPCs (Moyon et al., 2015). <i>Serpinb1</i> is found at the onset of EAE (Hou et al., 2019).
	p-value			7.42e-06		
	Adjusted p-value			2.74e-02		
<i>Slain1</i>	Log2 fold change			2.02		<i>Slain1</i> is widely expressed in brain and spinal cord tissues (Akila Parvathy Dharshini et al., 2019). Related to axon outgrowth (van der Vaart et al., 2012).
	p-value			1.05e-05		
	Adjusted p-value			2.74e-02		
<i>Cxcl10</i>	Log2 fold change			1.3		<i>CXCL10</i> regulates early microglial activation in cuprizone model, promoting neuroinflammation and resulting in oligodendrocytes apoptosis. However does not play a role in phagocytosis (Clarner et al., 2015). <i>CXCL10</i> is related to different demyelinating diseases (N. Zhang et al., 2020). Different studies show that <i>CXCL10</i> is upregulated during MS (Franciotta et al., 2001; Sørensen et al., 2002, 1999) and also that <i>CXCL10</i> values differ between the different MS subtypes (Scarpini et al., 2002). <i>CXCL10</i> neutralization exacerbates EAE symptomatology (Narumi et al., 2002). However, other study indicates that anti- <i>CXCL10</i> administration ameliorates the symptomatology in EAE (Fife et al., 2001) <i>CXCL10</i> is associated with EAE pathogenesis (Fife et al., 2001; Glabinski et al., 1995)
	p-value			1.35e-05		
	Adjusted p-value			2.74e-02		
<i>Sntn</i>	Log2 fold change			1.63		Not reported
	p-value			1.36e-05		
	Adjusted p-value			2.74e-02		
<i>Lrig3</i>	Log2 fold change			1.56		Not reported
	p-value			1.39e-05		
	Adjusted p-value			2.74e-02		
<i>Ppfibp2</i>	Log2 fold change			1.95		<i>Ppfibp2</i> mediates axonal extension and synapse formation (Brown et al., 2017)
	p-value			1.58e-05		

	Adjusted p-value			2.74e-02		
<i>Dusp15</i>	Log2 fold change			1.29		<i>Dusp15</i> plays an important role in oligodendrocytes differentiation (Schmidt et al., 2012)
	p-value			1.65e-05		
	Adjusted p-value			2.74e-02		
<i>Mog</i>	Log2 fold change				3.13	MOG Abs are associated with MS demyelination and other demyelinating diseases (Hennes et al., 2018; Peschl et al., 2017; Rosenthal et al., 2020) Remyelination of CC is accompanied by a increased of MOG immunoreactivity during the recovery period (Sachs et al., 2014). Transplantation of anti-MOG-immunosorted cells into locations with acute demyelination results in rising remyelinating oligodendrocytes (Crang et al., 2004). The function of MOG remains unknown but several studies point out MOG as responsible of triggering primary autoimmune-mediated demyelination (Ambrosius et al., 2020; Linington et al., 1988; Wynford-Thomas et al., 2019).
	p-value				7.39e-07	
	Adjusted p-value					
<i>Cyp3a13</i>	Log2 fold change				1.34	Not reported
	p-value				7.49e-07	
	Adjusted p-value				4.60e-03	
<i>Gm5067</i>	Log2 fold change				2.93	Not reported.
	p-value				1.52e-06	
	Adjusted p-value				7.10e-03	
<i>Sh3gl3</i>	Log2 fold change				1.87	Expressed in all CNS cells but higher expressed in myelinating oligodendrocytes and newly formed oligodendrocytes (Wasseff and Scherer, 2015). Upregulated in differentiated rat primary oligodendrocytes when compared to primary rat OPCs (Miyamoto et al., 2021).
	p-value				2.47e-06	
	Adjusted p-value					
<i>Msmo1</i>	Log2 fold change				1.47	Not reported.
	p-value				2.58e-06	

	Adjusted p-value				7.10e-03	
<i>E330037M01Rik</i>	Log2 fold change				3.05	Not reported.
	p-value				2.84e-06	
	Adjusted p-value				7.10e-03	
<i>Plekh1</i>	Log2 fold change				2.28	Not reported.
	p-value				2.93e-06	
	Adjusted p-value				7.10e-03	
<i>Insig1</i>	Adjusted p-value				1.39	Association in mature oligodendrocytes between glutamate exposure, increase of <i>Insig1</i> and reduction in the extension of human oligodendrocyte processes and in their ensheathing capacity (Larochelle et al., 2021)
	Adjusted p-value				3.13e-06	
	Adjusted p-value				7.10e-03	

One of the 10 most DEGs that was found upregulated during demyelination and remyelination was *Ninj2*, that has been related to neurite outgrowth and myelination network s(Allen et al., 2018; Araki and Milbrandt, 2000). Therefore, *Ninj2* upregulation could be linked to remyelination by sending signals for myelin recovery during demyelination and being necessary the continued activation of this signals to achieve remyelination once cuprizone diet is retired. Further studies will be needed to understand its role during de-/remyelination. As several DEGs were found associated with important process for a correct myelination, we decided to perform GO ontology and WikiPathways enrichment analysis to identify the different biological and molecular processes associated to the DEGs found in cuprizone. During late demyelination there were found 115 biological processes such as cholesterol biosynthesis, ensheathment of neurons, axon ensheathment in CNS, CNS myelination, glial cell differentiation, oligodendrocyte differentiation, neurogenesis, glial cell development, sphingolipid metabolic process, central nervous system development, oligodendrocyte development, myelin assembly and protein localization to paranode region of axon and regulation of neurogenesis (**Supplementary Table 14 in Chapter III**). However, when evaluating the molecular functions of the 20 most DEGs between control mice and 2 or 4-weeks-cuprizone treated mice, and 2 or 4-weeks-cuprizone treatment versus remyelination, it was observed that in all three cases some DEGs were associated to structural constituents of myelin sheath (**Figure 2E and H in Chapter III**). WikiPathways analysis in CC revealed that cholesterol biosynthesis or cholesterol metabolism were present at three time points of CC analysis (**Figure 2E and H in Chapter III**). Interestingly, cholesterol biosynthesis is a key pathway in myelination that is found affected in demyelination diseases (Raddatz et al., 2016). These biological and molecular

functions found in CC suggest the importance of these DEGs during (re)myelination and demyelination.

As previously said, CC is on the most affected areas in cuprizone model but there are present other cells than oligodendroglia lineage cells. Therefore, we cannot assure in which type of cells are found these DEGs. Hence, we decided to specifically study the involved molecules between microglia and OPCs crosstalk. In this case it was just possible to study the genes involved during late demyelination when compared to controls due to the available datasets (**Supplementary Table 1 in Chapter III**).

In microglia we found 12 DEGs upregulated (**Figure 1B and Figure 3 in Chapter III, Supplementary Table 4 and Supplementary Figure 2C in Chapter III**), and among these genes were found *Lpl* and *Olr1*. *Lpl* has been related to support remyelination by scavenging myelin-derived lipids in CNS and PNS (Bruce et al., 2018), and also has been found as a key player in microglia to achieve remyelination (Olah et al., 2012). Importantly, *Olr1*, has been described as an essential receptor for myelin phagocytosis (Gaultier et al., 2009). Among the other DEGs found in microglia, *Lgals3* was found in common between microglia and OPCs. *Lgals3* gene encodes for Galectin-3 that has been identified in microglia and oligodendrocytes in the cuprizone mode and also *Lgals3*^{-/-} mice show important deficits in remyelination and microglia activation (Hoyos et al., 2014). Therefore, upregulated genes found in microglia during demyelination would probably have an important role on sending signals to achieve remyelination.

The next step consisted in identifying the DEGs in OPCs between control and 4 week-cuprizone fed animals. In this case, several DEGs were found, concretely, 1372 downregulated and 1358 upregulated that make a total of 2730 DEGs (**Supplementary Table 5 in chapter III**). Among these DEGs, were found important key genes related to CNS as for example as *Mobp* and *Mog*. Interestingly, we found *Opalin* as a DEG that in our previous work (Enrich-Bengoia et al., 2022) was found interacting with the TRPV2 which is a key player in CNS myelin, and also *Opalin* was found severely decreased in a mouse model of an hypomyelinating disorder. Therefore, further studies of *Opalin* expression at in the whole oligodendroglial lineage and at different time points in cuprizone model could be very hopeful to unravel the role of *Opalin* in de-/remyelination and during physiological myelination. In OPCs, some of the most significantly DEGs were also found among the most DEGs in CC (**Supplementary Figure 2B and E**). Concretely, these genes were: *Atf5*, *Trib3* and *Cdkn1a*. Contrary to the obtained data in CC dataset, these genes were found upregulated in OPCs and downregulated in CC. *Atf5* downregulation is necessary for differentiation of neurons, astrocytes and OPCs and also *Atf5* is not expressed in mature oligodendrocytes (Mason et al., 2005). A plausible explanation to be

found *Atf5* downregulated in CC and upregulated OPCs is that *Atf5* overexpression during demyelination inhibits OPCs differentiation. Nevertheless, other cell types could counterbalance the effect by *Atf5* downregulation. *Trib3* overexpression has been described as associated to demyelination and was also found that cuprizone stimulates *Trib3* expression. Our obtained results in OPCs are in line with previous available bibliography (Abe et al., 2015; Shimotsuma et al., 2016), probably studies focused on *Trib3* expression at different cell types could be helpful to understand such differences. *Cdkn1a* has been described in the majority of oligodendrocytes in demyelinated lesions, being suggested as a possible marker for demyelination (Shen et al., 2021). GO terms and WikiPathways in OPCs revealed that the most significant DEGs were associated with 19 molecular functions (**Supplementary Table 15 in Chapter III**) and 226 biological processes including; regulation of axon extension, neurogenesis, and neuron projection development, among others. WikiPathways analysis revealed 6 significant WikiPathways associated to these DEGs such as cholesterol metabolism and sphingolipid metabolism (**Figure 2F in Chapter III**). Cholesterol and sphingolipids are major components of myelin and an impaired metabolism leads to different neurological and neurodegenerative disorders (Li et al., 2019).

All these obtained data reinforce the importance of microglia and OPCs communication to achieve (re)myelination and also the involvement of several of these genes during demyelinating processes. Therefore, we decided to go further and study the communication between microglia and OPCs. The microglia-OPCs crosstalk was studied through a putative ligand-receptor pair analysis using the NicheNet model. This model allowed us to identify 47 potential microglia ligands that could be interacting with 43 potential OPC receptors and 115 OPC target genes associated with demyelination (**Figure 4 in Chapter III**). The different identified microglia ligands (**Supplementary Table 10 in Chapter III**) and OPC receptors (**Supplementary Table 12 in Chapter III**) have been related to de-/(re-)myelinating processes.

When we performed the analysis of microglia ligands with OPC receptors after cuprizone treatment, we found that among the microglia-OPC interactions, the following ligand-receptor pairs presented the maximum potential of interaction: CSF1-CSFR, GAS6-AXL/TYRO3, IGF1-IGF1R, JAM2-JAM3, PTPRC-CD22, APOE-VLDLR, LRPAP1-VLDLR, SMAD4D-PLXNB1 (**Figure 3 and 4C in Chapter III**). All these interactions have been described as associated to demyelination, myelination or oligodendroglial cells. Upregulation of *Csf1* was described in demyelinated WM lesions of cuprizone treated mice. Also *Csf1r* inhibition overrides oligodendrocytes death, demyelination and astrogliosis in cuprizone treated mice (Marzan et al., 2021). *Gas6* and *Axl* have been reported as necessary for the maintenance of axonal integrity and remyelination after cuprizone treatment (Ray et al., 2017). Another study demonstrated that pro-myelinating effects of *Gas6* are lost in absence of *Tyro3* receptor (Akkermann et al., 2017).

Igf1 action that is mediated by the receptor *Igf1r* has been related to oligodendrocytes proliferation, differentiation, survival and myelination (Wrigley et al., 2017). Another study (Mason et al., 2000) demonstrated that *Igf1* prevents mature oligodendrocyte depletion during primary demyelination, facilitating a quick improvement from demyelination. Our results showed that *Jam3* was found as the most differentially expressed OPC receptors (**Figure 4C in chapter III**). Different studies observed that when *Jam2* interacts with its receptor, inhibits oligodendrocytes wrapping but does not affect oligodendrocytes density, differentiation proliferation or migration (Follis and Carter, 2016; Redmond et al., 2016). Another study described that members of the Jam family, such as *Jam-c*, has an important role on maintaining integrity of myelin sheaths (Scheiermann et al., 2007). Therefore, the observed *Jam3* downregulation in OPCs from cuprizone treated mice, could indicate that decreased levels of *Jam3* contribute to the loss of myelin integrity observed in cuprizone mice. Among the other ligand-receptors interactions, *Ptprc* has been described as involved in OPCs differentiation and *Ptprc* deficient mice showed dysmyelination (Nakahara et al., 2005). *ApoE* has been described as an important contributor in supporting and maintaining myelination but also it has been found upregulated after SCI (Gu et al., 2013), pointing out *ApoE* as an interesting target to repair CNS injury. However, another study found that MS patients that express some *ApoE* alleles have worse clinical course of the pathology (Carlin et al., 2000). The *ApoE* receptor, *Vldlr*, has been suggested as possibly playing an important role in myelin generation (Zhao et al., 2007). *Lrpap1* has been described as involved in myelin uptake (Fitzner et al., 2011). *Sema4D* triggers glial activation, inhibits OPCs migration and differentiation and also inhibits remyelination (Smith et al., 2015). Inhibition of *Sema4D* activity reduces OPCs death and enhances remyelination (Smith et al., 2015). Another study (Taniguchi et al., 2009) observed that lack of *Sema4D* results in increased number of oligodendrocytes, suggesting that *Sema4D* could be a negative regulator of oligodendrocyte development. In another article, was demonstrated that *Sema4D* inhibits OPCs differentiation by triggering apoptosis (Yamaguchi et al., 2012). A study performed on *Sema4D* knockdown in oligodendrocytes resulted in functional recovery after SCI (H.-L. Zhang et al., 2014). *Sema4D*-*Plxnb1* interaction is involved in microglial activation and pathogenesis of EAE, however, inhibition of *Sema4D* significantly arrests neuroinflammation in the EAE model (Okuno et al., 2010). Our obtained results with the ligand-receptor analysis showed that all these microglia ligands and OPC receptors are key to understand myelination in physiological conditions and pathological conditions.

Among the 43 identified OPC receptors there were 15 differentially expressed, concretely, 6 DEGs upregulated (*Plxnb2*, *TnfRsf1a*, *Acvr1*, *LRP1*, *Itgb5* and *AXL*) and 9 DEGs downregulated (*Jam3*, *HHIP*, *LDLR*, *Fgfr2*, *Itgb4*, *Ephb1*, *Lpar1*, *Tyro3* and *Sorl1*) after cuprizone treatment (**Figure 4C and Supplementary Table 12 in Chapter III**). Although the function of some of

them still remains unknown, several of these DEGs have been related to CNS myelin and related pathologies, and also with oligodendrocytes (**Table 4**).

Table 4. Associated functions of the differentially expressed OPC receptors.

	Gene ID	Function in CNS
Upregulated	<i>Plxnb2</i>	Involved to the maintenance of a stable synaptic connectivity in the adult hippocampus (Simonetti et al., 2021) and plays an important role in postnatal and adult neurogenesis (Saha et al., 2012).
	<i>Tnfrsf1a</i>	Mutations in <i>Tnfrsf1a</i> have been associated with a high risk to develop MS promoting the increase of pro-inflammatory signals (Caminero et al., 2011).
	<i>Acvr1</i>	Involved in OPCs differentiation and myelin production (Quan et al., 2022). Other studies also revealed that Mutations in <i>Acvr1</i> gene inhibits oligodendrocytes differentiation (Fortin et al., 2020).
	<i>Lrp1</i>	<i>Lrp1</i> is a direct negative regulator of OPC differentiation but does not influence proliferation. In addition, <i>Lrp1</i> blockade leads to myelin recovery (Auderset et al., 2020).
	<i>Itgb5</i>	Oligodendrocyte cells express integrins that necessary for oligodendrocytes proliferation, survival, and maturation (O'Meara et al., 2011).
	<i>Axl</i>	<i>Axl</i> is necessary for of axonal integrity and remyelination after cuprizone treatment (Ray et al., 2017).
Downregulated	<i>Jam3</i>	<i>Jam3</i> is the counter-receptor of <i>Jam2</i> which is responsible of inhibiting oligodendrocytes wrapping (Arrate et al., 2001; Liang et al., 2002).
	<i>Hhip</i>	<i>Hhip</i> interacts <i>shh</i> that protects from demyelination and favors OPC proliferation and subsequent remyelination (Ferent et al., 2013).
	<i>Ldlr</i>	<i>Ldlr</i> is necessary for a correct myelination and reduced levels of <i>Ldlr</i> are linked to an impaired OPCs differentiation (Pietiäinen et al., 2013).
	<i>Fgfr2</i>	Regulates myelin thickness, fosters remyelination just in chronic demyelinated lesions and promotes myelin growth during developmental (Furusho et al., 2012).
	<i>Itgb4</i>	Regulates OPCs proliferation (W. Zhang et al., 2020).
	<i>Ephb1</i>	Stimulates myelin sheath formation (Linneberg et al., 2015) and is involved in T cell differentiation and migration to inflammatory sites in both EAE and MS (Darling and Lamb, 2019).
	<i>Lpar1</i>	<i>Lpar1</i> is required for OPCs differentiation and myelination (García-Díaz et al., 2015). Lack of <i>Lpar1</i> is linked and its deletion has been correlated with myelin alterations and oligodendrocytes death (García-Díaz et al., 2015). correlated with myelin alterations and oligodendrocytes death (García-Díaz et al., 2015)
	<i>Tyro3</i>	Its expression is found at the onset of remyelination and promotes myelination (Akkermann et al., 2017).
<i>Sor11</i>	<i>Sor11</i> is involved in the communication between mature oligodendrocytes and activated microglia (Luan et al., 2021)	

The NicheNet model also allowed to identify 115 OPC target genes, being 107 differentially expressed between control mice and cuprizone-treated mice (**Figure 4D and E in Chapter III, Supplementary Table 13 in Chapter III**). The most DEGs were *Bbc3*, *Gadd45b* and *Hist1h3d*. Among these DEGS, *Bbc3* and *Gadd45b* have been related to different oligodendrocytes processes. *Bbc3* is a pro-apoptotic gene that fosters premyelinating oligodendrocytes cell death (Sun et al., 2018). Our results showed that that *Bbc3* is upregulated in cuprizone treated mice which could indicate that *Bbc3* leads to some oligodendroglia cells death. *Gadd45b* was also found upregulated in cuprizone treated mice downregulating a signal that is necessary for proliferation (J.-X. Zhang et al., 2014).

The latest results of this work demonstrate the importance of the microglia-OPCs crosstalk during de-/(re-)myelination. Our results showed that TRPV2 is a key player in CNS myelin disorders and also that is probably involved in the maturation of oligodendrocytes and myelination. Also, a role of TRPV2 in microglia is confirmed in EAE mice model. Therefore, with the available data supporting as necessary the crosstalk between microglia and oligodendrocytes to achieve re-/myelination we decided to go further and study the involved genes and interactions between microglia and OPCs. Further studies could be focused on studying some of the unraveled genes in tissue or cell samples from demyelinating animal models. Also the discovery of new ligands, receptors and target genes could be biochemically validated and study in *in vitro* and histological models.

Conclusions

Conclusions

The main conclusions of this thesis are:

Chapter I

- We have identified key proteins for the regulated and constitutive trafficking of TRPV2 towards the membrane. Most of these interactors are lipid-dependent and lipid-modifying proteins, key in the regulation of the lipid composition for membrane proteins when trafficked from internal compartments towards the plasma membrane.

Chapter II

- TRPV2 is present in several cell types in the CNS, such as microglia, OPCs and oligodendrocytes.
- Confirmation that NO translocates TRPV2 to the plasma membrane towards channels activity not only in microglia, but also in OPCs.
- TRPV2 interacts at the biochemical level with PLP1, Opalin, and NTM. The TRPV2-Opalin, and TRPV2-NTM interaction is highly likely to be mediated by the TRPV2 ankyrin repeat domain. TRPV2 and Opalin colocalize in oligodendrocyte-related cells.
- TRPV2 and Opalin expression patterns in jimpy mutant mice and in the cuprizone experimental model agree with the potential expression of TRPV2 in oligodendrocytes and the TRPV2-Opalin interaction in this cell-type.
- TRPV2 expression increases during the peak of demyelination in the mice cuprizone model due to the proliferative peak of OPCs, confirming the expression of TRPV2 in OPCs. In cuprizone model, TRPV2 increase is higher during the remyelination OPCs increase and the presence of mature oligodendrocytes. These results support the presence of TRPV2 in OPCs and oligodendrocytes.
- In the EAE model, TRPV2 expression increases during the demyelination peak, and decreases during the chronic phase. MSRA expression levels increase during demyelination in the EAE and the cuprizone models as a direct indicator of active methionine-oxidized TRPV2.
- MSRA expression levels increase and TRPV2 decrease in MS patients during demyelination, which agrees with the results shown in the EAE model, arguing for a protective mechanism against oxidative stress. MSRA expression levels are not affected

in hypomyelinating jimpy mutant mice, since this mutant does not suffer from a severe inflammatory/oxidative phenotype.

- TRPV2 activation increases microglia and infiltrating immune cells phagocytic activity as a necessary step to remove cell debris to restore demyelinated areas.

Chapter III

- Using transcriptomic data analysis of cuprizone treated animals, we observe that most DEGs found are robustly associated to remyelination, demyelination, neurite outgrowth, myelination networks, oligodendrocytes death, and myelin phagocytosis, but also to lipid metabolism.
- Crosstalk analysis identified 47 microglia ligands, 43 OPC receptors and 115 OPC target genes. Identified ligands, receptors and target genes, were differentially expressed in cuprizone treated samples and most of them are already associated with myelination. Also from our study we have identified several microglia ligands/OPCs receptor and microglia ligands/OPCs targets pairs, which require further experimental validation, but are highly promising novel myelination players.
- Our methodological approach highlights the potential of data analysis to study the cellular crosstalk not only in co-cultured cell types, but also with transcriptomic data of independent studies, as long as the cell types have received the same treatment, opening the possibility of analyzing the crosstalk between cell types that cannot be co-cultured for which transcriptomic data is available.

Bibliography

- Abe, H., Tanaka, T., Kimura, M., Mizukami, S., Saito, F., Imatanaka, N., Akahori, Y., Yoshida, T., Shibutani, M., 2015. Cuprizone decreases intermediate and late-stage progenitor cells in hippocampal neurogenesis of rats in a framework of 28-day oral dose toxicity study. *Toxicol. Appl. Pharmacol.* 287, 210–221. <https://doi.org/10.1016/j.taap.2015.06.005>
- Abumaria, N., Li, W., Clarkson, A.N., 2019. Role of the channel TRPM7 in the nervous system in health and disease. *Cell. Mol. Life Sci. CMLS* 76, 3301–3310. <https://doi.org/10.1007/s00018-019-03124-2>
- Ahmadian, E., Eftekhari, A., Samiei, M., Maleki Dizaj, S., Vinken, M., 2019. The role and therapeutic potential of connexins, pannexins and their channels in Parkinson's disease. *Cell. Signal.* 58, 111–118. <https://doi.org/10.1016/j.cellsig.2019.03.010>
- Akbarian, F., Tabatabaiefar, M.A., Shaygannejad, V., Shahpouri, M.M., Badihian, N., Sajjadi, R., Dabiri, A., Jalilian, N., Noori-Dalooi, M.R., 2020. Upregulation of MTOR, RPS6KB1, and EIF4EBP1 in the whole blood samples of Iranian patients with multiple sclerosis compared to healthy controls. *Metab. Brain Dis.* 35, 1309–1316. <https://doi.org/10.1007/s11011-020-00590-7>
- Akila Parvathy Dharshini, S., Taguchi, Y., Michael Gromiha, M., 2019. Exploring the selective vulnerability in Alzheimer disease using tissue specific variant analysis. *Genomics* 111, 936–949. <https://doi.org/10.1016/j.ygeno.2018.05.024>
- Akkermann, R., Aprico, A., Perera, A.A., Bujalka, H., Cole, A.E., Xiao, J., Field, J., Kilpatrick, T.J., Binder, M.D., 2017. The TAM receptor Tyro3 regulates myelination in the central nervous system. *Glia* 65, 581–591. <https://doi.org/10.1002/glia.23113>
- Alim, I., Teves, L., Li, R., Mori, Y., Tymianski, M., 2013. Modulation of NMDAR Subunit Expression by TRPM2 Channels Regulates Neuronal Vulnerability to Ischemic Cell Death. *J. Neurosci.* 33, 17264–17277. <https://doi.org/10.1523/JNEUROSCI.1729-13.2013>
- Allen, M., Wang, X., Burgess, J.D., Watzlawik, J., Serie, D.J., Younkin, C.S., Nguyen, T., Malphrus, K.G., Lincoln, S., Carrasquillo, M.M., Ho, C., Chakrabarty, P., Strickland, S., Murray, M.E., Swarup, V., Geschwind, D.H., Seyfried, N.T., Dammer, E.B., Lah, J.J., Levey, A.I., Golde, T.E., Funk, C., Li, H., Price, N.D., Petersen, R.C., Graff-Radford, N.R., Younkin, S.G., Dickson, D.W., Crook, J.R., Asmann, Y.W., Ertekin-Taner, N., 2018. Conserved brain myelination networks are altered in Alzheimer's and other neurodegenerative diseases. *Alzheimers Dement. J. Alzheimers Assoc.* 14, 352–366. <https://doi.org/10.1016/j.jalz.2017.09.012>
- Ambrosius, W., Michalak, S., Kozubski, W., Kalinowska, A., 2020. Myelin Oligodendrocyte Glycoprotein Antibody-Associated Disease: Current Insights into the Disease Pathophysiology, Diagnosis and Management. *Int. J. Mol. Sci.* 22, 100. <https://doi.org/10.3390/ijms22010100>
- Amstad, A., Coray, M., Frick, C., Barro, C., Oechtering, J., Amann, M., Wischhusen, J., Kappos, L., Naegelin, Y., Kuhle, J., Mehling, M., 2020. Growth differentiation factor 15 is increased in stable MS. *Neurol. Neuroimmunol. Neuroinflammation* 7, e675. <https://doi.org/10.1212/NXI.0000000000000675>

Araki, T., Milbrandt, J., 2000. Ninjurin2, a novel homophilic adhesion molecule, is expressed in mature sensory and enteric neurons and promotes neurite outgrowth. *J. Neurosci. Off. J. Soc. Neurosci.* 20, 187–195.

Arrate, M.P., Rodriguez, J.M., Tran, T.M., Brock, T.A., Cunningham, S.A., 2001. Cloning of human junctional adhesion molecule 3 (JAM3) and its identification as the JAM2 counter-receptor. *J. Biol. Chem.* 276, 45826–45832. <https://doi.org/10.1074/jbc.M105972200>

Auderset, L., Pitman, K.A., Cullen, C.L., Pepper, R.E., Taylor, B.V., Foa, L., Young, K.M., 2020. Low-Density Lipoprotein Receptor-Related Protein 1 (LRP1) Is a Negative Regulator of Oligodendrocyte Progenitor Cell Differentiation in the Adult Mouse Brain. *Front. Cell Dev. Biol.* 8, 1067. <https://doi.org/10.3389/fcell.2020.564351>

Bai, J.-Z., Lipski, J., 2014. Involvement of TRPV4 channels in A β (40)-induced hippocampal cell death and astrocytic Ca(2+) signalling. *Neurotoxicology* 41, 64–72. <https://doi.org/10.1016/j.neuro.2014.01.001>

Baker, D., Amor, S., 2015. Mouse models of multiple sclerosis: lost in translation? *Curr. Pharm. Des.* 21, 2440–2452. <https://doi.org/10.2174/1381612821666150316122706>

Barthelmes, J., Tafferner, N., Kurz, J., de Bruin, N., Parnham, M.J., Geisslinger, G., Schiffmann, S., 2016. Induction of Experimental Autoimmune Encephalomyelitis in Mice and Evaluation of the Disease-dependent Distribution of Immune Cells in Various Tissues. *J. Vis. Exp. JoVE* 53933. <https://doi.org/10.3791/53933>

Beecham, A.H., Patsopoulos, N.A., Xifara, D.K., Davis, M.F., Kempainen, A., Cotsapas, C., Shahi, T.S., Spencer, C., Booth, D., Goris, A., Oturai, A., Saarela, J., Fontaine, B., Hemmer, B., Martin, C., Zipp, F., D'alfonso, S., Martinelli-Boneschi, F., Taylor, B., Harbo, H.F., Kockum, I., Hillert, J., Olsson, T., Ban, M., Oksenberg, J.R., Hintzen, R., Barcellos, L.F., Agliardi, C., Alfredsson, L., Alizadeh, M., Anderson, C., Andrews, R., Søndergaard, H.B., Baker, A., Band, G., Baranzini, S.E., Barizzone, N., Barrett, J., Bellenguez, C., Bergamaschi, L., Bernardinelli, L., Berthele, A., Biberacher, V., Binder, T.M.C., Blackburn, H., Bomfim, I.L., Brambilla, P., Broadley, S., Brochet, B., Brundin, L., Buck, D., Butzkueven, H., Caillier, S.J., Camu, W., Carpentier, W., Cavalla, P., Celiuss, E.G., Coman, I., Comi, G., Corrado, L., Cosemans, L., Cournu-Rebeix, I., Cree, B.A.C., Cusi, D., Damotte, V., Defer, G., Delgado, S.R., Deloukas, P., di Sapio, A., Dilthey, A.T., Donnelly, P., Dubois, B., Duddy, M., Edkins, S., Elovaara, I., Esposito, F., Evangelou, N., Fiddes, B., Field, J., Franke, A., Freeman, C., Frohlich, I.Y., Galimberti, D., Gieger, C., Gourraud, P.-A., Graetz, C., Graham, A., Grummel, V., Guaschino, C., Hadjixenofontos, A., Hakonarson, H., Halfpenny, C., Hall, G., Hall, P., Hamsten, A., Harley, J., Harrower, T., Hawkins, C., Hellenthal, G., Hillier, C., Hobart, J., Hoshi, M., Hunt, S.E., Jagodic, M., Jelčić, I., Jochim, A., Kendall, B., Kermode, A., Kilpatrick, T., Koivisto, K., Konidari, I., Korn, T., Kronsbein, H., Langford, C., Larsson, M., Lathrop, M., Lebrun-Frenay, C., Lechner-Scott, J., Lee, M.H., Leone, M.A., Leppä, V., Liberatore, G., Lie, B.A., Lill, C.M., Lindén, M., Link, J., Luessi, F., Lycke, J., Macciardi, F., Männistö, S., Manrique, C.P., Martin, R., Martinelli, V., Mason, D., Mazibrada, G., McCabe, C., Mero, I.-L., Mescheriakova, J., Moutsianas, L., Myhr, K.-M., Nagels, G., Nicholas, R., Nilsson, P., Piehl, F., Pirinen, M., Price, S.E., Quach, H., Reunanen, M., Robberecht, W., Robertson, N.P., Rodegher, M., Rog, D., Salvetti, M., Schnetz-Boutaud, N.C., Sellebjerg, F., Selter, R.C., Schaefer, C., Shaunak, S., Shen, L., Shields, S., Siffrin, V., Slee, M., Sorensen, P.S., Sorosina, M., Sospedra, M., Spurkland, A., Strange, A., Sundqvist, E., Thijs, V., Thorpe, J., Ticca, A., Tienari, P., van Duijn,

- C., Visser, E.M., Vucic, S., Westerlind, H., Wiley, J.S., Wilkins, A., Wilson, J.F., Winkelmann, J., Zajicek, J., Zindler, E., Haines, J.L., Pericak-Vance, M.A., Ivinson, A.J., Stewart, G., Hafler, D., Hauser, S.L., Compston, A., McVean, G., De Jager, P., Sawcer, S., McCauley, J.L., 2013. Analysis of immune-related loci identifies 48 new susceptibility variants for multiple sclerosis. *Nat. Genet.* 45, 1353–1360. <https://doi.org/10.1038/ng.2770>
- Bénardais, K., Kotsiari, A., Skuljec, J., Koutsoudaki, P.N., Gudi, V., Singh, V., Vulinović, F., Skripuletz, T., Stangel, M., 2013. Cuprizone [bis(cyclohexylidenehydrazide)] is selectively toxic for mature oligodendrocytes. *Neurotox. Res.* 24, 244–250. <https://doi.org/10.1007/s12640-013-9380-9>
- Bennett, J., Basivireddy, J., Kollar, A., Biron, K.E., Reickmann, P., Jefferies, W.A., McQuaid, S., 2010. Blood-brain barrier disruption and enhanced vascular permeability in the multiple sclerosis model EAE. *J. Neuroimmunol.* 229, 180–191. <https://doi.org/10.1016/j.jneuroim.2010.08.011>
- Berger, T., Reindl, M., 2015. Antibody biomarkers in CNS demyelinating diseases – a long and winding road. *Eur. J. Neurol.* 22, 1162–1168. <https://doi.org/10.1111/ene.12759>
- Bergles, D.E., Richardson, W.D., 2016. Oligodendrocyte Development and Plasticity. *Cold Spring Harb. Perspect. Biol.* 8, a020453. <https://doi.org/10.1101/cshperspect.a020453>
- Bhatt, A., Fan, L.-W., Pang, Y., 2014. Strategies for myelin regeneration: lessons learned from development. *Neural Regen. Res.* 9, 1347–1350. <https://doi.org/10.4103/1673-5374.137586>
- Blackburn, D., Sargsyan, S., Monk, P.N., Shaw, P.J., 2009. Astrocyte function and role in motor neuron disease: a future therapeutic target? *Glia* 57, 1251–1264. <https://doi.org/10.1002/glia.20848>
- Blakemore, W.F., 1973a. Remyelination of the superior cerebellar peduncle in the mouse following demyelination induced by feeding cuprizone. *J. Neurol. Sci.* 20, 73–83. [https://doi.org/10.1016/0022-510x\(73\)90119-6](https://doi.org/10.1016/0022-510x(73)90119-6)
- Blakemore, W.F., 1973b. Demyelination of the superior cerebellar peduncle in the mouse induced by cuprizone. *J. Neurol. Sci.* 20, 63–72. [https://doi.org/10.1016/0022-510x\(73\)90118-4](https://doi.org/10.1016/0022-510x(73)90118-4)
- Blakemore, W.F., 1972. Observations on oligodendrocyte degeneration, the resolution of status spongiosus and remyelination in cuprizone intoxication in mice. *J. Neurocytol.* 1, 413–426. <https://doi.org/10.1007/BF01102943>
- Bolivar, V.J., Brown, R.E., 1994. The ontogeny of ultrasonic vocalizations and other behaviors in male jimpy (jp/Y) mice and their normal male littermates. *Dev. Psychobiol.* 27, 101–110. <https://doi.org/10.1002/dev.420270204>
- Bomben, V., Sontheimer, H., 2010. Disruption of Transient Receptor Potential Canonical Channel 1 Causes Incomplete Cytokinesis and Slows the Growth of Human Malignant Gliomas. *Glia* 58, 1145–56. <https://doi.org/10.1002/glia.20994>
- Bomben, V.C., Sontheimer, H.W., 2008. Inhibition of transient receptor potential canonical channels impairs cytokinesis in human malignant gliomas. *Cell Prolif.* 41, 98–121. <https://doi.org/10.1111/j.1365-2184.2007.00504.x>

- Bosson, A., Paumier, A., Boisseau, S., Jacquier-Sarlin, M., Buisson, A., Albrieux, M., 2017. TRPA1 channels promote astrocytic Ca²⁺ hyperactivity and synaptic dysfunction mediated by oligomeric forms of amyloid- β peptide. *Mol. Neurodegener.* 12, 53. <https://doi.org/10.1186/s13024-017-0194-8>
- Bourque, C.W., Ciura, S., Trudel, E., Stachniak, T.J.E., Sharif-Naeini, R., 2007. Neurophysiological characterization of mammalian osmosensitive neurones. *Exp. Physiol.* 92, 499–505. <https://doi.org/10.1113/expphysiol.2006.035634>
- Boziki, M., Sintila, S.-A., Ioannidis, P., Grigoriadis, N., 2020. Biomarkers in Rare Demyelinating Disease of the Central Nervous System. *Int. J. Mol. Sci.* 21, 8409. <https://doi.org/10.3390/ijms21218409>
- Brown, L.N., Xing, Y., Noble, K.V., Barth, J.L., Panganiban, C.H., Smythe, N.M., Bridges, M.C., Zhu, J., Lang, H., 2017. Macrophage-Mediated Glial Cell Elimination in the Postnatal Mouse Cochlea. *Front. Mol. Neurosci.* 10, 407. <https://doi.org/10.3389/fnmol.2017.00407>
- Bruce, K.D., Gorkhali, S., Given, K., Coates, A.M., Boyle, K.E., Macklin, W.B., Eckel, R.H., 2018. Lipoprotein Lipase Is a Feature of Alternatively-Activated Microglia and May Facilitate Lipid Uptake in the CNS During Demyelination. *Front. Mol. Neurosci.* 11, 57. <https://doi.org/10.3389/fnmol.2018.00057>
- Butenko, O., Dzamba, D., Benesova, J., Honsa, P., Benfenati, V., Rusnakova, V., Ferroni, S., Anderova, M., 2012. The increased activity of TRPV4 channel in the astrocytes of the adult rat hippocampus after cerebral hypoxia/ischemia. *PloS One* 7, e39959. <https://doi.org/10.1371/journal.pone.0039959>
- Butovsky, O., Ziv, Y., Schwartz, A., Landa, G., Talpalar, A.E., Pluchino, S., Martino, G., Schwartz, M., 2006. Microglia activated by IL-4 or IFN-gamma differentially induce neurogenesis and oligodendrogenesis from adult stem/progenitor cells. *Mol. Cell. Neurosci.* 31, 149–160. <https://doi.org/10.1016/j.mcn.2005.10.006>
- Cahoy, J.D., Emery, B., Kaushal, A., Foo, L.C., Zamanian, J.L., Christopherson, K.S., Xing, Y., Lubischer, J.L., Krieg, P.A., Krupenko, S.A., Thompson, W.J., Barres, B.A., 2008. A transcriptome database for astrocytes, neurons, and oligodendrocytes: a new resource for understanding brain development and function. *J. Neurosci. Off. J. Soc. Neurosci.* 28, 264–278. <https://doi.org/10.1523/JNEUROSCI.4178-07.2008>
- Cailloux, F., Gauthier-Barichard, F., Mimault, C., Isabelle, V., Courtois, V., Giraud, G., Dastugue, B., Boespflug-Tanguy, O., 2000. Genotype-phenotype correlation in inherited brain myelination defects due to proteolipid protein gene mutations. *Clinical European Network on Brain Demyelinating Disease. Eur. J. Hum. Genet. EJHG* 8, 837–845. <https://doi.org/10.1038/sj.ejhg.5200537>
- Califf, R.M., 2018. Biomarker definitions and their applications. *Exp. Biol. Med.* 243, 213–221. <https://doi.org/10.1177/1535370217750088>
- Camirero, A., Comabella, M., Montalban, X., 2011. Role of tumour necrosis factor (TNF)- α and TNFRSF1A R92Q mutation in the pathogenesis of TNF receptor-associated periodic syndrome and multiple sclerosis. *Clin. Exp. Immunol.* 166, 338–345. <https://doi.org/10.1111/j.1365-2249.2011.04484.x>

- Cao, S., Anishkin, A., Zinkevich, N.S., Nishijima, Y., Korishettar, A., Wang, Z., Fang, J., Wilcox, D.A., Zhang, D.X., 2018. Transient receptor potential vanilloid 4 (TRPV4) activation by arachidonic acid requires protein kinase A-mediated phosphorylation. *J. Biol. Chem.* 293, 5307–5322. <https://doi.org/10.1074/jbc.M117.811075>
- Carlin, C., Murray, L., Graham, D., Doyle, D., Nicoll, J., 2000. Involvement of apolipoprotein E in multiple sclerosis: absence of remyelination associated with possession of the APOE epsilon2 allele. *J. Neuropathol. Exp. Neurol.* 59, 361–367. <https://doi.org/10.1093/jnen/59.5.361>
- Carlton, W.W., 1966. Response of mice to the chelating agents sodium diethyldithiocarbamate, alpha-benzoinoxime, and biscyclohexanone oxaldihydrazone. *Toxicol. Appl. Pharmacol.* 8, 512–521. [https://doi.org/10.1016/0041-008x\(66\)90062-7](https://doi.org/10.1016/0041-008x(66)90062-7)
- Caterina, M.J., Julius, D., 2001. The vanilloid receptor: a molecular gateway to the pain pathway. *Annu. Rev. Neurosci.* 24, 487–517. <https://doi.org/10.1146/annurev.neuro.24.1.487>
- Caterina, M.J., Rosen, T.A., Tominaga, M., Brake, A.J., Julius, D., 1999. A capsaicin-receptor homologue with a high threshold for noxious heat. *Nature* 398, 436–441. <https://doi.org/10.1038/18906>
- Chen, X., Sun, F.-J., Wei, Y.-J., Wang, L.-K., Zang, Z.-L., Chen, B., Li, S., Liu, S.-Y., Yang, H., 2016. Increased Expression of Transient Receptor Potential Vanilloid 4 in Cortical Lesions of Patients with Focal Cortical Dysplasia. *CNS Neurosci. Ther.* 22, 280–290. <https://doi.org/10.1111/cns.12494>
- Choi, I.-Y., Lee, P., Adany, P., Hughes, A.J., Belliston, S., Denney, D.R., Lynch, S.G., 2018. In vivo evidence of oxidative stress in brains of patients with progressive multiple sclerosis. *Mult. Scler.* Houndmills Basingstoke Engl. 24, 1029–1038. <https://doi.org/10.1177/1352458517711568>
- Clapham, D.E., Montell, C., Schultz, G., Julius, D., International Union of Pharmacology, 2003. International Union of Pharmacology. XLIII. Compendium of voltage-gated ion channels: transient receptor potential channels. *Pharmacol. Rev.* 55, 591–596. <https://doi.org/10.1124/pr.55.4.6>
- Clarner, T., Janssen, K., Nellessen, L., Stangel, M., Skripuletz, T., Krauspe, B., Hess, F.-M., Denecke, B., Beutner, C., Linnartz-Gerlach, B., Neumann, H., Vallières, L., Amor, S., Ohl, K., Tenbrock, K., Beyer, C., Kipp, M., 2015. CXCL10 triggers early microglial activation in the cuprizone model. *J. Immunol. Baltim. Md* 1950 194, 3400–3413. <https://doi.org/10.4049/jimmunol.1401459>
- Cohen, M.R., Johnson, W.M., Pilat, J.M., Kiselar, J., DeFrancesco-Lisowitz, A., Zigmond, R.E., Moiseenkova-Bell, V.Y., 2015. Nerve Growth Factor Regulates Transient Receptor Potential Vanilloid 2 via Extracellular Signal-Regulated Kinase Signaling To Enhance Neurite Outgrowth in Developing Neurons. *Mol. Cell. Biol.* 35, 4238–4252. <https://doi.org/10.1128/MCB.00549-15>
- Cosens, D.J., Manning, A., 1969. Abnormal electroretinogram from a *Drosophila* mutant. *Nature* 224, 285–287. <https://doi.org/10.1038/224285a0>

- Crang, A.J., Gilson, J.M., Li, W.-W., Blakemore, W.F., 2004. The remyelinating potential and in vitro differentiation of MOG-expressing oligodendrocyte precursors isolated from the adult rat CNS. *Eur. J. Neurosci.* 20, 1445–1460. <https://doi.org/10.1111/j.1460-9568.2004.03606.x>
- Cuddapah, V.A., Turner, K.L., Sontheimer, H., 2013. Calcium entry via TRPC1 channels activates chloride currents in human glioma cells. *Cell Calcium* 53, 187–194. <https://doi.org/10.1016/j.ceca.2012.11.013>
- Darling, T.K., Lamb, T.J., 2019. Emerging Roles for Eph Receptors and Ephrin Ligands in Immunity. *Front. Immunol.* 10, 1473. <https://doi.org/10.3389/fimmu.2019.01473>
- de Faria, O., Dhaunchak, A.S., Kamen, Y., Roth, A.D., Kuhlmann, T., Colman, D.R., Kennedy, T.E., 2019. TMEM10 Promotes Oligodendrocyte Differentiation and is Expressed by Oligodendrocytes in Human Remyelinating Multiple Sclerosis Plaques. *Sci. Rep.* 9, 3606. <https://doi.org/10.1038/s41598-019-40342-x>
- Dobson, R., Giovannoni, G., 2019. Multiple sclerosis - a review. *Eur. J. Neurol.* 26, 27–40. <https://doi.org/10.1111/ene.13819>
- Doly, S., Fischer, J., Salio, C., Conrath, M., 2004. The vanilloid receptor-1 is expressed in rat spinal dorsal horn astrocytes. *Neurosci. Lett.* 357, 123–126. <https://doi.org/10.1016/j.neulet.2003.12.051>
- Domingues, H.S., Portugal, C.C., Socodato, R., Relvas, J.B., 2016. Oligodendrocyte, Astrocyte, and Microglia Crosstalk in Myelin Development, Damage, and Repair. *Front. Cell Dev. Biol.* 4. <https://doi.org/10.3389/fcell.2016.00071>
- Doñate-Macián, P., Enrich-Bengoa, J., Dégano, I.R., Quintana, D.G., Perálvarez-Marín, A., 2019. Trafficking of Stretch-Regulated TRPV2 and TRPV4 Channels Inferred Through Interactomics. *Biomolecules* 9, 791. <https://doi.org/10.3390/biom9120791>
- Doñate-Macián, Pau, Gómez, A., Dégano, I.R., Perálvarez-Marín, A., 2018. A TRPV2 interactome-based signature for prognosis in glioblastoma patients. *Oncotarget* 9, 18400–18409. <https://doi.org/10.18632/oncotarget.24843>
- Doñate-Macián, P., Jungfleisch, J., Pérez-Vilaró, G., Rubio-Moscardo, F., Perálvarez-Marín, A., Diez, J., Valverde, M.A., 2018. The TRPV4 channel links calcium influx to DDX3X activity and viral infectivity. *Nat. Commun.* 9, 2307. <https://doi.org/10.1038/s41467-018-04776-7>
- Dorboz, I., Dumay-Odelot, H., Boussaid, K., Bouyacoub, Y., Barreau, P., Samaan, S., Jmel, H., Eymard-Pierre, E., Cances, C., Bar, C., Poulat, A.-L., Rousselle, C., Renaldo, F., Bergès, M.E., Teichmann, M., Boespflug-Tanguy, O., 2018. Mutation in POLR3K causes hypomyelinating leukodystrophy and abnormal ribosomal RNA regulation. *Neurol. Genet.* 4. <https://doi.org/10.1212/NXG.0000000000000289>
- Dowling, P., Husar, W., Menonna, J., Donnenfeld, H., Cook, S., Sidhu, M., 1997. Cell death and birth in multiple sclerosis brain. *J. Neurol. Sci.* 149, 1–11. [https://doi.org/10.1016/s0022-510x\(97\)05213-1](https://doi.org/10.1016/s0022-510x(97)05213-1)
- Du, W., Huang, J., Yao, H., Zhou, K., Duan, B., Wang, Y., 2010. Inhibition of TRPC6 degradation suppresses ischemic brain damage in rats. *J. Clin. Invest.* 120, 3480–3492. <https://doi.org/10.1172/JCI43165>

- Dugas, J.C., Tai, Y.C., Speed, T.P., Ngai, J., Barres, B.A., 2006. Functional Genomic Analysis of Oligodendrocyte Differentiation. *J. Neurosci.* 26, 10967–10983. <https://doi.org/10.1523/JNEUROSCI.2572-06.2006>
- Duncan, I.D., Kondo, Y., Zhang, S.-C., 2011. The Myelin Mutants as Models to Study Myelin Repair in the Leukodystrophies. *Neurotherapeutics* 8, 607–624. <https://doi.org/10.1007/s13311-011-0080-y>
- Duncan, I.D., Marik, R.L., Broman, A.T., Heidari, M., 2017. Thin myelin sheaths as the hallmark of remyelination persist over time and preserve axon function. *Proc. Natl. Acad. Sci.* 114, E9685–E9691. <https://doi.org/10.1073/pnas.1714183114>
- Dusart, I., Marty, S., Peschanski, M., 1992. Demyelination, and remyelination by Schwann cells and oligodendrocytes after kainate-induced neuronal depletion in the central nervous system. *Neuroscience* 51, 137–148. [https://doi.org/10.1016/0306-4522\(92\)90478-k](https://doi.org/10.1016/0306-4522(92)90478-k)
- El Andaloussi-Lilja, J., Lundqvist, J., Forsby, A., 2009. TRPV1 expression and activity during retinoic acid-induced neuronal differentiation. *Neurochem. Int.* 55, 768–774. <https://doi.org/10.1016/j.neuint.2009.07.011>
- Elitt, M.S., Barbar, L., Shick, H.E., Powers, B.E., Maeno-Hikichi, Y., Madhavan, M., Allan, K.C., Nawash, B.S., Gevorgyan, A.S., Hung, S., Nevin, Z.S., Olsen, H.E., Hitomi, M., Schlatzer, D.M., Zhao, H.T., Swayze, A., LePage, D.F., Jiang, W., Conlon, R.A., Rigo, F., Tesar, P.J., 2020. Suppression of proteolipid protein rescues Pelizaeus-Merzbacher disease. *Nature* 585, 397–403. <https://doi.org/10.1038/s41586-020-2494-3>
- Elzamzamy, O.M., Penner, R., Hazlehurst, L.A., 2020. The Role of TRPC1 in Modulating Cancer Progression. *Cells* 9, 388. <https://doi.org/10.3390/cells9020388>
- Eng, L.F., Chao, F.C., Gerstl, B., Pratt, D., Tavaststjerna, M.G., 1968. The maturation of human white matter myelin. Fractionation of the myelin membrane proteins. *Biochemistry* 7, 4455–4465. <https://doi.org/10.1021/bi00852a042>
- Enrich-Bengoia, J., Manich, G., Valente, T., Sanchez-Molina, P., Almolda, B., Solà, C., Saura, J., González, B., Castellano, B., Perálvarez-Marín, A., 2022. TRPV2: A Key Player in Myelination Disorders of the Central Nervous System. *Int. J. Mol. Sci.* 23, 3617. <https://doi.org/10.3390/ijms23073617>
- Evilsizor, M.N., Ray-Jones, H.F., Ellis, T.W., Lifshitz, J., Ziebell, J.M., 2015. Microglia in Experimental Brain Injury: Implications on Neuronal Injury and Circuit Remodeling, in: Kobeissy, F.H. (Ed.), *Brain Neurotrauma: Molecular, Neuropsychological, and Rehabilitation Aspects*, Frontiers in Neuroengineering. CRC Press/Taylor & Francis, Boca Raton (FL).
- Fancy, S.P.J., Chan, J.R., Baranzini, S.E., Franklin, R.J.M., Rowitch, D.H., 2011. Myelin regeneration: a recapitulation of development? *Annu. Rev. Neurosci.* 34, 21–43. <https://doi.org/10.1146/annurev-neuro-061010-113629>
- Feng, X., Takayama, Y., Ohno, N., Kanda, H., Dai, Y., Sokabe, T., Tominaga, M., 2020. Increased TRPV4 expression in non-myelinating Schwann cells is associated with demyelination after sciatic nerve injury. *Commun. Biol.* 3, 716. <https://doi.org/10.1038/s42003-020-01444-9>

- Ferent, J., Zimmer, C., Durbec, P., Ruat, M., Traiffort, E., 2013. Sonic Hedgehog Signaling Is a Positive Oligodendrocyte Regulator during Demyelination. *J. Neurosci.* 33, 1759–1772. <https://doi.org/10.1523/JNEUROSCI.3334-12.2013>
- Fernandez-Castaneda, A., Gaultier, A., 2016. Adult oligodendrocyte progenitor cells - multifaceted regulators of the CNS in health and disease. *Brain. Behav. Immun.* 57, 1–7. <https://doi.org/10.1016/j.bbi.2016.01.005>
- Ferrandiz-Huertas, C., Mathivanan, S., Wolf, C.J., Devesa, I., Ferrer-Montiel, A., 2014. Trafficking of ThermoTRP Channels. *Membranes* 4, 525–564. <https://doi.org/10.3390/membranes4030525>
- Fife, B.T., Kennedy, K.J., Paniagua, M.C., Lukacs, N.W., Kunkel, S.L., Luster, A.D., Karpus, W.J., 2001. CXCL10 (IFN-gamma-inducible protein-10) control of encephalitogenic CD4+ T cell accumulation in the central nervous system during experimental autoimmune encephalomyelitis. *J. Immunol. Baltim. Md* 1950 166, 7617–7624. <https://doi.org/10.4049/jimmunol.166.12.7617>
- Fischbach, F., Nedelcu, J., Leopold, P., Zhan, J., Clarner, T., Nellessen, L., Beißel, C., Heuvel, Y. van, Goswami, A., Weis, J., Denecke, B., Schmitz, C., Hochstrasser, T., Nyamoya, S., Victor, M., Beyer, C., Kipp, M., 2019. Cuprizone-induced graded oligodendrocyte vulnerability is regulated by the transcription factor DNA damage-inducible transcript 3. *Glia* 67, 263–276. <https://doi.org/10.1002/glia.23538>
- Fitsiori, A., Nguyen, D., Karentzos, A., Delavelle, J., Vargas, M.I., 2011. The corpus callosum: white matter or terra incognita. *Br. J. Radiol.* 84, 5–18. <https://doi.org/10.1259/bjr/21946513>
- Fitzner, D., Schnaars, M., van Rossum, D., Krishnamoorthy, G., Dibaj, P., Bakhti, M., Regen, T., Hanisch, U.-K., Simons, M., 2011. Selective transfer of exosomes from oligodendrocytes to microglia by macropinocytosis. *J. Cell Sci.* 124, 447–458. <https://doi.org/10.1242/jcs.074088>
- Follis, R.M., Carter, B.D., 2016. Myelin Avoids the JAM. *Neuron* 91, 713–716. <https://doi.org/10.1016/j.neuron.2016.08.003>
- Fortin, J., Tian, R., Zarrabi, I., Hill, G., Williams, E., Sanchez-Duffhues, G., Thorikay, M., Ramachandran, P., Siddaway, R., Wong, J.F., Wu, A., Apuzzo, L.N., Haight, J., You-Ten, A., Snow, B.E., Wakeham, A., Goldhamer, D.J., Schramek, D., Bullock, A.N., Dijke, P. ten, Hawkins, C., Mak, T.W., 2020. Mutant ACVR1 Arrests Glial Cell Differentiation to Drive Tumorigenesis in Pediatric Gliomas. *Cancer Cell* 37, 308–323.e12. <https://doi.org/10.1016/j.ccell.2020.02.002>
- Franciotta, D., Martino, G., Zardini, E., Furlan, R., Bergamaschi, R., Andreoni, L., Cosi, V., 2001. Serum and CSF levels of MCP-1 and IP-10 in multiple sclerosis patients with acute and stable disease and undergoing immunomodulatory therapies. *J. Neuroimmunol.* 115, 192–198. [https://doi.org/10.1016/s0165-5728\(01\)00261-2](https://doi.org/10.1016/s0165-5728(01)00261-2)
- Franklin, R.J., Hinks, G.L., 1999. Understanding CNS remyelination: clues from developmental and regeneration biology. *J. Neurosci. Res.* 58, 207–213.
- Fricke, T.C., Echtermeyer, F., Zielke, J., de la Roche, J., Filipovic, M.R., Claverol, S., Herzog, C., Tominaga, M., Pumroy, R.A., Moiseenkova-Bell, V.Y., Zygmunt, P.M., Leffler, A.,

- Eberhardt, M.J., 2019. Oxidation of methionine residues activates the high-threshold heat-sensitive ion channel TRPV2. *Proc. Natl. Acad. Sci. U. S. A.* 116, 24359–24365. <https://doi.org/10.1073/pnas.1904332116>
- Furusho, M., Dupree, J.L., Nave, K.-A., Bansal, R., 2012. Fibroblast Growth Factor Receptor Signaling in Oligodendrocytes Regulates Myelin Sheath Thickness. *J. Neurosci.* 32, 6631–6641. <https://doi.org/10.1523/JNEUROSCI.6005-11.2012>
- Garbern, J., Cambi, F., Shy, M., Kamholz, J., 1999. The molecular pathogenesis of Pelizaeus-Merzbacher disease. *Arch. Neurol.* 56, 1210–1214. <https://doi.org/10.1001/archneur.56.10.1210>
- Garbern, J.Y., 2007. Pelizaeus-Merzbacher disease: Genetic and cellular pathogenesis. *Cell. Mol. Life Sci. CMLS* 64, 50–65. <https://doi.org/10.1007/s00018-006-6182-8>
- Garbern, J.Y., Yool, D.A., Moore, G.J., Wilds, I.B., Faulk, M.W., Klugmann, M., Nave, K.-A., Sistermans, E.A., van der Knaap, M.S., Bird, T.D., Shy, M.E., Kamholz, J.A., Griffiths, I.R., 2002. Patients lacking the major CNS myelin protein, proteolipid protein 1, develop length-dependent axonal degeneration in the absence of demyelination and inflammation. *Brain J. Neurol.* 125, 551–561. <https://doi.org/10.1093/brain/awf043>
- García-Díaz, B., Riquelme, R., Varela-Nieto, I., Jiménez, A.J., de Diego, I., Gómez-Conde, A.I., Matas-Rico, E., Aguirre, J.Á., Chun, J., Pedraza, C., Santín, L.J., Fernández, O., Rodríguez de Fonseca, F., Estivill-Torrús, G., 2015. Loss of lysophosphatidic acid receptor LPA1 alters oligodendrocyte differentiation and myelination in the mouse cerebral cortex. *Brain Struct. Funct.* 220, 3701–3720. <https://doi.org/10.1007/s00429-014-0885-7>
- Gaultier, A., Wu, X., Le Moan, N., Takimoto, S., Mukandala, G., Akassoglou, K., Campana, W.M., Gonias, S.L., 2009. Low-density lipoprotein receptor-related protein 1 is an essential receptor for myelin phagocytosis. *J. Cell Sci.* 122, 1155–1162. <https://doi.org/10.1242/jcs.040717>
- Gelfand, J.M., 2014. Multiple sclerosis: diagnosis, differential diagnosis, and clinical presentation. *Handb. Clin. Neurol.* 122, 269–290. <https://doi.org/10.1016/B978-0-444-52001-2.00011-X>
- Gencic, S., Abuelo, D., Ambler, M., Hudson, L.D., 1989. Pelizaeus-Merzbacher disease: an X-linked neurologic disorder of myelin metabolism with a novel mutation in the gene encoding proteolipid protein. *Am. J. Hum. Genet.* 45, 435–442.
- Ghasemi, N., Razavi, S., Nikzad, E., 2017. Multiple Sclerosis: Pathogenesis, Symptoms, Diagnoses and Cell-Based Therapy. *Cell J.* 19, 1–10.
- Gilgun-Sherki, Y., Melamed, E., Offen, D., 2004. The role of oxidative stress in the pathogenesis of multiple sclerosis: the need for effective antioxidant therapy. *J. Neurol.* 251, 261–268. <https://doi.org/10.1007/s00415-004-0348-9>
- Giovannoni, G., Heales, S.J., Silver, N.C., O’Riordan, J., Miller, R.F., Land, J.M., Clark, J.B., Thompson, E.J., 1997. Raised serum nitrate and nitrite levels in patients with multiple sclerosis. *J. Neurol. Sci.* 145, 77–81. [https://doi.org/10.1016/s0022-510x\(96\)00246-8](https://doi.org/10.1016/s0022-510x(96)00246-8)
- Giovannoni, G., Silver, N.C., O’Riordan, J., Miller, R.F., Heales, S.J., Land, J.M., Elliot, M., Feldmann, M., Miller, D.H., Thompson, E.J., 1999. Increased urinary nitric oxide metabolites in

- patients with multiple sclerosis correlates with early and relapsing disease. *Mult. Scler. Houndmills Basingstoke Engl.* 5, 335–341. <https://doi.org/10.1177/135245859900500506>
- Girolamo, F., Ferrara, G., Strippoli, M., Rizzi, M., Errede, M., Trojano, M., Perris, R., Roncali, L., Svelto, M., Mennini, T., Virgintino, D., 2011. Cerebral cortex demyelination and oligodendrocyte precursor response to experimental autoimmune encephalomyelitis. *Neurobiol. Dis.* 43, 678–689. <https://doi.org/10.1016/j.nbd.2011.05.021>
- Glabinski, A.R., Tani, M., Tuohy, V.K., Tuthill, R.J., Ransohoff, R.M., 1995. Central nervous system chemokine mRNA accumulation follows initial leukocyte entry at the onset of acute murine experimental autoimmune encephalomyelitis. *Brain. Behav. Immun.* 9, 315–330. <https://doi.org/10.1006/brbi.1995.1030>
- Golan, N., Adamsky, K., Kartvelishvily, E., Brockschnieder, D., Möbius, W., Spiegel, I., Roth, A.D., Thomson, C.E., Rechavi, G., Peles, E., 2008. Identification of Tmem10/Opalin as an oligodendrocyte enriched gene using expression profiling combined with genetic cell ablation. *Glia* 56, 1176–1186. <https://doi.org/10.1002/glia.20688>
- Goldenberg, M.M., 2012. Multiple Sclerosis Review. *Pharm. Ther.* 37, 175–184.
- Goldstein, A., Covington, B.P., Mahabadi, N., Mesfin, F.B., 2021. Neuroanatomy, Corpus Callosum, in: *StatPearls*. StatPearls Publishing, Treasure Island (FL).
- Gonzalez-Reyes, L.E., Ladas, T.P., Chiang, C.-C., Durand, D.M., 2013. TRPV1 antagonist capsazepine suppresses 4-AP-induced epileptiform activity in vitro and electrographic seizures in vivo. *Exp. Neurol.* 250, 321–332. <https://doi.org/10.1016/j.expneurol.2013.10.010>
- Gonzalez-Teran, B., Pittman, M., Felix, F., Thomas, R., Richmond-Buccola, D., Hüttenhain, R., Choudhary, K., Moroni, E., Costa, M.W., Huang, Y., Padmanabhan, A., Alexanian, M., Lee, C.Y., Maven, B.E.J., Samse-Knapp, K., Morton, S.U., McGregor, M., Gifford, C.A., Seidman, J.G., Seidman, C.E., Gelb, B.D., Colombo, G., Conklin, B.R., Black, B.L., Bruneau, B.G., Krogan, N.J., Pollard, K.S., Srivastava, D., 2022. Transcription factor protein interactomes reveal genetic determinants in heart disease. *Cell* 185, 794-814.e30. <https://doi.org/10.1016/j.cell.2022.01.021>
- Goswami, C., Rademacher, N., Smalla, K.-H., Kalscheuer, V., Ropers, H.-H., Gundelfinger, E.D., Hucho, T., 2010. TRPV1 acts as a synaptic protein and regulates vesicle recycling. *J. Cell Sci.* 123, 2045–2057. <https://doi.org/10.1242/jcs.065144>
- Greka, A., Navarro, B., Oancea, E., Duggan, A., Clapham, D.E., 2003. TRPC5 is a regulator of hippocampal neurite length and growth cone morphology. *Nat. Neurosci.* 6, 837–845. <https://doi.org/10.1038/nn1092>
- Gu, Z., Li, F., Zhang, Y.P., Shields, L.B.E., Hu, X., Zheng, Y., Yu, P., Zhang, Y., Cai, J., Vitek, M.P., Shields, C.B., 2013. Apolipoprotein E Mimetic Promotes Functional and Histological Recovery in Lysolecithin-Induced Spinal Cord Demyelination in Mice. *J. Neurol. Neurophysiol.* 2014, 10. <https://doi.org/10.4172/2155-9562.S12-010>
- Gudi, V., Gingele, S., Skripuletz, T., Stangel, M., 2014. Glial response during cuprizone-induced de- and remyelination in the CNS: lessons learned. *Front. Cell. Neurosci.* 8. <https://doi.org/10.3389/fncel.2014.00073>

- Gul, M., Azari Jafari, A., Shah, M., Mirmoenei, S., Haider, S.U., Moinuddin, S., Chaudhry, A., 2020. Molecular Biomarkers in Multiple Sclerosis and Its Related Disorders: A Critical Review. *Int. J. Mol. Sci.* 21, 6020. <https://doi.org/10.3390/ijms21176020>
- Haenig, C., Atias, N., Taylor, A.K., Mazza, A., Schaefer, M.H., Russ, J., Riechers, S.-P., Jain, S., Coughlin, M., Fontaine, J.-F., Freibaum, B.D., Brusendorf, L., Zenkner, M., Porras, P., Stroedicke, M., Schnoegl, S., Arnsburg, K., Boeddrich, A., Pigazzini, L., Heutink, P., Taylor, J.P., Kirstein, J., Andrade-Navarro, M.A., Sharan, R., Wanker, E.E., 2020. Interactome Mapping Provides a Network of Neurodegenerative Disease Proteins and Uncovers Widespread Protein Aggregation in Affected Brains. *Cell Rep.* 32. <https://doi.org/10.1016/j.celrep.2020.108050>
- Hainz, N., Becker, P., Rapp, D., Wagenpfeil, S., Wonnenberg, B., Beisswenger, C., Tschernig, T., Meier, C., 2017a. Probenecid-treatment reduces demyelination induced by cuprizone feeding. *J. Chem. Neuroanat.* 85, 21–26. <https://doi.org/10.1016/j.jchemneu.2017.06.003>
- Hainz, N., Wolf, S., Beck, A., Wagenpfeil, S., Tschernig, T., Meier, C., 2017b. Probenecid arrests the progression of pronounced clinical symptoms in a mouse model of multiple sclerosis. *Sci. Rep.* 7, 17214. <https://doi.org/10.1038/s41598-017-17517-5>
- Hainz, N., Wolf, S., Tschernig, T., Meier, C., 2016. Probenecid Application Prevents Clinical Symptoms and Inflammation in Experimental Autoimmune Encephalomyelitis. *Inflammation* 39, 123–128. <https://doi.org/10.1007/s10753-015-0230-1>
- Hamilton, S.P., Rome, L.H., 1994. Stimulation of in vitro myelin synthesis by microglia. *Glia* 11, 326–335. <https://doi.org/10.1002/glia.440110405>
- Hammond, T.R., Gadea, A., Dupree, J., Kerninon, C., Nait-Oumesmar, B., Aguirre, A., Gallo, V., 2014. Astrocyte-derived endothelin-1 inhibits remyelination through notch activation. *Neuron* 81, 588–602. <https://doi.org/10.1016/j.neuron.2013.11.015>
- Hansen, T., Skytthe, A., Stenager, E., Petersen, H.C., Brønnum-Hansen, H., Kyvik, K.O., 2005. Concordance for multiple sclerosis in Danish twins: an update of a nationwide study. *Mult. Scler. Houndmills Basingstoke Engl.* 11, 504–510. <https://doi.org/10.1191/1352458505ms1220oa>
- Harbo, H.F., Gold, R., Tintoré, M., 2013. Sex and gender issues in multiple sclerosis. *Ther. Adv. Neurol. Disord.* 6, 237–248. <https://doi.org/10.1177/1756285613488434>
- Hardy, R., Reynolds, R., 1993. Neuron-oligodendroglial interactions during central nervous system development. *J. Neurosci. Res.* 36, 121–126. <https://doi.org/10.1002/jnr.490360202>
- Harirchian, M.H., Fatehi, F., Sarraf, P., Honarvar, N.M., Bitarafan, S., 2018. Worldwide prevalence of familial multiple sclerosis: A systematic review and meta-analysis. *Mult. Scler. Relat. Disord.* 20, 43–47. <https://doi.org/10.1016/j.msard.2017.12.015>
- Harris, V.K., Sadiq, S.A., 2009. Disease biomarkers in multiple sclerosis: potential for use in therapeutic decision making. *Mol. Diagn. Ther.* 13, 225–244. <https://doi.org/10.1007/BF03256329>
- Hassanpour Golakani, M., Mohammad, M.G., Li, H., Gamble, J., Breit, S.N., Ruitenber, M.J., Brown, D.A., 2019. MIC-1/GDF15 Overexpression Is Associated with Increased Functional

- Recovery in Traumatic Spinal Cord Injury. *J. Neurotrauma* 36, 3410–3421. <https://doi.org/10.1089/neu.2019.6421>
- Hauser, S.L., Cree, B.A.C., 2020. Treatment of Multiple Sclerosis: A Review. *Am. J. Med.* 133, 1380–1390.e2. <https://doi.org/10.1016/j.amjmed.2020.05.049>
- Hengel, H., Magee, A., Mahanjah, M., Vallat, J.-M., Ouvrier, R., Abu-Rashid, M., Mahamid, J., Schüle, R., Schulze, M., Krägeloh-Mann, I., Bauer, P., Züchner, S., Sharkia, R., Schöls, L., 2017. CNTNAP1 mutations cause CNS hypomyelination and neuropathy with or without arthrogyriposis. *Neurol. Genet.* 3, e144. <https://doi.org/10.1212/NXG.0000000000000144>
- Hennes, E.-M., Baumann, M., Lechner, C., Rostásy, K., 2018. MOG Spectrum Disorders and Role of MOG-Antibodies in Clinical Practice. *Neuropediatrics* 49, 3–11. <https://doi.org/10.1055/s-0037-1604404>
- Hibbits, N., Pannu, R., Wu, T.J., Armstrong, R.C., 2009. Cuprizone demyelination of the corpus callosum in mice correlates with altered social interaction and impaired bilateral sensorimotor coordination. *ASN Neuro* 1, e00013. <https://doi.org/10.1042/AN20090032>
- Hisanaga, E., Nagasawa, M., Ueki, K., Kulkarni, R.N., Mori, M., Kojima, I., 2009. Regulation of Calcium-Permeable TRPV2 Channel by Insulin in Pancreatic β -Cells. *Diabetes* 58, 174–184. <https://doi.org/10.2337/db08-0862>
- Ho, K.W., Ward, N.J., Calkins, D.J., 2012. TRPV1: a stress response protein in the central nervous system. *Am. J. Neurodegener. Dis.* 1, 1–14.
- Hobson, G.M., Garbern, J.Y., 2012. Pelizaeus-Merzbacher disease, Pelizaeus-Merzbacher-like disease 1, and related hypomyelinating disorders. *Semin. Neurol.* 32, 62–67. <https://doi.org/10.1055/s-0032-1306388>
- Hoffmann, A., Grimm, C., Kraft, R., Goldbaum, O., Wrede, A., Nolte, C., Hanisch, U.-K., Richter-Landsberg, C., Brück, W., Kettenmann, H., Harteneck, C., 2010. TRPM3 is expressed in sphingosine-responsive myelinating oligodendrocytes. *J. Neurochem.* 114, 654–665. <https://doi.org/10.1111/j.1471-4159.2010.06644.x>
- Hosking, M.P., Tirota, E., Ransohoff, R.M., Lane, T.E., 2010. CXCR2 Signaling Protects Oligodendrocytes and Restricts Demyelination in a Mouse Model of Viral-Induced Demyelination. *PLOS ONE* 5, e11340. <https://doi.org/10.1371/journal.pone.0011340>
- Hou, L., Rao, D.A., Yuki, K., Cooley, J., Henderson, L.A., Jonsson, A.H., Kaiserman, D., Gorman, M.P., Nigrovic, P.A., Bird, P.I., Becher, B., Remold-O'Donnell, E., 2019. SerpinB1 controls encephalitogenic T helper cells in neuroinflammation. *Proc. Natl. Acad. Sci.* 116, 20635–20643. <https://doi.org/10.1073/pnas.1905762116>
- Hoyos, H.C., Rinaldi, M., Mendez-Huergo, S.P., Marder, M., Rabinovich, G.A., Pasquini, J.M., Pasquini, L.A., 2014. Galectin-3 controls the response of microglial cells to limit cuprizone-induced demyelination. *Neurobiol. Dis.* 62, 441–455. <https://doi.org/10.1016/j.nbd.2013.10.023>
- Hudson, L.D., Puckett, C., Berndt, J., Chan, J., Gencic, S., 1989. Mutation of the proteolipid protein gene PLP in a human X chromosome-linked myelin disorder. *Proc. Natl. Acad. Sci. U. S. A.* 86, 8128–8131. <https://doi.org/10.1073/pnas.86.20.8128>

Inoue, K., 2019. Pelizaeus-Merzbacher Disease: Molecular and Cellular Pathologies and Associated Phenotypes. *Adv. Exp. Med. Biol.* 1190, 201–216. https://doi.org/10.1007/978-981-32-9636-7_13

International Multiple Sclerosis Genetics Consortium, Wellcome Trust Case Control Consortium 2, Sawcer, S., Hellenthal, G., Pirinen, M., Spencer, C.C.A., Patsopoulos, N.A., Moutsianas, L., Dilthey, A., Su, Z., Freeman, C., Hunt, S.E., Edkins, S., Gray, E., Booth, D.R., Potter, S.C., Goris, A., Band, G., Oturai, A.B., Strange, A., Saarela, J., Bellenguez, C., Fontaine, B., Gillman, M., Hemmer, B., Gwilliam, R., Zipp, F., Jayakumar, A., Martin, R., Leslie, S., Hawkins, S., Giannoulatou, E., D'alfonso, S., Blackburn, H., Martinelli Boneschi, F., Liddle, J., Harbo, H.F., Perez, M.L., Spurkland, A., Waller, M.J., Mycko, M.P., Ricketts, M., Comabella, M., Hammond, N., Kockum, I., McCann, O.T., Ban, M., Whittaker, P., Kempainen, A., Weston, P., Hawkins, C., Widaa, S., Zajicek, J., Dronov, S., Robertson, N., Bumpstead, S.J., Barcellos, L.F., Ravindrarajah, R., Abraham, R., Alfredsson, L., Ardlie, K., Aubin, C., Baker, A., Baker, K., Baranzini, S.E., Bergamaschi, L., Bergamaschi, R., Bernstein, A., Berthele, A., Boggild, M., Bradfield, J.P., Brassat, D., Broadley, S.A., Buck, D., Butzkueven, H., Capra, R., Carroll, W.M., Cavalla, P., Celius, E.G., Cepok, S., Chiavacci, R., Clerget-Darpoux, F., Clysters, K., Comi, G., Cossburn, M., Cournu-Rebeix, I., Cox, M.B., Cozen, W., Cree, B.A.C., Cross, A.H., Cusi, D., Daly, M.J., Davis, E., de Bakker, P.I.W., Debouverie, M., D'hooghe, M.B., Dixon, K., Dobosi, R., Dubois, B., Ellinghaus, D., Elovaara, I., Esposito, F., Fontenille, C., Foote, S., Franke, A., Galimberti, D., Ghezzi, A., Glessner, J., Gomez, R., Gout, O., Graham, C., Grant, S.F.A., Guerini, F.R., Hakonarson, H., Hall, P., Hamsten, A., Hartung, H.-P., Heard, R.N., Heath, S., Hobart, J., Hoshi, M., Infante-Duarte, C., Ingram, G., Ingram, W., Islam, T., Jagodic, M., Kabesch, M., Kermodé, A.G., Kilpatrick, T.J., Kim, C., Klopp, N., Koivisto, K., Larsson, M., Lathrop, M., Lechner-Scott, J.S., Leone, M.A., Leppä, V., Liljedahl, U., Bomfim, I.L., Lincoln, R.R., Link, J., Liu, J., Lorentzen, A.R., Lupoli, S., Macciardi, F., Mack, T., Marriott, M., Martinelli, V., Mason, D., McCauley, J.L., Mentch, F., Mero, I.-L., Mihalova, T., Montalban, X., Mottershead, J., Myhr, K.-M., Naldi, P., Ollier, W., Page, A., Palotie, A., Pelletier, J., Piccio, L., Pickersgill, T., Piehl, F., Pobywajlo, S., Quach, H.L., Ramsay, P.P., Reunanen, M., Reynolds, R., Rioux, J.D., Rodegher, M., Roesner, S., Rubio, J.P., Rückert, I.-M., Salvetti, M., Salvi, E., Santaniello, A., Schaefer, C.A., Schreiber, S., Schulze, C., Scott, R.J., Sellebjerg, F., Selmaj, K.W., Sexton, D., Shen, L., Simms-Acuna, B., Skidmore, S., Sleiman, P.M.A., Smestad, C., Sørensen, P.S., Søndergaard, H.B., Stankovich, J., Strange, R.C., Sulonen, A.-M., Sundqvist, E., Syvänen, A.-C., Taddeo, F., Taylor, B., Blackwell, J.M., Tienari, P., Bramon, E., Tourbah, A., Brown, M.A., Tronczynska, E., Casas, J.P., Tubridy, N., Corvin, A., Vickery, J., Jankowski, J., Villoslada, P., Markus, H.S., Wang, K., Mathew, C.G., Wason, J., Palmer, C.N.A., Wichmann, H.-E., Plomin, R., Willoughby, E., Rautanen, A., Winkelmann, J., Wittig, M., Trembath, R.C., Yaouanq, J., Viswanathan, A.C., Zhang, H., Wood, N.W., Zuvich, R., Deloukas, P., Langford, C., Duncanson, A., Oksenberg, J.R., Pericak-Vance, M.A., Haines, J.L., Olsson, T., Hillert, J., Ivinson, A.J., De Jager, P.L., Peltonen, L., Stewart, G.J., Hafler, D.A., Hauser, S.L., McVean, G., Donnelly, P., Compston, A., 2011. Genetic risk and a primary role for cell-mediated immune mechanisms in multiple sclerosis. *Nature* 476, 214–219. <https://doi.org/10.1038/nature10251>

Islas-Hernandez, A., Aguilar-Talamantes, H.S., Bertado-Cortes, B., Mejia-delCastillo, G. de J., Carrera-Pineda, R., Cuevas-Garcia, C.F., Garcia-delaTorre, P., 2018. BDNF and Tau as biomarkers of severity in multiple sclerosis. *Biomark. Med.* 12, 717–726. <https://doi.org/10.2217/bmm-2017-0374>

- Itoyama, Y., Webster, H.D., Richardson, E.P., Trapp, B.D., 1983. Schwann cell remyelination of demyelinated axons in spinal cord multiple sclerosis lesions. *Ann. Neurol.* 14, 339–346. <https://doi.org/10.1002/ana.410140313>
- Iwata, Y., Katanosaka, Y., Arai, Y., Komamura, K., Miyatake, K., Shigekawa, M., 2003. A novel mechanism of myocyte degeneration involving the Ca²⁺-permeable growth factor–regulated channel. *J. Cell Biol.* 161, 957–967. <https://doi.org/10.1083/jcb.200301101>
- Jafari, A., Babajani, A., Rezaei-Tavirani, M., 2021. Multiple Sclerosis Biomarker Discoveries by Proteomics and Metabolomics Approaches. *Biomark. Insights* 16, 11772719211013352. <https://doi.org/10.1177/11772719211013352>
- Jahan-Abad, A.J., Karima, S., Shateri, S., Baram, S.M., Rajaei, S., Morteza-Zadeh, P., Borhani-Haghighi, M., Salari, A.-A., Nikzamid, A., Gorji, A., 2020. Serum pro-inflammatory and anti-inflammatory cytokines and the pathogenesis of experimental autoimmune encephalomyelitis. *Neuropathol. Off. J. Jpn. Soc. Neuropathol.* 40, 84–92. <https://doi.org/10.1111/neup.12612>
- Jeon, J.-P., Roh, S.-E., Wie, J., Kim, J., Kim, H., Lee, K.-P., Yang, D., Jeon, J.-H., Cho, N.-H., Kim, I.-G., Kang, D.E., Kim, H.J., So, I., 2013. Activation of TRPC4 β by G α i subunit increases Ca²⁺ selectivity and controls neurite morphogenesis in cultured hippocampal neuron. *Cell Calcium* 54, 307–319. <https://doi.org/10.1016/j.ceca.2013.07.006>
- Ji, H., Li, D., Wu, Y., Zhang, Q., Gu, Q., Xie, H., Ji, T., Wang, H., Zhao, L., Zhao, H., Yang, Y., Feng, H., Xiong, H., Ji, J., Yang, Z., Kou, L., Li, M., Bao, X., Chang, X., Zhang, Y., Li, L., Li, H., Niu, Z., Wu, X., Xiao, J., Jiang, Y., Wang, J., 2018. Hypomyelinating disorders in China: The clinical and genetic heterogeneity in 119 patients. *PLOS ONE* 13, e0188869. <https://doi.org/10.1371/journal.pone.0188869>
- Jiang, W., Yang, Wanchun, Yang, Weiwei, Zhang, J., Pang, D., Gan, L., Luo, L., Fan, Y., Liu, Y., Chen, M., 2013. Identification of Tmem10 as a Novel Late-stage Oligodendrocytes Marker for Detecting Hypomyelination. *Int. J. Biol. Sci.* 10, 33–42. <https://doi.org/10.7150/ijbs.7526>
- Kalafatakis, I., Karagogeos, D., 2021. Oligodendrocytes and Microglia: Key Players in Myelin Development, Damage and Repair. *Biomolecules* 11, 1058. <https://doi.org/10.3390/biom11071058>
- Kanzaki, M., Zhang, Y.Q., Mashima, H., Li, L., Shibata, H., Kojima, I., 1999. Translocation of a calcium-permeable cation channel induced by insulin-like growth factor-I. *Nat. Cell Biol.* 1, 165–170. <https://doi.org/10.1038/11086>
- Kashani, I.R., Chavoshi, H., Pasbakhsh, P., Hassani, M., Omid, A., Mahmoudi, R., Beyer, C., Zendedel, A., 2017. Protective effects of erythropoietin against cuprizone-induced oxidative stress and demyelination in the mouse corpus callosum. *Iran. J. Basic Med. Sci.* 20, 886–893. <https://doi.org/10.22038/IJBMS.2017.9110>
- Kempner, Z.L.E. van, Kryscio, R.J., Costa, G.D., 2020. Serum neurofilament light as a prognostic marker for MS disability: Are we there yet? *Neurology* 94, 1013–1014. <https://doi.org/10.1212/WNL.0000000000009576>

- Kippert, A., Trajkovic, K., Fitzner, D., Opitz, L., Simons, M., 2008. Identification of Tmem10/Opalin as a novel marker for oligodendrocytes using gene expression profiling. *BMC Neurosci.* 9, 40. <https://doi.org/10.1186/1471-2202-9-40>
- Kira, J.I., 2017. New biomarker in demyelinating disorders. *J. Neurol. Sci.* 381, 9. <https://doi.org/10.1016/j.jns.2017.08.055>
- Kisucká, A., Bimbová, K., Bačová, M., Gálik, J., Lukáčová, N., 2021. Activation of Neuroprotective Microglia and Astrocytes at the Lesion Site and in the Adjacent Segments Is Crucial for Spontaneous Locomotor Recovery after Spinal Cord Injury. *Cells* 10, 1943. <https://doi.org/10.3390/cells10081943>
- Klinkert, W.E., Kojima, K., Lesslauer, W., Rinner, W., Lassmann, H., Wekerle, H., 1997. TNF-alpha receptor fusion protein prevents experimental auto-immune encephalomyelitis and demyelination in Lewis rats: an overview. *J. Neuroimmunol.* 72, 163–168. [https://doi.org/10.1016/s0165-5728\(96\)00183-x](https://doi.org/10.1016/s0165-5728(96)00183-x)
- Knapp, P., Skoff, R., Redstone, D., 1986. Oligodendroglial cell death in jimpy mice: an explanation for the myelin deficit. *J. Neurosci.* 6, 2813–2822. <https://doi.org/10.1523/JNEUROSCI.06-10-02813.1986>
- Knapp, P.E., 1996. Proteolipid protein: is it more than just a structural component of myelin? *Dev. Neurosci.* 18, 297–308. <https://doi.org/10.1159/000111420>
- Koeppen, A.H., Robitaille, Y., 2002. Pelizaeus-Merzbacher disease. *J. Neuropathol. Exp. Neurol.* 61, 747–759. <https://doi.org/10.1093/jnen/61.9.747>
- Kojima, I., Nagasawa, M., 2014. TRPV2. *Handb. Exp. Pharmacol.* 222, 247–272. https://doi.org/10.1007/978-3-642-54215-2_10
- Kolodny, E.H., 1993. Dysmyelinating and demyelinating conditions in infancy. *Curr. Opin. Neurol. Neurosurg.* 6, 379–386.
- Krauss, M., Haucke, V., 2007. Phosphoinositides: regulators of membrane traffic and protein function. *FEBS Lett.* 581, 2105–2111. <https://doi.org/10.1016/j.febslet.2007.01.089>
- Krumbholz, M., Theil, D., Cepok, S., Hemmer, B., Kivisäkk, P., Ransohoff, R.M., Hofbauer, M., Farina, C., Derfuss, T., Hartle, C., Newcombe, J., Hohlfeld, R., Meinl, E., 2006. Chemokines in multiple sclerosis: CXCL12 and CXCL13 up-regulation is differentially linked to CNS immune cell recruitment. *Brain J. Neurol.* 129, 200–211. <https://doi.org/10.1093/brain/awh680>
- Kumar, S., Chakraborty, S., Barbosa, C., Brustovetsky, T., Brustovetsky, N., Obukhov, A.G., 2012. Mechanisms controlling neurite outgrowth in a pheochromocytoma cell line: The role of TRPC channels. *J. Cell. Physiol.* 227, 1408–1419. <https://doi.org/10.1002/jcp.22855>
- Kumar, S., Singh, U., Goswami, C., Singru, P.S., 2017. Transient receptor potential vanilloid 5 (TRPV5), a highly Ca²⁺-selective TRP channel in the rat brain: relevance to neuroendocrine regulation. *J. Neuroendocrinol.* 29. <https://doi.org/10.1111/jne.12466>
- Kumar, Santosh, Singh, U., Singh, O., Goswami, C., Singru, P.S., 2017. Transient receptor potential vanilloid 6 (TRPV6) in the mouse brain: Distribution and estrous cycle-related

changes in the hypothalamus. *Neuroscience* 344, 204–216. <https://doi.org/10.1016/j.neuroscience.2016.12.025>

Larochelle, C., Wasser, B., Jamann, H., Löffel, J.T., Cui, Q.-L., Tastet, O., Schillner, M., Luchtman, D., Birkenstock, J., Stroh, A., Antel, J., Bittner, S., Zipp, F., 2021. Pro-inflammatory T helper 17 directly harms oligodendrocytes in neuroinflammation. *Proc. Natl. Acad. Sci.* 118, e2025813118. <https://doi.org/10.1073/pnas.2025813118>

Lassmann, H., 2018. Multiple Sclerosis Pathology. *Cold Spring Harb. Perspect. Med.* 8, a028936. <https://doi.org/10.1101/cshperspect.a028936>

Lassmann, H., 2011. Pathophysiology of inflammation and tissue injury in multiple sclerosis: What are the targets for therapy. *J. Neurol. Sci., Special Section: ECF 2009* 306, 167–169. <https://doi.org/10.1016/j.jns.2010.07.023>

Lassmann, H., Bradl, M., 2017. Multiple sclerosis: experimental models and reality. *Acta Neuropathol. (Berl.)* 133, 223–244. <https://doi.org/10.1007/s00401-016-1631-4>

Lee, B.C., Le, D.T., Gladyshev, V.N., 2008. Mammals Reduce Methionine-S-sulfoxide with MsrA and Are Unable to Reduce Methionine-R-sulfoxide, and This Function Can Be Restored with a Yeast Reductase. *J. Biol. Chem.* 283, 28361–28369. <https://doi.org/10.1074/jbc.M805059200>

Lee, J., Hamanaka, G., Lo, E.H., Arai, K., 2019. Heterogeneity of microglia and their differential roles in white matter pathology. *CNS Neurosci. Ther.* 25, 1290–1298. <https://doi.org/10.1111/cns.13266>

Lee, K., Jo, Y.Y., Chung, G., Jung, J.H., Kim, Y.H., Park, C.-K., 2021. Functional Importance of Transient Receptor Potential (TRP) Channels in Neurological Disorders. *Front. Cell Dev. Biol.* 9, 410. <https://doi.org/10.3389/fcell.2021.611773>

Levine, J.M., Stincone, F., Lee, Y.S., 1993. Development and differentiation of glial precursor cells in the rat cerebellum. *Glia* 7, 307–321. <https://doi.org/10.1002/glia.440070406>

Li, Y., Xu, X., Zhang, D., Cheng, W., Zhang, Yanan, Yu, B., Zhang, Yao, 2019. Genetic variation in the leukotriene pathway is associated with myocardial infarction in the Chinese population. *Lipids Health Dis.* 18, 25. <https://doi.org/10.1186/s12944-019-0968-9>

Liang, T.W., Chiu, H.H., Gurney, A., Sidle, A., Tumas, D.B., Schow, P., Foster, J., Klassen, T., Dennis, K., DeMarco, R.A., Pham, T., Frantz, G., Fong, S., 2002. Vascular endothelial-junctional adhesion molecule (VE-JAM)/JAM 2 interacts with T, NK, and dendritic cells through JAM 3. *J. Immunol. Baltim. Md* 168, 1618–1626. <https://doi.org/10.4049/jimmunol.168.4.1618>

Liapi, A., Wood, J.N., 2005. Extensive co-localization and heteromultimer formation of the vanilloid receptor-like protein TRPV2 and the capsaicin receptor TRPV1 in the adult rat cerebral cortex. *Eur. J. Neurosci.* 22, 825–834. <https://doi.org/10.1111/j.1460-9568.2005.04270.x>

Liebers, M., 1928. Zur Histopathologie des zweiten Falles von PelizaeusMerzbacherscher Krankheit. *Zeitschr Ges Neurol Psychiat* 115, 487–509.

- Linington, C., Bradl, M., Lassmann, H., Brunner, C., Vass, K., 1988. Augmentation of demyelination in rat acute allergic encephalomyelitis by circulating mouse monoclonal antibodies directed against a myelin/oligodendrocyte glycoprotein. *Am. J. Pathol.* 130, 443–454.
- Link, T.M., Park, U., Vonakis, B.M., Raben, D.M., Soloski, M.J., Caterina, M.J., 2010. TRPV2 plays a pivotal role in macrophage particle binding and phagocytosis. *Nat. Immunol.* 11, 232–239. <https://doi.org/10.1038/ni.1842>
- Linneberg, C., Harboe, M., Laursen, L.S., 2015. Axo-Glia Interaction Preceding CNS Myelination Is Regulated by Bidirectional Eph-Ephrin Signaling. *ASN NEURO* 7, 1759091415602859. <https://doi.org/10.1177/1759091415602859>
- Liu, M., Liu, X., Wang, L., Wang, Y., Dong, F., Wu, J., Qu, X., Liu, Y., Liu, Z., Fan, H., Yao, R., 2018. TRPV4 Inhibition Improved Myelination and Reduced Glia Reactivity and Inflammation in a Cuprizone-Induced Mouse Model of Demyelination. *Front. Cell. Neurosci.* 12, 392. <https://doi.org/10.3389/fncel.2018.00392>
- Liu, R.Y., Snider, W.D., 2001. Different signaling pathways mediate regenerative versus developmental sensory axon growth. *J. Neurosci. Off. J. Soc. Neurosci.* 21, RC164.
- Liu, Z., Xu, D., Wang, S., Chen, Y., Li, Z., Gao, X., Jiang, L., Tang, Y., Peng, Y., 2017. Astrocytes induce proliferation of oligodendrocyte progenitor cells via connexin 47-mediated activation of the ERK/Id4 pathway. *Cell Cycle Georget. Tex* 16, 714–722. <https://doi.org/10.1080/15384101.2017.1295183>
- Love, S., 2006. Demyelinating diseases. *J. Clin. Pathol.* 59, 1151–1159. <https://doi.org/10.1136/jcp.2005.031195>
- Luan, W., Qi, X., Liang, F., Zhang, X., Jin, Z., Shi, L., Luo, B., Dai, X., 2021. Microglia Impede Oligodendrocyte Generation in Aged Brain. *J. Inflamm. Res.* 14, 6813–6831. <https://doi.org/10.2147/JIR.S338242>
- Lucchinetti, C., Brück, W., Parisi, J., Scheithauer, B., Rodriguez, M., Lassmann, H., 2000. Heterogeneity of multiple sclerosis lesions: implications for the pathogenesis of demyelination. *Ann. Neurol.* 47, 707–717. [https://doi.org/10.1002/1531-8249\(200006\)47:6<707::aid-ana3>3.0.co;2-q](https://doi.org/10.1002/1531-8249(200006)47:6<707::aid-ana3>3.0.co;2-q)
- Lüders, K.A., Nessler, S., Kusch, K., Patzig, J., Jung, R.B., Möbius, W., Nave, K.-A., Werner, H.B., 2019. Maintenance of high proteolipid protein level in adult central nervous system myelin is required to preserve the integrity of myelin and axons. *Glia* 67, 634–649. <https://doi.org/10.1002/glia.23549>
- Ludwig, P.E., Reddy, V., Varacallo, M., 2021. Neuroanatomy, Neurons, in: *StatPearls*. StatPearls Publishing, Treasure Island (FL).
- Maiorino, E., Baek, S.H., Guo, F., Zhou, X., Kothari, P.H., Silverman, E.K., Barabási, A.-L., Weiss, S.T., Raby, B.A., Sharma, A., 2020. Discovering the genes mediating the interactions between chronic respiratory diseases in the human interactome. *Nat. Commun.* 11, 811. <https://doi.org/10.1038/s41467-020-14600-w>

- Maksoud, M.J.E., Tellios, V., An, D., Xiang, Y.-Y., Lu, W.-Y., 2019. Nitric oxide upregulates microglia phagocytosis and increases transient receptor potential vanilloid type 2 channel expression on the plasma membrane. *Glia* 67, 2294–2311. <https://doi.org/10.1002/glia.23685>
- Malmeström, C., Haghghi, S., Rosengren, L., Andersen, O., Lycke, J., 2003. Neurofilament light protein and glial fibrillary acidic protein as biological markers in MS. *Neurology* 61, 1720–1725. <https://doi.org/10.1212/01.wnl.0000098880.19793.b6>
- Mangiardi, M., Crawford, D.K., Xia, X., Du, S., Simon-Freeman, R., Voskuhl, R.R., Tiwari-Woodruff, S.K., 2011. An Animal Model of Cortical and Callosal Pathology in Multiple Sclerosis. *Brain Pathol. Zurich Switz.* 21, 263–278. <https://doi.org/10.1111/j.1750-3639.2010.00444.x>
- Martin, N.A., Nawrocki, A., Molnar, V., Elkjaer, M.L., Thygesen, E.K., Palkovits, M., Acs, P., Sejbaek, T., Nielsen, H.H., Hegedus, Z., Sellebjerg, F., Molnar, T., Barbosa, E.G.V., Alcaraz, N., Gallyas, F., Svenningsen, A.F., Baumbach, J., Lassmann, H., Larsen, M.R., Illes, Z., 2018. Orthologous proteins of experimental de- and remyelination are differentially regulated in the CSF proteome of multiple sclerosis subtypes. *PLoS ONE* 13. <https://doi.org/10.1371/journal.pone.0202530>
- Martínez, Y., Li, X., Liu, G., Bin, P., Yan, W., Más, D., Valdivié, M., Hu, C.-A.A., Ren, W., Yin, Y., 2017. The role of methionine on metabolism, oxidative stress, and diseases. *Amino Acids* 49, 2091–2098. <https://doi.org/10.1007/s00726-017-2494-2>
- Marzan, D.E., Brügger-Verdon, V., West, B.L., Liddelow, S., Samanta, J., Salzer, J.L., 2021. Activated microglia drive demyelination via CSF1R signaling. *Glia* 69, 1583–1604. <https://doi.org/10.1002/glia.23980>
- Mason, J.L., Angelastro, J.M., Ignatova, T.N., Kukekov, V.G., Lin, G., Greene, L.A., Goldman, J.E., 2005. ATF5 regulates the proliferation and differentiation of oligodendrocytes. *Mol. Cell Neurosci.* 29, 372–380. <https://doi.org/10.1016/j.mcn.2005.03.004>
- Mason, J.L., Ye, P., Suzuki, K., D’Ercole, A.J., Matsushima, G.K., 2000. Insulin-like growth factor-1 inhibits mature oligodendrocyte apoptosis during primary demyelination. *J. Neurosci. Off. J. Soc. Neurosci.* 20, 5703–5708.
- Medina, E., 1993. Demyelinating and Dysmyelinating Diseases. *Riv. Neuroradiol.* 6, 33–38. <https://doi.org/10.1177/19714009930060S205>
- Menn, B., Garcia-Verdugo, J.M., Yaschine, C., Gonzalez-Perez, O., Rowitch, D., Alvarez-Buylla, A., 2006. Origin of Oligodendrocytes in the Subventricular Zone of the Adult Brain. *J. Neurosci.* 26, 7907–7918. <https://doi.org/10.1523/JNEUROSCI.1299-06.2006>
- Merzbacher, L., 1910. Eine eigenartige familiär-hereditäre erkrankungsform (Aplasia axialis extracorticalis congenita). *Z. Für Gesamte Neurol. Psychiatr.* 3, 1. <https://doi.org/10.1007/BF02893591>
- Meyer, N., Richter, N., Fan, Z., Siemonsmeier, G., Pivneva, T., Jordan, P., Steinhäuser, C., Semtner, M., Nolte, C., Kettenmann, H., 2018. Oligodendrocytes in the Mouse Corpus Callosum Maintain Axonal Function by Delivery of Glucose. *Cell Rep.* 22, 2383–2394. <https://doi.org/10.1016/j.celrep.2018.02.022>

- Mihara, H., Boudaka, A., Shibasaki, K., Yamanaka, A., Sugiyama, T., Tominaga, M., 2010. Involvement of TRPV2 Activation in Intestinal Movement through Nitric Oxide Production in Mice. *J. Neurosci.* 30, 16536–16544. <https://doi.org/10.1523/JNEUROSCI.4426-10.2010>
- Miljkovic, D., Drulovic, J., Trajkovic, V., Mesaros, S., Dujmovic, I., Maksimovic, D., Samardzic, T., Stojavljevic, N., Levic, Z., Mostarica Stojkovic, M., 2002. Nitric oxide metabolites and interleukin-6 in cerebrospinal fluid from multiple sclerosis patients. *Eur. J. Neurol.* 9, 413–418. <https://doi.org/10.1046/j.1468-1331.2002.00437.x>
- Miller, M.J., Kangas, C.D., Macklin, W.B., 2009. Neuronal expression of the proteolipid protein gene in the medulla of the mouse. *J. Neurosci. Res.* 87, 2842–2853. <https://doi.org/10.1002/jnr.22121>
- Miller, S.D., Karpus, W.J., Davidson, T.S., 2007. Experimental Autoimmune Encephalomyelitis in the Mouse. *Curr. Protoc. Immunol.* Ed. John E Coligan AI CHAPTER, Unit-15.1. <https://doi.org/10.1002/0471142735.im1501s77>
- Mix, E., Meyer-Rienecker, H., Hartung, H.-P., Zettl, U.K., 2010. Animal models of multiple sclerosis—Potentials and limitations. *Prog. Neurobiol.* 92, 386–404. <https://doi.org/10.1016/j.pneurobio.2010.06.005>
- Miyamoto, Y., Torii, T., Terao, M., Takada, S., Tanoue, A., Katoh, H., Yamauchi, J., 2021. Rnd2 differentially regulates oligodendrocyte myelination at different developmental periods. *Mol. Biol. Cell* 32, 769–787. <https://doi.org/10.1091/mbc.E20-05-0332>
- Molina-Gonzalez, I., Miron, V.E., 2019. Astrocytes in myelination and remyelination. *Neurosci. Lett.* 713, 134532. <https://doi.org/10.1016/j.neulet.2019.134532>
- Monet, M., Gkika, D., Lehen'kyi, V., Pournier, A., Abeele, F.V., Bidaux, G., Juvin, V., Rassendren, F., Humez, S., Prevarsakaya, N., 2009. Lysophospholipids stimulate prostate cancer cell migration via TRPV2 channel activation. *Biochim. Biophys. Acta BBA - Mol. Cell Res.* 1793, 528–539. <https://doi.org/10.1016/j.bbamcr.2009.01.003>
- Montell, C., 2005. The TRP superfamily of cation channels. *Sci. STKE Signal Transduct. Knowl. Environ.* 2005, re3. <https://doi.org/10.1126/stke.2722005re3>
- Morell, P., Quarles, R.H., 1999. Characteristic Composition of Myelin. *Basic Neurochem. Mol. Cell. Med. Asp.* 6th Ed.
- Morelli, M.B., Amantini, C., Tomassoni, D., Nabissi, M., Arcella, A., Santoni, G., 2019. Transient Receptor Potential Mucolipin-1 Channels in Glioblastoma: Role in Patient's Survival. *Cancers* 11, 525. <https://doi.org/10.3390/cancers11040525>
- Moyon, S., Dubessy, A.L., Aigrot, M.S., Trotter, M., Huang, J.K., Dauphinot, L., Potier, M.C., Kerninon, C., Melik Parsadaniantz, S., Franklin, R.J.M., Lubetzki, C., 2015. Demyelination Causes Adult CNS Progenitors to Revert to an Immature State and Express Immune Cues That Support Their Migration. *J. Neurosci.* 35, 4–20. <https://doi.org/10.1523/JNEUROSCI.0849-14.2015>
- Muraki, K., Iwata, Y., Katanosaka, Y., Ito, T., Ohya, S., Shigekawa, M., Imaizumi, Y., 2003. TRPV2 is a component of osmotically sensitive cation channels in murine aortic myocytes. *Circ. Res.* 93, 829–838. <https://doi.org/10.1161/01.RES.0000097263.10220.0C>

- Nabissi, M., Morelli, M.B., Amantini, C., Farfariello, V., Ricci-Vitiani, L., Caprodossi, S., Arcella, A., Santoni, M., Giangaspero, F., De Maria, R., Santoni, G., 2010. TRPV2 channel negatively controls glioma cell proliferation and resistance to Fas-induced apoptosis in ERK-dependent manner. *Carcinogenesis* 31, 794–803. <https://doi.org/10.1093/carcin/bgq019>
- Nabissi, M., Morelli, M.B., Santoni, M., Santoni, G., 2013. Triggering of the TRPV2 channel by cannabidiol sensitizes glioblastoma cells to cytotoxic chemotherapeutic agents. *Carcinogenesis* 34, 48–57. <https://doi.org/10.1093/carcin/bgs328>
- Nadon, N.L., West, M., 1998. Myelin proteolipid protein: function in myelin structure is distinct from its role in oligodendrocyte development. *Dev. Neurosci.* 20, 533–539. <https://doi.org/10.1159/000017354>
- Nagasawa, M., Kojima, I., 2012. Translocation of calcium-permeable TRPV2 channel to the podosome: Its role in the regulation of podosome assembly. *Cell Calcium* 51, 186–193. <https://doi.org/10.1016/j.ceca.2011.12.012>
- Nahas, N., Conant, A., Hamilton, E., Curiel, J., Simons, C., van der Knaap, M., Vanderver, A., 1993. TUBB4A-Related Leukodystrophy, in: Adam, M.P., Ardinger, H.H., Pagon, R.A., Wallace, S.E., Bean, L.J., Mirzaa, G., Amemiya, A. (Eds.), *GeneReviews®*. University of Washington, Seattle, Seattle (WA).
- Nakahara, J., Seiwa, C., Tan-Takeuchi, K., Gotoh, M., Kishihara, K., Ogawa, M., Asou, H., Aiso, S., 2005. Involvement of CD45 in central nervous system myelination. *Neurosci. Lett.* 379, 116–121. <https://doi.org/10.1016/j.neulet.2004.12.066>
- Narumi, S., Kaburaki, T., Yoneyama, H., Iwamura, H., Kobayashi, Y., Matsushima, K., 2002. Neutralization of IFN-inducible protein 10/CXCL10 exacerbates experimental autoimmune encephalomyelitis. *Eur. J. Immunol.* 32, 1784–1791. [https://doi.org/10.1002/1521-4141\(200206\)32:6<1784::AID-IMMU1784>3.0.CO;2-R](https://doi.org/10.1002/1521-4141(200206)32:6<1784::AID-IMMU1784>3.0.CO;2-R)
- Nash, B., Ioannidou, K., Barnett, S.C., 2011. Astrocyte phenotypes and their relationship to myelination. *J. Anat.* 219, 44–52. <https://doi.org/10.1111/j.1469-7580.2010.01330.x>
- Nave, K.A., Bloom, F.E., Milner, R.J., 1987. A single nucleotide difference in the gene for myelin proteolipid protein defines the jimpy mutation in mouse. *J. Neurochem.* 49, 1873–1877. <https://doi.org/10.1111/j.1471-4159.1987.tb02449.x>
- Nedungadi, T.P., Dutta, M., Bathina, C.S., Caterina, M.J., Cunningham, J.T., 2012. Expression and distribution of TRPV2 in rat brain. *Exp. Neurol.* 237, 223–237. <https://doi.org/10.1016/j.expneurol.2012.06.017>
- Neumann, H., Kotter, M.R., Franklin, R.J.M., 2009. Debris clearance by microglia: an essential link between degeneration and regeneration. *Brain* 132, 288–295. <https://doi.org/10.1093/brain/awn109>
- Nicholas, R.S., Wing, M.G., Compston, A., 2001. Nonactivated microglia promote oligodendrocyte precursor survival and maturation through the transcription factor NF-kappa B. *Eur. J. Neurosci.* 13, 959–967. <https://doi.org/10.1046/j.0953-816x.2001.01470.x>
- Nilsson, G., 1950. A New colour reaction on copper and certain carbonyl compounds. *Acta Chem Scand* 4, 205–205.

- Noble, P.G., Antel, J.P., Yong, V.W., 1994. Astrocytes and catalase prevent the toxicity of catecholamines to oligodendrocytes. *Brain Res.* 633, 83–90. [https://doi.org/10.1016/0006-8993\(94\)91525-3](https://doi.org/10.1016/0006-8993(94)91525-3)
- Numata, Y., Gotoh, L., Iwaki, A., Kurosawa, K., Takanashi, J.-I., Deguchi, K., Yamamoto, T., Osaka, H., Inoue, K., 2014. Epidemiological, clinical, and genetic landscapes of hypomyelinating leukodystrophies. *J. Neurol.* 261, 752–758. <https://doi.org/10.1007/s00415-014-7263-5>
- Nutma, E., van Gent, D., Amor, S., Peferoen, L.A.N., 2020. Astrocyte and Oligodendrocyte Cross-Talk in the Central Nervous System. *Cells* 9, 600. <https://doi.org/10.3390/cells9030600>
- Ohl, K., Tenbrock, K., Kipp, M., 2016. Oxidative stress in multiple sclerosis: Central and peripheral mode of action. *Exp. Neurol.* 277, 58–67. <https://doi.org/10.1016/j.expneurol.2015.11.010>
- Okuno, T., Nakatsuji, Y., Moriya, M., Takamatsu, H., Nojima, S., Takegahara, N., Toyofuku, T., Nakagawa, Y., Kang, S., Friedel, R.H., Sakoda, S., Kikutani, H., Kumanogoh, A., 2010. Roles of Sema4D–Plexin-B1 Interactions in the Central Nervous System for Pathogenesis of Experimental Autoimmune Encephalomyelitis. *J. Immunol.* 184, 1499–1506. <https://doi.org/10.4049/jimmunol.0903302>
- Olitsky, P.K., Yager, R.H., 1949. Experimental disseminated encephalomyelitis in white mice. *J. Exp. Med.* 90, 213–224. <https://doi.org/10.1084/jem.90.3.213>
- Omari, K.M., Lutz, S.E., Santambrogio, L., Lira, S.A., Raine, C.S., 2009. Neuroprotection and remyelination after autoimmune demyelination in mice that inducibly overexpress CXCL1. *Am. J. Pathol.* 174, 164–176. <https://doi.org/10.2353/ajpath.2009.080350>
- O’Meara, R.W., Michalski, J.-P., Kothary, R., 2011. Integrin Signaling in Oligodendrocytes and Its Importance in CNS Myelination. *J. Signal Transduct.* 2011, 354091. <https://doi.org/10.1155/2011/354091>
- Órpez-Zafra, T., Pavía, J., Hurtado-Guerrero, I., Pinto-Medel, M.J., Rodríguez Bada, J.L., Urbaneja, P., Suardíaz, M., Villar, L.M., Comabella, M., Montalban, X., Alvarez-Cermeño, J.C., Leyva, L., Fernández, Ó., Oliver-Martos, B., 2017. Decreased soluble IFN- β receptor (sIFNAR2) in multiple sclerosis patients: A potential serum diagnostic biomarker. *Mult. Scler. J.* 23, 937–945. <https://doi.org/10.1177/1352458516667564>
- Osorio, J.M., Goldman, S.A., 2018. Neurogenetics of Pelizaeus-Merzbacher disease. *Handb. Clin. Neurol.* 148, 701–722. <https://doi.org/10.1016/B978-0-444-64076-5.00045-4>
- Packialakshmi, B., Zhou, X., 2018. Experimental autoimmune encephalomyelitis (EAE) up-regulates the mitochondrial activity and manganese superoxide dismutase (MnSOD) in the mouse renal cortex. *PLoS ONE* 13, e0196277. <https://doi.org/10.1371/journal.pone.0196277>
- Paez, P.M., Fulton, D., Spreuer, V., Handley, V., Campagnoni, A.T., 2011. Modulation of Canonical Transient Receptor Potential Channel 1 in the Proliferation of Oligodendrocyte Precursor Cells by the Golli Products of the Myelin Basic Protein Gene. *J. Neurosci.* 31, 3625–3637. <https://doi.org/10.1523/JNEUROSCI.4424-10.2011>

- Pandur, E., Pap, R., Varga, E., Jánosa, G., Komoly, S., Fórizs, J., Sipos, K., 2019. Relationship of Iron Metabolism and Short-Term Cuprizone Treatment of C57BL/6 Mice. *Int. J. Mol. Sci.* 20, 2257. <https://doi.org/10.3390/ijms20092257>
- Pang, Y., Cai, Z., Rhodes, P.G., 2000. Effects of lipopolysaccharide on oligodendrocyte progenitor cells are mediated by astrocytes and microglia. *J. Neurosci. Res.* 62, 510–520. [https://doi.org/10.1002/1097-4547\(20001115\)62:4<510::AID-JNR5>3.0.CO;2-F](https://doi.org/10.1002/1097-4547(20001115)62:4<510::AID-JNR5>3.0.CO;2-F)
- Parnell, G.P., Booth, D.R., 2017. The Multiple Sclerosis (MS) Genetic Risk Factors Indicate both Acquired and Innate Immune Cell Subsets Contribute to MS Pathogenesis and Identify Novel Therapeutic Opportunities. *Front. Immunol.* 8, 425. <https://doi.org/10.3389/fimmu.2017.00425>
- Pasquini, L.A., Millet, V., Hoyos, H.C., Giannoni, J.P., Croci, D.O., Marder, M., Liu, F.T., Rabinovich, G.A., Pasquini, J.M., 2011. Galectin-3 drives oligodendrocyte differentiation to control myelin integrity and function. *Cell Death Differ.* 18, 1746–1756. <https://doi.org/10.1038/cdd.2011.40>
- Pelizaeus, F., 1885. Über eine eigenthümliche Form spastischer Lähmung mit Cerebralerschinungen auf hereditärer Grundlage (Multiple Sklerose). *Arch Psychiatr* 16, 698–710.
- Penna, A., Juvin, V., Chemin, J., Compan, V., Monet, M., Rassendren, F.-A., 2006. PI3-kinase promotes TRPV2 activity independently of channel translocation to the plasma membrane. *Cell Calcium* 39, 495–507. <https://doi.org/10.1016/j.ceca.2006.01.009>
- Perálvarez-Marín, A., Doñate-Macian, P., Gaudet, R., 2013. What do we know about the transient receptor potential vanilloid 2 (TRPV2) ion channel? *FEBS J.* 280, 5471–5487. <https://doi.org/10.1111/febs.12302>
- Perlman, S.J., Mar, S., 2012. Leukodystrophies. *Adv. Exp. Med. Biol.* 724, 154–171. https://doi.org/10.1007/978-1-4614-0653-2_13
- Peschl, P., Bradl, M., Höftberger, R., Berger, T., Reindl, M., 2017. Myelin Oligodendrocyte Glycoprotein: Deciphering a Target in Inflammatory Demyelinating Diseases. *Front. Immunol.* 8. <https://doi.org/10.3389/fimmu.2017.00529>
- Pietiäinen, V., Vassilev, B., Blom, T., Wang, W., Nelson, J., Bittman, R., Bäck, N., Zelcer, N., Ikonen, E., 2013. NDRG1 functions in LDL receptor trafficking by regulating endosomal recycling and degradation. *J. Cell Sci.* 126, 3961–3971. <https://doi.org/10.1242/jcs.128132>
- Plastini, M.J., Desu, H.L., Brambilla, R., 2020. Dynamic Responses of Microglia in Animal Models of Multiple Sclerosis. *Front. Cell. Neurosci.* 14. <https://doi.org/10.3389/fncel.2020.00269>
- Platten, M., Ho, P.P., Youssef, S., Fontoura, P., Garren, H., Hur, E.M., Gupta, R., Lee, L.Y., Kidd, B.A., Robinson, W.H., Sobel, R.A., Selley, M.L., Steinman, L., 2005. Treatment of Autoimmune Neuroinflammation with a Synthetic Tryptophan Metabolite. *Science* 310, 850–855. <https://doi.org/10.1126/science.1117634>
- Popescu, B.F.G., Lucchinetti, C.F., 2012. Pathology of demyelinating diseases. *Annu. Rev. Pathol.* 7, 185–217. <https://doi.org/10.1146/annurev-pathol-011811-132443>

- Popescu, B.F.Gh., Pirko, I., Lucchinetti, C.F., 2013. Pathology of Multiple Sclerosis: Where Do We Stand? *Contin. Lifelong Learn. Neurol.* 19, 901–921. <https://doi.org/10.1212/01.CON.0000433291.23091.65>
- Poser, C.M., 1978. Demyelination revisited. *Arch. Neurol.* 35, 401–408. <https://doi.org/10.1001/archneur.1978.00500310003001>
- Prodan, C.I., Holland, N.R., Wisdom, P.J., Burstein, S.A., Bottomley, S.S., 2002. CNS demyelination associated with copper deficiency and hyperzincemia. *Neurology* 59, 1453–1456. <https://doi.org/10.1212/01.wnl.0000032497.30439.f6>
- Puntambekar, P., Mukherjea, D., Jajoo, S., Ramkumar, V., 2005. Essential role of Rac1/NADPH oxidase in nerve growth factor induction of TRPV1 expression. *J. Neurochem.* 95, 1689–1703. <https://doi.org/10.1111/j.1471-4159.2005.03518.x>
- Purves, D., Augustine, G.J., Fitzpatrick, D., Katz, L.C., LaMantia, A.-S., McNamara, J.O., Williams, S.M., 2001. *Increased Conduction Velocity as a Result of Myelination*. Neurosci. 2nd Ed.
- Quan, L., Uyeda, A., Muramatsu, R., 2022. Central nervous system regeneration: the roles of glial cells in the potential molecular mechanism underlying remyelination. *Inflamm. Regen.* 42, 7. <https://doi.org/10.1186/s41232-022-00193-y>
- Qureshi, M., Al-Suhaimi, E.A., Wahid, F., Shehzad, O., Shehzad, A., 2018. Therapeutic potential of curcumin for multiple sclerosis. *Neurol. Sci. Off. J. Ital. Neurol. Soc. Ital. Soc. Clin. Neurophysiol.* 39, 207–214. <https://doi.org/10.1007/s10072-017-3149-5>
- Raddatz, B.B., Sun, W., Brogden, G., Sun, Y., Kammeyer, P., Kalkuhl, A., Colbatzky, F., Deschl, U., Naim, H.Y., Baumgärtner, W., Ulrich, R., 2016. Central Nervous System Demyelination and Remyelination is Independent from Systemic Cholesterol Level in Theiler's Murine Encephalomyelitis. *Brain Pathol. Zurich Switz.* 26, 102–119. <https://doi.org/10.1111/bpa.12266>
- Rao, P., Segal, B.M., 2004. Experimental autoimmune encephalomyelitis. *Methods Mol. Med.* 102, 363–375. <https://doi.org/10.1385/1-59259-805-6:363>
- Ray, A.K., DuBois, J.C., Gruber, R.C., Guzik, H.M., Gulinello, M.E., Perumal, G., Raine, C., Kozakiewicz, L., Williamson, J., Shafit-Zagardo, B., 2017. Loss of Gas6 and Axl signaling results in extensive axonal damage, motor deficits, prolonged neuroinflammation and less remyelination following cuprizone exposure. *Glia* 65, 2051–2069. <https://doi.org/10.1002/glia.23214>
- Redmond, S., Mei, F., Eshed-Eisenbach, Y., Osso, L.A., Leshkowitz, D., Shen, Y.-A., Kay, J.N., Aurrand-Lions, M., Lyons, D.A., Peles, E., Chan, J.R., 2016. Somatodendritic Expression of JAM2 Inhibits Oligodendrocyte Myelination. *Neuron* 91. <https://doi.org/10.1016/j.neuron.2016.07.021>
- Reiche, L., Göttle, P., Lane, L., Duek, P., Park, M., Azim, K., Schütte, J., Manousi, A., Schira-Heinen, J., Küry, P., 2021. C21orf91 Regulates Oligodendroglial Precursor Cell Fate—A Switch in the Glial Lineage? *Front. Cell. Neurosci.* 15, 653075. <https://doi.org/10.3389/fncel.2021.653075>

- Richardson, W.D., Kessaris, N., Pringle, N., 2006. Oligodendrocyte Wars. *Nat. Rev. Neurosci.* 7, 11–18. <https://doi.org/10.1038/nrn1826>
- Rivers, T.M., Sprunt, D.H., Berry, G.P., 1933. OBSERVATIONS ON ATTEMPTS TO PRODUCE ACUTE DISSEMINATED ENCEPHALOMYELITIS IN MONKEYS. *J. Exp. Med.* 58, 39–53. <https://doi.org/10.1084/jem.58.1.39>
- Robinson, A.P., Harp, C.T., Noronha, A., Miller, S.D., 2014. The experimental autoimmune encephalomyelitis (EAE) model of MS: utility for understanding disease pathophysiology and treatment. *Handb. Clin. Neurol.* 122, 173–189. <https://doi.org/10.1016/B978-0-444-52001-2.00008-X>
- Rosenthal, J.F., Hoffman, B.M., Tyor, W.R., 2020. CNS inflammatory demyelinating disorders: MS, NMOSD and MOG antibody associated disease. *J. Investig. Med. Off. Publ. Am. Fed. Clin. Res.* 68, 321–330. <https://doi.org/10.1136/jim-2019-001126>
- Ruiz, C., Zitnik, M., Leskovec, J., 2021. Identification of disease treatment mechanisms through the multiscale interactome. *Nat. Commun.* 12, 1796. <https://doi.org/10.1038/s41467-021-21770-8>
- Ruiz, M., Bégou, M., Launay, N., Ranea-Robles, P., Bianchi, P., López-Erauskin, J., Morató, L., Guilera, C., Petit, B., Vauris-Barriere, C., Guéret-Gonthier, C., Bonnet-Dupeyron, M.-N., Fourcade, S., Auwerx, J., Boespflug-Tanguy, O., Pujol, A., 2018. Oxidative stress and mitochondrial dynamics malfunction are linked in Pelizaeus-Merzbacher disease. *Brain Pathol. Zurich Switz.* 28, 611–630. <https://doi.org/10.1111/bpa.12571>
- Sachs, H.H., Bercury, K.K., Popescu, D.C., Narayanan, S.P., Macklin, W.B., 2014. A New Model of Cuprizone-Mediated Demyelination/Remyelination. *ASN Neuro* 6, 1759091414551955. <https://doi.org/10.1177/1759091414551955>
- Saha, B., Ypsilanti, A.R., Boutin, C., Cremer, H., Chédotal, A., 2012. Plexin-B2 Regulates the Proliferation and Migration of Neuroblasts in the Postnatal and Adult Subventricular Zone. *J. Neurosci.* 32, 16892–16905. <https://doi.org/10.1523/JNEUROSCI.0344-12.2012>
- Saito, S., Fukuta, N., Shingai, R., Tominaga, M., 2011. Evolution of Vertebrate Transient Receptor Potential Vanilloid 3 Channels: Opposite Temperature Sensitivity between Mammals and Western Clawed Frogs. *PLoS Genet.* 7. <https://doi.org/10.1371/journal.pgen.1002041>
- Salzer, J., Svenningsson, A., Sundström, P., 2010. Neurofilament light as a prognostic marker in multiple sclerosis. *Mult. Scler. Houndmills Basingstoke Engl.* 16, 287–292. <https://doi.org/10.1177/1352458509359725>
- Salzer, J.L., Zalc, B., 2016. Myelination. *Curr. Biol.* 26, R971–R975. <https://doi.org/10.1016/j.cub.2016.07.074>
- Santoni, G., Amantini, C., 2019. The Transient Receptor Potential Vanilloid Type-2 (TRPV2) Ion Channels in Neurogenesis and Gliomagenesis: Cross-Talk between Transcription Factors and Signaling Molecules. *Cancers* 11. <https://doi.org/10.3390/cancers11030322>
- Santos, B.S. dos, Silva, L.C.N. da, Silva, T.D. da, Rodrigues, J.F.S., Grisotto, M.A.G., Correia, M.T. dos S., Napoleão, T.H., Silva, M.V. da, Paiva, P.M.G., 2016. Application of Omics

Technologies for Evaluation of Antibacterial Mechanisms of Action of Plant-Derived Products. *Front. Microbiol.* 7.

Sappington, R.M., Calkins, D.J., 2008. Contribution of TRPV1 to Microglia-Derived IL-6 and NF κ B Translocation with Elevated Hydrostatic Pressure. *Invest. Ophthalmol. Vis. Sci.* 49, 3004–3017. <https://doi.org/10.1167/iovs.07-1355>

Saugier-Weber, P., Munnich, A., 1994. La maladie de Pelizaeus-Merzbacher et une forme de paraplégie spastique liée à l’X sont toutes deux associées au gène PLP. *MS Médecine Sci. Rev. Pap.* ISSN 0767-0974 1994 Vol 10 N° 4 P487-488. <https://doi.org/10.4267/10608/2649>

Saunders, C.I., Kunde, D.A., Crawford, A., Geraghty, D.P., 2007. Expression of transient receptor potential vanilloid 1 (TRPV1) and 2 (TRPV2) in human peripheral blood. *Mol. Immunol.* 44, 1429–1435. <https://doi.org/10.1016/j.molimm.2006.04.027>

Scarpini, E., Galimberti, D., Baron, P., Clerici, R., Ronzoni, M., Conti, G., Scarlato, G., 2002. IP-10 and MCP-1 levels in CSF and serum from multiple sclerosis patients with different clinical subtypes of the disease. *J. Neurol. Sci.* 195, 41–46. [https://doi.org/10.1016/s0022-510x\(01\)00680-3](https://doi.org/10.1016/s0022-510x(01)00680-3)

Scheiermann, C., Meda, P., Aurrand-Lions, M., Madani, R., Yiangou, Y., Coffey, P., Salt, T.E., Ducrest-Gay, D., Caille, D., Howell, O., Reynolds, R., Lobrinus, A., Adams, R.H., Yu, A.S.L., Anand, P., Imhof, B.A., Nourshargh, S., 2007. Expression and function of junctional adhesion molecule-C in myelinated peripheral nerves. *Science* 318, 1472–1475. <https://doi.org/10.1126/science.1149276>

Schmidt, F., van den Eijnden, M., Pescini Gobert, R., Saborio, G.P., Carboni, S., Alliod, C., Pouly, S., Staugaitis, S.M., Dutta, R., Trapp, B., van Huijsduijnen, R.H., 2012. Identification of VHY/Dusp15 as a Regulator of Oligodendrocyte Differentiation through a Systematic Genomics Approach. *PLoS ONE* 7, e40457. <https://doi.org/10.1371/journal.pone.0040457>

Seitelberger, F., 1995. Neuropathology and genetics of Pelizaeus-Merzbacher disease. *Brain Pathol. Zurich Switz.* 5, 267–273. <https://doi.org/10.1111/j.1750-3639.1995.tb00603.x>

Seitelberger, F., Vinken, P., Bruyn, G., 1970. Pelizaeus-Merzbacher disease. Leukodystrophies and Poliodystrophies, in: *Handbook of Clinical Neurology*. Elsevier, Amsterdam, pp. 150–202.

Shachuan, F., Zhou, L., Huang, C., Xie, K., Nice, E., 2015. Interactomics: Toward protein function and regulation. *Expert Rev. Proteomics* 12, 1–24. <https://doi.org/10.1586/14789450.2015.1000870>

Shen, K., Reichelt, M., Kyauk, R.V., Ngu, H., Shen, Y.-A.A., Foreman, O., Modrusan, Z., Friedman, B.A., Sheng, M., Yuen, T.J., 2021. Multiple sclerosis risk gene Mertk is required for microglial activation and subsequent remyelination. *Cell Rep.* 34, 108835. <https://doi.org/10.1016/j.celrep.2021.108835>

Shibasaki, K., Ikenaka, K., Tamalu, F., Tominaga, M., Ishizaki, Y., 2014. A novel subtype of astrocytes expressing TRPV4 (transient receptor potential vanilloid 4) regulates neuronal excitability via release of gliotransmitters. *J. Biol. Chem.* 289, 14470–14480. <https://doi.org/10.1074/jbc.M114.557132>

Shibasaki, K., Ishizaki, Y., Mandadi, S., 2013. Astrocytes express functional TRPV2 ion channels. *Biochem. Biophys. Res. Commun.* 441, 327–332. <https://doi.org/10.1016/j.bbrc.2013.10.046>

Shibasaki, K., Murayama, N., Ono, K., Ishizaki, Y., Tominaga, M., 2010. TRPV2 enhances axon outgrowth through its activation by membrane stretch in developing sensory and motor neurons. *J. Neurosci. Off. J. Soc. Neurosci.* 30, 4601–4612. <https://doi.org/10.1523/JNEUROSCI.5830-09.2010>

Shibasaki, K., Sugio, S., Takao, K., Yamanaka, A., Miyakawa, T., Tominaga, M., Ishizaki, Y., 2015. TRPV4 activation at the physiological temperature is a critical determinant of neuronal excitability and behavior. *Pflugers Arch.* 467, 2495–2507. <https://doi.org/10.1007/s00424-015-1726-0>

Shibasaki, K., Suzuki, M., Mizuno, A., Tominaga, M., 2007. Effects of body temperature on neural activity in the hippocampus: regulation of resting membrane potentials by transient receptor potential vanilloid 4. *J. Neurosci. Off. J. Soc. Neurosci.* 27, 1566–1575. <https://doi.org/10.1523/JNEUROSCI.4284-06.2007>

Shimizu, T., Dietz, R.M., Cruz-Torres, I., Strnad, F., Garske, A.K., Moreno, M., Venna, V.R., Quillinan, N., Herson, P.S., 2016. Extended therapeutic window of a novel peptide inhibitor of TRPM2 channels following focal cerebral ischemia. *Exp. Neurol.* 283, 151–156. <https://doi.org/10.1016/j.expneurol.2016.06.015>

Shimotsuma, Y., Tanaka, M., Izawa, T., Yamate, J., Kuwamura, M., 2016. Enhanced Expression of Trib3 during the Development of Myelin Breakdown in dmy Myelin Mutant Rats. *PLoS ONE* 11. <https://doi.org/10.1371/journal.pone.0168250>

Sidman, R.L., Dickie, M.M., Appel, S.H., 1964. MUTANT MICE (QUAKING AND JIMPY) WITH DEFICIENT MYELINATION IN THE CENTRAL NERVOUS SYSTEM. *Science* 144, 309–311. <https://doi.org/10.1126/science.144.3616.309>

Simonetti, M., Paldy, E., Njoo, C., Bali, K.K., Worzfeld, T., Pitzer, C., Kuner, T., Offermanns, S., Mauceri, D., Kuner, R., 2021. The impact of Semaphorin 4C/Plexin-B2 signaling on fear memory via remodeling of neuronal and synaptic morphology. *Mol. Psychiatry* 26, 1376–1398. <https://doi.org/10.1038/s41380-019-0491-4>

Singh, U., Upadhyaya, M., Basu, S., Singh, O., Kumar, S., Kokare, D.M., Singru, P.S., 2020. Transient Receptor Potential Vanilloid 3 (TRPV3) in the Cerebellum of Rat and Its Role in Motor Coordination. *Neuroscience* 424, 121–132. <https://doi.org/10.1016/j.neuroscience.2019.10.047>

Sinha, S., Boyden, A.W., Itani, F.R., Crawford, M.P., Karandikar, N.J., 2015. CD8+ T-Cells as Immune Regulators of Multiple Sclerosis. *Front. Immunol.* 6, 619. <https://doi.org/10.3389/fimmu.2015.00619>

Smith, E.S., Jonason, A., Reilly, C., Veeraraghavan, J., Fisher, T., Doherty, M., Klimatcheva, E., Mallow, C., Cornelius, C., Leonard, J.E., Marchi, N., Janigro, D., Argaw, A.T., Pham, T., Seils, J., Bussler, H., Torno, S., Kirk, R., Howell, A., Evans, E.E., Paris, M., Bowers, W.J., John, G., Zauderer, M., 2015. SEMA4D compromises blood–brain barrier, activates microglia,

- and inhibits remyelination in neurodegenerative disease. *Neurobiol. Dis.* 73, 254–268. <https://doi.org/10.1016/j.nbd.2014.10.008>
- Smith, K.J., Lassmann, H., 2002. The role of nitric oxide in multiple sclerosis. *Lancet Neurol.* 1, 232–241. [https://doi.org/10.1016/s1474-4422\(02\)00102-3](https://doi.org/10.1016/s1474-4422(02)00102-3)
- Smith-Bouvier, D.L., Divekar, A.A., Sasidhar, M., Du, S., Tiwari-Woodruff, S.K., King, J.K., Arnold, A.P., Singh, R.R., Voskuhl, R.R., 2008. A role for sex chromosome complement in the female bias in autoimmune disease. *J. Exp. Med.* 205, 1099–1108. <https://doi.org/10.1084/jem.20070850>
- Sørensen, T.L., Tani, M., Jensen, J., Pierce, V., Lucchinetti, C., Folcik, V.A., Qin, S., Rottman, J., Sellebjerg, F., Strieter, R.M., Frederiksen, J.L., Ransohoff, R.M., 1999. Expression of specific chemokines and chemokine receptors in the central nervous system of multiple sclerosis patients. *J. Clin. Invest.* 103, 807–815.
- Sørensen, T.L., Trebst, C., Kivisäkk, P., Klaege, K.L., Majmudar, A., Ravid, R., Lassmann, H., Olsen, D.B., Strieter, R.M., Ransohoff, R.M., Sellebjerg, F., 2002. Multiple sclerosis: a study of CXCL10 and CXCR3 co-localization in the inflamed central nervous system. *J. Neuroimmunol.* 127, 59–68. [https://doi.org/10.1016/s0165-5728\(02\)00097-8](https://doi.org/10.1016/s0165-5728(02)00097-8)
- Sriram, S., Steiner, I., 2005. Experimental allergic encephalomyelitis: a misleading model of multiple sclerosis. *Ann. Neurol.* 58, 939–945. <https://doi.org/10.1002/ana.20743>
- Stadtman, E.R., Berlett, B.S., 1998. Reactive oxygen-mediated protein oxidation in aging and disease. *Drug Metab. Rev.* 30, 225–243. <https://doi.org/10.3109/03602539808996310>
- Stern, B.R., Solioz, M., Krewski, D., Aggett, P., Aw, T.-C., Baker, S., Crump, K., Dourson, M., Haber, L., Hertzberg, R., Keen, C., Meek, B., Rudenko, L., Schoeny, R., Slob, W., Starr, T., 2007. Copper and human health: biochemistry, genetics, and strategies for modeling dose-response relationships. *J. Toxicol. Environ. Health B Crit. Rev.* 10, 157–222. <https://doi.org/10.1080/10937400600755911>
- Strimbu, K., Tavel, J.A., 2010. What are Biomarkers? *Curr. Opin. HIV AIDS* 5, 463–466. <https://doi.org/10.1097/COH.0b013e32833ed177>
- Suminaite, D., Lyons, D.A., Livesey, M.R., 2019. Myelinated axon physiology and regulation of neural circuit function. *Glia* 67, 2050–2062. <https://doi.org/10.1002/glia.23665>
- Sun, L.O., Mulinyawe, S.B., Collins, H.Y., Ibrahim, A., Li, Q., Simon, D.J., Tessier-Lavigne, M., Barres, B.A., 2018. Spatiotemporal Control of CNS Myelination by Oligodendrocyte Programmed Cell Death through the TFEB-PUMA Axis. *Cell* 175, 1811–1826.e21. <https://doi.org/10.1016/j.cell.2018.10.044>
- Sun, Y., Chen, X., Ou, Z., Wang, Y., Chen, W., Zhao, T., Liu, C., Chen, Y., 2021. Dysmyelination by Oligodendrocyte-Specific Ablation of Ninj2 Contributes to Depressive-Like Behaviors. *Adv. Sci.* 9, 2103065. <https://doi.org/10.1002/advs.202103065>
- 't Hart, B.A., Gran, B., Weissert, R., 2011. EAE: imperfect but useful models of multiple sclerosis. *Trends Mol. Med.* 17, 119–125. <https://doi.org/10.1016/j.molmed.2010.11.006>

- Tafti, D., Ehsan, M., Xixis, K.L., 2021. Multiple Sclerosis, in: StatPearls. StatPearls Publishing, Treasure Island (FL).
- Takeuchi, H., Wang, J., Kawanokuchi, J., Mitsuma, N., Mizuno, T., Suzumura, A., 2006. Interferon-gamma induces microglial-activation-induced cell death: a hypothetical mechanism of relapse and remission in multiple sclerosis. *Neurobiol. Dis.* 22, 33–39. <https://doi.org/10.1016/j.nbd.2005.09.014>
- Taniguchi, Y., Amazaki, M., Furuyama, T., Yamaguchi, W., Takahara, M., Saino, O., Wada, T., Niwa, H., Tashiro, F., Miyazaki, J., Kogo, M., Matsuyama, T., Inagaki, S., 2009. Sema4D deficiency results in an increase in the number of oligodendrocytes in healthy and injured mouse brains. *J. Neurosci. Res.* 87, 2833–2841. <https://doi.org/10.1002/jnr.22124>
- Tarrago, L., Laugier, E., Rey, P., 2009. Protein-Repairing Methionine Sulfoxide Reductases in Photosynthetic Organisms: Gene Organization, Reduction Mechanisms, and Physiological Roles. *Mol. Plant* 2, 202–217. <https://doi.org/10.1093/mp/ssn067>
- Thilo, F., Suess, O., Liu, Y., Tepel, M., 2011. Decreased expression of transient receptor potential channels in cerebral vascular tissue from patients after hypertensive intracerebral hemorrhage. *Clin. Exp. Hypertens. N. Y.* N 1993 33, 533–537. <https://doi.org/10.3109/10641963.2011.561903>
- Thomson, C.E., Anderson, T.J., McCulloch, M.C., Dickinson, P., Vouyiouklis, D.A., Griffiths, I.R., 1999. The early phenotype associated with the jimpy mutation of the proteolipid protein gene. *J. Neurocytol.* 28, 207–221. <https://doi.org/10.1023/A:1007024022663>
- Thorburne, S.K., Juurlink, B.H., 1996. Low glutathione and high iron govern the susceptibility of oligodendroglial precursors to oxidative stress. *J. Neurochem.* 67, 1014–1022. <https://doi.org/10.1046/j.1471-4159.1996.67031014.x>
- Torii, T., Miyamoto, Y., Yamauchi, J., Tanoue, A., 2014. Pelizaeus–Merzbacher disease: Cellular pathogenesis and pharmacologic therapy. *Pediatr. Int.* 56, 659–666. <https://doi.org/10.1111/ped.12450>
- Torkildsen, O., Brunborg, L.A., Myhr, K.-M., Bø, L., 2008. The cuprizone model for demyelination. *Acta Neurol. Scand. Suppl.* 188, 72–76. <https://doi.org/10.1111/j.1600-0404.2008.01036.x>
- Torre-Fuentes, L., Moreno-Jiménez, L., Pytel, V., Matías-Guiu, J.A., Gómez-Pinedo, U., Matías-Guiu, J., 2020. Modelos experimentales de desmielinización-remielinización. *Neurología* 35, 32–39. <https://doi.org/10.1016/j.nrl.2017.07.002>
- Toscano, S., Patti, F., 2021. CSF biomarkers in multiple sclerosis: beyond neuroinflammation. *Neuroimmunol. Neuroinflammation* 8, 14–41. <https://doi.org/10.20517/2347-8659.2020.12>
- Tóth, A., Boczán, J., Kedei, N., Lizanecz, E., Bagi, Z., Papp, Z., Edes, I., Csiba, L., Blumberg, P.M., 2005. Expression and distribution of vanilloid receptor 1 (TRPV1) in the adult rat brain. *Brain Res. Mol. Brain Res.* 135, 162–168. <https://doi.org/10.1016/j.molbrainres.2004.12.003>
- Traiffort, E., Kassoussi, A., Zahaf, A., Laouarem, Y., 2020. Astrocytes and Microglia as Major Players of Myelin Production in Normal and Pathological Conditions. *Front. Cell. Neurosci.* 14, 79. <https://doi.org/10.3389/fncel.2020.00079>

- Trebst, C., König, F., Ransohoff, R., Brück, W., Stangel, M., 2008. CCR5 expression on macrophages/microglia is associated with early remyelination in multiple sclerosis lesions. *Mult. Scler. Houndmills Basingstoke Engl.* 14, 728–733. <https://doi.org/10.1177/1352458508089359>
- Trofatter, J.A., Dlouhy, S.R., DeMyer, W., Conneally, P.M., Hodes, M.E., 1989. Pelizaeus-Merzbacher disease: tight linkage to proteolipid protein gene exon variant. *Proc. Natl. Acad. Sci. U. S. A.* 86, 9427–9430. <https://doi.org/10.1073/pnas.86.23.9427>
- Udvardia, A.J., Köster, R.W., Skene, J.H., 2001. GAP-43 promoter elements in transgenic zebrafish reveal a difference in signals for axon growth during CNS development and regeneration. *Dev. Camb. Engl.* 128, 1175–1182.
- Urbanski, M.M., Brendel, M.B., Melendez-Vasquez, C.V., 2019. Acute and chronic demyelinated CNS lesions exhibit opposite elastic properties. *Sci. Rep.* 9, 999. <https://doi.org/10.1038/s41598-018-37745-7>
- Valério-Gomes, B., Guimarães, D.M., Szczupak, D., Lent, R., 2018. The Absolute Number of Oligodendrocytes in the Adult Mouse Brain. *Front. Neuroanat.* 12. <https://doi.org/10.3389/fnana.2018.00090>
- van der Knaap, M.S., Wolf, N.I., Heine, V.M., 2016. Leukodystrophies. *Neurol. Clin. Pract.* 6, 506–514. <https://doi.org/10.1212/CPJ.0000000000000289>
- van der Star, B.J., Vogel, D.Y.S., Kipp, M., Puentes, F., Baker, D., Amor, S., 2012. In vitro and in vivo models of multiple sclerosis. *CNS Neurol. Disord. Drug Targets* 11, 570–588. <https://doi.org/10.2174/187152712801661284>
- van der Vaart, B., Franker, M.A.M., Kuijpers, M., Hua, S., Bouchet, B.P., Jiang, K., Grigoriev, I., Hoogenraad, C.C., Akhmanova, A., 2012. Microtubule Plus-End Tracking Proteins SLAIN1/2 and ch-TOG Promote Axonal Development. *J. Neurosci.* 32, 14722–14728a. <https://doi.org/10.1523/JNEUROSCI.1240-12.2012>
- Vanderver, A., Prust, M., Tonduti, D., Mochel, F., Hussey, H.M., Helman, G., Garbern, J., Eichler, F., Labauge, P., Aubourg, P., Rodriguez, D., Patterson, M.C., Van Hove, J.L.K., Schmidt, J., Wolf, N.I., Boespflug-Tanguy, O., Schiffmann, R., van der Knaap, M.S., 2015. Case Definition and Classification of Leukodystrophies and Leukoencephalopathies. *Mol. Genet. Metab.* 114, 494–500. <https://doi.org/10.1016/j.ymgme.2015.01.006>
- Vega-Riquer, J.M., Mendez-Victoriano, G., Morales-Luckie, R.A., Gonzalez-Perez, O., 2019. Five Decades of Cuprizone, an Updated Model to Replicate Demyelinating Diseases. *Curr. Neuropharmacol.* 17, 129–141. <https://doi.org/10.2174/1570159X15666170717120343>
- Vela, J.M., González, B., Castellano, B., 1998. Understanding glial abnormalities associated with myelin deficiency in the jimpy mutant mouse. *Brain Res. Brain Res. Rev.* 26, 29–42. [https://doi.org/10.1016/s0165-0173\(97\)00055-6](https://doi.org/10.1016/s0165-0173(97)00055-6)
- Velilla, J., Marchetti, M.M., Toth-Petroczy, A., Grosogeat, C., Bennett, A.H., Carmichael, N., Estrella, E., Darras, B.T., Frank, N.Y., Krier, J., Gaudet, R., Gupta, V.A., 2019. Homozygous TRPV4 mutation causes congenital distal spinal muscular atrophy and arthrogyriposis. *Neurol. Genet.* 5, e312. <https://doi.org/10.1212/NXG.0000000000000312>

- Vennekens, R., Menigoz, A., Nilius, B., 2012. TRPs in the Brain. *Rev. Physiol. Biochem. Pharmacol.* 163, 27–64. https://doi.org/10.1007/112_2012_8
- Verkhatsky, A., Reyes, R.C., Papura, V., 2014. TRP Channels Coordinate Ion Signalling in Astroglia. *Rev. Physiol. Biochem. Pharmacol.* 166, 1–22. https://doi.org/10.1007/112_2013_15
- Verma, P., Kumar, A., Goswami, C., 2010. TRPV4-mediated channelopathies. *Channels Austin Tex* 4, 319–328. <https://doi.org/10.4161/chan.4.4.12905>
- Vidal, M., Cusick, M.E., Barabási, A.-L., 2011. Interactome Networks and Human Disease. *Cell* 144, 986–998. <https://doi.org/10.1016/j.cell.2011.02.016>
- Wade, B.J., 2014. Spatial Analysis of Global Prevalence of Multiple Sclerosis Suggests Need for an Updated Prevalence Scale. *Mult. Scler. Int.* 2014, 124578. <https://doi.org/10.1155/2014/124578>
- Wainwright, A., Rutter, A.R., Seabrook, G.R., Reilly, K., Oliver, K.R., 2004. Discrete expression of TRPV2 within the hypothalamo-neurohypophysial system: Implications for regulatory activity within the hypothalamic-pituitary-adrenal axis. *J. Comp. Neurol.* 474, 24–42. <https://doi.org/10.1002/cne.20100>
- Walton, C., King, R., Rechtman, L., Kaye, W., Leray, E., Marrie, R.A., Robertson, N., La Rocca, N., Uitdehaag, B., van der Mei, I., Wallin, M., Helme, A., Angood Napier, C., Rijke, N., Baneke, P., 2020. Rising prevalence of multiple sclerosis worldwide: Insights from the Atlas of MS, third edition. *Mult. Scler. Houndmills Basingstoke Engl.* 26, 1816–1821. <https://doi.org/10.1177/1352458520970841>
- Wang, R., Tu, S., Zhang, J., Shao, A., 2020. Roles of TRP Channels in Neurological Diseases. *Oxid. Med. Cell. Longev.* 2020, 7289194. <https://doi.org/10.1155/2020/7289194>
- Wang, X., Zhao, L., Zhang, J., Fariss, R.N., Ma, W., Kretschmer, F., Wang, M., Qian, H. hua, Badea, T.C., Diamond, J.S., Gan, W.-B., Roger, J.E., Wong, W.T., 2016. Requirement for Microglia for the Maintenance of Synaptic Function and Integrity in the Mature Retina. *J. Neurosci.* 36, 2827–2842. <https://doi.org/10.1523/JNEUROSCI.3575-15.2016>
- Warf, B., Fok-Seang, J., Miller, R., 1991. Evidence for the ventral origin of oligodendrocyte precursors in the rat spinal cord. *J. Neurosci.* 11, 2477–2488. <https://doi.org/10.1523/JNEUROSCI.11-08-02477.1991>
- Wasseff, S.K., Scherer, S.S., 2015. Activated Immune Response in an Inherited Leukodystrophy Disease Caused by the Loss of Oligodendrocyte Gap Junctions. *Neurobiol. Dis.* 82, 86–98. <https://doi.org/10.1016/j.nbd.2015.05.018>
- Weissbach, H., Resnick, L., Brot, N., 2005. Methionine sulfoxide reductases: history and cellular role in protecting against oxidative damage. *Biochim. Biophys. Acta* 1703, 203–212. <https://doi.org/10.1016/j.bbapap.2004.10.004>
- Willard, H.F., Riordan, J.R., 1985. Assignment of the gene for myelin proteolipid protein to the X chromosome: implications for X-linked myelin disorders. *Science* 230, 940–942. <https://doi.org/10.1126/science.3840606>

- Willer, C.J., Dymont, D.A., Risch, N.J., Sadovnick, A.D., Ebers, G.C., Canadian Collaborative Study Group, 2003. Twin concordance and sibling recurrence rates in multiple sclerosis. *Proc. Natl. Acad. Sci. U. S. A.* 100, 12877–12882. <https://doi.org/10.1073/pnas.1932604100>
- Willis, C.M., Nicaise, A.M., Bongarzone, E.R., Givogri, M., Reiter, C.R., Heintz, O., Jellison, E.R., Sutter, P.A., TeHennepe, G., Ananda, G., Vella, A.T., Crocker, S.J., 2020. Astrocyte Support for Oligodendrocyte Differentiation can be Conveyed via Extracellular Vesicles but Diminishes with Age. *Sci. Rep.* 10. <https://doi.org/10.1038/s41598-020-57663-x>
- Wrigley, S., Arafa, D., Tropea, D., 2017. Insulin-Like Growth Factor 1: At the Crossroads of Brain Development and Aging. *Front. Cell. Neurosci.* 11, 14. <https://doi.org/10.3389/fncel.2017.00014>
- Wynford-Thomas, R., Jacob, A., Tomassini, V., 2019. Neurological update: MOG antibody disease. *J. Neurol.* 266, 1280–1286. <https://doi.org/10.1007/s00415-018-9122-2>
- Xu, C., Li, P.P., Cooke, R.G., Parikh, S.V., Wang, K., Kennedy, J.L., Warsh, J.J., 2009. TRPM2 variants and bipolar disorder risk: confirmation in a family-based association study. *Bipolar Disord.* 11, 1–10. <https://doi.org/10.1111/j.1399-5618.2008.00655.x>
- Xu, C., Macciardi, F., Li, P.P., Yoon, I.-S., Cooke, R.G., Hughes, B., Parikh, S.V., McIntyre, R.S., Kennedy, J.L., Warsh, J.J., 2006. Association of the putative susceptibility gene, transient receptor potential protein melastatin type 2, with bipolar disorder. *Am. J. Med. Genet. Part B Neuropsychiatr. Genet. Off. Publ. Int. Soc. Psychiatr. Genet.* 141B, 36–43. <https://doi.org/10.1002/ajmg.b.30239>
- Xu, H., Ramsey, I.S., Kotecha, S.A., Moran, M.M., Chong, J.A., Lawson, D., Ge, P., Lilly, J., Silos-Santiago, I., Xie, Y., DiStefano, P.S., Curtis, R., Clapham, D.E., 2002. TRPV3 is a calcium-permeable temperature-sensitive cation channel. *Nature* 418, 181–186. <https://doi.org/10.1038/nature00882>
- Yamaguchi, W., Tamai, R., Kageura, M., Furuyama, T., Inagaki, S., 2012. Sema4D as an inhibitory regulator in oligodendrocyte development. *Mol. Cell. Neurosci.* 49, 290–299. <https://doi.org/10.1016/j.mcn.2011.12.004>
- Yamashita, T., Ando, Y., Obayashi, K., Uchino, M., Ando, M., 1997. Changes in nitrite and nitrate (NO₂-/NO₃-) levels in cerebrospinal fluid of patients with multiple sclerosis. *J. Neurol. Sci.* 153, 32–34. [https://doi.org/10.1016/s0022-510x\(97\)00183-4](https://doi.org/10.1016/s0022-510x(97)00183-4)
- Yamate-Morgan, H., Lauderdale, K., Horeczko, J., Merchant, U., Tiwari-Woodruff, S.K., 2019. Functional Effects of Cuprizone-Induced Demyelination in the Presence of the mTOR-Inhibitor Rapamycin. *Neuroscience* 406, 667–683. <https://doi.org/10.1016/j.neuroscience.2019.01.038>
- Yan, S., Nagle, D.G., Zhou, Y., Zhang, W., 2018. Chapter 3 - Application of Systems Biology in the Research of TCM Formulae, in: Zhang, W.-D. (Ed.), *Systems Biology and Its Application in TCM Formulas Research*. Academic Press, pp. 31–67. <https://doi.org/10.1016/B978-0-12-812744-5.00003-5>
- Yatsenko, A.S., Kucherenko, M.M., Xie, Y., Aweida, D., Urlaub, H., Scheibe, R.J., Cohen, S., Shcherbata, H.R., 2020. Profiling of the muscle-specific dystroglycan interactome reveals the

- role of Hippo signaling in muscular dystrophy and age-dependent muscle atrophy. *BMC Med.* 18, 8. <https://doi.org/10.1186/s12916-019-1478-3>
- Yeo, Y.A., Martínez Gómez, J.M., Croxford, J.L., Gasser, S., Ling, E.-A., Schwarz, H., 2012. CD137 ligand activated microglia induces oligodendrocyte apoptosis via reactive oxygen species. *J. Neuroinflammation* 9, 173. <https://doi.org/10.1186/1742-2094-9-173>
- Yin, J., Valin, K.L., Dixon, M.L., Leavenworth, J.W., 2017. The Role of Microglia and Macrophages in CNS Homeostasis, Autoimmunity, and Cancer. *J. Immunol. Res.* 2017. <https://doi.org/10.1155/2017/5150678>
- Zawadzka, M., Rivers, L.E., Fancy, S.P.J., Zhao, C., Tripathi, R., Jamen, F., Young, K., Goncharevich, A., Pohl, H., Rizzi, M., Rowitch, D.H., Kessler, N., Suter, U., Richardson, W.D., Franklin, R.J.M., 2010. CNS-Resident Glial Progenitor/Stem Cells Produce Schwann Cells as well as Oligodendrocytes during Repair of CNS Demyelination. *Cell Stem Cell* 6, 10.1016/j.stem.2010.04.002. <https://doi.org/10.1016/j.stem.2010.04.002>
- Zeman, W., Demyer, W., Falls, H.F., 1964. PELIZAEUS-MERZBACHER DISEASE. A STUDY IN NOSOLOGY. *J. Neuropathol. Exp. Neurol.* 23, 334–354. <https://doi.org/10.1097/00005072-196404000-00008>
- Zhan, J., Mann, T., Joost, S., Behrangi, N., Frank, M., Kipp, M., 2020. The Cuprizone Model: Dos and Do Nots. *Cells* 9, 843. <https://doi.org/10.3390/cells9040843>
- Zhang, C., Jia, P., Jia, Y., Weissbach, H., Webster, K.A., Huang, X., Lemanski, S.L., Achary, M., Lemanski, L.F., 2010. Methionine Sulfoxide Reductase A (MsrA) Protects Cultured Mouse Embryonic Stem Cells From H₂O₂-Mediated Oxidative Stress. *J. Cell. Biochem.* 111, 94–103. <https://doi.org/10.1002/jcb.22666>
- Zhang, H.-L., Wang, J., Tang, L., 2014. Sema4D knockdown in oligodendrocytes promotes functional recovery after spinal cord injury. *Cell Biochem. Biophys.* 68, 489–496. <https://doi.org/10.1007/s12013-013-9727-0>
- Zhang, J.-X., Feng, Y.-F., Qi, Q., Shen, L., Wang, R., Zhou, J.-S., Lü, H.-Z., Hu, J.-G., 2014. JNK is necessary for oligodendrocyte precursor cell proliferation induced by the conditioned medium from B104 neuroblastoma cells. *J. Mol. Neurosci.* MN 52, 269–276. <https://doi.org/10.1007/s12031-013-0135-0>
- Zhang, N., Liu, C., Zhang, R., Jin, L., Yin, X., Zheng, X., Siebert, H.-C., Li, Y., Wang, Z., Loers, G., Petridis, A.K., 2020. Amelioration of clinical course and demyelination in the cuprizone mouse model in relation to ketogenic diet. *Food Funct.* 11, 5647–5663. <https://doi.org/10.1039/c9fo02944c>
- Zhang, W., Zhang, X., Zhang, L., Xu, D., Cheng, N., Tang, Y., Peng, Y., 2020. Astrocytes increase exosomal secretion of oligodendrocyte precursor cells to promote their proliferation via integrin β 4-mediated cell adhesion. *Biochem. Biophys. Res. Commun.* 526, 341–348. <https://doi.org/10.1016/j.bbrc.2020.03.092>
- Zhang, Y., Yin, L., Zheng, N., Zhang, L., Liu, J., Liang, W., Wang, Q., 2017. Icaritin enhances remyelination process after acute demyelination induced by cuprizone exposure. *Brain Res. Bull.* 130, 180–187. <https://doi.org/10.1016/j.brainresbull.2017.01.025>

- Zhang, Z., Ma, Z., Zou, W., Guo, H., Liu, M., Ma, Y., Zhang, L., 2019. The Appropriate Marker for Astrocytes: Comparing the Distribution and Expression of Three Astrocytic Markers in Different Mouse Cerebral Regions. *BioMed Res. Int.* 2019, e9605265. <https://doi.org/10.1155/2019/9605265>
- Zhao, S., Hu, X., Park, J., Zhu, Y., Zhu, Q., Li, H., Luo, C., Han, R., Cooper, N., Qiu, M., 2007. Selective expression of LDLR and VLDLR in myelinating oligodendrocytes. *Dev. Dyn. Off. Publ. Am. Assoc. Anat.* 236, 2708–12. <https://doi.org/10.1002/dvdy.21283>
- Zheng, J., 2013. Molecular Mechanism of TRP Channels. *Compr. Physiol.* 3, 221–242. <https://doi.org/10.1002/cphy.c120001>
- Zhou, J., Du, W., Zhou, K., Tai, Y., Yao, H., Jia, Y., Ding, Y., Wang, Y., 2008. Critical role of TRPC6 channels in the formation of excitatory synapses. *Nat. Neurosci.* 11, 741–743. <https://doi.org/10.1038/nn.2127>
- Ziemssen, T., Akgün, K., Brück, W., 2019. Molecular biomarkers in multiple sclerosis. *J. Neuroinflammation* 16, 272. <https://doi.org/10.1186/s12974-019-1674-2>
- Zipp, F., 2000. Apoptosis in multiple sclerosis. *Cell Tissue Res.* 301, 163–171. <https://doi.org/10.1007/s004410000179>